U.PORTO

DOUTORAMENTO

CIÊNCIAS FARMACÊUTICAS

Biomarker discovery and metabolic characterization of prostate cancer through tissue and urine metabolomic studies

Ana Rita Couto Machado Lima

D

2021

Ana Rita Couto Machado Lima

Biomarker discovery and metabolic characterization of prostate cancer through tissue and urine metabolomic studies

Tese do 3º Ciclo de Estudos Conducente ao Grau de Doutoramento em Ciências Farmacêuticas – Especialidade de Toxicologia

Trabalho realizado sob a orientação de:

Doutora Maria Paula do Amaral Alegria Guedes de Pinho (Orientadora)

Professora Doutora Márcia Cláudia Dias de Carvalho (Coorientadora)

Doutora Joana Isabel Monteiro Pinto (Coorientadora)

Professora Doutora Maria de Lourdes Pinho de Almeida Souteiro Bastos (Coorientadora)

Porto

Junho, 2021

A candidata agradece à Fundação para a Ciência e Tecnologia (FCT) pela atribuição da bolsa individual de Doutoramento (SFRH/BD/123012/2016); à Unidade de Ciências Biomoleculares Aplicadas - UCIBIO financiada por fundos nacionais através da FCT (UIDB/04378/2020 e UIDP/04423/2020); ao Fundo Europeu de Desenvolvimento Regional (FEDER) no âmbito do projeto POCI/01/0145/FEDER/07728; ao programa Operacional Regional do Norte (NORTE 2020), através do Portugal 2020 e do FEDER no âmbito do projeto NORTE-01-0145-FEDER-000024; a Fundos FEDER através do Programa Operacional Competitividade e Internacionalização - COMPETE 2020 e Fundos Nacionais através da FCT no âmbito do projeto POCI-01-0145-FEDER-030388 - PTDC/SAU-SER/30388/2017.

Publications

Author's declaration

The following original articles/communications were prepared in the scope of this thesis. The author declares to have a major contribution to the conception design and technical execution of the work, acquisition of data, analysis, and interpretation of the results as well as manuscript preparation of the published work included in this thesis.

- **Manuscripts published in international peer-reviewed journals**

General introduction

I. **Ana Rita Lima,** Joana Pinto, Maria de Lourdes Bastos, Márcia Carvalho and Paula Guedes de Pinho. NMR-based metabolomics studies of human prostate cancer tissue. *Metabolomics*, 2018; 14:88. doi: 10.1007/s11306-018-1384-2

II. **Ana Rita Lima,** Joana Pinto, Filipa Amaro, Maria de Lourdes Bastos, Márcia Carvalho and Paula Guedes de Pinho. Advances and perspectives in prostate cancer biomarker discovery in the last 5 years through tissue and urine metabolomics. *Metabolites*, 2021; 11:181. doi: 10.3390/metabo11030181

Original research

I. **Ana Rita Lima,** Joana Pinto, Ana Isabel Azevedo, Daniela Barros-Silva, Carmen Jerónimo, Rui Henrique, Maria de Lourdes Bastos, Paula Guedes de Pinho and Márcia Carvalho. Identification of a biomarker panel for improvement of prostate cancer diagnosis by volatile metabolic profiling of urine. *British Journal of Cancer*, 2019; 121:857-868. doi: 10.1038/s41416-019-0585-4

II. **Ana Rita Lima,** Joana Pinto, Carina Carvalho-Maia, Carmen Jerónimo, Rui Henrique, Maria de Lourdes Bastos, Márcia Carvalho and Paula Guedes de Pinho. A panel of urinary volatile biomarkers for differential diagnosis of prostate cancer from other urological cancers. *Cancers*, 2020; 12:2017. doi: 10.3390/cancers12082017.10.3390

III. **Ana Rita Lima,** Joana Pinto, Daniela Barros-Silva, Carmen Jerónimo, Rui Henrique, Maria de Lourdes Bastos, Márcia Carvalho and Paula Guedes de Pinho. New findings on urinary prostate cancer metabolome through combined GC-MS and ^{1}H NMR analytical platforms. *Metabolomics*, 2020; 16:70. doi: 10.1007/s11306-020-01691-1

IV. **Ana Rita Lima**, Márcia Carvalho, Susana S. Aveiro, Tânia Melo, M. Rosário Domingues, Catarina Macedo-Silva, Nuno Coimbra, Carmen Jerónimo, Rui Henrique, Maria de Lourdes Bastos, Paula Guedes de Pinho, Joana Pinto. Comprehensive metabolomics and lipidomics profiling of prostate cancer tissue reveals metabolic dysregulations associated with disease development. Submited to *Cancers.*

- **Conference papers in international peer-reviewed journals**

I. **Ana Rita Lima**, Joana Pinto, Carmen Jerónimo, Rui Henrique, Maria de Lourdes Bastos, Márcia Carvalho and Paula Guedes de Pinho. Metabolomics evaluation of urine from PCa patients by GC-MS and NMR spectroscopy. *Toxicology Letters*, 2019; 314S:S89. doi: 10.1016/j.toxlet.2019.09.002

- **Oral communications in scientific meetings**

I. **Ana Rita Lima**, Ana Isabel Azevedo, Joana Pinto, Carmen Jerónimo, Rui Henrique, Maria de Lourdes Bastos, Márcia Carvalho and Paula Guedes de Pinho. Investigation of urinary volatile metabolites as potential prostate cancer biomarkers by headspace solid-phase microextraction in combination with gas chromatography-mass spectrometry. In XLIX Reunião da Sociedade

Portuguesa de Farmacologia, XXXVII Reunião de Farmacologia Clínica, e XVIII Reunião de Toxicologia (SPF 2019), 6-8 February 2019, Porto, Portugal.

II. **Ana Rita Lima**, Joana Pinto, Ana Isabel Azevedo, Carmen Jerónimo, Rui Henrique, Maria de Lourdes Bastos, Márcia Carvalho and Paula Guedes de Pinho. Potentialities of volatile organic compounds in human urine for urological cancers diagnosis. In EMN Workshop – Volatilomics in Human Health: An Introduction, Metabolomics 2019, 23-27 June 2019, The Hague, Netherlands.

- **Poster communications in scientific meetings**

I. **Ana Rita Lima**, Joana Pinto, Ana Isabel Azevedo, Carmen Jerónimo, Rui Henrique, Maria de Lourdes Bastos, Márcia Carvalho and Paula Guedes de Pinho. Evaluation of urinary volatile metabolites as potential biomarkers for prostate cancer diagnosis. In Metabolomics 2019 - the 15th International Conference of the Metabolomics Society, 23-27 June 2019, The Hague, Netherlands.

II. **Ana Rita Lima**, Joana Pinto, Carmen Jerónimo, Rui Henrique, Maria de Lourdes Bastos, Márcia Carvalho and Paula Guedes de Pinho. Metabolomics evaluation of urine from PCa patients by GC-MS and NMR spectroscopy. In 55th Congress of the European Societies of Toxicology (EUROTOX 2019), 8-11 September 2019, Helsinki, Finland.

III. **Ana Rita Lima**, Joana Pinto, Ana Isabel Azevedo, Daniela Barros-Silva, Carmen Jerónimo, Rui Henrique, Maria de Lourdes Bastos, Márcia Carvalho and Paula Guedes de Pinho. Identificação de um painel de biomarcadores para diagnóstico do cancro de próstata através do estudo do perfil metabólico volátil da urina. In 1º Encontro Nacional de Jovens Investigadores em Oncologia, 24 September 2019, Porto, Portugal.

IV. **Ana Rita Lima**, Joana Pinto, Daniela Barros-Silva, Carmen Jerónimo, Rui Henrique, Maria de Lourdes Bastos, Márcia Carvalho and Paula Guedes Pinho. Caracterização da assinatura metabólica do cancro da próstata em

urina. In 2º Encontro Nacional de Jovens Investigadores em Oncologia, 24 September 2020, Porto, Portugal.

V. **Ana Rita Lima**, Joana Pinto, Carina Carvalho-Maia, Carmen Jerónimo, Rui Henrique, Maria de Lourdes Bastos, Márcia Carvalho and Paula Guedes de Pinho. A volatile 10-biomarker panel in urine for an improved prostate cancer diagnosis. In Metabolomics 2020 - the 16th International Conference of the Metabolomics Society, 27-29 October 2020.

VI. **Ana Rita Lima,** Márcia Carvalho, Susana S. Aveiro, Tânia Melo, M. Rosário Domingues, Catarina Macedo-Silva, Nuno Coimbra, Carmen Jerónimo, Rui Henrique, Maria de Lourdes Bastos, Paula Guedes de Pinho and Joana Pinto. Integration of metabolomics and lipidomics for prostate cancer tissue fingerprinting. In Metabolomics 2021 - the 17th International Conference of the Metabolomics Society, 22-24 June 2021.

Acknowledgements

O espaço limitado desta secção de agradecimentos, seguramente, não me permite agradecer, como devia, a todas as pessoas que me ajudaram e acompanharam durante todos estes anos e que foram indispensáveis para eu conseguir concluir mais esta etapa na minha vida. Por isso, peço desculpa se as palavras forem poucas quando comparadas com todo o apoio que me deram, mas garanto que são acompanhadas de um sincero e profundo sentimento de reconhecimento e agradecimento.

Assim, gostaria de agradecer...

Às minhas orientadoras, esta tese é tanto minha como delas, muito obrigada por orientarem este trabalho, mas sobretudo por todas as vezes que me orientaram a mim própria. Foi uma honra poder trabalhar com todas. Muito obrigada por tudo que fizeram por mim e por tudo o que me ensinaram nos últimos 6 anos (2 relativos ao mestrado e 4 ao doutoramento).

À Doutora Paula Guedes, obrigada pela sua orientação, por todos os momentos em que ouviu as minhas ideias, dúvidas e inseguranças. Pela paciência, incentivo, simpatia e disponibilidade constantes. E sobretudo obrigada por acreditar e confiar em mim, e dar-me esta oportunidade de aprender e de investir no meu sonho.

À Professora Doutora Márcia Carvalho por todo o tempo que dispensou para me ajudar, por todos comentários e sugestões, por ser tão exigente e sobretudo por me incentivar a melhorar constantemente, a procurar respostas, a querer saber mais e fazer melhor. Obrigada por toda a paciência, preocupação e disponibilidade, sem dúvida que a sua orientação fez de mim uma investigadora melhor e mais competente.

À Doutora Joana Pinto por toda a ajuda, por todos os ensinamentos, por todos os conselhos e opiniões, pela paciência e por todas as vezes (e foram muitas) que ‘’invadi’’ o teu gabinete com dúvidas, obrigada pela disponibilidade.

À Professora Doutora Maria de Lourdes Bastos em primeiro lugar por me ter dado a oportunidade de poder integrar esta maravilhosa equipa e ter depositado essa confiança em mim. Obrigada por ter orientado este trabalho, pela sua disponibilidade, por tantas

vezes abdicar do seu tempo de descanso para me ajudar e por todos os conhecimentos que me transmitiu.

À Professora Doutora Carmen Jerónimo e ao Professor Doutor Rui Henrique, assim como à restante equipa do Grupo de Epigenética e Biologia do Cancro do Centro de Investigação do IPO do Porto, por terem colaborado neste projeto.

À Professora Doutora Rosário Domingues, à Doutora Susana Aveiro e à Doutora Tânia Melo por me terem recebido em Aveiro e por toda a colaboração neste projeto.

A todos os meus colegas e restantes colaboradores do Laboratório de Toxicologia da Faculdade de Farmácia da Universidade do Porto por me fazerem sentir sempre bem recebida e em casa. Em especial à Cátia e à Margarida por todas as vezes que me salvaram e por todos os miminhos, à Filipa por me fazer ver sempre o lado ‘’cor-de-rosa’’ de todas as situações e à Sandra por me ter adotado, por todas as conversas, jantares e por toda a “acidez” partilhada.

À Bárbara, ao Brandon, ao Jorge, à Maria, à Renata e à Sofia, por todos os momentos que passámos, por todos os almoços, lanches, jantares e pausas, por todas as gargalhadas que partilhámos, por todas as vezes que me ouviram, e sobretudo por estarem sempre presentes e nunca me deixarem a “apanhar bonés” sozinha. Sem todos vós tenho a certeza que esta jornada não teria tido nem metade do brilho e da alegria que teve. Quando comecei esta jornada éramos simples colegas; agora, que terminou, levo-vos no coração como amigos.

À minha família, em especial à minha Mãe e à avó Maria, definitivamente não há palavras no mundo que cheguem para vos agradecer. Tudo que sou hoje devo-o a vós e só espero ter-vos deixado orgulhosas. Foram e sempre serão o meu porto seguro, obrigada por me apoiarem sempre e por continuarem a acreditar em mim mesmo quando eu não acreditava. Amo-vos.

Por tudo isto e muito mais…
Obrigada a todos!

Abstract

Prostate cancer (PCa) was the second most diagnosed cancer and the fifth leading cause of mortality worldwide in 2020. Since the mid-1990s, PCa mortality rates have decreased due to advancements in treatment and increased screening among men over 50 years of age. However, the currently available screening and diagnostic tools show critical limitations (e.g., false negatives, overdiagnosis and overtreatment), which impairs patient's quality of live. Therefore, the search for new and more precise PCa biomarkers is of utmost importance to assure timely detection and treatment with better patients' quality of life, as well as to reduce the mortality rate. In the last decade, metabolomics has been widely used to unravel the complexity of PCa development and progression, advancing new promising diagnostic and prognostic biomarkers along with new potential therapeutic targets.

The work presented in this thesis aimed to contribute for the identification of metabolite biomarkers for timely detection of PCa to improve the current screening strategies, as well as to get further insights into metabolic characterization of the dysregulations associated with PCa development. For this purpose, advanced analytical tools, namely mass spectrometry (MS) and nuclear magnetic resonance (NMR) spectroscopy-based metabolomic approaches, were applied for analysis of urine and tissue samples collected from PCa patients.

In the first study, a headspace solid-phase microextraction (HS-SPME) gas chromatography-mass spectrometry (GC-MS)-based metabolomics approach was used to investigate the performance of urinary volatilome to unveil novel non-invasive biomarkers for PCa detection. The results revealed a multi-biomarker panel composed by 6 volatile compounds, which was able to identify this type of cancer with 89% sensitivity, 83% specificity and 86% accuracy. Considering the promising results obtained, a new cohort of samples was collected to validate the 6-biomarker panel in a completely independent study using the same methodology. Furthermore, the biomarker panel was improved in terms of organ specificity by comparison of detection performance for other urological cancers (renal cancer and bladder cancer) leading to a candidate 10-biomarker panel which comprised the former panel plus 4 new metabolites. This 10-biomarker panel showed an excellent discriminatory performance to distinguish PCa from cancer-free controls and other urological cancers, with 76% sensitivity, 90% specificity, and 92% accuracy. Indeed, this accuracy outperformed serum prostate specific antigen (PSA), which is currently the most frequently used biomarker for PCa screening.

Considering that tissue is the ideal matrix to disclose specific-organ metabolic changes associated with PCa development, in the next study, matched pairs of tumor and adjacent non-malignant tissues were collected from patients who underwent radical prostatectomy PCa and analyzed through a multi-platform untargeted metabolomics approach. The combination of GC-MS, ^{1}H NMR and hydrophilic interaction liquid chromatography-tandem mass spectrometry (HILIC-MS/MS) allowed a more holistic metabolic profiling of tissue, including amino acids, organic acids, fatty acids, nucleotides, purines, pyrimidine and pyridines, phospholipids, among others. The results showed alterations in the levels of 27 metabolites and 21 phospholipid species associated with PCa development, suggesting dysregulation in 13 metabolic pathways, predominantly in amino acid and glycerophospholipid metabolisms.

Lastly, a dual analytical platform study combining GC-MS and ^{1}H NMR spectroscopy was carried out to obtain a more comprehensive characterization of the urinary non-volatile metabolome of PCa patients. In this study, we were able to associate PCa development and progression with the dysregulations in the levels of 28 metabolites participating in 14 metabolic pathways. These results emphasized the participation of amino acid and energetic metabolisms in PCa development.

In summary, this thesis demonstrated the potential of metabolomics to provide accurate and non-invasive biomarkers for PCa screening as well as for the characterization of metabolic dysregulations associated with PCa development and progression.

Keywords: Metabolomics; biomarkers; prostate cancer; urine; tissue

Resumo

O cancro da próstata (PCa) foi o segundo cancro mais diagnosticado e a quinta principal causa de morte, em todo o mundo, em 2020. Desde meados da década de 1990, a taxa de mortalidade por PCa diminuiu devido aos avanços no tratamento e ao aumento do rastreio em homens com mais de 50 anos. No entanto, as ferramentas de rastreio e diagnóstico disponíveis atualmente apresentam limitações significativas (por exemplo, falsos negativos, sobrediagnóstico e sobretratamento), o que prejudica a qualidade de vida dos doentes. Portanto, a descoberta de biomarcadores mais precisos para o PCa é de extrema importância para garantir a deteção e tratamento adequados, melhorando assim a qualidade de vida dos doentes, e reduzindo a taxa de mortalidade. A metabolómica tem sido amplamente usada na última década na elucidação dos processos metabólicos envolvidos no desenvolvimento e na progressão do PCa, avançando biomarcadores promissores para o diagnóstico e prognóstico, bem como potenciais alvos terapêuticos.

O trabalho apresentado nesta tese teve como objetivo identificar novos biomarcadores para a deteção precoce do PCa, melhorando assim as técnicas de rastreio atuais, bem como aprofundar o conhecimento sobre as desregulações metabólicas associadas ao desenvolvimento do PCa. Para o efeito, realizaram-se estudos metabolómicos em amostras de urina e tecido recolhidas de doentes com PCa, recorrendo a ferramentas analíticas avançadas, nomeadamente espectrometria de massa (MS) e espectroscopia de ressonância magnética nuclear (NMR).

No primeiro estudo, foi aplicada uma abordagem metabolómica usando como metodologia analítica a cromatografia gasosa acoplada à espectrometria de massa (GC-MS) com microextração em fase sólida por *headspace* (HS-SPME), para investigar o potencial do volatiloma urinário revelando novos biomarcadores não invasivos para a deteção do PCa. Os resultados revelaram um painel de biomarcadores constituído por 6 compostos voláteis, capaz de identificar este tipo de cancro com uma sensibilidade de 89%, uma especificidade de 83% e uma precisão de 86%. Tendo em conta os resultados obtidos, foi realizado um estudo independente incluindo amostras recolhidas de doentes com PCa, assim como outros cancros urológicos (cancro renal e cancro de bexiga) para avaliar a especificidade deste painel. Com vista a melhorar a especificidade em relação a outros tipos de cancro, foi necessário introduzir 4 novos metabolitos ao painel anterior dando origem a um painel de 10 biomarcadores que mostrou um excelente desempenho para distinguir doentes com PCa de indivíduos controlo e de doentes com outros cancros urológicos, com sensibilidade de 76%, especificidade de 90% e precisão de 92%. De facto,

a precisão deste painel mostrou ser superior à do teste do antigénio específico da próstata (PSA), que é o biomarcador mais frequentemente usado para rastreio do PCa.

Considerando que o tecido da próstata é a matriz ideal para revelar as alterações metabólicas específicas associadas ao desenvolvimento do PCa, no estudo seguinte foram colhidos pares de tecido prostático tumoral e não maligno adjacente de doentes com PCa submetidos a prostatectomia radical. Estes tecidos foram analisados por meio de uma abordagem não direcionada, usando várias plataformas analíticas. A combinação de GC-MS, ^{1}H NMR e cromatografia líquida de interação hidrofílica acoplada a espectrometria de massa (HILIC-MS/MS) permitiu obter um perfil metabólico mais completo do tecido, incluindo aminoácidos, ácidos orgânicos, ácidos gordos, nucleótidos, purinas, pirimidinas e piridinas, fosfolípidos, entre outros. Os resultados revelaram desregulações nos níveis de 27 metabolitos e 21 espécies moleculares fosfolipídicas no tecido de PCa em comparação com o tecido não maligno adjacente, sugerindo desregulação em 13 vias metabólicas, predominantemente no metabolismo de aminoácidos e glicerofosfolipídios.

Para obter uma caracterização mais abrangente do metaboloma urinário considerando a composição não volátil, foi realizado um estudo combinando GC-MS e ^{1}H NMR em doentes com PCa *vs*. controlos. Neste estudo, foi possível associar o desenvolvimento e a progressão do PCa com as desregulações nos níveis de 28 metabolitos que participam em 14 vias metabólicas. Estes resultados enfatizam a importância do metabolismo dos aminoácidos e do metabolismo energético no desenvolvimento do PCa.

Em conclusão, os resultados obtidos nesta tese demonstraram o potencial da metabolómica para fornecer novos biomarcadores precisos e não invasivos para o rastreio do PCa, bem como para a caracterização das desregulações metabólicas associadas ao desenvolvimento e progressão do PCa.

Palavras-chave: Metabolómica; biomarcadores; cancro da próstata; urina; tecido

Graphical abstract

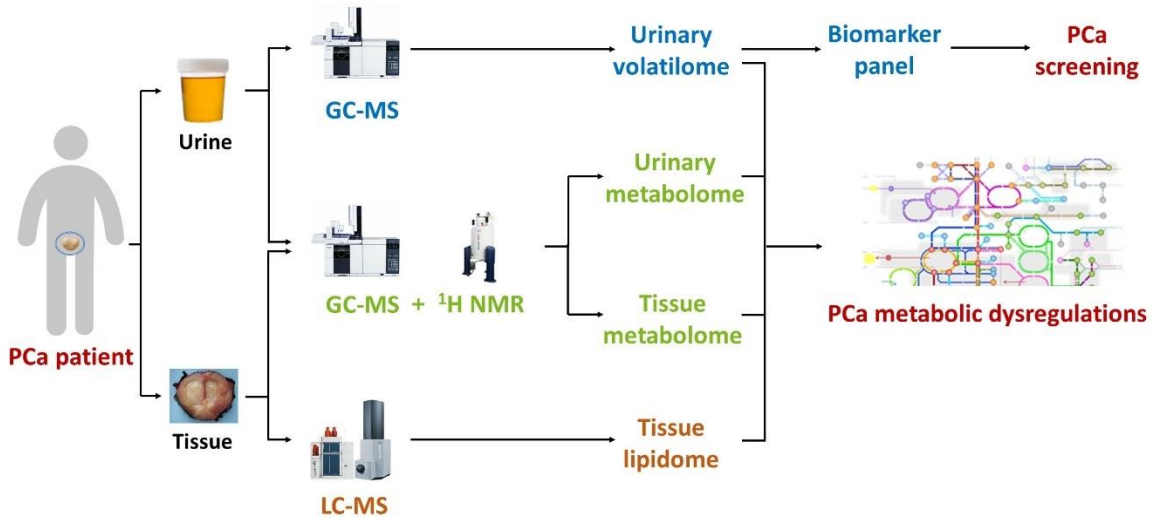

Thesis Layout

This thesis will be divided into six main chapters:

- **Chapter 1 – General introduction**

  In this section, the theoretical principles at the basis of this thesis will be presented, including a brief description of prostate cancer (PCa) diagnosis and prognosis, as well as the state of the art of metabolomics in PCa research, highlighting the major contributions of metabolomics for PCa biomarker discovery and metabolic characterization. The main goal of this section is to provide the knowledge to comprehend the aims and the results obtained in original research studies. This chapter includes two review articles:

  - **Section 1.1:** Ana Rita Lima, Joana Pinto, Filipa Amaro, Maria de Lourdes Bastos, Márcia Carvalho and Paula Guedes de Pinho. Advances and perspectives in prostate cancer biomarker discovery in the last 5 years through tissue and urine metabolomics. *Metabolites*, 2021; 11(3):181. doi: 10.3390/metabo11030181.

  - **Section 1.2:** Ana Rita Lima, Joana Pinto, Maria de Lourdes Bastos, Márcia Carvalho and Paula Guedes de Pinho. NMR-based metabolomics studies of human prostate cancer tissue. *Metabolomics*, 2018; 14, 88. doi: 10.1007/s11306-018-1384-2.

- **Chapter 2 – Aims and scope**

  This section will explain the main goals and objectives intended to be achieved in the scope of this thesis.

✦ **Chapter 3 – PCa biomarker discovery**

This section presents the main results obtained throughout the experimental studies regarding PCa biomarker discovery performed in the scope of this thesis, divided into two original research manuscripts:

- **Section 3.1:** Ana Rita Lima, Joana Pinto, Ana Isabel Azevedo, Daniela Barros-Silva, Carmen Jerónimo, Rui Henrique, Maria de Lourdes Bastos, Paula Guedes de Pinho and Márcia Carvalho. Identification of a biomarker panel for improvement of prostate cancer diagnosis by volatile metabolic profiling of urine. *British Journal of Cancer*, 2019; 121, 857-868. doi: 10.1038/s41416-019-0585-4.

- **Section 3.2:** Ana Rita Lima, Joana Pinto, Carina Carvalho-Maia, Carmen Jerónimo, Rui Henrique, Maria de Lourdes Bastos, Márcia Carvalho and Paula Guedes de Pinho. A Panel of Urinary Volatile Biomarkers for Differential Diagnosis of Prostate Cancer from Other Urological Cancers. *Cancers*, 2020; 12(8):2017. doi: 10.3390/cancers12082017.10.3390.

✦ **Chapter 4 – Metabolic characterization of PCa**

This section presents the main results obtained throughout the experimental studies performed regarding metabolic characterization of PCa, in the scope of this thesis, divided into two original research manuscripts:

- **Section 4.1:** Ana Rita Lima, Márcia Carvalho, Susana S. Aveiro, Tânia Melo, M. Rosário Domingues, Catarina Macedo-Silva, Nuno Coimbra, Carmen Jerónimo, Rui Henrique, Maria de Lourdes Bastos, Paula Guedes de Pinho and Joana Pinto. Comprehensive metabolomics and lipidomics profiling of prostate cancer tissue reveals metabolic dysregulations associated with disease development. Submited to *International Journal of cancer.*

- **Section 4.2:** Ana Rita Lima, Joana Pinto, Daniela Barros-Silva, Carmen Jerónimo, Rui Henrique, Maria de Lourdes Bastos, Márcia Carvalho and Paula Guedes de Pinho. New findings on urinary prostate cancer metabolome through combined GC-MS and ^{1}H NMR analytical platforms. *Metabolomics*, 2020; 16:70. doi: 10.1007/s11306-020-01691-1.

✦ **Chapter 5 – Integrated discussion**

The findings achieved by the original research described in Chapter 3 and 4 will be discussed and interpreted in this section.

✦ **Chapter 6 – Conclusions and future perspectives**

A general conclusion highlighting the major achievements of this thesis, as well as the future perspectives in this area will be presented in this section.

✦ **References**

This section lists all the references of the literature used in the integrated discussion. The review papers and the original manuscripts included in this thesis have their own list of references, according to the guidelines of the publishing journal.

Table of contents

List of figures

Chapter 5

List of tables

Abbreviations

^{1}H NMR	Proton nuclear magnetic resonance spectroscopy
1-MH	1-Methylhistidine
αKG	α-Ketoglutarate
accu	Accuracy
ADPR	ADP-ribose
ADT	Androgen deprivation therapy
AGC	Automatic gain control
AH	Arterial hypertension
Ala	Alanine
AR	Androgen receptor
Asp	Aspartic acid
ATP	Adenosine triphosphate
AUC	Area under the curve
BC	Bladder cancer
BCAAs	Branched-chain amino acids
BCR	Biochemical recurrence
BPH	Benign prostate hyperplasia
BSTFA	N,O-bis(trimethylsilyl) trifluoroacetamide
CCD	Central composite design
CE	Collision energy
Chol	Choline
CoA	Coenzyme A
CTs	Circulating tumor cells
CYP 450	Cytochrome P450
D_2O	Deuterium oxide

DRE	Digital rectal examination
dMPA	1,2-Dimyristoyl-sn-glycero-3-phosphate
dMPC	1,2-Dimyristoyl-sn-glycero-3-phosphocholine
dMPE	1,2-Dimyristoyl-sn-glycero-3-phosphoethanolamine
dMPG	1,2-Dimyristoyl-sn-glycero-3-phospho-(10-rac-) glycerol
dMPS	1,2-Dimyristoyl-sn-glycero-3-phospho-L-serine
DNA	Deoxyribonucleic acid
dPPI	1,2-Dipalmitoyl-sn-glycero-3-phosphatidylinositol
DVB/CAR/PDMS	Divinylbenzene/carboxen/polydimethylsiloxane
EI	Electron impact
e-nose	Electronic nose
ERSPC-RC	European Randomized Study for Screening of Prostate Cancer-Risk Calculator
ES_{SE}	Effect size and standard error
FDA	Food and Drug administration
FH	Fumarate hydratase
fPSA	Free PSA
Fum	Fumaric acid
G6P	Glucose-6-phosphate
G6PD	Glucose-6-phosphate dehydrogenase
GC-MS	Gas chromatography-mass spectrometry
Glu	Glutamine
GLUT	Glucose transporters
GNMT	Glycine N-methyltransferase
GPLs	Glycerophospholipids
GS	Gleason score
HIF1α	Hypoxia-inducible factor 1-subunit alfa

HILIC-MS/MS	Hydrophilic interaction liquid chromatography-tandem mass spectrometry
hK2	Human glandular kallikrein
HR-MAS	High resolution magic angle spinning
HSQC	Heteronuclear single quantum coherence
HS-SPME	Headspace solid-phase microextraction
Hyp	Hypoxanthine
iPSA	Intact PSA
IS	Internal standard
Iso	Isoleucine
Isocit	Isocitrate
IT	Inject time
KI	Kovats indices
LC-MS	Liquid chromatography-mass spectrometry
Leu	Leucine
LPC	Lysophosphatidylcholine
LPCAT1	Lysophosphatidylcholine transferase 1
LPLs	Lysophospholipids
MA	Malic acid
Met	Methionine
MG	Methylglyoxal
MRSI	Magnetic resonance spectroscopy imaging
MS	Mass spectrometry
mTOR	Mammalian target of rapamycin
MVA	Multivariate statistical analysis
NAD	Nicotinamide-adenine dinucleotide
NADP	Nicotinamide-adenine dinucleotide phosphate

NAMPT	Nicotinamide phosphoribosyltransferase
NFκB	Nuclear factor κ B
NMR	Nuclear magnetic resonance spectroscopy
NM	Niacinamide
NO	Nitric oxide
NPSM	N-palmitoyl-D-erythro-sphingosyl-phosphorylcholine
OAA	Oxaloacetate
p2PSA	[-2]proPSA
PB	Prostate biopsy
PC	Phosphatidylcholines
PCA	Principal component analysis
PCa	Prostate cancer
PCA3	Prostate cancer antigen 3
PDMS/DVB	Polydimethylsiloxane/divinylbenzene
PE	Phosphatidylethanolamines
PFBHA	O-(2,3,4,5,6-pentafluorobenzyl)hydroxylamine
PI	Phosphatidylinositols
PIP3	Phosphatidylinositol (3,4,5)-trisphosphate
Phe	Phenylalanine
PHI	Prostate health index
PLs	Phospholipids
PLS-DA	Partial least squares-discriminant analysis
PPP	Pentose phosphate pathway
Pro	Proline
PSA	Prostate specific antigen
PUFA	Polyunsaturated fatty acid
Q^2	Goodness of prediction or prediction power

QCs	Quality control samples
R^2X	Variation explained by the X matrix
R^2Y	Variation explained by the Y matrix
R5P	Ribose-5-phosphate
RC	Renal cancer
RNA	Ribonucleic acid
ROC	Receiver operating characteristic
ROS	Reactive oxygen species
RP	Radical prostatectomy
RT	Retention time
SAH	S-adenosylhomocysteine
SAM	S-adenosylmethionine
SARDH	Sarcosine dehydrogenase
SDH	Succinate dehydrogenase
sens	Sensitivity
SL	Sphingolipids
spec	Specificity
SQ	Single quadrupole
SM	Sphingomyelins
Tau	Taurine
TCA cycle	Tricarboxylic acid cycle
TG	Triglycerides
TOCSY	Total correlation spectroscopy
TQ	Triple quadrupole
Typ	Tryptophan
Tyr	Tyrosine
TSP	3-(Trimethylsilyl)propionic-2,2,3,3-d^4 acid

U	Uracil
UDP-Glu/UDP-Gal	UDP-glucose/UDP-galactose
UV	Unit variance
Val	Valine
VCCs	Volatile carbonyl compounds
VIP	Variable importance to the projection
VOCs	Volatile organic compounds

Chapter 1 - General introduction

This chapter comprises two complementary review papers. The first review paper (**Section 1.1**) introduces the current limitations on PCa diagnosis and management, the fundaments and basis of metabolomics and related subareas, the metabolic dysregulations associated with PCa development and progression, and provides a state of the art of the most recent metabolomic studies on PCa (2015-2020). The second review paper (**Section 1.2**) gives more emphasis on PCa metabolomic studies performed in tissue by NMR spectroscopy (2007-2018).

Section 1.1 - Advances and perspectives in prostate cancer biomarker discovery in the last 5 years through tissue and urine metabolomics

Ana Rita Lima, Joana Pinto, Filipa Amaro, Maria de Lourdes Bastos, Márcia Carvalho, Paula Guedes de Pinho

The article (DOI: 10.3390/metabo11030181) presented in this chapter was published by MDPI, in *Metabolites*, in 2021, and is here presented in the form of "Accepted Manuscript". It is available online on:

https://www.mdpi.com/2218-1989/11/3/181

1.1.1 Abstract

Prostate cancer (PCa) is the second most diagnosed cancer in men worldwide. For its screening, serum prostate specific antigen (PSA) test has been largely performed over the past decade, despite its lack of accuracy and inability to distinguish indolent from aggressive disease. Metabolomics has been widely applied in cancer biomarker discovery due to the well-known metabolic reprogramming characteristic of cancer cells. Most of the metabolomic studies have reported alterations in urine of PCa patients due its non-invasive collection, but the analysis of prostate tissue metabolome is an ideal approach to disclose specific modifications in PCa development. This review aims to summarize and discuss the most recent findings from tissue and urine metabolomic studies applied to PCa biomarker discovery. Eighteen metabolites were found consistently altered in PCa tissue among different studies, including alanine, arginine, uracil, glutamate, fumarate and citrate. Urine metabolomic studies also showed consistency in the dysregulation of fifteen metabolites and, interestingly, alterations in the levels of valine, taurine, leucine and citrate were found in common between urine and tissue studies. These findings unveil that the impact of PCa development in human metabolome may offer a promising strategy to find novel biomarkers for PCa diagnosis.

Keywords: metabolomics; volatilomics; lipidomics; prostate cancer; urine; tissue; biomarkers; metabolic pathways

1.1.2 Introduction

Cancer diseases are one of the most important health problems worldwide, being prostate cancer (PCa) one of the most prevalent. Indeed, PCa is globally the second most frequently diagnosed male malignancy and the fifth leading cause of cancer, with more than 1 000 000 new cases and more than 350 000 deaths, each year [1]. PCa is a heterogeneous disease [2] with a broad spectrum of aggressiveness, going from indolent PCa, which is a non-life-threatening cancer, to metastatic PCa with a five-year survival of 28% [3].

Currently, PCa screening is based in serum prostate specific antigen (PSA) test and digital rectal examination (DRE) [4], whereas prostate biopsy (PB) is mandatory for a final diagnosis [5]. High levels of PSA (> 4 ng/mL) are considered a sign of PCa [4]. However, this biomarker shows important limitations [6], due to its reduced accuracy (accu) (62–75%) [7], sensitivity (sens) (20.5%), specificity (spec) (ranging from 51 to 91%) [4,8] and area under the curve (AUC) (varying from 0.53 to 0.83) [7]. These low performance values can be due to interference from other diseases, like benign prostate hyperplasia (BPH) or prostatitis, that may also lead to an increase in serum PSA levels [2,6]. Furthermore, PSA testing is unable to distinguish indolent from aggressive disease, leading to unnecessary PB [2]. As matter of fact, about 70% of the PB performed due to high levels of PSA do not detect PCa and could be avoided with a more accurate PCa screening test [6]. PB is an invasive procedure that is associated to several adverse effects, like haemoejaculate, haematuria, fever, pain and haematochezia. Although more rare, other complications, like bleeding, acute urinary retention, local infection, sepsis, vasovagal syncope and erectile dysfunction, can also occur as a consequence of PB [9]. Moreover, PB can fail to diagnose over 30% of clinically significant PCa (non-indolent). On the other hand, PB can also lead to overdiagnosis and overtreatment of indolent PCa, that will not bring advantages to the patients' health and can negatively affect patients' quality of life [5].

PCa can be curable if diagnosed when the development is still in its early stages [3]. For localized PCa, the gold standard treatment is radical prostatectomy (RP). However, around 40% of the patients will develop biochemical recurrence (BCR) after RP, which indicates PCa progression [10]. After RP, levels of PSA decrease until undetectable, and the resurgence of high PSA levels is the first indication of BCR. The ideal PSA cut-off to define BCR is still controversial [10], with the American Urological Association and the European Association of Urology defining BCR for a serum PSA ≥ 0.2 ng/ml [10,11]. For aggressive PCa, one of the most frequently used treatments is androgen deprivation therapy (castration). However, the treatment can be hampered by the development of resistance to castration [12].

Considering the limitations of the currently available PCa diagnostic tools, the scientific community has performed massive efforts to discover new biomarkers for PCa detection. These biomarkers include several derivatives of PSA, like the prostate health index (PHI) and the 4Kscore tests. PHI test combines the PSA precursor isoform that circulates uncomplexed [-2]proPSA (p2PSA), free PSA (fPSA) and total PSA, through the formula PHI = (p2PSA/fPSA) x √(tPSA) [13,14]. Higher levels of PHI are correlated with PCa [13,14] and this test obtained FDA approval for men with PSA between 2.5-10 ng/ml and negative DRE [2]. The 4Kscore test includes total PSA, fPSA, intact PSA (iPSA), and human glandular kallikrein (hK2), a protein similar to PSA [2]. Despite the promising results, 4Kscore test did not obtain FDA approval [2].

With the raising of "omics'' technologies, other biomarkers for PCa detection have been proposed, such as prostate cancer antigen 3 (PCA3), which is a biomarker coming from transcriptomic methodologies. PCA3 gene encodes a non-coding RNA which is specific of prostate and is increased in urine of PCa patients collected after DRE. Despite the controversy around the ideal cut-off for the levels of this biomarker, this test obtained FDA approval for men with high PSA levels and/or positive DRE and/or previous negative PB [15,16]. Prostarix test, which is also performed in urine after DRE, was developed using metabolomic approaches and detects four amino acids [17], namely sarcosine, glycine, alanine and glutamate [13,16]. This test has not yet obtained FDA approval [13], but it is commercially available and is recommended for men with persistent PSA increase and previously negative PB [13,17].

Despite such great efforts to discover new biomarkers for PCa detection and the promising perspectives, no biomarker has so far been able to replace PSA in clinical practice for PCa screening, highlighting the need to pursue research in this field. In this review, we explore the potentialities and challenges of metabolomics for PCa biomarker discovery. In addition, we update our earlier review [18] by presenting the most recent metabolomic studies performed in urine and tissues from PCa patients aimed at evaluating metabolic pathways perturbed in this disease and the altered metabolites as potential biomarkers for PCa detection. For this, a search was conducted in the PubMed database for articles published between January of 2015 and December 2020, using the keywords "metabolomics", "prostate cancer", "biomarker", "urine" or "tissue". A total of twenty-five studies were included, of which twelve were performed in PCa tissue samples, twelve in PCa urine samples and one study included both matrices.

1.1.3 Metabolomic approaches to biomarker discovery

Nicholson et al. (1999) defined metabonomics as “the quantitative measurement of the dynamic multiparametric metabolic response of living systems to pathophysiological stimuli or genetic modification” [19]. Nowadays, the term metabonomics is often used interchangeably with the terms metabolic phenotyping, metabolic profiling, or simply metabolomics in the context of the comprehensive analysis of all metabolites of a biological sample representative of an organism or cell. Metabolomics is the last “omic” platform in the “omics” cascade (genomics – transcriptomics – proteomics – metabolomics), and it focus in the study of small molecules (<1500 Da) [20] in several complex matrices like serum, saliva, exhaled air, urine, tissue, among others [21]. When compared with other omics, metabolomics shows important advantages: i) the dynamic feature of metabolome, once it modifies rapidly in response to changes in cell status, allowing a continuous evaluation of the cell state [22]; ii) minor changes in gene expression or protein synthesis are translated into major alterations in metabolite levels [23]; iii) the response of metabolome to pathophysiological alterations is much more sensitive than gene or protein response [24]; iv) the alterations in metabolome are closely related with the observed phenotype; v) the levels of several metabolites can simultaneously be measured, allowing to establish a pattern of alterations associated with an specific pathophysiological state [22]; and vi) allows to define patterns of disease progression [25].

Human metabolome comprises metabolites of low molecular weight from very different chemical families, such as amino acids, lipids, nucleotides, carbohydrates, organic acids, among others. They are present in a wide range of concentrations and have distinct physicochemical characteristics [26]. When a metabolomics study is designed, the selection of the analytical technique is a critical step, once this choice will restrict the metabolites detected and consequently the obtained results [27]. This selection needs to take into consideration the characteristics of the analytical technique like sensitivity, resolution, limits of detection of the instrumental technique [27], but also the characteristics of the samples and of the metabolites of interest, e.g., metabolite physicochemical properties and abundance [27,28].

Currently, the majority of the metabolic studies are performed using mass spectrometry (MS), frequently coupled with a separation technique like gas or liquid chromatography (GC-MS or LC-MS), and nuclear magnetic resonance spectroscopy (NMR) [26,29]. MS and NMR show several differences, including in the detected range of concentrations, namely, MS allows the detection of metabolites in concentrations ranging from picomolar (pM) to millimolar (mM) [30] and NMR from micromolar (μM) to millimolar (mM) [31]. Table 1.1

summarizes the advantages and limitations of the three analytical techniques (GC-MS, LC-MS and NMR), for metabolomic studies. As depicted in table 1.1, none of these methods are able to cover the entire metabolome. For example, GC-MS is only suitable for the analysis of thermally stable compounds, such as volatile organic compounds (VOCs) [26]. In turn, LC-MS is used for profiling of compounds with medium and low polarities (reversed-phase LC) and polar compounds (hydrophilic-interaction LC), but the datasets generated are complex, spectrometer dependent, and require additional MS/MS experiments, as well as spiking with authentic standards, in order to perform metabolite annotation and identification [26,32,33]. NMR shows a lower sensitivity, which compromise the detection of low abundance metabolites. Importantly, due to NMR non-destructive nature, the samples can be recovered after analysis and used in complementary studies (e.g., MS analysis) to obtain a more comprehensive characterization of the metabolome [34]. Indeed, the combination of more than one analytical platform is desirable to allow a more comprehensive analysis of a sample metabolome [26,29].

Table 1.1: Main advantages and limitations of gas or liquid chromatography coupled with mass spectrometry (GC–MS or LC–MS), and nuclear magnetic resonance spectroscopy (NMR) in metabolomic studies.

Analytical platform	Advantages	Limitations
GC-MS	-Ideal for volatile organic compounds detection [26] -High sensitivity and resolution [26] -Available database for metabolite identification [26] -High peak capacity to cover a wide range of concentrations [22] -Small amounts of sample used [32] -High dynamic range, selectivity and throughput [26,29,35] -Retention times are highly reproducible [22,26]	-Only suitable for thermally stable compounds [26] -Derivatization step is required for nonvolatile compounds [26] -Formation of new compounds due the derivatization step [28] -Destructive nature [32]

Analytical platform	Advantages	Limitations
LC-MS	-Detects a wide range of metabolites, including conjugates, of varying molecular weight and different natures (hydrophilic and hydrophobic compounds) [22,26] -Easy sample preparation [26,28] -Does not require derivatization [22] -Small amounts of sample used [32]	-Destructive nature [32] -MS/MS experiments are usually required for metabolite identification, which implies additional experimental time [33]
NMR	-Relatively high throughput and efficiency [22,36] -High reproducibility and selectivity [34,37] -Non-destructive nature [22,34] -Analysis of liquid and solid matrices [34] -Easy sample preparation [37] -Provides information about chemical structure, chemical environment and molecular interactions [34,36]	-Low sensitivity [34,37] -High costs [22] -Not optimal for targeted analysis [37] -Peak overlapping which difficult quantification [34]

Metabolomic studies can follow two distinct approaches, namely the untargeted or the targeted approach. In the first, the goal is to cover the maximum of the metabolome detecting as many metabolites as possible in a matrix and is frequently denominated as hypothesis generation [23]. In the second, a single metabolite or a group of metabolites (e.g., metabolites from a specific metabolic pathway) are previously selected and all the study is designed to detect and quantify these metabolites. This approach can be applied to validate the results obtained through an untargeted approach and is called hypothesis-driven [23,25].

Regarding PCa metabolomic studies, two main goals are recognized: i) the discovery of biomarkers with high sensitivity and specificity for PCa timely detection and ii) to understand the metabolic basis of PCa pathogenesis identifying altered metabolic pathways in consequence of PCa development and progression [25]. Nevertheless, the potential application of metabolomic studies is not limited to these two main goals, once metabolomic

studies can also be applied to study the effectiveness of treatments, as well as the mechanism of action of therapeutic drugs and the mechanism of drug resistance or contribute to achieve the goal of personalized medicine [38].

Over the years, several independent subareas emerged from metabolomics, like volatilomics, lipidomics, among others. Volatilomics is based on the analysis of VOCs, like aldehydes, ketones, alcohols, hydrocarbons or aromatic compounds [39], that are produced by human body and released into breath, blood, sweat, urine, feces or saliva [39,40]. All VOCs share some physicochemical characteristics, such as low molecular weight and low boiling point and/or elevate vapor pressure in normal conditions [41]. The interest to investigate VOCs as potential cancer biomarkers gained strength after the observation that dogs were able to ‘’smell’’ urine or skin samples of cancer patients with high sensitivity and specificity, indicating that the composition of VOCs is different in cancer individuals [42-44]. VOCs are end products of human biological activity and their composition in biological samples can reflect pathological processes [40], alterations in normal biochemical pathways and/or a response to a damage or disease. Indeed, cancer development and progression can lead to the production of new VOCs and/or to change their concentration [41], making them suitable candidates to cancer biomarkers [39]. One of the greatest advantages of VOCs as biomarkers is the possibility to easily, inexpensively and quickly detect them in clinical point of care through the most recent technological developments in biological sensors (e.g., electronic noses (e-nose)) [39].

Lipidomics is the subarea of metabolomics focused on the qualitative and quantitative profile of the lipid species in biological samples [45]. The knowledge of lipid metabolism is crucial to understand cancer development and progression for several reasons: i) *de novo* synthesis provide phospholipids for cancer cell proliferation, ii) fatty acid β-oxidation is important in energetics and redox homeostasis, iii) lipids play an important role in signaling pathways [46] and, finally, iv) lipids are extremely dynamic and can reflect physiological, pathological, and environmental alterations [47]. For these reasons, the interest to study the lipid profile of cancer cells has increased in the last years. It is estimated that mammalian cells comprise around 10 000 individual lipid species [48]. These lipids can be classified into different classes: i) fatty acids, ii) glycerophospholipids (GPLs), iii) glycerolipids (e.g. triglycerides (TG)), iv) saccharolipids, v) sphingolipids (SL) and vi) sterols. Each class of lipids show different biological functions. For instance, TG are important for energy storage, while sterols are key elements in cellular membrane and have also hormonal functions [49]. GPLs and SL are important components of cellular membranes and lysophospholipids (LPLs) (a subclass of GPLs) are important molecules for cellular signaling. These three

classes (GPLs, SL and LPLs) are the most frequently studied in cancer lipidomic studies. GPLs can still be divided into phosphatidylcholine, phosphatidylethanolamine (major components of human cellular membranes), phosphatidic acid, phosphatidylglycerol, phosphatidylinositol and phosphatidylserine, considering the molecular structure of these molecules. SLs can also be divided into several subclasses like ceramides, sphingomyelins, among others [45]. This summary reflects the importance and the complexity of the lipidome and justify that lipidomics comprises an independent subarea of metabolomics. Furthermore, several studies revealed that cancer cells show alterations in lipidome fingerprint demonstrating the potential of lipids as biomarkers and/or therapeutic targets [46,49].

1.1.4 The metabolic phenotype of prostate cancer

It is well established that cancer cells suffer profound metabolic alterations that are indispensable for cancer development and progression [50]. One of the most well described metabolic alterations of cancer cells is the Warburg effect, which is characterized by a change in the preferential pathway to produce energy. Indeed, cancer cells preferentially produce ATP via aerobic glycolysis, even in the presence of oxygen, while normal cells produce ATP through oxidative phosphorylation [50,51]. This shift leads to an increase in glucose uptake and in lactate secretion [50,52]. The increase in lactate levels seems to play an important role in cancer development and progression [50]. Lactate can be utilized as fuel for oxidative metabolism, metabolized into alanine and glutamine and can also intervene in cancer cell mobility, immune escape and angiogenesis [50].

To comprehend how the Warburg effect impacts PCa cell metabolism, it is important to revisit the peculiar metabolic phenotype of normal prostate cells. Contrarily to other human cells, prostate cells favor citrate accumulation instead of citrate oxidation for energy production through tricarboxylic (TCA) cycle, also known as Krebs cycle or citric acid cycle [53]. Prostate cells have an increase in the zinc transporter ZIP1 and, consequently, zinc accumulates in prostate tissue [52]. The high levels of zinc are responsible for the inhibition of m-aconitase, which is the enzyme responsible for citrate oxidation in TCA cycle [53]. However, one of the first metabolic alterations associated with PCa development is the loss of cell ability to accumulate zinc and subsequent reduction of citrate levels in PCa cells [53]. Indeed, there is an increment of citrate oxidation in TCA cycle to produce energy in PCa cells [52,53]. For this reason, the Warburg effect and consequent increase in aerobic glycolysis is described mainly in advanced stages of PCa, where the increase in glycolytic

pathway is associated with metastases formation and thereafter to a poor prognosis [52,54]. Furthermore, citrate can also be used in PCa cell to produce acetyl-coenzyme A (acetyl-CoA) (important for fatty acids and cholesterol synthesis) and oxaloacetate (amino acid precursor) [55] (Figure 1.1). Beyond citrate accumulation, normal prostate cells can also accumulate polyamines, such as spermine and spermidine once they are important components of prostatic secretions [56]. Polyamine levels also decrease, similarly to citrate, during cancer development and progression (Figure 1.1). Indeed, this reduction in polyamine levels may promote PCa cell survival by preventing apoptosis [55,56].

Pentose phosphate pathway (PPP) is also altered in PCa cells, once the levels of glucose-6-phosphate dehydrogenase (a key enzyme in PPP) are increased through androgen receptor (AR) signaling [54], which is essential for PCa progression. AR signaling also promotes glycolysis and anabolism [55]. As previously referred, one of the most frequently used treatments for aggressive PCa is androgen deprivation therapy, which is associated to the development of castration-resistant state and consequently alterations in the lipid profile, and to a worst prognosis [55,57]. Furthermore, PCa cells show the ability to synthesize sterols, highlighting the importance of androgen signaling in PCa [57] (Figure 1.1).

Alterations in different amino acids, such as glutamine, have been associated with PCa and other cancers [50,52]. Glutamine is one of the most abundant amino acids in human plasma and has important roles in human metabolism [54], as it can be converted in glutamate, and subsequently be transformed in α-ketoglutarate, an intermediate in TCA cycle [50,52]. This amino acid can also be used by cancer cells for acetyl-CoA production [54], for fatty acid synthesis [52] and as a nitrogen and carbon donor for nucleotide, lipids and protein synthesis [50,54]. The glutamate resulting from glutamine is an essential substrate for glutathione synthesis, and therefore important for the protection of the cells against oxidative damage [50] (Figure 1.1). Arginine is an important amino acid involved in PCa metabolism. Arginine is converted by PCa cells in glutamine and/or proline [52]. The increase in proline levels is needed to the maintenance of the levels of pyridine nucleotides [54]. Arginine has also an important role in nitric oxide (NO) production [52] (Figure 1.1).

Sreekumar et al (2009), reported higher levels of sarcosine in urine of PCa patients, which was a milestone in PCa metabolomics [58], but its importance as potential PCa biomarker was refuted in the following years [59-61]. Sarcosine is synthesized from other amino acid, glycine, and vice versa. This reaction can be linked to methionine cycle, and the produced methionine can be up-taken to folate cycle. The combination of these two cycles is referred frequently as one-carbon metabolism. One-carbon metabolism fuels

building blocks for purines and thymidylates synthesis, which are essential for DNA synthesis and repair [62,63]. Methionine cycle also plays a role in polyamines and glutathione synthesis [54,63] (Figure 1.1).

Another prominent characteristic of a cancer cell is its ability to proliferate constantly. Lipids are major components of cellular membranes, so alterations in lipids, and in choline or choline derivative metabolites, have a very important role in cancer cells proliferation [53,54]. Furthermore, lipids are also essential as energy resource, for energy storage and for intracellular signaling [54]. So, increase in *de novo* fatty acids synthesis is an initial event in PCa development, which is stimulated by androgen signaling [52], as well as the increase in fatty acids oxidation to produce energy [52,54]. The importance of lipogenesis in PCa is patent in the increase of the expression of lipogenic and lipid-modifying enzymes, occurring in PCa [52,54] and by the accumulation of triglycerides, cholesterol esters and phospholipids (phosphatidylcholine), mainly in aggressive PCa [53]. Furthermore, metastatic PCa cells also show an upregulation of acetyl-CoA synthetase 2, allowing PCa cells to produce acetyl-CoA (essential for fatty acids synthesis) from acetate, while normal cells produce acetyl-CoA essentially from glucose and glutamine [54] (Figure 1.1). Moreover, PCa cells show the ability to take up exogenous lipids and to synthetize and mobilize lipids storage in other cells, like adipocytes [54]. From this brief explanation, it is reasonable to infer that the study of the metabolic signature of cancer cells has an enormous potential in the discovery of new biomarkers, as well as to elucidate cancer pathophysiological mechanisms, which can be used to define new therapeutic strategies.

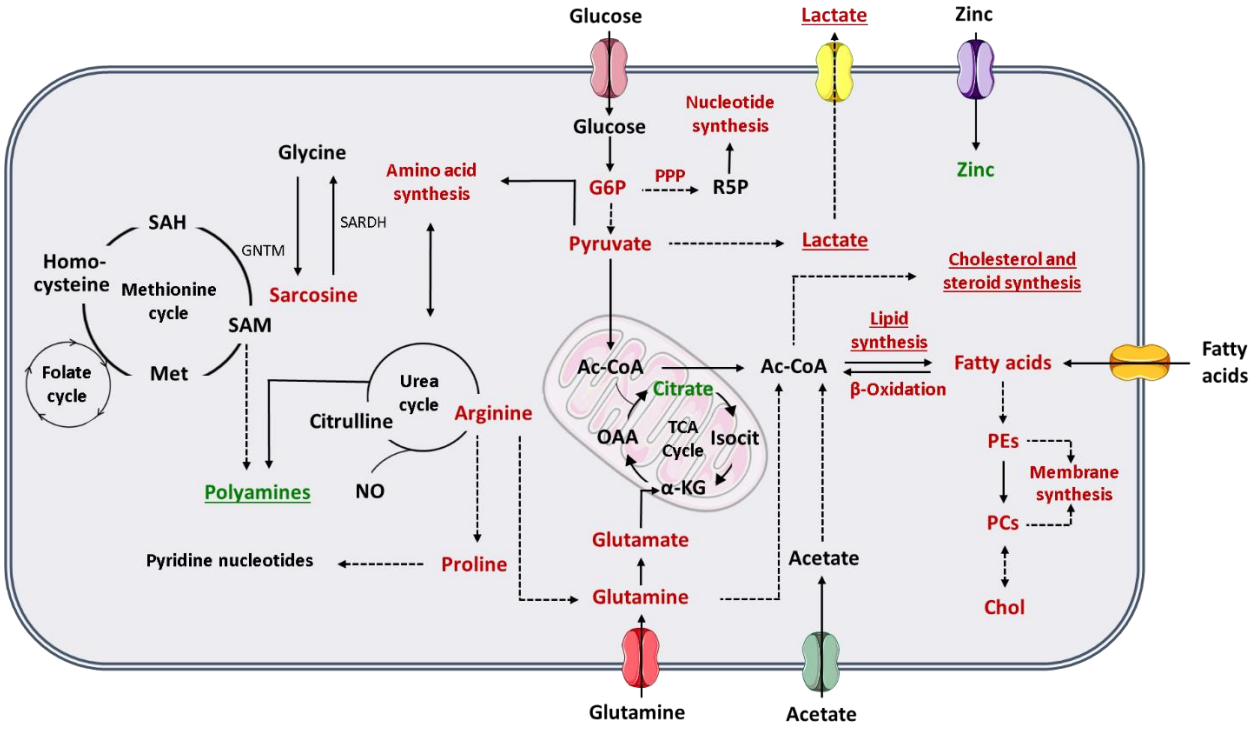

Figure 1.1: Schematic representation of the metabolic phenotype of prostate cancer cells. Red indicates increase in either metabolites or metabolic pathway flux and green indicates decrease in either metabolites or metabolic pathway flux. Underlined indicate changes especially important in advanced PCa. The dashed lines represent multiple steps reactions. (α-KG, alpha-ketoglutarate; Ac-CoA, acetyl-coenzyme A; Chol, choline; G6P, glucose-6-phosphate; GNMT, glycine N-methyltransferase; Isocit, isocitrate; Met, methionine; NO, nitric oxide; OAA, oxaloacetate; PCs, phosphatidylcholines; PEs, phosphatidylethanolamines; PPP, pentose phosphate pathway; R5P, ribose-5-phosphate; SAH, S-adenosylhomocysteine; SAM, S-adenosylmethionine; SARDH, sarcosine dehydrogenase; TCA cycle, tricarboxylic acid cycle).

1.1.5 Tissue metabolomic studies

The collection of tissue samples is very invasive, hampering their use for PCa screening. However, the study of the tissue metabolome has important advantages, once this is the ideal matrix to establish which metabolic alterations are specific to PCa development and progression. Furthermore, tissue studies have been performed using matched tumoral and non-tumoral samples from the same individual, thus minimizing the contribution of confounding factors (e.g., age, comorbidities, lifestyle).

Thirteen metabolomic studies performed in PCa tissue samples were published in the last 5 years, including two lipidomic studies. Table 1.2 summarizes the study design and

main outcomes obtained in those studies. Overall, a total of 98 different metabolites were associated with PCa, indicating that PCa is related with dysregulations in 32 different metabolic pathways (Table 1.2). Interestingly, 18 metabolites were found to be common among the included studies (Figure 1.2). It is important to note that these studies were performed under different analytical conditions, with different sample selection criteria and using different statistical approaches, foreseeing difficulties to compare results across studies. The fact that these metabolites were found common in the various studies, highlights their importance in PCa metabolism and their potential as specific PCa biomarkers.

Table 1.2: Metabolomic studies performed in tissue samples from PCa patients in the last five years (2015-2020).

PCa group	Control group	Analytical platform	Statistical methods	Altered metabolites (direction of variation)	Dysregulated metabolic pathways	Candidate biomarkers	Ref.
n=31	*n*=14 (benign adjacent tissue)	HR-MALDI-IMS MS/MS	Univariate and Multivariate Cox Regression Analyses	1. LPC (16:0) (-) 2. SM [(d18:1/16:0) (-) Predictor of biochemical recurrence: 1. LPC (16:0) (-)	1. FAs *de novo* synthesis and remodeling pathway (Lands' pathway) 2. Arachidonic acid metabolism	LPC (16:0)	[64]
n=25 Validation set 1: *n*=19 Validation set 2: *n*=12	*n*=25 (normal adjacent tissue) Validation set 1: *n*=17 (normal adjacent tissue) Validation set 2: *n*=12 (normal adjacent tissue)	LC-MS	PCA OPLS-DA Model performance: Sens: 85% Spec: 83- 91% AUC: 0.90	1. Adenosine monophosphate (-) 2. Spermidine (+) 3. Uracil (+)	1. Purine metabolism 2. Polyamines synthesis 3. Pyrimidine metabolism	Adenosine monophosphate (AUC: 0.82) Spermidine (AUC: 0.85) Uracil (AUC: 0.91)	[65]
n=25 Validation set: *n*=51	*n*=25 (normal adjacent tissue) Validation set: *n*=19 (BPH)	LC-MS	PCA PLS-DA Model performance: AUC: 0.90-0.94 External validation: AUC: 0.84-0.91	1. PCs (alkyl/acyl-PCs, PC-O) (-); PEs (alkenyl/acyl-PEs, plasmalogens, PE-P) (-); Free saturated FAs (-); Diacyl-PC (+); Diacyl-PE (+); Free mono- and poly-unsaturated FAs (+) 2. CEs (+); Cholesteryl oleate (+)	1. Lipogenesis, lipid uptake and phospholipids remodeling 2. Cholesterol metabolism	Cholesteryl oleate (AUC: 0.91(PCa *vs*. normal adjacent tissue) and AUC: 0.96 (PCa *vs*. BPH))	[66]

PCa group	Control group	Analytical platform	Statistical methods	Altered metabolites (direction of variation)	Dysregulated metabolic pathways	Candidate biomarkers	Ref.
n=25 Validation set: *n*=51	*n*=25 (normal adjacent tissue) Validation set: *n*=51 (benign adjacent tissue) + *n*=16 (BPH)	LC-MS	PCA PLS-DA	1. Choline (+); Citicoline (+) Nicotinamide adenine dinucleotide (+); S-Adenosylhomoserine (+); 5-Methylthioadensine (+); S-Adenosylmethionine (+); Nicotinamide mononucleotide (+); Nicotinamide adenine dinucleotide phosphate (+); Adenosine (-); Uric acid (-) 2. D-Glucosamine 6-phosphate (+); N-Acetyl-D-glucosamine (+); N-Acetyl-D-glucosamine 6-phosphate (+); UDP-Acetyl-glucosamine (+) 3. 2-Aminoadipic acid (+); Saccharopine (+); Trimethyllysine (+); Carnitine C4-OH (+); Carnitine C14:2 4. Sphingosine (+) 5. Pantothenic acid (+) 6. Dehydroepiandrosterone sulfate (-); Etiocholanolone sulfate (-) 7. Phenylacetylglutamine (-)	1.Cysteine and methionine metabolism; NAD metabolism; phospholipid membrane metabolism 2. Hexosamine biosynthesis 3. Lysine degradation; β-oxidation of FAs 4. Sphingolipid metabolism 5. CoA homeostasis 6. Dihydro-testosterone synthesis 7. Unavailable	Sphingosine (AUC: 0.81-0.87)	[67]
n=34 (ERG_{high} PCa)	*n*=30 (ERG_{low} PCa)	HR-MAS ^{1}H-NMR	PCA PLS-DA Model performance: Sens: 79% Spec: 74% Accu: 77%	<u>ERG_{high} PCa *vs*. ERG_{low} PCa</u> 1. Citrate (-) 2. Spermine (-)	1. TCA cycle 2. Polyamines synthesis	Citrate and spermine ERG_{high} for stratification	[68]

PCa group	Control group	Analytical platform	Statistical methods	Altered metabolites (direction of variation)	Dysregulated metabolic pathways	Candidate biomarkers	Ref.
n=6 (patients treated with Degarelix) + *n*=7 (untreated)	*n*=10 (benign from untreated patients)	HR-MAS ^{1}H-NMR	PCA OPLS-DA	Untreated patients: 1. Lactate (+); Alanine (+) 2. Total choline (+) Patients treated with Degarelix: 1. Lactate (-) 2. Total choline (-)	1. Energetic metabolism 2. Choline metabolism; Phospholipid membrane metabolism	Lactate Total choline	[69]
n=50 (patients that developed recurrence after prostatectomy)	*n*=60 (patients that did not develop recurrence after prostatectomy)	HR-MAS ^{1}H-NMR	PLS-DA Model performance: Sens: 92% Spec: 92% Accu: 92%	Increased risk of recurrence 1. (Total-choline + creatine)/spermine (+); (Total-choline + creatine)/citrate (+) 2. Spermine (-) 3. Citrate (-)	1. Choline metabolism; Phospholipid membrane metabolism 2. Polyamines synthesis 3. TCA cycle	Spermine Total-choline + creatine/ spermine	[70]
n=21 Validation set: *n*=50	*n*=21 (benign adjacent tissue) Validation set: *n*=50	GC-MS	OSC-PLS-DA	1. Fumarate (+); Malate (+); Succinate (+); 2- Hydroxyglutaric acid (+); Alanine (+); Glycerol-3-phosphate (+) 2. 11-Eicosenoic acid (+); Docosanoic acid (+); Eicosanoic acid (+) 3. Glycerolipids (+); *Myo*-inositol (+) 4. Uracil (+) 5. Proline (+)	1. Energetic metabolism (TCA cycle) 2. FAs metabolism 3. Membrane metabolism 4. Pyrimidine metabolism 5. Amino acid metabolism	-	[71]
n=199 Validation set *n*=166	*n*=179 (benign adjacent tissue) *n*=15 (BPH) + *n*=14 (cancer-free patients) Validation set *n*=159 (benign adjacent tissue)	HR-MAS ^{1}H-NMR	Linear Regressions	1. *Myo*-inositol (+); Phosphocholine (+); Glycerophosphocholine (+) 2. Lactate (+); Taurine (-) 3. Histidine (+) 4. Phenylalanine (-); Glutamate (+)	1. Membrane metabolism 2. Energetic metabolismo 3. Histidine metabolism 4. Amino acid metabolism	*Myo*-inositol	[72]

PCa group	Control group	Analytical platform	Statistical methods	Altered metabolites (direction of variation)	Dysregulated metabolic pathways	Candidate biomarkers	Ref.
n=13 (American African population) + n=13 (Caucasian American population)	*n*=12 (American African population) + n=9 (Caucasian American population) (benign adjacent tissue)	GC-FID ESI-MS	Generalized linear model	Saturated total FAs (+); Arachidic acid (+); Myristic acid (+) Monounsaturated total FAs (+); Polyunsaturated FAs (+); n-6 Total FAs (+); n-3 Free FAs (+)	Lipid metabolism	Arachidic acid (sens: 78%; spec: 75%; accu: 80%) (American African population) Myristic acid (sens: 85%; spec: 89%; accu: 98%) (Caucasian American population)	[72]
n=13	*n*=13 (benign adjacent tissue)	LC-MS CE-MS	OPLS-DA	1. Cysteine (+); Lysine (+); Methionine (+); Phenylalanine (+); Tyrosine (+); Branched-chain amino acids (leucine, isoleucine, and valine) (+); Fumarate (+) 2. Glycerophospholipids (+) 3. Fructose 6-phosphate (-); Fructose 1,2-biphosphate (-); Pyruvate (-); Citrate (-); *cis*-aconitate (-); Isocitrate (-) 4. N-Acetylglucosamine (+); N-Acetylglucosamine 1-phosphate (+), N-acetylglucosamine 6-phosphate (+); Galacturonate 1-phosphate (+) 5. Aspartate (+); Argininosuccinate (+); Arginine (+); Proline (+); Fumarate (+)	1. Amino acid metabolism 2. Lipid metabolism 3. TCA cycle 4. Hexosamine pathway 5. Urea cycle	Fumarate Citrate Isocitrate	[74]

PCa group	Control group	Analytical platform	Statistical methods	Altered metabolites (direction of variation)	Dysregulated metabolic pathways	Candidate biomarkers	Ref.
n=58	*n*=18 (BPH)	^{1}H-NMR	PCA PLS-DA	1. Creatine (-); Creatinine (-); Glutamate (+); Glutamine (+); Formate (+); Tyrosine (+); Uridine (+) 2. Citrate (-) 3. Trimethylamine (+)	1. Amino acid metabolism 2. TCA cycle 3. Membrane metabolism	Citrate Glutamine	[75]
n=70 43 GS (3+3) 16 GS (3+4) 10 GS (4+3) 1 GS (4+4)	*n*=59 (benign adjacent tissue)	^{1}H HR MAS NMR ^{1}H/^{31}P NMR LC-MS	PCA OPLS-DA	PCa *vs*. Benign 1. Citrate (-); Succinate/ malate (+); Fumarate (+) 2. Putrescine (-); Spermidine (-) Spermine (-) 3. Glutamate (+) 4. Uracil (+) 5. Hypoxanthine (+); Inosine (+) 6. α-Glucose (-) 7. SM (-) 8. NAD^{+} (-) 9. Phosphocholine (+); PE (+); LPC (-); 10. Arginine (+); 11. Docosapentanoic acid (22:5) (+); Oleic acid (18:1) (+); Linoleic acid (+); Docosahexaenoic acid (22:6) (+); Maleic acid (+);	1. TCA cycle 2. Polyamines synthesis 3. Glutamate metabolism 4. Pyrimidine metabolism 5. Purine metabolism 6. Glycolysis 7. Sphingolipid metabolism 8. Nicotinate and nicotinamide metabolism 9. Glycerophosphocholine metabolism; Phospholipid membrane metabolism 10. Urea cycle 11. Free FAs oxidation 12. Branched-chain amino acid metabolism 13. Inositol metabolism 14. Propanoate metabolism 15. Aminoacyl-tRNA biosynthesis	Phosphocholine Glutamate Hypoxanthine Arginine α-Glucose	[76]

PCa group	Control group	Analytical platform	Statistical methods	Altered metabolites (direction of variation)	Dysregulated metabolic pathways	Candidate biomarkers	Ref.
				GS ≥7 *vs* GS 6 3. Glutamate (+) 5. Hypoxanthine (+) 6. α-Glucose (-) 7. Sphingosine (+) 9. Glycerophosphorylcholine (+); Phosphocholine (+) 10. Arginine (+) 11. Hexanoylcarnitine (+) 12. Tyrosine (+); Valine (+); Phenylalanine (+) 13. Ascorbate (+) 14. 2-Hydroxybutyrate (+) 15. Lysine (+); Threonine (+)			

Notes: (+) indicates increased levels in PCa, (-) indicates decreased levels in PCa; (-); the numbering of the column Altered Metabolites is related with the numbering of the column Dysregulated metabolic pathways. Abbreviations: ^{1}H-NMR, proton nuclear magnetic resonance spectroscopy; ^{31}P NMR, phosphorus-31 nuclear magnetic resonance spectroscopy; accu, accuracy; AUC, area under the curve; BPH, benign prostatic hyperplasia; CE-MS, capillary electrophoresis-mass spectrometry; CEs, cholesteryl esters; PCs, ether-linked phosphatidylcholines; ESI-MS, electrospray ionization-mass spectrometry; ERG, ETS-related gene; FAs, fatty acids; GC-FID, gas chromatography-flame ionization detector; GC-MS, gas chromatography-mass spectrometry; GS, Gleason score; HR-MALDI-IMS, high-resolution matrix-assisted laser desorption/ionization imaging mass spectrometry; HR-MAS ^{1}H-NMR, high resolution magic angle spinning proton nuclear magnetic resonance; LC-MS, liquid chromatography-mass spectrometry; LPC, lysophosphatidylcholine; OPLS-DA, orthogonal projections to latent structures discriminant analysis; OSC-PLS-DA, orthogonal signal corrected partial least squares-discriminant analysis; PCA, principal component analysis; PEs, phosphatidylethanolamines; PLS-DA, partial least squares-discriminant analysis; sens, sensitivity; spec, specificity; SM, sphingomyelin; TCA, tricarboxylic acid cycle.

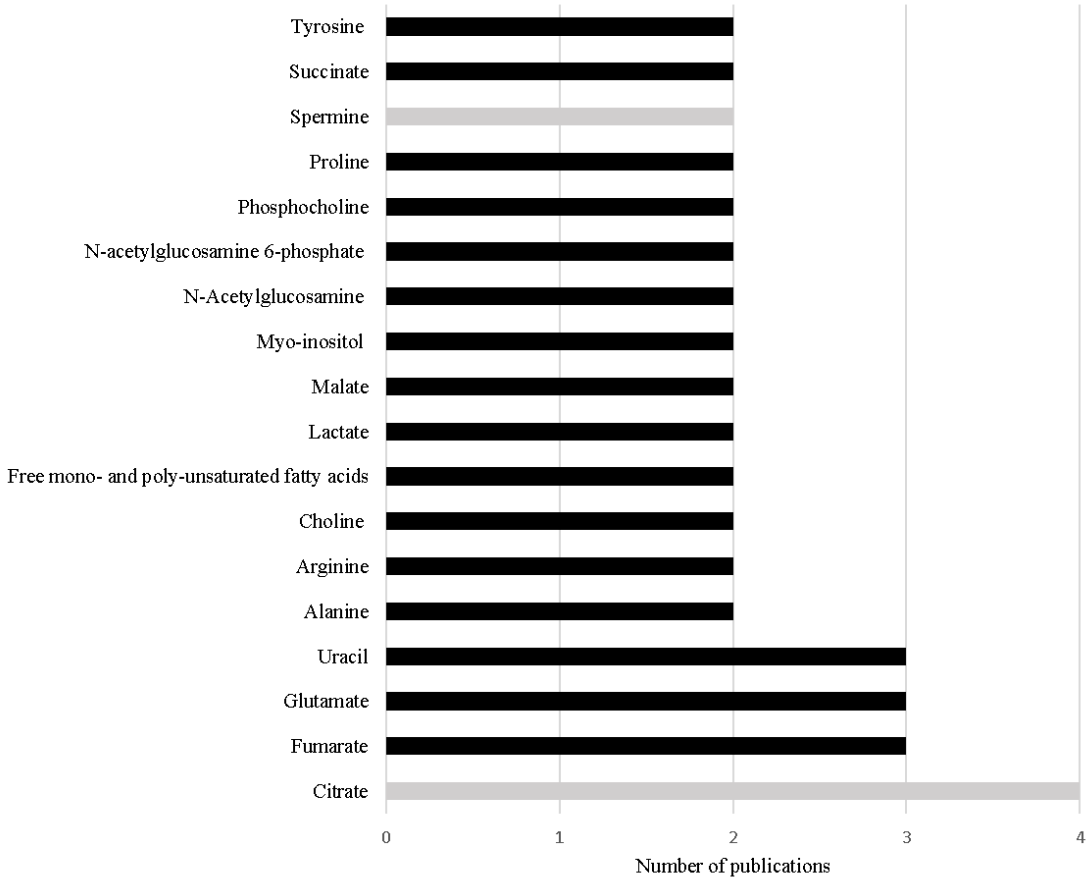

Figure 1.2: Metabolites referred with the same variation in more than one study performed in PCa tissue in the last 5 years. The black bars represent metabolites increased in PCa and the grey bars represent metabolites decreased in PCa.

The most frequent alteration reported among the studies conducted in the last 5 years is the significant decrease in citrate levels in PCa tissue [68,74-76] (Table 1.2 and Figure 1.2). This result is not unexpected as the loss of capability to accumulate citrate is one of the first metabolic alterations observed in prostate cells during malignant transformation. This loss of capability to accumulate citrate translates in a profound alteration in energetic metabolism of PCa cells, once PCa cells start to use citrate in TCA cycle more efficiently than normal prostate cells [51,52]. Furthermore, Braadland et al (2017) compared PCa tissue from men that suffered PCa recurrence after prostatectomy with tissue from men that, until the date of the study, did not show signals of recurrence, unveiling that lower levels of citrate in PCa tissue were associated with shorter time of recurrence [70]. Additionally, lower levels of citrate were also associated with more aggressive PCa [77]. Beyond citrate, two other metabolites involved in energetic metabolism, namely alanine [69,71] and lactate [69,72] showed significant alteration in PCa tissue.

The increased levels of other key metabolites of TCA cycle have also been frequently cited in the reviewed studies, namely succinate [71,76], malate [71,76] and fumarate [71,74,76] (Table 1.2, Figure 1.2). The increase in malate and fumarate levels was also correlated with Gleason score [71,78] and tumor stage [71]. Notably, both succinate and fumarate were previously considered oncometabolites [49] once their accumulation leads to cancer progression [79]. The increased levels of succinate and fumarate have been associated in other cancer types (e.g., paraganglioma, pheochromocytoma or kidney cancers [78]) with mutation in the enzymes succinate dehydrogenase (SDH) and fumarate hydratase (FH), respectively [49,80]. However, these results were not observed in PCa studies performed by Shao et al (2018), which suggested the involvement of other mechanisms that could also be related with the increase of the levels of these metabolites in PCa [71]. Once fumarate is also linked with urea cycle [74,76], this metabolic pathway could be responsible for keeping the high levels of fumarate in PCa tissue [74,79]. As previously referred, the accumulation of fumarate leads to cancer progression, this could involve the activation of hypoxia-inducible factor 1-subunit alfa (HIF1α) and NFκB pathways [74]. HIF1α plays an important oncogenic role in PCa once this pathway is responsible for many essential mechanisms to guarantee PCa cell survival, like anti-apoptosis, angiogenesis and increased glycolytic metabolism. Furthermore, HIF1α protects PCa cells against oxidative stress and against the cytotoxicity caused by androgen deprivation therapy, chemotherapy, or radiation [81]. Similarly, NFκB pathways support PCa cell survival, proliferation, and invasion, playing an important role in the development of resistance to castration therapy [82].

The increase in uracil levels is another alteration consistently reported in PCa tissue (Table 1.2, Figure 1.2), suggesting that PCa cells have alterations in pyrimidine metabolism [65,71,76]. Pyrimidine metabolism is a complex biochemical pathway that comprises different reactions, namely *de novo* nucleotide synthesis, nucleoside salvage, and pyrimidines degradation [83]. Pyrimidines, like uracil [84], are essential in cells metabolism once they are constituents of nucleotides, nucleic acids, vitamins, proteins and folates [85]. Furthermore, they are key intermediates in RNA and DNA synthesis, protein and lipids glycosylation, synthesis of phospholipid precursors [84,85] and in reactions of glucuronidation [84]. Cancer cells are dependent on *de novo* nucleotide synthesis for cell proliferation and consequently for cancer development and progression [83,84]. Importantly, the inhibition of this metabolic pathway is a strategy adopted in the treatment of several cancers (e.g. colorectal cancer and pancreatic cancer) [84,86,87].

One of the main functions of normal prostate is to synthesize polyamines like spermine but apparently this function is impaired with PCa development and progression [70] leading to a decrease in the levels of spermine [68,76]. Indeed, the reduction of spermine levels was proposed as a biomarker able to predict BCR [70]. Interestingly, levels of spermidine, a spermine precursor, were also reported as significantly altered in PCa tissue samples; however, the obtained results were contradictory. Huan et al (2016) found a significant increase in the levels of spermidine [65], whereas Dudka et al (2020) showed a significant decrease in the levels of this metabolite in PCa tissue samples [76].

As previously referred, lipid metabolism can be an important source of PCa biomarkers, emphasizing the relevance of lipidomic studies. The major reported lipidic alterations occurring in PCa cells involved phospholipids from cellular membrane [64,66,67,69,71-73,76] which was expected taking into consideration that cancer cells show a high proliferative phenotype. Notably, the significant decrease in the levels of LPC (16:0) was able to predict BCR [64]. This observation is supported by a transcriptomic study, that evaluate the expression of the enzyme LPC transferase 1 (LPCAT1). The increase in the expression of this enzyme was able to discriminate PCa from benign tissue, as well as to differentiate PCa with different GS and to predict BCR and/or metastasis development [88]. Furthermore, phosphocholine also revealed to be able to discriminate PCa tissue with different GS [76].

Finally, alterations in amino acid metabolism have also been widely reported in PCa, mainly in the increase levels of glutamate [72,75,76], tyrosine [74,75], arginine [74,76] and proline [71,74]. Importantly, the significant alteration in the levels of the first three amino acids was associated with GS and consequently PCa aggressiveness [76], making these metabolites potential diagnosis and prognosis biomarkers.

1.1.6 Urine metabolomic studies

Urine is the ideal matrix to be used in a screening test, due to its non-invasive nature, along with ease collection and handling, high volume which allow repeated analysis, and lower complexity when compared with other biofluids (e.g. serum or plasma) [20,37,89]. Furthermore, urinary metabolites are concentrated by the kidneys, which are anatomically close to the prostate [89,90]. However, urine composition can vary due to several external factors, like diet, smoking habits, genetic factors, microbiota, diurnal cycles, diabetes and other diseases which can affect urine metabolome [91].

From 2015 to 2020, thirteen studies performed in PCa urine samples were published, including four volatilomic studies. Table 1.3 summarizes these studies, highlighting study design, altered metabolites, metabolic pathways, as well as candidate biomarkers, whenever available. Overall, 179 different metabolites were associated with PCa, indicating that PCa is correlated with dysregulations in 48 different metabolic pathways. In this section, the metabolites that hold greatest potential as PCa biomarkers will be highlighted, considering different selection criteria: i) consistency among different urinary studies, ii) AUC greater than PSA and iii) translatability between tissue and urine studies.

Table 1.3: Metabolomic studies performed in urine samples from PCa patients in the last five years (2015-2020)

PCa group	Control group	Analytical platform	Statistical methods	Altered metabolites (direction of variation)	Dysregulated metabolic pathways	Candidate Biomarkers	Ref.
n=32	*n*=32	LC-MS GC-MS	PCA PLS-DA	1. Glycine (-); Serine (-); Threonine (-); Alanine (-) 2. Glutamine (-); Isocitrate/Citrate (-); Aconitate (-); Succinate (-) 3. Sucrose (-); Sorbose (-); Arabinose (-); Arabitol (-); Inositol (-); Galactarate (-); Acetate (-); Propanoic acid (-); Propenoic acid (-); Butanoic acid (-) 4. Carnitines (-) 5. Sphingolipids (+)	1. Amino acid metabolism 2. Energetic metabolism 3. Carbohydrates metabolism 4. Long-chain FAs metabolism 5. Sphingolipid metabolism	-	[92]
n=59	*n*=43	GC-MS	RF LDA	1. 2,6-Dimethyl-7-octen-2-ol (-); 3-Octanone (-); 2-Octanone (-) 2. Pentanal (+)	1. Increased energy consumption 2. Inflammatory conditions via the excessive production of reactive oxygen species, known to induce lipid peroxidation	4-Biomarker panel: 2,6-Dimethyl-7-octen-2-ol 3-Octanone 2-Octanone Pentanal (accu: 63-65%)	[93]
n=66	*n*=88 (BPH) + *n*=11 (cancer-free)	UPLC-MS/MS	ROC Student's t-test	Spermine (-)	Polyamines synthesis	Spermine (AUC: 0.83)	[94]

PCa group	Control group	Analytical platform	Statistical methods	Altered metabolites (direction of variation)	Dysregulated metabolic pathways	Candidate Biomarkers	Ref.
n=62	*n*=42	LC-QTOF	PLS-DA Model Performance: Sens: 88%; Spec: 93%	1. Dimethyllysine (-); 5-Acetamidovalerate (-); Acetyllysine (-); Trimethyllysine (-) 2. Imidazole lactate (-); Histidine (-); Methylhistidine (-); Acetylhistidine (-) 3. Urea (-); Acetylarginine (-); Acetylcitrulline (-); Acetylputrescine (-); Dimethylarginine (-); Citrulline (-) 4. Tyrosine (-) 5. 8-Methoxykynurenate (-); Kynurenic acid (-); Xanthurenic acid (-) 6. Sulfoacetate (-); Isethionate (-); Acetyltaurine (-) 7. Acetylaspartylglutamic acid (-); Acetylaspartate (-); 2-Oxoglutaramate (-) 8. 2-Pyrrolidone-5-carboxylate (-) 9. 5-Methyldeoxycytidine-5′-phosphate(-); 7-Methylguanosine (-); 7-Methylguanine (+)	1. Lysine degradation 2. Histidine degradation 3. Arginine metabolism 4. Tyrosine metabolism 5. Tryptophan metabolism 6. Taurine metabolism 7. Alanine, aspartate and glutamate metabolism 8. Glutamine and glutamate metabolism 9. Purine and pyrimidine metabolism	-	[95]

PCa group	Control group	Analytical platform	Statistical methods	Altered metabolites (direction of variation)	Dysregulated metabolic pathways	Candidate Biomarkers	Ref.
n=30 Validation set *n*=19	*n*=25 Validation set *n*=15	LC-ESI-MS/MS	PLS-DA Model performance: Sens: 90% Spec: 73%	1. Taurine (+) 2. Ethanolamine (-); Phosphoethanolamine (-) 3. Arginine (-); Homocitrulline (-); Citrulline (-) 4. Isoleucine (-); Leucine (-); Phenylalanine (-); Serine (-); Tyrosine (-); Tryptophan (-); Asparagine (-); Glutamate (-); Ornithine (-); Glutamine (-) 5. Lysine (-); δ-Hydroxylysine (-) 6. 1-Methylhistidine (-); 3-Methylhistidine (-); Histidine (-) 7. α-Aminoadipic acid (-); γ-Amino-*n*-butyric acid (-) 8. Cystathionine (-); Cystine (-); Methionine (-)	1. Energetic metabolism 2. Phospholipid metabolism 3. Arginine metabolism 4. Amino acid metabolism 5. Lysine degradation 6. Histidine degradation 7. FAs metabolism 8. Methionine metabolism	γ-Amino-n-butyric acid (AUC: 0.93) Phosphoethanolamine (AUC: 0.88) Ethanolamine (AUC: 0.86) Homocitrulline (AUC: 0.84) Arginine (AUC: 0.83) δ-Hydroxylysine (AUC: 0.80) Asparagine (AUC: 0.77)	[96]
n=64	*n*=51 (BPH)	^{1}H-NMR	OPLS-DA	1. Branched-chain amino acids (+); Glutamate (+); Glycine (-); Dimethylglycine (-) 2. 4-Imidazole-acetate (-) 3. Fumarate (-) 4. Pseudouridine (+)	1. Amino acid metabolism 2. Histidine metabolism 3. TCA cycle 4. RNA synthesis	-	[97]
n=29	*n*=21 (BPH)	HS-SPME-GC-MS	Shapiro-Wilks test, Levene's test, ANOVA, Kruskal-Wallis test, Pearson test	<u>Before prostate massage:</u> 1. 3,5-Dimethylbenzaldehyde (-) 2. 2,6-Dimethyl-7-octen-2-ol (-); 2-Ethylhexanol (-) 3. Santolin triene (-) 4. Furan (+) <u>After prostate massage:</u> 2. 3-Methylphenol (+); Phenol (+) 4. Furan (+) 5. 2-Butanone (+) 6. *p*-Xylene (+)	1. Alcohols and FAs metabolism 2. Lipid metabolism 3. Energetic metabolism 4. FAs oxidation 5. FAs and carbohydrate metabolism 6. Unavailable	Furan *p*-Xylene (correlation with GS)	[98]

PCa group	Control group	Analytical platform	Statistical methods	Altered metabolites (direction of variation)	Dysregulated metabolic pathways	Candidate Biomarkers	Ref.
n=40 Validation set *n*=18	*n*=42 Validation set *n*=18	GC-MS	PCA PLS-DA Model performance: Sens: 78% Spec: 94%-100% Accu: 86%-89% AUC: 0.90-094	1. Methylglyoxal (-) 2. Hexanal (-) 3. 3-Phenylpropionaldehyde (+); Decanal (-); 4. 4-Methylhexan-3-one (-), Hexan-2-one (-); 2-Methylcyclopentan-1-one (-); 5-Methylheptan-2-one (-); 4,6-Dimethylheptan-2-one (-);2-Hydroxy-2-methyl-1-phenylpropan-1-one (-); Pentan-2-one (+); Cyclohexanone (+) 5. 2.5-Dimethylbenzaldehyde (+) 6. 2,6-Dimethyl-6-hepten-2-ol (-);1-Methyl-4-propan-2-ylcyclohex-2-en-1-ol (-); Linalool (-); Terpinen-4-ol (-); 3-Carene (-); Isoterpinolene (-); Menthyl acetate (-); 7. Theaspirane (-) 8. Glyoxal (-); 9. 2-Butenal (-) 10. Phenylacetaldehyde (+) 11. Butan-2-one (+) 12. Dihydroedulan IA (-); 3,4-Dimethylcyclohex-3-ene-1-carbaldehyde (-); 4-Methyldec-1-ene (-); Hexadecane (+)	1. Pyruvate metabolism; Glycine, serine and threonine metabolism 2. Steroid hormone biosynthesis 3. Alcohols and FAs metabolism; Amino acids and carbohydrate catabolism 4. FAs metabolism 5. Alcohols and FAs metabolism 6. Lipid metabolism 7. Steroid metabolism 8. Energetic metabolism; metabolites related to cell signaling and membrane stabilization 9. Metabolites linked to lipid peroxidation 10. Phenylalanine metabolism 11. FAs and carbohydrate metabolism 12. Unavailable	6-Biomarker-panel: Hexanal 2,5-Dimethyl-benzaldehyde 4- Methylhexan-3-one Dihydroedulan IA Methylglyoxal 3- Phenylpropional-dehyde (AUC: 0.90; sens: 89%; spec: 83%; accu: 86%)	[99]

PCa group	Control group	Analytical platform	Statistical methods	Altered metabolites (direction of variation)	Dysregulated metabolic pathways	Candidate Biomarkers	Ref.
n=10	*n*=30	GC-MS LC-MS	PCA OPLS-DA	1. Pseudouridine/Uridine (+); Dihydrouridine(+) 2. Citrate (-) Pyruvate (+); Lactate (+); Hexose (-); Pentose (+); 3. Hippuric acid (-); Aminohippuric acid (+); Phenylpyruvic acid (-); Tyrosine (-) 4. Sphinganine (-); Sphingosine (-); Serine (+) 5. Succinate (-); Glucosamine phosphate (+) 6. Xanthosine (+); Hypoxanthine (+); Xanthine (+) 7. Hydroxytryptophan (+) 8. N-linoleoyl taurine (-); Taurine (+) 9. Creatinine (+) 10. Sialyl-N-acetyllactosamine (+); Suberic acid (+); Dihydrocaffeic acid sulfate (+); Hydroxyethanesulfonate (+); Hydroxyglutaric acid (+); Acetylaminoadipic acid (+); Adipic acid (+); Hydantoinpropionate (+); Nicotine glucuronide (-); Benzoic acid (-); Oxo-heptanoic acid (+); Glucoheptonic acid (-); Aminohexadecanoic acid (-); Glucocaffeic acid (-); Trimethyluric acid (+); 3,7 Dimethyluric acid (-); 3' Sialyllactose (+)	1. Pyrimidine metabolism 2. Energetic metabolism (gluconeogenesis; pyruvate metabolism pathways; glycolysis; pentose phosphate pathway) 3. Phenylalanine metabolism 4. Sphingolipid metabolism 5. Alanine, aspartate and glutamate metabolism 6. Purine metabolism 7. Tryptophan metabolism 8. Taurine metabolism 9. Amino acid metabolism 10. Unavailable	-	[100]
n=43	*n*=48 (BPH)	GC-MS	PLS-DA PARAFAC2 Model performance: Sens: 93% Spec: 89%	1. Androsterone (+); 16-Hydroxydehydroisoandrosterone (+); 5β-Pregnanediol (-); Enterodiol (-); Pregnanetriol (-) 2. 5-Hydroxyindoleacetic acid (+) 3. Vanillyl alcohol (+)	1. Steroidal biosynthesis 2. Tryptophan metabolism 3. Unavailable	-	[101]

PCa group	Control group	Analytical platform	Statistical methods	Altered metabolites (direction of variation)	Dysregulated metabolic pathways	Candidate Biomarkers	Ref.
n=41 Validation set *n*=18	*n*=42 Validation set *n*=18	GC-MS ^{1}H-NMR	PCA PLS-DA Model performance: GC-MS Sens: 89% Spec: 83%, Accu: 86% AUC: 0.96 ^{1}H NMR Sens:67% Spec: 89% Accu:78% AUC: 0.82	1. Pyruvate (+); Leucine (+); Valine (+) 2. Gluconic acid (-); d-Glucose (-); d-Mannitol (-); d-Threitol (+); l-Fucitol (-); l-Threose (+) 3. Sarcosine (+); Hydroxyacetone (+); 2-Furoylglycine (-) 4. l-Arabitol (-); Ribitol (-) 5. Propylene glycol (+) 6. Acetone (+) 7. Trigonelline (-) 8. Oxalate (+) 9. *Myo*-inositol (-) 10. 2-Hydroxyisobutyrate (+); 2-Hydroxyvalerate (+)	1. Valine, leucine and isoleucine biosynthesis and degradation 2. Energetic metabolism (Pentose phosphate pathway; Glycolysis or gluconeogenesis) 3. Glycine, serine and threonine metabolism 4. Pentose and glucuronate interconversions 5. Pyruvate metabolism 6. Propanoate metabolism; Synthesis and degradation of ketone bodies 7. Nicotinate and nicotinamide metabolism 8. Glyoxylate and dicarboxylate metabolism 9. Galactose metabolism; Ascorbate and aldarate metabolism; Membrane metabolism 10. Unavailable	2-Hydroxyvalerate (sens: 86%; spec: 61%; AUC 0.76) 2-Furoylglycine (sens: 85%; spec: 62%; AUC 0.74) d-Glucose (sens: 70%; spec: 69%; AUC 0.69) d-Mannitol (sens: 78%; spec: 60%; AUC 0.69)	[102]

PCa group	Control group	Analytical platform	Statistical methods	Altered metabolites (direction of variation)	Dysregulated metabolic pathways	Candidate Biomarkers	Ref.
n=20	*n*=20 (cancer-free) *n*=20 (bladder cancer) *n*=20 (renal cancer)	GC-MS	PCA PLS-DA	1. Methylglyoxal (-) 2. Hexanal (-) 3. 3-Phenylpropionaldehyde (+) 4. 4-Methylhexan-3-one (-) 5. 2.5-Dimethylbenzaldehyde (+) 6. Dihydroedulan IA (-) 7. Ethylbenzene (+) 8. Heptan-2-one (+); Heptan-3-one (+); 4-(2-Methylpropoxy) butan-2-one (+) 9. Methyl benzoate (+) 10. 3-Methyl-benzaldehyde(+)	1. Pyruvate metabolism; Glycine, serine and threonine metabolism 2. Steroid hormone biosynthesis 3. Alcohols and FAs metabolism; amino acid and carbohydrate catabolism 4. FAs metabolism 5. Alcohols and FAs metabolism 7. Metabolites linked to oxidative stress 8. Protein metabolism; Ketogenic pathway 9. Lipid hydrolysis 10. Metabolites linked to lipid peroxidation	10-biomarker panel Methylglyoxal Hexanal 3-Phenylpropionaldehyde 4-Methylhexan-3-one 2.5-Dimethylbenzaldehyde Dihydroedulan IA Ethylbenzene Heptan-2-one Heptan-3-one 4-(2-Methylpropoxy)butan-2-one Methyl benzoate 3-Methyl-benzaldehyde Discrimination of PCa from control, bladder cancer and renal cancer (AUC 0.90; sens: 76%, spec: 90%, accu: 92%)	[103]
n=58	*n*=18 (BPH)	^{1}H-NMR	PCA PLS-DA	1. Glutamate (-); Glutamine (-); Glycine (-) 2. Citrate (-); Taurine (-) 3. Trimethylamine (+) 4. Choline (-)	1. Amino acid metabolism 2. Energetic metabolism 3. Membrane metabolism 4. Choline metabolism; phospholipid membrane metabolism	Citrate Glutamine	[75]

Notes: (+) indicates increased levels in PCa, (-) indicates decreased levels in PCa; the numbering of the column Altered Metabolites is related with the numbering of the column Dysregulated metabolic pathways. Abbreviations: ^{1}H-NMR, proton nuclear magnetic resonance spectroscopy; accu, accuracy; AUC, area under the curve; BPH, benign prostatic hyperplasia; FAs, fatty acids; GC-MS, gas chromatography–mass spectrometry; GS, gleason score; HS-SPME, headspace solid-phase microextraction; LC-ESI-MS/MS, liquid chromatography electrospray ionization tandem mass spectrometry; LC-MS, liquid chromatography–mass spectrometry; LC-QTOF, liquid chromatography quadrupole time of flight; LDA, linear discriminant analysis; OPLS-DA, orthogonal projections to latent structures discriminant analysis; PCA, principal component analysis; PLS-DA, partial least squares-discriminant analysis; RF, random forest; ROC, receiver operating characteristics curve; sens, sensitivity; spec, specificity; TCA, tricarboxylic acid cycle; UPLC-MS/MS, ultra-performance liquid chromatography-tandem mass spectrometry.

Despite the great differences (e.g different analytical platform, samples preparation or different inclusion/ exclusion criteria) among the study designs, 15 metabolites have been consistently reported with the same variation among different urinary studies, as represented in Figure 1.3. Importantly, 4 metabolites out of the 15 have also been reported with the same alteration in PCa tissue, namely decreased levels of citrate [68,74-76,92,100], increased levels of leucine [74,97,102], increased levels of valine [74,97,102] and increased levels of taurine [96,100,104], suggesting that these alterations may be specific of PCa tumors and suggesting their translatability between tissue and urine samples (Figure 1.3).

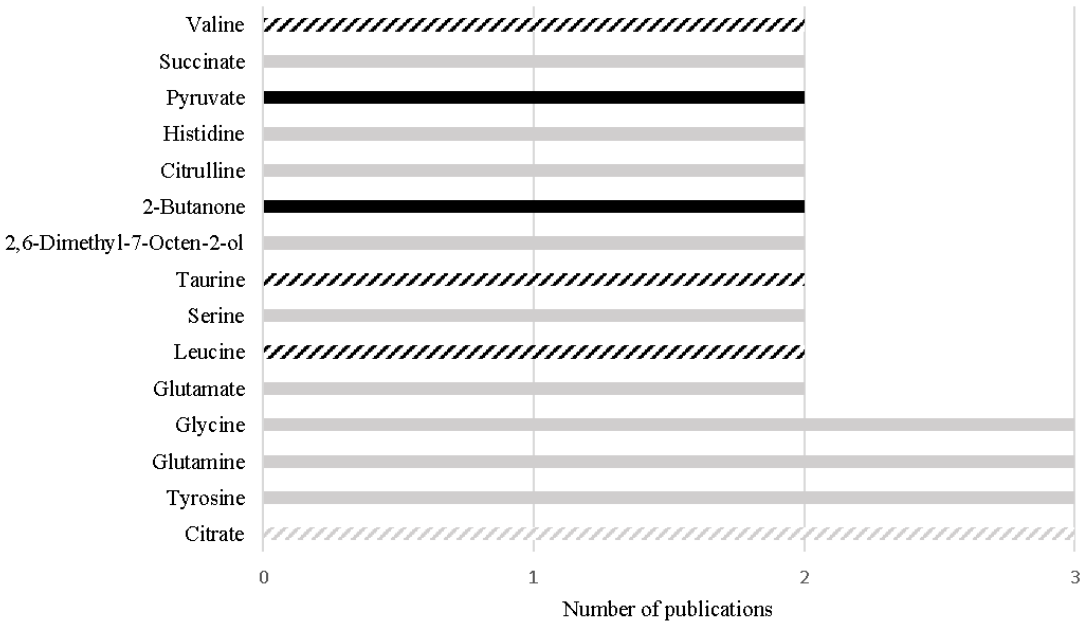

Figure 1.3: Metabolites found with the same alteration in urine metabolome of PCa patients in more than one study, in the last 5 years. The black bars represent metabolites increased in PCa and the grey bars represent metabolites decreased in PCa. The listed bars correspond to the metabolites that were previously found with the same variation in PCa tissue.

In addition, 12 metabolites stood out once they unveiled similar or even better performance than PSA (AUC ranging from 0.53 to 0.83) for PCa detection [7], namely γ-amino-n-butyric acid (AUC: 0.93), phosphoethanolamine (AUC: 0.88), ethanolamine (AUC: 0.86), homocitrulline (AUC: 0.84), asparagine (AUC: 0.773), arginine (AUC: 0.83) [96], spermine (AUC: 0.83) [94], δ-hydroxylysine (AUC: 0.80) [96], 2-hydroxyvalerate (AUC: 0.76), 2-furoylglycine (AUC: 0.74), mannitol (AUC: 0.69) and glucose (AUC 0.69) [102]. From these 12 metabolites, the alterations observed in the levels of 3 metabolites were

previously reported in PCa tissues, namely spermine [68,76], ethanolamine [105] and glucose [76]. Importantly, the decrease in glucose levels was also correlated with GS [76]. The significant alterations observed in the other 9 metabolites, to the best of our knowledge, were not previously reported in PCa tissue. It is important to highlight that even if it is not possible to prove translatability of a metabolite from tissue to urine, this does not invalidate its potential as PCa biomarker once its alteration can for example be driven from a systemic response to PCa development and progression.

The volatilomic studies have been more focused in the definition of biomarker panels for possible detection through biosensors rather than proposing individual biomarkers [93,99,103]. The smallest biomarker panel reported included four metabolites (2,6-dimethyl-7-octen-2-ol, 3-octanone, 2-octanone and pentanal) [93], which unveiled accuracies at least equal to PSA (accu. of 62-75% for PSA *vs*. accu. of 63-65% for the 4-biomarker panel [7,93]. Remarkably, a 6-biomarker panel (hexanal, 2,5-dimethylbenzaldehyde, 4-methylhexan-3-one, dihydroedulan IA, methylglyoxal, 3-phenylpropionaldehyde) [99] and an improved 10-biomarker panel (methylglyoxal, hexanal, 3-phenylpropionaldehyde, 4-methylhexan-3-one, 2.5-dimethylbenzaldehyde, dihydroedulan IA, ethylbenzene, heptan-2-one, heptan-3-one, 4-(2-methylpropoxy)butan-2-one, methyl benzoate, 3-methyl-benzaldehyde) [103] were recently proposed that outperformed PSA in all performance parameters (PSA: acc = 62%-75% , Sens = 20.5%, spec = 51%-91% [4,7,8]; 6-biomarker panel: acc = 86%, sens = 89%, spec = 83% [99]; 10-biomarker panel: acc = 92%, sens = 76%, spec = 90% [103]). Notably, the 10-biomarker panel proved to be able to differentiate PCa from cancer-free individuals as well as from other urological cancers (renal and bladder cancers) [103].

Overall, findings from the reviewed studies showed that PCa development and progression is mainly associated with alterations in amino acid metabolism, energy metabolism, especially in TCA cycle, and membrane metabolism (Tables 1.2 and 1.3).

1.1.7 Current challenges and future perspectives

There are no doubts that the scientific community has made enormous efforts to define the impact of PCa in human metabolome with dozens of studies focused in this topic, not only using tissue and urine matrices but also other biological samples as serum, plasma, seminal fluid, prostatic fluid and even cell lines [18]. However, some biological and technical challenges should be addressed before we can translate all the potentialities of metabolomics into clinical practice.

The traditional paradigm is to find a single biomarker for PCa screening. However, during the last years, the idea of using a panel of biomarkers instead of a single biomarker has gained strength, especially in volatilomic studies. The use of a biomarker panel has important advantages, once a multi-biomarker panel may be able to capture more deeply the various metabolic dysregulations occurring during cancer development and progression than a single biomarker [106]. Hence, a multi-biomarker panel allows the definition of a more robust signature of PCa providing a better evaluation of cancer progression. Furthermore, the use of a biomarker panel avoids that an arbitrary change in a single metabolite leads to a false result [22].

As referred in the previous section, the comparison of the findings from different studies is compromised by the lack of standardized procedures in metabolomic studies, especially in study design which consequently increases inter-laboratory variability [107]. Many efforts have been made to accomplish the goal of standardized procedures in metabolomics studies in the last years [107,108]. There is still a long way to go until the desired standardization, but the first steps have already been taken [108].

Other crucial technical challenge is metabolite identification. This is particularly true in volatilomics studies. Also, the interpretation of the urinary volatilome signature of PCa is particularly challenging once there is no clearly understand of the biological origin of VOCs [39]. In addition, the volatilome of PCa tissue has not been explored so far, to our knowledge, hindering the elucidation of a potential translatability of VOCs from tissues to urine samples. In future, this issue can be addressed through volatilomic studies of PCa tissue and fluxomic studies. Fluxomic studies allow the understanding of the metabolic origin of endogenous VOCs by labeling and tracking metabolic precursors (e.g., glucose), throughout the metabolic pathways [109].

Perhaps the greatest limitation to biomarker discovery relies on the fact that several metabolomic studies are essentially descriptive and skip the validation step. Indeed, the vast majority of the papers just list which metabolites are statistically different between the groups in study, not proposing candidate biomarkers and/or clearly state the performance of the proposed metabolites/biomarkers (e.g., AUC, sensitivity, specificity and/or accuracy), thus impairing the discussion of which would be the most promising biomarkers for PCa. Hence, future studies should be less descriptive and more assertive, proposing and evaluating potential biomarkers. Furthermore, it is also important to include external sets for model/results validation to improve the robustness of candidate biomarkers and to include unambiguous biochemical and biological interpretation of PCa metabolic dysregulations. Remarkably, some of the studies included in this revision are already

following this direction. In addition, it is well known that especially urinary metabolic profile can be affected by several factors (e.g., diet, lifestyle, microbiota, race, among others) [107], so it is also crucial to perform studies in large and more heterogeneous populations (e.g., American, African, Caucasian), to ensure that the proposed biomarkers can be applied among different countries and different lifestyles.

To conclude, metabolomics is a powerful tool to uncover the metabolic signature of PCa development and progression. The results obtained so far in tissue and urine metabolomic studies unveiled potential to define new screening/diagnosis biomarkers.

1.1.8 References

1. Bray, F.; Ferlay, J.; Soerjomataram, I.; Siegel, R.L.; Torre, L.A.; Jemal, A. Global cancer statistics 2018: GLOBOCAN estimates of incidence and mortality worldwide for 36 cancers in 185 countries. CA Cancer J Clin 2018, 68, 394-424, doi:10.3322/caac.21492.
2. Filella, X.; Foj, L. Novel Biomarkers for Prostate Cancer Detection and Prognosis. Adv Exp Med Biol 2018, 1095, 15-39, doi:10.1007/978-3-319-95693-0_2.
3. Rigau, M.; Olivan, M.; Garcia, M.; Sequeiros, T.; Montes, M.; Colas, E.; Llaurado, M.; Planas, J.; Torres, I.; Morote, J., et al. The present and future of prostate cancer urine biomarkers. Int J Mol Sci 2013, 14, 12620-12649, doi:10.3390/ijms140612620.
4. Wolf, A.M.; Wender, R.C.; Etzioni, R.B.; Thompson, I.M.; D'Amico, A.V.; Volk, R.J.; Brooks, D.D.; Dash, C.; Guessous, I.; Andrews, K., et al. American Cancer Society guideline for the early detection of prostate cancer: update 2010. CA Cancer J Clin 2010, 60, 70-98, doi:10.3322/caac.20066.
5. Hubner, N.; Shariat, S.; Remzi, M. Prostate biopsy: guidelines and evidence. Curr Opin Urol 2018, 28, 354-359, doi:10.1097/MOU.0000000000000510.
6. Eskra, J.N.; Rabizadeh, D.; Pavlovich, C.P.; Catalona, W.J.; Luo, J. Approaches to urinary detection of prostate cancer. Prostate Cancer Prostatic Dis 2019, 22, 362-381, doi:10.1038/s41391-019-0127-4.
7. Louie, K.S.; Seigneurin, A.; Cathcart, P.; Sasieni, P. Do prostate cancer risk models improve the predictive accuracy of PSA screening? A meta-analysis. Ann Oncol 2015, 26, 848-864, doi:10.1093/annonc/mdu525.
8. Kearns, J.T.; Lin, D.W. Improving the Specificity of PSA Screening with Serum and Urine Markers. Curr Urol Rep 2018, 19, 80, doi:10.1007/s11934-018-0828-6.
9. Das, C.J.; Razik, A.; Sharma, S.; Verma, S. Prostate biopsy: when and how to perform. Clin Radiol 2019, 74, 853-864, doi:10.1016/j.crad.2019.03.016.

10. Tourinho-Barbosa, R.; Srougi, V.; Nunes-Silva, I.; Baghdadi, M.; Rembeyo, G.; Eiffel, S.S.; Barret, E.; Rozet, F.; Galiano, M.; Cathelineau, X., et al. Biochemical recurrence after radical prostatectomy: what does it mean? Int Braz J Urol 2018, 44, 14-21, doi:10.1590/S1677-5538.IBJU.2016.0656.

11. Fakhrejahani, F.; Madan, R.A.; Dahut, W.L. Management Options for Biochemically Recurrent Prostate Cancer. Curr Treat Options Oncol 2017, 18, 26, doi:10.1007/s11864-017-0462-4.

12. Teo, M.Y.; Rathkopf, D.E.; Kantoff, P. Treatment of Advanced Prostate Cancer. Annual review of medicine 2019, 70, 479-499, doi:10.1146/annurev-med-051517-011947.

13. Narayan, V.M.; Konety, B.R.; Warlick, C. Novel biomarkers for prostate cancer: An evidence-based review for use in clinical practice. Int J Urol 2017, 24, 352-360, doi:10.1111/iju.13326.

14. Park, H.; Lee, S.W.; Song, G.; Kang, T.W.; Jung, J.H.; Chung, H.C.; Kim, S.J.; Park, C.-H.; Park, J.Y.; Shin, T.Y., et al. Diagnostic Performance of %[-2]proPSA and Prostate Health Index for Prostate Cancer: Prospective, Multi-institutional Study. J Korean Med Sci 2018, 33.

15. Sartori, D.A.; Chan, D.W. Biomarkers in prostate cancer: what's new? Curr Opin Oncol 2014, 26, 259-264, doi:10.1097/CCO.0000000000000065.

16. Chistiakov, D.A.; Myasoedova, V.A.; Grechko, A.V.; Melnichenko, A.A.; Orekhov, A.N. New biomarkers for diagnosis and prognosis of localized prostate cancer. Semin Cancer Biol 2018, 52, 9-16, doi:10.1016/j.semcancer.2018.01.012.

17. Murphy, L.; Prencipe, M.; Gallagher, W.M.; Watson, R.W. Commercialized biomarkers: new horizons in prostate cancer diagnostics. Expert Rev Mol Diagn 2015, 15, 491-503, doi:10.1586/14737159.2015.1011622.

18. Lima, A.R.; Bastos Mde, L.; Carvalho, M.; Guedes de Pinho, P. Biomarker Discovery in Human Prostate Cancer: an Update in Metabolomics Studies. Transl Oncol 2016, 9, 357-370, doi:10.1016/j.tranon.2016.05.004.

19. Nicholson, J.K.; Lindon, J.C.; Holmes, E. 'Metabonomics': understanding the metabolic responses of living systems to pathophysiological stimuli via multivariate statistical analysis of biological NMR spectroscopic data. Xenobiotica; the fate of foreign compounds in biological systems 1999, 29, 1181-1189, doi:10.1080/004982599238047.

20. Bujak, R.; Struck-Lewicka, W.; Markuszewski, M.J.; Kaliszan, R. Metabolomics for laboratory diagnostics. J Pharm Biomed Anal 2015, 113, 108-120, doi:10.1016/j.jpba.2014.12.017.

21. Armitage, E.G.; Barbas, C. Metabolomics in cancer biomarker discovery: current trends and future perspectives. J Pharm Biomed Anal 2014, 87, 1-11, doi:10.1016/j.jpba.2013.08.041.
22. Marchand, C.R.; Farshidfar, F.; Rattner, J.; Bathe, O.F. A Framework for Development of Useful Metabolomic Biomarkers and Their Effective Knowledge Translation. Metabolites 2018, 8, doi:10.3390/metabo8040059.
23. Lopez-Lopez, A.; Lopez-Gonzalvez, A.; Barker-Tejeda, T.C.; Barbas, C. A review of validated biomarkers obtained through metabolomics. Expert Rev Mol Diagn 2018, 18, 557-575, doi:10.1080/14737159.2018.1481391.
24. Nagrath, D.; Caneba, C.; Karedath, T.; Bellance, N. Metabolomics for mitochondrial and cancer studies. Biochim Biophys Acta 2011, 1807, 650-663, doi:10.1016/j.bbabio.2011.03.006.
25. Nagana Gowda, G.A.; Raftery, D. Biomarker Discovery and Translation in Metabolomics. Curr Metabolomics 2013, 1, 227-240, doi:10.2174/2213235X113019990005.
26. Ren, J.-L.; Zhang, A.-H.; Kong, L.; Wang, X.-J. Advances in mass spectrometry-based metabolomics for investigation of metabolites. RSC Advances 2018, 8, 22335-22350, doi:10.1039/C8RA01574K.
27. Marshall, D.D.; Powers, R. Beyond the paradigm: Combining mass spectrometry and nuclear magnetic resonance for metabolomics. Prog Nucl Magn Reson Spectrosc 2017, 100, 1-16, doi:10.1016/j.pnmrs.2017.01.001.
28. Segers, K.; Declerck, S.; Mangelings, D.; Heyden, Y.V.; Eeckhaut, A.V. Analytical techniques for metabolomic studies: a review. Bioanalysis 2019, 11, 2297-2318, doi:10.4155/bio-2019-0014.
29. Dettmer, K.; Aronov, P.A.; Hammock, B.D. Mass spectrometry-based metabolomics. Mass Spectrom Rev 2007, 26, 51-78, doi:10.1002/mas.20108.
30. Han, J.; Datla, R.; Chan, S.; Borchers, C.H. Mass spectrometry-based technologies for high-throughput metabolomics. Bioanalysis 2009, 1, 1665-1684, doi:10.4155/bio.09.158.
31. Crook, A.A.; Powers, R. Quantitative NMR-Based Biomedical Metabolomics: Current Status and Applications. Molecules (Basel, Switzerland) 2020, 25, 5128, doi:10.3390/molecules25215128.
32. Lindon, J.C.; Nicholson, J.K. Spectroscopic and statistical techniques for information recovery in metabonomics and metabolomics. Annual review of analytical chemistry (Palo Alto, Calif.) 2008, 1, 45-69, doi:10.1146/annurev.anchem.1.031207.113026.

33. Xiao, J.F.; Zhou, B.; Ressom, H.W. Metabolite identification and quantitation in LC-MS/MS-based metabolomics. Trends Analyt Chem 2012, 32, 1-14, doi:10.1016/j.trac.2011.08.009.
34. Lima, A.R.; Pinto, J.; Bastos, M.L.; Carvalho, M.; Guedes de Pinho, P. NMR-based metabolomics studies of human prostate cancer tissue. Metabolomics 2018, 14, 88, doi:10.1007/s11306-018-1384-2.
35. Zou, W.; She, J.; Tolstikov, V.V. A comprehensive workflow of mass spectrometry-based untargeted metabolomics in cancer metabolic biomarker discovery using human plasma and urine. Metabolites 2013, 3, 787-819, doi:10.3390/metabo3030787.
36. Fan, T.W.; Lane, A.N. Applications of NMR spectroscopy to systems biochemistry. Prog Nucl Magn Reson Spectrosc 2016, 92-93, 18-53, doi:10.1016/j.pnmrs.2016.01.005.
37. Turi, K.N.; Romick-Rosendale, L.; Ryckman, K.K.; Hartert, T.V. A review of metabolomics approaches and their application in identifying causal pathways of childhood asthma. The Journal of allergy and clinical immunology 2018, 141, 1191-1201, doi:10.1016/j.jaci.2017.04.021.
38. Armitage, E.G.; Ciborowski, M. Applications of Metabolomics in Cancer Studies. Adv Exp Med Biol 2017, 965, 209-234, doi:10.1007/978-3-319-47656-8_9.
39. Janfaza, S.; Khorsand, B.; Nikkhah, M.; Zahiri, J. Digging deeper into volatile organic compounds associated with cancer. Biol Methods Protoc 2019, 4, bpz014, doi:10.1093/biomethods/bpz014.
40. Gao, Q.; Lee, W.Y. Urinary metabolites for urological cancer detection: a review on the application of volatile organic compounds for cancers. Am J Clin Exp Urol 2019, 7, 232-248.
41. Lubes, G.; Goodarzi, M. GC-MS based metabolomics used for the identification of cancer volatile organic compounds as biomarkers. J Pharm Biomed Anal 2018, 147, 313-322, doi:10.1016/j.jpba.2017.07.013.
42. Cornu, J.N.; Cancel-Tassin, G.; Ondet, V.; Girardet, C.; Cussenot, O. Olfactory detection of prostate cancer by dogs sniffing urine: a step forward in early diagnosis. Eur Urol 2011, 59, 197-201, doi:10.1016/j.eururo.2010.10.006.
43. Taverna, G.; Tidu, L.; Grizzi, F.; Torri, V.; Mandressi, A.; Sardella, P.; La Torre, G.; Cocciolone, G.; Seveso, M.; Giusti, G., et al. Olfactory system of highly trained dogs detects prostate cancer in urine samples. J Urol 2015, 193, 1382-1387, doi:10.1016/j.juro.2014.09.099.

44. Pirrone, F.; Albertini, M. Olfactory detection of cancer by trained sniffer dogs: A systematic review of the literature. Journal of Veterinary Behavior 2017, 19, 105-117, doi:https://doi.org/10.1016/j.jveb.2017.03.004.
45. Perrotti, F.; Rosa, C.; Cicalini, I.; Sacchetta, P.; Del Boccio, P.; Genovesi, D.; Pieragostino, D. Advances in Lipidomics for Cancer Biomarkers Discovery. Int J Mol Sci 2016, 17, doi:10.3390/ijms17121992.
46. Park, J.K.; Coffey, N.J.; Limoges, A.; Le, A. The Heterogeneity of Lipid Metabolism in Cancer. Adv Exp Med Biol 2018, 1063, 33-55, doi:10.1007/978-3-319-77736-8_3.
47. Yang, K.; Han, X. Lipidomics: Techniques, Applications, and Outcomes Related to Biomedical Sciences. Trends Biochem Sci 2016, 41, 954-969, doi:10.1016/j.tibs.2016.08.010.
48. Tumanov, S.; Kamphorst, J.J. Recent advances in expanding the coverage of the lipidome. Curr Opin Biotechnol 2017, 43, 127-133, doi:10.1016/j.copbio.2016.11.008.
49. Islam, S.R.; Manna, S.K. Lipidomic Analysis of Cancer Cell and Tumor Tissues. Methods Mol Biol 2019, 1928, 175-204, doi:10.1007/978-1-4939-9027-6_11.
50. Kwon, H.; Oh, S.; Jin, X.; An, Y.J.; Park, S. Cancer metabolomics in basic science perspective. Arch Pharm Res 2015, 38, 372-380, doi:10.1007/s12272-015-0552-4.
51. Warburg, O. On the origin of cancer cells. Science 1956, 123, 309-314, doi:10.1126/science.123.3191.309.
52. Eidelman, E.; Twum-Ampofo, J.; Ansari, J.; Siddiqui, M.M. The Metabolic Phenotype of Prostate Cancer. Front Oncol 2017, 7, 131, doi:10.3389/fonc.2017.00131.
53. Andersen, M.K.; Giskeødegård, G.F.; Tessem, M.-B. Metabolic alterations in tissues and biofluids of patients with prostate cancer. Current Opinion in Endocrine and Metabolic Research 2020, 10, 23-28, doi: 10.1016/j.coemr.2020.02.003.
54. Zadra, G.; Loda, M. Metabolic Vulnerabilities of Prostate Cancer: Diagnostic and Therapeutic Opportunities. Cold Spring Harb Perspect Med 2018, 8, doi:10.1101/cshperspect.a030569.
55. Lloyd, S.M.; Arnold, J.; Sreekumar, A. Metabolomic profiling of hormone-dependent cancers: a bird's eye view. Trends Endocrinol Metab 2015, 26, 477-485, doi:10.1016/j.tem.2015.07.001.
56. Schipper, R.G.; Romijn, J.C.; Cuijpers, V.M.; Verhofstad, A.A. Polyamines and prostatic cancer. Biochem Soc Trans 2003, 31, 375-380, doi:10.1042/bst0310375.
57. Dai, C.; Heemers, H.; Sharifi, N. Androgen Signaling in Prostate Cancer. Cold Spring Harb Perspect Med 2017, 7, doi:10.1101/cshperspect.a030452.

58. Sreekumar, A.; Poisson, L.M.; Rajendiran, T.M.; Khan, A.P.; Cao, Q.; Yu, J.; Laxman, B.; Mehra, R.; Lonigro, R.J.; Li, Y., et al. Metabolomic profiles delineate potential role for sarcosine in prostate cancer progression. Nature 2009, 457, 910-914, doi:10.1038/nature07762.

59. Wu, H.; Liu, T.; Ma, C.; Xue, R.; Deng, C.; Zeng, H.; Shen, X. GC/MS-based metabolomic approach to validate the role of urinary sarcosine and target biomarkers for human prostate cancer by microwave-assisted derivatization. Anal Bioanal Chem 2011, 401, 635-646, doi:10.1007/s00216-011-5098-9.

60. Jentzmik, F.; Stephan, C.; Lein, M.; Miller, K.; Kamlage, B.; Bethan, B.; Kristiansen, G.; Jung, K. Sarcosine in prostate cancer tissue is not a differential metabolite for prostate cancer aggressiveness and biochemical progression. J Urol 2011, 185, 706-711, doi:10.1016/j.juro.2010.09.077.

61. Jentzmik, F.; Stephan, C.; Miller, K.; Schrader, M.; Erbersdobler, A.; Kristiansen, G.; Lein, M.; Jung, K. Sarcosine in urine after digital rectal examination fails as a marker in prostate cancer detection and identification of aggressive tumours. Eur Urol 2010, 58, 12-18; discussion 20-11, doi:10.1016/j.eururo.2010.01.035.

62. Green, T.; Chen, X.; Ryan, S.; Asch, A.S.; Ruiz-Echevarria, M.J. TMEFF2 and SARDH cooperate to modulate one-carbon metabolism and invasion of prostate cancer cells. Prostate 2013, 73, 1561-1575, doi:10.1002/pros.22706.

63. Donkena, K.V.; Yuan, H.; Young, C.Y. Vitamin Bs, one carbon metabolism and prostate cancer. Mini Rev Med Chem 2010, 10, 1385-1392, doi:10.2174/138955710793564106.

64. Goto, T.; Terada, N.; Inoue, T.; Kobayashi, T.; Nakayama, K.; Okada, Y.; Yoshikawa, T.; Miyazaki, Y.; Uegaki, M.; Utsunomiya, N., et al. Decreased expression of lysophosphatidylcholine (16:0/OH) in high resolution imaging mass spectrometry independently predicts biochemical recurrence after surgical treatment for prostate cancer. Prostate 2015, 75, 1821-1830, doi:10.1002/pros.23088.

65. Huan, T.; Troyer, D.A.; Li, L. Metabolite Analysis and Histology on the Exact Same Tissue: Comprehensive Metabolomic Profiling and Metabolic Classification of Prostate Cancer. Sci Rep 2016, 6, 32272, doi:10.1038/srep32272.

66. Li, J.; Ren, S.; Piao, H.L.; Wang, F.; Yin, P.; Xu, C.; Lu, X.; Ye, G.; Shao, Y.; Yan, M., et al. Integration of lipidomics and transcriptomics unravels aberrant lipid metabolism and defines cholesteryl oleate as potential biomarker of prostate cancer. Sci Rep 2016, 6, 20984, doi:10.1038/srep20984.

67. Ren, S.; Shao, Y.; Zhao, X.; Hong, C.S.; Wang, F.; Lu, X.; Li, J.; Ye, G.; Yan, M.; Zhuang, Z., et al. Integration of Metabolomics and Transcriptomics Reveals Major Metabolic Pathways and Potential Biomarker Involved in Prostate Cancer. Mol Cell Proteomics 2016, 15, 154-163, doi:10.1074/mcp.M115.052381.
68. Hansen, A.F.; Sandsmark, E.; Rye, M.B.; Wright, A.J.; Bertilsson, H.; Richardsen, E.; Viset, T.; Bofin, A.M.; Angelsen, A.; Selnaes, K.M., et al. Presence of TMPRSS2-ERG is associated with alterations of the metabolic profile in human prostate cancer. Oncotarget 2016, 7, 42071-42085, doi:10.18632/oncotarget.9817.
69. Madhu, B.; Shaw, G.L.; Warren, A.Y.; Neal, D.E.; Griffiths, J.R. Response of Degarelix treatment in human prostate cancer monitored by HR-MAS 1H NMR spectroscopy. Metabolomics 2016, 12, 120, doi:10.1007/s11306-016-1055-0.
70. Braadland, P.R.; Giskeodegard, G.; Sandsmark, E.; Bertilsson, H.; Euceda, L.R.; Hansen, A.F.; Guldvik, I.J.; Selnaes, K.M.; Grytli, H.H.; Katz, B., et al. Ex vivo metabolic fingerprinting identifies biomarkers predictive of prostate cancer recurrence following radical prostatectomy. Br J Cancer 2017, 117, 1656-1664, doi:10.1038/bjc.2017.346.
71. Shao, Y.; Ye, G.; Ren, S.; Piao, H.L.; Zhao, X.; Lu, X.; Wang, F.; Ma, W.; Li, J.; Yin, P., et al. Metabolomics and transcriptomics profiles reveal the dysregulation of the tricarboxylic acid cycle and related mechanisms in prostate cancer. Int J Cancer 2018, 143, 396-407, doi:10.1002/ijc.31313.
72. Vandergrift, L.A.; Decelle, E.A.; Kurth, J.; Wu, S.; Fuss, T.L.; DeFeo, E.M.; Halpern, E.F.; Taupitz, M.; McDougal, W.S.; Olumi, A.F., et al. Metabolomic Prediction of Human Prostate Cancer Aggressiveness: Magnetic Resonance Spectroscopy of Histologically Benign Tissue. Sci Rep 2018, 8, 4997, doi:10.1038/s41598-018-23177-w.
73. Zhou, X.; Mei, H.; Agee, J.; Brown, T.; Mao, J. Racial differences in distribution of fatty acids in prostate cancer and benign prostatic tissues. Lipids Health Dis 2019, 18, 189, doi:10.1186/s12944-019-1130-4.
74. Franko, A.; Shao, Y.; Heni, M.; Hennenlotter, J.; Hoene, M.; Hu, C.; Liu, X.; Zhao, X.; Wang, Q.; Birkenfeld, A.L., et al. Human Prostate Cancer is Characterized by an Increase in Urea Cycle Metabolites. Cancers (Basel) 2020, 12, doi:10.3390/cancers12071814.
75. Zheng, H.; Dong, B.; Ning, J.; Shao, X.; Zhao, L.; Jiang, Q.; Ji, H.; Cai, A.; Xue, W.; Gao, H. NMR-based metabolomics analysis identifies discriminatory metabolic disturbances in tissue and biofluid samples for progressive prostate cancer. Clin Chim Acta 2020, 501, 241-251, doi:10.1016/j.cca.2019.10.046.

76. Dudka, I.; Thysell, E.; Lundquist, K.; Antti, H.; Iglesias-Gato, D.; Flores-Morales, A.; Bergh, A.; Wikstrom, P.; Grobner, G. Comprehensive metabolomics analysis of prostate cancer tissue in relation to tumor aggressiveness and TMPRSS2-ERG fusion status. BMC Cancer 2020, 20, 437, doi:10.1186/s12885-020-06908-z.
77. Bertilsson, H.; Tessem, M.-B.; Flatberg, A.; Viset, T.; Gribbestad, I.; Angelsen, A.; Halgunset, J. Changes in Gene Transcription Underlying the Aberrant Citrate and Choline Metabolism in Human Prostate Cancer Samples. Clinical Cancer Research 2012, 18, 3261-3269, doi:10.1158/1078-0432.ccr-11-2929.
78. Pollard, P.J.; Briere, J.J.; Alam, N.A.; Barwell, J.; Barclay, E.; Wortham, N.C.; Hunt, T.; Mitchell, M.; Olpin, S.; Moat, S.J., et al. Accumulation of Krebs cycle intermediates and over-expression of HIF1alpha in tumours which result from germline FH and SDH mutations. Hum Mol Genet 2005, 14, 2231-2239, doi:10.1093/hmg/ddi227.
79. Yang, M.; Soga, T.; Pollard, P.J. Oncometabolites: linking altered metabolism with cancer. The Journal of clinical investigation 2013, 123, 3652-3658, doi:10.1172/jci67228.
80. King, A.; Selak, M.A.; Gottlieb, E. Succinate dehydrogenase and fumarate hydratase: linking mitochondrial dysfunction and cancer. Oncogene 2006, 25, 4675-4682, doi:10.1038/sj.onc.1209594.
81. Ranasinghe, W.K.; Baldwin, G.S.; Bolton, D.; Shulkes, A.; Ischia, J.; Patel, O. HIF1alpha expression under normoxia in prostate cancer--which pathways to target? J Urol 2015, 193, 763-770, doi:10.1016/j.juro.2014.10.085.
82. Staal, J.; Beyaert, R. Inflammation and NF-kappaB Signaling in Prostate Cancer: Mechanisms and Clinical Implications. Cells 2018, 7, doi:10.3390/cells7090122.
83. Siddiqui, A.; Ceppi, P. A non-proliferative role of pyrimidine metabolism in cancer. Mol Metab 2020, 35, 100962, doi:10.1016/j.molmet.2020.02.005.
84. Loffler, M.; Fairbanks, L.D.; Zameitat, E.; Marinaki, A.M.; Simmonds, H.A. Pyrimidine pathways in health and disease. Trends Mol Med 2005, 11, 430-437, doi:10.1016/j.molmed.2005.07.003.
85. Garavito, M.F.; Narvaez-Ortiz, H.Y.; Zimmermann, B.H. Pyrimidine Metabolism: Dynamic and Versatile Pathways in Pathogens and Cellular Development. J Genet Genomics 2015, 42, 195-205, doi:10.1016/j.jgg.2015.04.004.
86. Konno, M.; Asai, A.; Kawamoto, K.; Nishida, N.; Satoh, T.; Doki, Y.; Mori, M.; Ishii, H. The one-carbon metabolism pathway highlights therapeutic targets for gastrointestinal cancer (Review). Int J Oncol 2017, 50, 1057-1063, doi:10.3892/ijo.2017.3885.
87. Vasan, K.; Werner, M.; Chandel, N.S. Mitochondrial Metabolism as a Target for Cancer Therapy. Cell Metab 2020, 32, 341-352, doi:10.1016/j.cmet.2020.06.019.

88. Zhou, X.; Lawrence, T.J.; He, Z.; Pound, C.R.; Mao, J.; Bigler, S.A. The expression level of lysophosphatidylcholine acyltransferase 1 (LPCAT1) correlates to the progression of prostate cancer. Experimental and molecular pathology 2012, 92, 105-110, doi:10.1016/j.yexmp.2011.11.001.
89. Gomez-Cebrian, N.; Rojas-Benedicto, A.; Albors-Vaquer, A.; Lopez-Guerrero, J.A.; Pineda-Lucena, A.; Puchades-Carrasco, L. Metabolomics Contributions to the Discovery of Prostate Cancer Biomarkers. Metabolites 2019, 9, doi:10.3390/metabo9030048.
90. Schmidt, K.; Podmore, I. Current Challenges in Volatile Organic Compounds Analysis as Potential Biomarkers of Cancer. J Biomark 2015, 2015, 981458, doi:10.1155/2015/981458.
91. Walsh, M.C.; Brennan, L.; Malthouse, J.P.; Roche, H.M.; Gibney, M.J. Effect of acute dietary standardization on the urinary, plasma, and salivary metabolomic profiles of healthy humans. Am J Clin Nutr 2006, 84, 531-539, doi:10.1093/ajcn/84.3.531.
92. Struck-Lewicka, W.; Kordalewska, M.; Bujak, R.; Yumba Mpanga, A.; Markuszewski, M.; Jacyna, J.; Matuszewski, M.; Kaliszan, R.; Markuszewski, M.J. Urine metabolic fingerprinting using LC-MS and GC-MS reveals metabolite changes in prostate cancer: A pilot study. J Pharm Biomed Anal 2015, 111, 351-361, doi:10.1016/j.jpba.2014.12.026.
93. Khalid, T.; Aggio, R.; White, P.; De Lacy Costello, B.; Persad, R.; Al-Kateb, H.; Jones, P.; Probert, C.S.; Ratcliffe, N. Urinary Volatile Organic Compounds for the Detection of Prostate Cancer. PloS one 2015, 10, e0143283, doi:10.1371/journal.pone.0143283.
94. Tsoi, T.H.; Chan, C.F.; Chan, W.L.; Chiu, K.F.; Wong, W.T.; Ng, C.F.; Wong, K.L. Urinary Polyamines: A Pilot Study on Their Roles as Prostate Cancer Detection Biomarkers. PloS one 2016, 11, e0162217, doi:10.1371/journal.pone.0162217.
95. Fernandez-Peralbo, M.A.; Gomez-Gomez, E.; Calderon-Santiago, M.; Carrasco-Valiente, J.; Ruiz-Garcia, J.; Requena-Tapia, M.J.; Luque de Castro, M.D.; Priego-Capote, F. Prostate Cancer Patients-Negative Biopsy Controls Discrimination by Untargeted Metabolomics Analysis of Urine by LC-QTOF: Upstream Information on Other Omics. Sci Rep 2016, 6, 38243, doi:10.1038/srep38243.
96. Derezinski, P.; Klupczynska, A.; Sawicki, W.; Palka, J.A.; Kokot, Z.J. Amino Acid Profiles of Serum and Urine in Search for Prostate Cancer Biomarkers: a Pilot Study. Int J Med Sci 2017, 14, 1-12, doi:10.7150/ijms.15783.
97. Perez-Rambla, C.; Puchades-Carrasco, L.; Garcia-Flores, M.; Rubio-Briones, J.; Lopez-Guerrero, J.A.; Pineda-Lucena, A. Non-invasive urinary metabolomic profiling

discriminates prostate cancer from benign prostatic hyperplasia. Metabolomics 2017, 13, 52, doi:10.1007/s11306-017-1194-y.
98. Jimenez-Pacheco, A.; Salinero-Bachiller, M.; Iribar, M.C.; Lopez-Luque, A.; Mijan-Ortiz, J.L.; Peinado, J.M. Furan and p-xylene as candidate biomarkers for prostate cancer. Urol Oncol 2018, 36, 243 e221-243 e227, doi:10.1016/j.urolonc.2017.12.026.
99. Lima, A.R.; Pinto, J.; Azevedo, A.I.; Barros-Silva, D.; Jeronimo, C.; Henrique, R.; de Lourdes Bastos, M.; Guedes de Pinho, P.; Carvalho, M. Identification of a biomarker panel for improvement of prostate cancer diagnosis by volatile metabolic profiling of urine. Br J Cancer 2019, 121, 857-868, doi:10.1038/s41416-019-0585-4.
100. Arlette, Y.-M.; Wiktoria, S.-L.; Renata, W.; Marcin, M.; Marek, R.; Roman, K.; Michał Jan, M. Metabolomic Heterogeneity of Urogenital Tract Cancers Analyzed by Complementary Chromatographic Techniques Coupled with Mass Spectrometry. Current Medicinal Chemistry 2019, 26, 216-231, doi: 10.2174/0929867324666171006150326.
101. Amante, E.; Salomone, A.; Alladio, E.; Vincenti, M.; Porpiglia, F.; Bro, R. Untargeted Metabolomic Profile for the Detection of Prostate Carcinoma-Preliminary Results from PARAFAC2 and PLS-DA Models. Molecules 2019, 24, doi:10.3390/molecules24173063.
102. Lima, A.R.; Pinto, J.; Barros-Silva, D.; Jeronimo, C.; Henrique, R.; Bastos, M.L.; Carvalho, M.; Guedes Pinho, P. New findings on urinary prostate cancer metabolome through combined GC-MS and (1)H NMR analytical platforms. Metabolomics 2020, 16, 70, doi:10.1007/s11306-020-01691-1.
103. Lima, A.R.; Pinto, J.; Carvalho-Maia, C.; Jeronimo, C.; Henrique, R.; Bastos, M.L.; Carvalho, M.; Guedes de Pinho, P. A Panel of Urinary Volatile Biomarkers for Differential Diagnosis of Prostate Cancer from Other Urological Cancers. Cancers (Basel) 2020, 12, doi:10.3390/cancers12082017.
104. Swanson, M.G.; Vigneron, D.B.; Tabatabai, Z.L.; Males, R.G.; Schmitt, L.; Carroll, P.R.; James, J.K.; Hurd, R.E.; Kurhanewicz, J. Proton HR-MAS spectroscopy and quantitative pathologic analysis of MRI/3D-MRSI-targeted postsurgical prostate tissues. Magnetic resonance in medicine 2003, 50, 944-954, doi:10.1002/mrm.10614.
105. Swanson, M.G.; Keshari, K.R.; Tabatabai, Z.L.; Simko, J.P.; Shinohara, K.; Carroll, P.R.; Zektzer, A.S.; Kurhanewicz, J. Quantification of choline- and ethanolamine-containing metabolites in human prostate tissues using ^{1}H HR-MAS total correlation spectroscopy. Magnetic resonance in medicine 2008, 60, 33-40, doi:10.1002/mrm.21647.
106. Tripathi, P.; Somashekar, B.S.; Ponnusamy, M.; Gursky, A.; Dailey, S.; Kunju, P.; Lee, C.T.; Chinnaiyan, A.M.; Rajendiran, T.M.; Ramamoorthy, A. HR-MAS NMR tissue

metabolomic signatures cross-validated by mass spectrometry distinguish bladder cancer from benign disease. J Proteome Res 2013, 12, 3519-3528, doi:10.1021/pr4004135.

107. Emwas, A.H.; Luchinat, C.; Turano, P.; Tenori, L.; Roy, R.; Salek, R.M.; Ryan, D.; Merzaban, J.S.; Kaddurah-Daouk, R.; Zeri, A.C., et al. Standardizing the experimental conditions for using urine in NMR-based metabolomic studies with a particular focus on diagnostic studies: a review. Metabolomics 2015, 11, 872-894, doi:10.1007/s11306-014-0746-7.

108. Spicer, R.A.; Salek, R.; Steinbeck, C. A decade after the metabolomics standards initiative it's time for a revision. Scientific Data 2017, 4, 170138, doi:10.1038/sdata.2017.138.

109. Lee, D.K.; Na, E.; Park, S.; Park, J.H.; Lim, J.; Kwon, S.W. *In Vitro* Tracking of Intracellular Metabolism-Derived Cancer Volatiles via Isotope Labeling. ACS Cent Sci 2018, 4, 1037-1044, doi:10.1021/acscentsci.8b00296.

Section 1.2 - NMR-based metabolomics studies of human prostate cancer tissue

Ana Rita Lima, Joana Pinto, Maria de Lourdes Bastos, Márcia Carvalho, Paula Guedes de Pinho

The article (DOI: 10.1007/s11306-018-1384-2) presented in this chapter was published by Springer Nature, in *Metabolomics*, in 2018, and is here presented in the form of "Accepted Manuscript". It is available online on:

https://link.springer.com/article/10.1007/s11306-018-1384-2

1.2.1 Abstract

Introduction: Prostate cancer (PCa) is one of the most prevalent cancers in men worldwide. Serum prostate-specific antigen (PSA) remains the most used biomarker in the detection and management of patients with PCa, in spite of the problems related with its low specificity, false positive rate and overdiagnosis. Furthermore, PSA is unable to discriminate indolent from aggressive PCa, which can lead to overtreatment. Early diagnosed and treated PCa can have a good prognosis and is potentially curable. Therefore, the discovery of new biomarkers able to detect clinically significant aggressive PCa is urgently needed.

Methods: This revision was based on an electronic literature search, using Pubmed, with Nuclear Magnetic Resonance (NMR), tissue and prostate cancer as keywords. All metabolomic studies performed in PCa tissues by NMR spectroscopy, from 2007 until March 2018, were included in this review.

Results: In the context of cancer, metabolomics allows the analysis of the entire metabolic profile of cancer cells. Several metabolic alterations occur in cancer cells to sustain their abnormal rates of proliferation. NMR proved to be a suitable methodology for the evaluation of these metabolic alterations in PCa tissues, allowing to unveil alterations in citrate, spermine, choline, choline-related compounds, lactate, alanine and glutamate.

Conclusion: The study of the metabolic alterations associated with PCa progression, accomplished by the analysis of PCa tissue by NMR, offers a promising approach for elucidating biochemical pathways affected by PCa and also for discovering new clinical biomarkers. The main metabolomic alterations associated with PCa development and promising biomarker metabolites for diagnosis of PCa were outlined.

Keywords:
Prostate cancer; Metabolomics; Tissues; Nuclear magnetic resonance spectroscopy

1.2.2 Introduction

Cancer is a serious health concern in the world, being one of the most important causes of death (Fuss and Cheng 2016). Prostate cancer (PCa) is one of the most prevalent cancers in men worldwide (Siegel et al. 2017) and the early-stage disease is usually asymptomatic. Currently available PCa diagnosis is mainly based on serum prostate-specific antigen (PSA) quantification, digital rectal examination (DRE) and prostate biopsy (PB). However, PSA is far from being an ideal biomarker as it lacks sensitivity and specificity and it is unable to distinguish indolent from aggressive PCa. PB is a very invasive technique giving false negative results, mainly in low grade and in heterogeneously distributed PCa (Spur et al. 2013). Furthermore, PCa if early diagnosed, when organ-confined, has a good prognosis and it is potentially curable, but advanced or metastatic PCa can be deadly. Given the magnitude of the PCa burden, continuous efforts have been made by the scientific community toward the discovery of new biomarkers for PCa diagnosis.

Metabolomics is a relatively novel approach for evaluating the entire measurable metabolome, that includes all endogenous and exogenous low molecular weight compounds in a biological system, giving a biochemical “snapshot” of an organism’s metabolic state. The detection of metabolite profile deviations in fluids (Sreekumar et al. 2009), cells (Lima et al. 2018a, b), or tissues (Kumar et al. 2014) by comparing the relative amount of these compounds in the samples under study with that of the control group (e.g., PCa patients *vs*. healthy individuals) may be translated into valuable disease biomarkers (Lima et al. 2016). It is well-established that cancer cells display distinct phenotypes from normal cells. These different phenotypes translate into deep metabolic alterations, which are indispensable to cancer development and progression. Metabolomics is an ideal approach to identify these metabolic alterations and consequently to discover new diagnostic and prognostic biomarkers, new therapeutic targets and also to better understand the cancer cell biochemistry (Lima et al. 2016).

Several different matrices can be used in metabolomic studies. In biomedical field, the most commonly used matrices are immortalized or primary cultured cells, tissues and biofluids, mainly urine and blood. Tissue samples are collected in an invasive way but present the value of being the most suitable matrix to determine organ-specific metabolic fingerprints (Lin et al. 2007).

Taking into consideration the high prevalence of PCa and the important drawbacks of the currently available biomarker, this review will focus on the metabolomic studies performed in PCa tissues by nuclear magnetic resonance (NMR) spectroscopy, updating previous reviews in this area (DeFeo et al. 2011; Decelle and Cheng 2014) and

summarizing the most frequent metabolic alterations associated with PCa. We believe that, in the future, these metabolic alterations could be used as novel biomarkers for PCa, as well as potential targets for more efficient treatments.

1.2.3 Prostate cancer diagnosis and prognosis

PCa is one of the most commonly diagnosed cancers in men. In fact, the predictions for 2017 indicated that PCa will be the most prevalent cancer in men in USA, with 161,360 new cases and 26,730 estimated deaths (Siegel et al. 2017). PCa is characterized by a slow growing nature (Kumar et al. 2016), though more aggressive forms of PCa (approximately 25%) can metastasize to the bones (majority) and other organs like lymph nodes and lungs (Aoun et al. 2014; Dimakakos et al. 2014; Yang et al. 2010). Metastatic PCa is a heterogeneous disease with an extensive range of different malignant progression and aggressiveness, and hence, the 5-year survival for men with metastatic disease is very low (28%). Despite this, PCa has a long latency period and is potentially curable if diagnosed at early stages and appropriately treated (Kumar et al. 2016). Since PCa is often initially asymptomatic, highly efficient screening technologies for effective detection of PCa potential biomarkers are indispensable in order to diagnose and treat PCa patients at an early stage (Yang et al. 2010).

Since the earliest 1990s, the introduction of PSA screening test markedly changed the management of PCa, with the number of PCa cases diagnosed at an early stage of the disease largely increased (Decelle and Cheng 2014). Serum PSA levels higher than 4.0 ng/mL were considered an indication of PCa (Dimakakos et al. 2014). However, after biopsy (mandatory for definitive diagnosis), only ~ 25% of men with PSA > 3.0 ng/mL were diagnosed with PCa (Alberts et al. 2017). Recently, the use of serum PSA for PCa screening of all senior male population started to be contested (Moyer and Force 2012), since this biomarker is not able to differentiate patients with aggressive PCa from those with indolent disease (slow growing, asymptomatic, non-life-threatening cancers) (McDunn et al. 2013), which may lead to an overdiagnosis (Welch and Black 2010). The overdiagnosis leads to prescription of aggressive treatments (prostatectomy, chemotherapy and radiotherapy) in PCa patients with indolent disease, with important side effects (e.g., androgen deprivation therapy leads to hypogonadism and consequently increased risk of cardiovascular disease, diabetes, and osteoporosis). For indolent PCa, those aggressive treatments have more disadvantages than advantages for the patient´s health and life quality (Drake et al. 2009; Decelle and Cheng 2014). Although PSA presents limited sensitivity and specificity to PCa

(Roberts et al. 2011; Trock 2011), this test has a good specificity for prostate diseases in general, meaning that it is organ- but not cancer-specific (Schalken et al. 2014) and, therefore, its levels may be elevated as a consequence of benign prostate hyperplasia (BPH) or other prostate diseases. In addition, some PCa patients may present PSA levels below the established cutoff value (4.0 ng/mL) (Dimakakos et al. 2014) and false negative results may occur (Roberts et al. 2011; Barry 2009; Dimakakos et al. 2014). Furthermore, there are also ethnic variations which influence the performance of the serum PSA test, as only 25–35% of Caucasians and Hispanics with a PSA level in the 2–10 ng/mL range have positive biopsies for PCa, whereas up to 70–80% of African-Americans in this same range have a positive biopsy (Lam et al. 2003). As the sensitivity and specificity of the serum PSA test is less than 75%, this is a rather imperfect PCa marker. In order to try to minimize this problem, at least two PSA measurements are recommended by European Association of Urology Guidelines on Prostate Cancer before PB (Gomez-Gomez et al. 2017; Heidenreich et al. 2014). Although several PSA derived indices have been developed (e.g., free PSA, complex PSA, PSA density and PSA velocity), none has so far attained widespread acceptance.

DRE is another commonly used PCa diagnostic technique, frequently used in combination with PSA. Although, definitive diagnosis of PCa is based on histopathological verification of adenocarcinoma in PB specimens. The diagnosis based on DRE alone can miss more than 50% of PCa patients, whereas PB is an invasive diagnostic technique (Drake et al. 2009; Decelle and Cheng 2014). Furthermore, PB may also lead to false negative results specially when PCa has a small size, and the lesions are dispersal (Fuss and Cheng 2016).

Other strategy used to try to improve PCa diagnosis and decrease overdiagnosis is the use of Nomogram-based PCa risk calculators (RC) (e.g. European Randomised Study for Screening of Prostate Cancer (ERSPC-RC)) (GomezGomez et al. 2017). RC are easy and accessible tools that can be used in the clinical practice to help in the decision of performing or not a PB, thus decreasing the number of unnecessary PB. However, these tools can also lead to PCa underestimation, mainly in patients with low risk values, and overestimation in patients with high risk values (GomezGomez et al. 2017).

The lack of a consistent biomarker for PCa diagnosis and monitoring, highlights the need for novel, specific, sensitive, and cost effective biomarkers (Dimakakos et al. 2014). Taking into consideration the problems associated with the currently used PCa diagnostic tools, and consequently the important problems of overdiagnosis and overtreatment observed, it is urgent to discover a new biomarker (or a panel of biomarkers) capable to

discriminate aggressive PCa from indolent PCa. For this purpose, metabolomic studies performed by NMR spectroscopy of PCa tissues are a very promising approach (Fuss and Cheng 2016).

1.2.4 Metabolomics: an "omic" platform technology for biological systems

The well-known "omics" technologies include genomics (evaluation of genome), transcriptomics (evaluation of gene expression) and proteomics (evaluation of proteins). Importantly, the integration of these three approaches may not be enough to explain all alterations occurring in the organism as a consequence of a disease or a xenobiotic exposure, as these "omics" do not evaluate the end point markers of the occurred alteration. To overcome this limitation, another "omic" technique was proposed, known as metabolomics (evaluation of all metabolites in a biological system), to enable the assessment of alterations that are not visible at a genomic and/or proteomic level. Metabolites are the end products of cellular metabolism and reflect a combination between environment and alterations in gene activation, gene expression, proteins, enzyme activity, microbiome, and alterations in metabolic pathways (Spratlin et al. 2009; Roberts et al. 2011; Markley et al. 2017). Other advantage of metabolomics is that the study of the entire metabolome gives a much more comprehensive perspective of cancer biochemistry than the measurement of a single metabolite and/or a single metabolic pathway, allowing a better understanding of cancer development and progression (Fuss and Cheng 2016). The total number of metabolites present in human organism is at the moment unknown, but it is believed that the human metabolome encompasses more than several thousands of metabolites (Spratlin et al. 2009; Zhang et al. 2014).

During neoplastic transformation, the energy needs and synthesis requirements of cells increase leading to metabolic alterations, which can be assessed by metabolomics approaches (Roberts et al. 2011; Lucarelli et al. 2015). Furthermore, metabolomics can be combined with other "omics" methodologies to better understand cancer cell biochemistry. The use of NMR spectroscopy in metabolomic studies has the advantage to preserve the samples (nondestructive), which can be further used for other metabolomic studies and/or gene expression evaluation, for example (Hansen et al. 2016).

Despite the advantages of NMR-based metabolomics, problems with the design of the metabolomic studies have challenged the validation of new biomarkers. The most relevant issues include the heterogeneity in patient populations, the small number of subjects in the tested and control groups, which leads to lack of statistical power, and the presentation of

the results in form of metabolite lists without reference to the critical metabolites that are altered or the degree of their perturbations. Regardless all aforementioned difficulties to obtain relevant and reliable results, metabolomics has great potential for the discovery of new cancer biomarkers.

1.2.5 Nuclear magnetic resonance spectroscopy: an analytical technique used in metabolomic studies

The human metabolic profile has a huge complexity and, hence, the combination of different analytical techniques is usually required in order to detect the maximum number of metabolites, as a single analytical technique allows the assessment of only part of the metabolome. The most commonly used analytical techniques in metabolomic studies are mass spectrometry (MS) and nuclear magnetic resonance (NMR) spectroscopy (Roberts et al. 2011; Kumar et al. 2016). The combination of NMR and MS platforms offers the best approach available nowadays for a more holistic evaluation of the metabolome (Monteiro et al. 2013; Cuperlovic-Culf et al. 2010). Both MS and NMR can be combined with multivariate statistical analysis (MVA), facilitating data interpretation, to investigate the metabolic state of the individual through analysis of biological samples (e.g., tissues or biological fluids) (Gao et al. 2012). MS, compared with NMR, is able to detect metabolites that exist at lower concentrations (< μM) due to its higher sensitivity (Monteiro et al. 2013). Nevertheless, MS techniques have some disadvantages, such as the requirement of sample pre-treatment procedures and the bias introduced by several factors, such as ionization efficiency, extraction efficiency, and molecule fragmentation behavior (Trock 2011; Roberts et al. 2011; Spratlin et al. 2009). On the other hand, NMR spectroscopy has several advantages over MS that include (i) minimal sample preparation, (ii) non-destructive analysis, (iii) analysis of liquid and solid matrices, (iv) high intra- and inter-laboratory reproducibility, (v) information about the chemical environment, (vi) detection of different nuclei, such as ^{1}H, ^{13}C, ^{15}N or ^{18}O. In addition, NMR acquisition is faster and gives results in a single experiment (ca. 10–30 min for 1D ^{1}H NMR) (Trock 2011; Kosmides et al. 2013; Kumar et al. 2014; Cuperlovic-Culf et al. 2010; Lenz and Wilson 2007; Markley et al. 2017). Another important advantage of NMR studies in prostate cancer tissues is that the results obtained through the evaluation of PCa tissues by NMR can be used in clinical practice since there is a relationship between the results obtained through NMR tissue analysis and the results obtained in *in vivo* assays (Hansen et al. 2016; Fuss and Cheng 2016). Hence, the results obtained through the evaluation of PCa tissues by NMR have the potential to be

translated to clinical practice in a noninvasive manner. Using magnetic resonance spectroscopy imaging (MRSI), it is possible to visualize *in vivo* prostate metabolites and not only the tissue anatomy, this will improve a noninvasive PCa diagnosis by translation to the clinic the results obtained by NMR tissue analysis (Fuss and Cheng 2016; Hansen et al.2016).

The NMR spectra from biological samples are very complex with several overlapped signals. However, it is possible to suppress or enhance specific signals through the optimization of pulse sequences and acquisition parameters, taking advantage of physical properties of the different resonating functional groups (Moestue et al. 2011). In the standard one dimension (1D) experiment, called 1D pulse-and-acquire experiment, both large (broad resonances) and small molecules (narrow resonances) contribute to the spectrum with the intensity proportional to their concentration (Dunn et al. 2005).

It is also possible to use edited pulse programs such as diffusion-edited experiment to select only the signals from macromolecules or transverse relaxation (T2)-edited experiment (Carr–Purcell–Meiboom–Gill experiment) for detection of small molecules (Dunn et al. 2005). In addition, 2D NMR methods are of paramount importance to facilitate the identification of overlapped metabolites (Ebbels and Cavill 2009; Cuperlovic-Culf et al. 2010). 1H–1H Total correlation spectroscopy (TOCSY) and 1H–13C heteronuclear single quantum coherence (HSQC) are the most commonly used 2D NMR experiments in metabolomic studies (Ebbels and Cavill 2009; Cuperlovic-Culf et al. 2010).

Before 1990s, the analysis of intact tissue by traditional NMR techniques was possible although the NMR spectra unveiled very low resolution and sensitivity due to the high heterogeneity of semi-solid samples which caused differences in magnetic field (DeFeo et al. 2011). In addition, molecules having low internal molecular motion lead to formation of 1H–1H dipolar couplings, quadrupolar interactions and anisotropic chemical shift. With the development of high-resolution magic angle spinning (HR-MAS) NMR, in the late 1990s, these limitations were overcome. In HR-MAS, the sample is spinning (at 4–6 kHz) at an angle of 54.7° (magic angle) with respect to the direction of the external magnetic field applied, which increase internal molecular motion allowing the reduction of the line broadening effects (Kumar et al. 2014; Moestue et al. 2011; DeFeo et al. 2011; Beckonert et al. 2010). Thus, the HR-MAS NMR spectra of tissues show the metabolites present in the sample with better resolution and reproducibility, in a non-destructive fashion, allowing to perform further analysis (e.g., histopathological analysis or gene expression assays) on the same tissue (Moestue et al. 2011). This is particularly important in PCa diagnosis once the histopathological evaluation of prostate tissue is mandatory (Fuss and Cheng 2016).

Furthermore, it is also possible to perform transcriptomic studies in the same tissue samples used in HRMAS NMR metabolomic studies since no transcriptomic data is lost during acquisition, as concluded by Santos et al. (2010).

Beyond the analysis of intact tissue, it is also possible to perform extraction of polar and non-polar metabolites for subsequent liquid NMR analysis (Beckonert et al. 2007). The spectral pattern obtained for tissue extracts and intact tissue is similar (Kumar et al. 2014). The extraction step presents some limitations such as time-consuming, destructive, larger amount of tissue required, lower accuracy, and chemical degradation of some metabolites (Lenz and Wilson 2007; Kumar et al. 2014). Nevertheless, when tissue extracts are used, it is possible to concentrate samples through lyophilization followed by resuspension in a small volume of deuterated solvent (Lenz and Wilson 2007; Kumar et al. 2014). In addition, some metabolites can only be observed using the extraction protocol, likely due to the location of metabolites in highly restricted environments (Dunn et al. 2005). Furthermore, the use of extraction protocols has also the advantage to completely stop the metabolism, allowing to capture an unbiased snapshot of the metabolism (Kumar et al. 2014; Moestue et al. 2011; Dunn et al. 2005).

1.2.6 PCa metabolomic studies using tissue by NMR spectroscopy

The first NMR studies performed in PCa tissue have more than twenty years and, despite these studies look archaic, they established the basis for the metabolomic studies (DeFeo et al. 2011). These studies were mainly performed in tissues extracts or intact tissues from prostate before HR-MAS development, showing poor spectral resolution.

A healthy prostate accumulates and secretes citrate and spermine, once these two metabolites are important constituents of prostatic fluid, though both these functions are lost during PCa progression (Lima et al. 2016). Several NMR studies confirmed the reduction in spermine levels associated with PCa development and progression (Table 1.4; Fig. 1.4) (Giskeodegard et al. 2013; Swanson et al. 2008; Stenman et al. 2011). The high levels of citrate characteristic of healthy prostate result from the inhibition of mitochondrial aconitase (*m*-aconitase), that prevents citrate oxidation in these cells. *m*-Aconitase is inhibited by high intracellular concentrations of zinc. With PCa development, the zinc levels decrease and consequently *m*-aconitase is no longer inhibited and can catalyze citrate oxidation (Lima et al. 2016; Kumar et al. 2016). The reduction in citrate levels, observed in PCa tissues, was confirmed in several NMR studies (Table 1.4; Fig. 1.4) (Dittrich et al. 2012; Giskeodegard et al. 2013; Swanson et al. 2008; Stenman et al. 2011; Keshari et al. 2011; van Asten et al.

2008). In a more recent study, the reduction of citrate and spermine levels was correlated with ERGhigh (overexpression of ERG which is associated with cells proliferation and invasion) in intact PCa tissues (Hansen et al. 2016) (Table 1.4). One of the most promising gene rearrangements for PCa diagnosis is the TMPRSS2: ERG fusion gene. This fusion gene is formed by the translocation between the androgen-regulated transmembrane protease, serine 2 (TMPRSS2) gene transcriptional promoter and the ETS related oncogene (ERG (protooncogene)) (Hansen et al. 2016). This alteration results in an increased expression of transcription factors involved in cell proliferation, namely the overexpression of ETS genes encoding the E26 family (ERG gene), which affects the androgen pathway. This alteration leads to androgen independency and, consequently, PCa progression (Rostad et al. 2009). Hansen et al. (2016) correlated the overexpression of this fusion gene (ERGhigh) with low levels of citrate and spermine and with an increase of PCa aggressiveness (Hansen et al. 2016).

Other frequent alterations associated with PCa are the increase in choline and/or choline-related metabolites and lipid levels (Table 1.4; Fig. 1.4) (Keshari et al. 2011; van Asten et al. 2008; Madhu et al. 2014). Choline and choline-related metabolites are the major precursors and degradation products of phospholipid membrane assembly and catabolism, and since cancer cells show a high proliferative phenotype and high rates of cellular division, it was expected to see alterations in those metabolites. Other deviation that can be related with the alteration in membrane metabolism is the increase of *myo*-inositol (Vandergrift et al. 2018) and *scyllo*-inositol levels, which are involved in cell proliferation (Table 1.4; Fig. 1.4) (Swanson et al. 2008; Stenman et al. 2011).

Taking into consideration the results that highlight deviations in cellular membrane metabolism and since one of the major components of membranes are phospholipids, several studies (Komoroski et al. 2011; Keshari et al. 2011) were performed by ^{31}P and ^{1}H NMR aiming to evaluate the alterations occurring in phospholipid metabolism in the presence of PCa. These studies unveiled significant alterations in the levels of important constituents of phospholipid cell membranes, such as phosphoethanolamine and glycerophosphoethanolamine (Table 1.4) (Komoroski et al. 2011; Keshari et al. 2011).

Madhu et al. (2014) determined the alanine levels in prostate tissues by HR-MAS ^{1}H NMR spectroscopy (Madhu et al. 2014). Consistent with previous studies, alanine levels were increased in PCa tissues (Table 1.4; Fig. 1.4) (Madhu et al. 2014; Tessem et al. 2008; van Asten et al. 2008). The results of these studies also revealed an increase in glutamate levels in high grade PCa when compared with low grade PCa and benign prostate samples, which may be due to an increase in glutaminolysis, as this mechanism can be used by

cancer cells to produce energy (Table 1.4; Fig. 1.4) (Madhu et al. 2014). Through glutaminolysis, glutamate is converted into α-ketoglutarate, which is further incorporated into the tricarboxylic acid cycle (Krebs cycle) leading to citrate formation. However, the transformation of α-ketoglutarate into citrate can be accomplished to the reversal of the tricarboxylic acid cycle through reductive carboxylation. Hypoxia promotes this transformation of oxidation to reductive carboxylation and this shift results in lipid synthesis and tumor growth (Lima et al. 2016; Kumar et al. 2016). The significant increase in lactate concentration found in prostate cancer biopsies (Tessem et al. 2008; van Asten et al. 2008) can be explained by the alteration in energy metabolism due to “Warburg effect”. “Warburg effect” is a well-established metabolic alteration associated with cancer development and progression that is characterized by an increase in the use of anaerobic pathway (glycolytic pathway) to produce energy even in presence of oxygen, which leads to lactate production (Lima et al. 2016). Increased levels of lactate may be associated with the tumor stage and cancer outcome (Tessem et al. 2008). The intensification in glycolytic flux and the increased protein synthesis in cancer cells are possible explanations for the elevated levels of alanine (Table 1.4; Fig. 1.4) (Tessem et al. 2008).

Table 1.4: Metabolomic studies performed in tissues from PCa patients using NMR technology.

Analytical platform	PCa group	Control group	Sample treatment	Statistical methods	Main results	Ref.
HR-MAS ^{1}H-NMR	*n*=15	*n*=32 benign	Intact	Z statistics	↑ Phosphocholine; Glycerolphosphocholine; Phosphoethanolamine; Glycerophosphoethanolamine ↓ Ethanolamine	(Swanson et al. 2008)
HR-MAS ^{1}H-NMR	*n*=16 malignant prostate biopsies	*n*=82 benign biopsies	Intact	Linear mixed effects model procedure	↑ Lactate; Alanine	(Tessem et al. 2008)
HR-MAS ^{1}H-NMR	*n*=18 malignant prostate needle biopsies	*n*=30 benign needle biopsies	Intact	Two-tailed unpaired t-test	↑ total choline/citrate; choline/creatinine; (glycerol-phosphocholine +phosphorylcholine)/creatinine; lactate/alanine ↓ Citrate/creatinine	(van Asten et al. 2008)
HR-MAS ^{1}H-NMR	*n*=27 from RP	*n*=54 nonmalignant from RP	Intact	NA	↑ Omega-6 PUFA	(Stenman et al. 2009)

Analytical platform	PCa group	Control group	Sample treatment	Statistical methods	Main results	Ref.
HR-MAS ^{1}H-NMR	*n*=16 from patients with recurrence after prostatectomy	*n*=16 from patients without recurrence after prostatectomy	Intact	PCA	Alteration in the levels of spermine, glutamine, *myo*-inositol, phosphoryl choline, *scyllo*-inositol, and glutamate Metabolic profiles obtained were able to predict recurrences with an accuracy of 78%.	(Maxeiner et al. 2010)
HR-MAS ^{1}H-NMR	*n*=13 LG + 22 HG	*n*=14 benign	Intact	Student t test	↑ Phosphocholine and glycerophosphocholine in high grade PCa when compared with low grade ↑ Choline + creatinine; phosphocholine; glycerophosphocholine; phosphoethanolamine; glycerolphosphoethanolamine ↓ Citrate	(Keshari et al. 2011)
^{31}P NMR	*n*=8 from transurethral resections or RP	*n*=13 BPH samples from transurethral resections or RP	Extraction with perchloric acid	NA	Significant alterations in phosphoethanolamine and glycerophosphoethanolamine	(Komoroski et al. 2011)

Analytical platform	PCa group	Control group	Sample treatment	Statistical methods	Main results	Ref.
HR-MAS ^{1}H-NMR	*n*=41 from RP	*n*=108 nonmalignant from RP	Intact	Linear Regression	↑ Choline compounds; *Scyllo*-inositol ↓ *Myo*-inositol	(Stenman et al. 2011)
HR-MAS ^{1}H-NMR	*n*=30 from LG + 81 from HG cancer from prostatectomies	*n*=47 normal adjacent	Intact	PLS PLS-DA	↑ (total choline+creatine+polyamines)/ citrate ↓ Citrate; spermine The metabolic alterations were correlated with Gleason score and can differentiate malignant from normal adjacent tissues samples with a sensitivity of 86.9% and a specificity of 85.2%	(Giskeodegard et al. 2013)
HR-MAS ^{1}H-NMR	*n*=6 LG + 6 HG	*n*=10 benign	Intact	Student t test	↑ Alanine; ↑ Glutamate and total choline in high grade PCa	(Madhu et al. 2014)
HR-MAS ^{1}H-NMR	*n*=95	n=34 benign adjacent tissue	Intact	PCA PLS-DA	↓ Citrate and spermine in ERG_{high} PCa samples	(Hansen et al. 2016)

Analytical platform	PCa group	Control group	Sample treatment	Statistical methods	Main results	Ref.
HR-MAS ^{1}H-NMR	*n*=6 from patients treated with Degarelix + 7 untreated PCa from prostatectomies	*n*=10 benign from untreated patients from prostatectomies	Intact	PCA OPLS-DA	↑ Lactate, alanine and total choline in high grade PCa when compared with benign samples from untreated patients ↓ Lactate and total choline in samples treated with Degarelix	(Madhu et al. 2016)
HR-MAS ^{1}H-NMR	*n*=50 patients that developed recurrence after prostatectomy	*n*=60 patients that do not develop recurrence after prostatectomy	Intact	PLS-DA LMM Mann–Whitney U-tests Spearman's rank	↓ Spermine and citrate associated with increased risk of recurrence ↑ Total choline + Creatine /Spermine and total Choline + Creatine /Citrate ratios were associated with increased risk of recurrence	(Braadland et al. 2017)
HR-MAS ^{1}H-NMR	*n*=365 from prostatectomies	*n*=15 from BPH *n*=14 from from cancer-negative patients	Intact	Linear regressions ANOVA Kruskal-Wallis-Wilcoxon test Student's t-test Mann-Whitney-Wilcoxon test Canonical analysis	↑ *Myo*-inositol HRMAS NMR-based metabolomics was able to predict prostate cancer biochemical recurrence and survival time.	(Vandergrift et al. 2018)

↑increased in PCa; ↓decreased in PCa; ^{1}H NMR: proton nuclear magnetic resonance; LLM: Linear mixed modelling; ^{31}P NMR: phosphorus nuclear magnetic resonance; BPH: benign prostate hyperplasia; HG: high grade; HR-MAS: high resolution magic angle spinning; LG: low grade; NA: not available; OPLS-DA: orthogonal partial least squares discriminant analysis; PCA: principal component analysis; PCa: prostate cancer; PUFA: polyunsaturated fatty acids; RP: radical prostatectomy; TURP: transurethral resection.

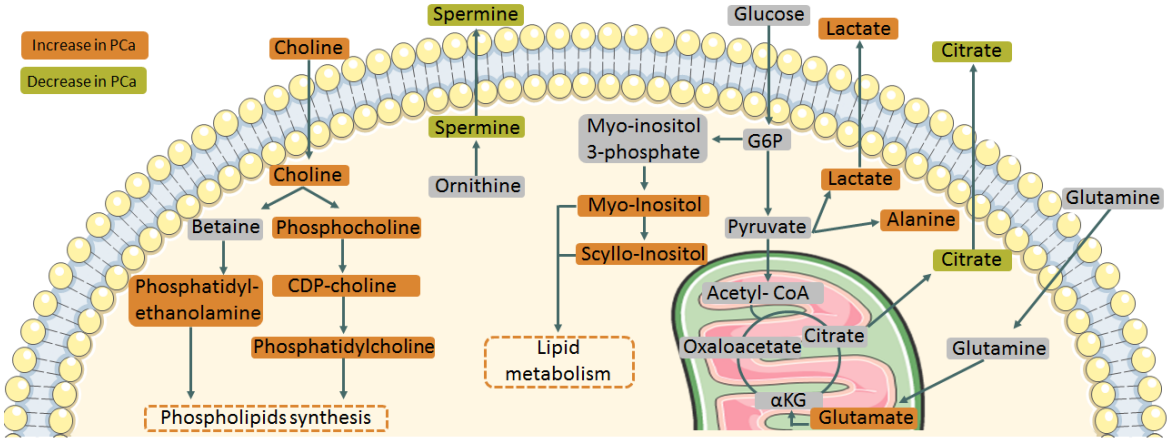

Figure 1.4: Schematic representation of the main metabolomic alterations associated to PCa development based in the NMR metabolomic studies presented in Table 1.4. (G6P, glucose 6-phosphate; αKG, α-ketoglutarate).

In another study, Stenman et al. (2009) evaluated the levels of polyunsaturated omega-6 fatty acids (PUFAs) in nonmalignant and malignant prostate tissue samples by HR-MAS ^{1}H NMR. There are two types of PUFAs associated with PCa development: omega-3, which are believed to inhibit PCa development, and omega-6, which promote PCa development. The results obtained from this study revealed that omega-6 fatty acids were only detected in PCa samples and were correlated with Gleason scores and worst tumor stages (Table 1.4) (Stenman et al. 2009).

Metabolomics can also be applied to follow up the patient's response to therapeutics. One of the major concerns of PCa treatment is the development of recurrences after treatment. Hence, in order to discriminate the PCa cases that will develop recurrences from PCa cases that will not develop recurrence after treatment, Maxeiner et al. (2010) compared the metabolic profile at the time of prostatectomy of PCa patients that developed recurrence after prostatectomy with that of PCa patients that did not develop recurrence (Maxeiner et al. 2010). The results showed that the levels of some metabolites, namely spermine, glutamine, *myo*-inositol, phosphoryl choline, *scyllo*-inositol, and glutamate, previously associated with PCa development, were also altered when comparing these two groups of PCa patients. These results indicated that the metabolic alterations occurring in the recurrence cases after prostatectomy are similar to that accompanying the development of PCa. It was also shown that significant alterations in spermine synthesis, phospholipid membrane synthesis and hydrolysis, and energy metabolism were associated with the development of PCa recurrence (Table 1.4) (Maxeiner et al. 2010). More recently, another study with a similar aim was performed by Braadland et al. (2017). In this study, the

increase in the levels of citrate, spermine and total choline + creatine/ spermine and total choline + creatine/citrate ratios were associated with an increased risk of recurrence (Braadland et al. 2017).

One of the most frequent treatments for PCa is the use of androgen deprivation therapy (Merseburger et al. 2015) to decrease androgen levels and consequently cancer remission. The metabolomic effects of a new gonadotropin-releasing hormone antagonist (degarelix) were recently studied by HR-MAS ^{1}H NMR (Madhu et al. 2016). In this study, malignant tissues from PCa patients treated with degarelix were compared with malignant and benign tissues from untreated PCa patients. The results showed a significant reduction in levels of lactate and total choline in tissues from patients treated with degarelix which may indicate a reversion of the "Warburg effect" (decreased glycolysis), and alteration in membrane phospholipid metabolism, which may indicate a reduction of cell division (cancer progression). In addition, an increase in lactate, alanine and total choline levels was also observed in high grade PCa when compared to benign samples from untreated patients (Table 1.4) (Madhu et al. 2016). Complementary information of all aforementioned studies is compiled in Table 1.4.

1.2.7 Conclusion

Metabolomics is a relatively new "omics" approach that already proved to have a tremendous potential for biomarker discovery. Beyond the discovery of new biomarkers for PCa detection, metabolomics also allows to find indicative biomarkers of cancer prognosis, disease progression, therapeutic response and may also help to identify new therapeutic targets, potentially leading to better therapeutic outcomes and improvement on the quality of life of treated patients.

The use of tissues in metabolomic studies allows the evaluation of the specific metabolic fingerprint of PCa and the identification of metabolic differences between PCa and normal prostate. However, and taking into consideration that PCa is a very complex disease, for a reliable diagnosis it will be important to use more than one parameter. Focusing in tissue PCa metabolomic studies performed by NMR spectroscopy, the mainly reported metabolic alterations included:

(i) the decrease in citrate and spermine levels, which indicates that prostate cells lose their ability to accumulate both metabolites with cancer development;

(ii) the increase in choline and choline-related compounds which indicates alterations in cell membrane synthesis and catabolism. The dysfunction in membrane metabolism was

also confirmed by alterations in the levels of phospholipid components and in *myo*-inositol and *scyllo*-inositol;

(iii) the increase in lactate and alanine levels which may be due to alterations in energy metabolism, probably associated with the “Warburg effect”, and the increase of energy demand caused by the high proliferative state of cancer cells;

(iv) alteration in glutamate levels, once glutaminolysis pathway can be used by cancer cells for energy production.

In the future, the results obtained by NMR analysis of prostate tissues have the potential to be translated into clinical practice. Furthermore, these results have the potential to be correlated with *in vivo* assays. Despite the potential of NMR-based metabolomics to identify and interpret the metabolic alterations occurring in PCa, there are still some challenges that need to be addressed in future studies before a new biomarker can be translated to clinical practice, namely the evaluation of inter-laboratory and inter-population reproducibility of cancer metabolic profile, aiming to prove the specificity of metabolic signature to cancer type. The influence of important confounder factors, such as age, lifestyle habits or other diseases, that can seriously interfere in the biological interpretation have to be considered. Furthermore, the NMR analyses requires expensive instrumentation and specialized technicians, which could difficult the implementation of NMR in the clinical practice.

1.2.8 References

Alberts, A. R., Schoots, I. G., Bokhorst, L. P., Drost, F. H., van Leenders, G. J., Krestin, G. P., et al. (2017). Characteristics of Prostate Cancer Found at Fifth Screening in the European Randomized Study of Screening for Prostate Cancer Rotterdam: Can we selectively detect high-grade prostate cancer with upfront multivariable risk stratification and magnetic resonance imaging? European Urology. https://doi.org/10.1016/j.eurur o.2017.06.019.

Aoun, F., Peltier, A., & van Velthoven, R. (2014). A comprehensive review of contemporary role of local treatment of the primary tumor and/or the metastases in metastatic prostate cancer. BioMed Research International. https ://doi.org/10.1155/2014/50121 3.

Barry, M. J. (2009). Screening for prostate cancer: The controversy that refuses to die. The New England Journal of Medicine, 360(13), 1351–1354. https ://doi.org/10.1056/NEJMe 09011 66.

Beckonert, O., Coen, M., Keun, H. C., Wang, Y., Ebbels, T. M., Holmes, E., et al. (2010). High-resolution magic-angle-spinning NMR spectroscopy for metabolic profiling of intact tissues. Nature Protocols, 5(6), 1019–1032. https ://doi.org/10.1038/nprot .2010.45.

Beckonert, O., Keun, H. C., Ebbels, T. M., Bundy, J., Holmes, E., Lindon, J. C., et al. (2007). Metabolic profiling, metabolomic and metabonomic procedures for NMR spectroscopy of urine, plasma, serum and tissue extracts. Nature Protocols, 2(11), 2692–2703. https ://doi.org/10.1038/nprot .2007.376.

Braadland, P. R., Giskeodegard, G., Sandsmark, E., Bertilsson, H., Euceda, L. R., Hansen, A. F., et al. (2017). Ex vivo metabolic fingerprinting identifies biomarkers predictive of prostate cancer recurrence following radical prostatectomy. British Journal of Cancer, 117(11), 1656–1664. https ://doi.org/10.1038/ bjc.2017.346.

Cuperlovic-Culf, M., Barnett, D. A., Culf, A. S., & Chute, I. (2010). Cell culture metabolomics: Applications and future directions. Drug Discovery Today, 15(15–16), 610–621. https ://doi. org/10.1016/j.drudi s.2010.06.012.

Decelle, E. A., & Cheng, L. L. (2014). High-resolution magic angle spinning 1H MRS in prostate cancer. NMR in Biomedicine, 27(1), 90–99. https ://doi.org/10.1002/nbm.2944.

DeFeo, E. M., Wu, C. L., McDougal, W. S., & Cheng, L. L. (2011). A decade in prostate cancer: From NMR to metabolomics. Nature Reviews Urology, 8(6), 301–311. https ://doi.org/10.1038/nruro l.2011.53.

Dimakakos, A., Armakolas, A., & Koutsilieris, M. (2014). Novel tools for prostate cancer prognosis, diagnosis, and follow-up. BioMed Research International. https ://doi.org/10.1155/2014/89069 7.

Dittrich, R., Kurth, J., Decelle, E. A., DeFeo, E. M., Taupitz, M., Wu, S., et al. (2012). Assessing prostate cancer growth with citrate measured by intact tissue proton magnetic resonance spectroscopy. Prostate Cancer and Prostatic Diseases, 15(3), 278–282. https ://doi.org/10.1038/pcan.2011.70.

Drake, R. R., White, K. Y., Fuller, T. W., Igwe, E., Clements, M. A., Nyalwidhe, J. O., et al. (2009). Clinical collection and protein properties of expressed prostatic secretions as a source for biomarkers of prostatic disease. Journal of Proteomics, 72(6), 907– 917. https ://doi.org/10.1016/j.jprot .2009.01.007.

Dunn, W. B., Bailey, N. J., & Johnson, H. E. (2005). Measuring the metabolome: Current analytical technologies. Analyst, 130(5), 606–625. https ://doi.org/10.1039/b4182 88j.

Ebbels, T., & Cavill, R. (2009). Bioinformatic methods in NMR-based metabolic profiling. Progress in Nuclear Magnetic Resonance Spectroscopy, 55, 361–374.

Fuss, T. L., & Cheng, L. L. (2016). Evaluation of cancer metabolomics using ex vivo high resolution magic angle spinning (HRMAS) magnetic resonance spectroscopy (MRS). Metabolites. https: //doi. org/10.3390/metab o6010 011.

Gao, H., Dong, B., Jia, J., Zhu, H., Diao, C., Yan, Z., et al. (2012). Application of ex vivo (1)H NMR metabonomics to the characterization and possible detection of renal cell carcinoma metastases. Journal of Cancer Research and Clinical Oncology, 138(5), 753–761. https ://doi.org/10.1007/s0043 2-011-1134-6.

Giskeodegard, G. F., Bertilsson, H., Selnaes, K. M., Wright, A. J., Bathen, T. F., Viset, T., et al. (2013). Spermine and citrate as metabolic biomarkers for assessing prostate cancer aggressiveness. PLoS ONE, 8(4), e62375. https://doi.org/10.1371/journ al.pone.00623 75.

Gomez-Gomez, E., Carrasco-Valiente, J., Blanca-Pedregosa, A., BarcoSanchez, B., Fernandez-Rueda, J. L., Molina-Abril, H., et al. (2017). European Randomized Study of Screening for Prostate Cancer Risk Calculator: External validation, variability, and clinical significance. Urology, 102, 85–91. https ://doi.org/10.1016/j. urolo gy.2016.11.004.

Hansen, A. F., Sandsmark, E., Rye, M. B., Wright, A. J., Bertilsson, H., Richardsen, E., et al. (2016). Presence of TMPRSS2-ERG is associated with alterations of the metabolic profile in human prostate cancer. Oncotarget, 7(27), 42071–42085. https: //doi.org/10.18632 /oncot arget .9817.

Heidenreich, A., Bastian, P. J., Bellmunt, J., Bolla, M., Joniau, S., van der Kwast, T., et al. (2014). EAU guidelines on prostate cancer part 1: Screening, diagnosis, and local treatment with curative intent-update 2013. European Urology, 65(1), 124–137. https :// doi.org/10.1016/j.eurur o.2013.09.046.

Keshari, K. R., Tsachres, H., Iman, R., Delos Santos, L., Tabatabai, Z. L., Shinohara, K., et al. (2011). Correlation of phospholipid metabolites with prostate cancer pathologic grade, proliferative status and surgical stage: Impact of tissue environment. NMR in Biomedicine, 24(6), 691–699. https: //doi.org/10.1002/nbm.1738.

Komoroski, R. A., Holder, J. C., Pappas, A. A., & Finkbeiner, A. E. (2011). 31P NMR of phospholipid metabolites in prostate cancer and benign prostatic hyperplasia. Magnetic Resonance in Medicine, 65(4), 911–913. https ://doi.org/10.1002/mrm.22677.

Kosmides, A. K., Kamisoglu, K., Calvano, S. E., Corbett, S. A., & Androulakis, I. P. (2013). Metabolomic fingerprinting: Challenges and opportunities. Critical Reviews in Biomedical Engineering, 41(3), 205–221.

Kumar, D., Gupta, A., & Nath, K. (2016). NMR-based metabolomics of prostate cancer: A protagonist in clinical diagnostics. Expert Review of Molecular Diagnostics, 16(6), 651–661. https ://doi. org/10.1586/14737 159.2016.11640 37.

Kumar, V., Dwivedi, D. K., & Jagannathan, N. R. (2014). High-resolution NMR spectroscopy of human body fluids and tissues in relation to prostate cancer. NMR in Biomedicine, 27(1), 80–89. https ://doi.org/10.1002/nbm.2979.

Lam, J. S., Cheung, Y. K., Benson, M. C., & Goluboff, E. T. (2003). Comparison of the predictive accuracy of serum prostate specific antigen levels and prostate specific antigen density in the detection of prostate cancer in Hispanic-American and white men. The Journal of Urology, 170(2 Pt 1), 451–456. https ://doi. org/10.1097/01.ju.00000 74707 .49775 .46.

Lenz, E. M., & Wilson, I. D. (2007). Analytical strategies in metabonomics. Journal of Proteome Research, 6(2), 443–458. https: // doi.org/10.1021/pr060 5217.

Lima, A. R., Araujo, A. M., Pinto, J., Jeronimo, C., Henrique, R., Bastos, M. L., et al. (2018a). Discrimination between the human prostate normal and cancer cell exometabolome by GC-MS. Scientific Reports, 8(1), 5539. https: //doi.org/10.1038/s41598-018-23847- 9.

Lima, A. R., Araujo, A. M., Pinto, J., Jeronimo, C., Henrique, R., Bastos, M. L., et al. (2018b). GC-MS-based endometabolome analysis differentiates prostate cancer from normal prostate cells. Metabolites. https ://doi.org/10.3390/metab o8010 023.

Lima, A. R., Mde, B., Carvalho, L., M., & Guedes de Pinho, P. (2016). Biomarker discovery in human prostate cancer: An update in metabolomics studies. Translational Oncology, 9(4), 357–370. https ://doi.org/10.1016/j.trano n.2016.05.004.

Lin, C. Y., Wu, H., Tjeerdema, R. S., & Viant, M. R. (2007). Evaluation of metabolite extraction strategies from tissue samples using NMR metabolomics. Metabolomics, 3(1), 55–67. https: // doi.org/10.1007/s1130 6-006-0043-1.

Lucarelli, G., Rutigliano, M., Galleggiante, V., Giglio, A., Palazzo, S., Ferro, M., et al. (2015). Metabolomic profiling for the identification of novel diagnostic markers in prostate cancer. Expert Review of Molecular Diagnostics, 15(9), 1211–1224. https :// doi.org/10.1586/14737 159.2015.10697 11.

Madhu, B., Shaw, G. L., Warren, A. Y., Neal, D. E., & Griffiths, J. R. (2014). Absolute quantitation of metabolites in human prostate cancer biopsies by HR-MAS ^{1}H NMR spectroscopy. Proceedings of the International Society for Magnetic Resonance in Medicine, 2014, 22.

Madhu, B., Shaw, G. L., Warren, A. Y., Neal, D. E., & Griffiths, J. R. (2016). Response of Degarelix treatment in human prostate cancer monitored by HR-MAS ^{1}H NMR spectroscopy. Metabolomics, 12, 120. https ://doi.org/10.1007/s1130 6-016-1055-0.

Markley, J. L., Bruschweiler, R., Edison, A. S., Eghbalnia, H. R., Powers, R., Raftery, D., et al. (2017). The future of NMR-based metabolomics. Current Opinion in Biotechnology, 43, 34–40.
https ://doi.org/10.1016/j.copbi o.2016.08.001.

Maxeiner, A., Adkins, C. B., Zhang, Y., Taupitz, M., Halpern, E. F., McDougal, W. S., et al. (2010). Retrospective analysis of prostate cancer recurrence potential with tissue metabolomic profiles. Prostate, 70(7), 710–717. https ://doi.org/10.1002/ pros.21103.

McDunn, J. E., Li, Z., Adam, K. P., Neri, B. P., Wolfert, R. L., Milburn, M. V., et al. (2013). Metabolomic signatures of aggressive prostate cancer. Prostate, 73(14), 1547–1560. https: //doi.org/10.1002/ pros.22704.

Merseburger, A. S., Haas, G. P., & von Klot, C. A. (2015). An update on enzalutamide in the treatment of prostate cancer. Therapeutic Advances in Urology, 7(1), 9–21. https ://doi.org/10.1177/17562 87214 55533 6.

Moestue, S., Sitter, B., Bathen, T. F., Tessem, M. B., & Gribbestad, I. S. (2011). HR MAS MR spectroscopy in metabolic characterization of cancer. Current Topics in Medicinal Chemistry, 11(1), 2–26.

Monteiro, M., Carvalho, M., Bastos, M. L., & de Pinho, P. G. (2013). Metabolomics analysis for biomarker discovery: Advances and challenges. Current Medicinal Chemistry, 20(2), 257–271.

Moyer, V. A., & Force, U. S. P. S. T. (2012). Screening for prostate cancer: U.S. Preventive Services Task Force recommendation statement. Annals of Internal Medicine, 157(2), 120–134. https: // doi.org/10.7326/0003-4819-157-2-20120 7170-00459.

Roberts, M. J., Schirra, H. J., Lavin, M. F., & Gardiner, R. A. (2011). Metabolomics: A novel approach to early and noninvasive prostate cancer detection. Korean Journal of Urology, 52(2), 79–89. https ://doi.org/10.4111/kju.2011.52.2.79.

Rostad, K., Hellwinkel, O. J., Haukaas, S. A., Halvorsen, O. J., Oyan, A. M., Haese, A., et al. (2009). TMPRSS2: ERG fusion transcripts in urine from prostate cancer patients correlate with a less favorable prognosis. APMIS, 117(8), 575–582. https ://doi.org/10.111 1/j.1600-0463.2009.02517x.

Santos, C. F., Kurhanewicz, J., Tabatabai, Z. L., Simko, J. P., Keshari, K. R., Gbegnon, A., et al. (2010). Metabolic, pathologic, and genetic analysis of prostate tissues: Quantitative

evaluation of histopathologic and mRNA integrity after HR-MAS spectroscopy. NMR in Biomedicine, 23(4), 391–398. https ://doi.org/10.1002/ nbm.1474.

Schalken, J., Dijkstra, S., Baskin-Bey, E., & van Oort, I. (2014). Potential utility of cancer-specific biomarkers for assessing response to hormonal treatments in metastatic prostate cancer. Therapeutic Advances in Urology, 6(6), 245–252. https ://doi.org/10.1177/17562 87214 54532 8.

Siegel, R. L., Miller, K. D., & Jemal, A. (2017). Cancer Statistics 2017. CA: A Cancer Journal for Clinicians, 67(1), 7–30. https ://doi. org/10.3322/caac.21387.

Spratlin, J. L., Serkova, N. J., & Eckhardt, S. G. (2009). Clinical applications of metabolomics in oncology: A review. Clinical Cancer Research, 15(2), 431–440. https ://doi.org/10.1158/1078-0432.CCR-08-1059.

Spur, E. M., Decelle, E. A., & Cheng, L. L. (2013). Metabolomic imaging of prostate cancer with magnetic resonance spectroscopy and mass spectrometry. European Journal of Nuclear Medicine and Molecular Imaging, 40(Suppl 1), S60–S71. https ://doi. org/10.1007/s0025 9-013-2379-x.

Sreekumar, A., Poisson, L. M., Rajendiran, T. M., Khan, A. P., Cao, Q., Yu, J., et al. (2009). Metabolomic profiles delineate potential role for sarcosine in prostate cancer progression. Nature, 457(7231), 910–914. https ://doi.org/10.1038/natur e0776 2.

Stenman, K., Hauksson, J. B., Grobner, G., Stattin, P., Bergh, A., & Riklund, K. (2009). Detection of polyunsaturated omega-6 fatty acid in human malignant prostate tissue by 1D and 2D high-resolution magic angle spinning NMR spectroscopy. MAGMA, 22(6), 327–331. https ://doi.org/10.1007/s1033 4-009-0187-x.

Stenman, K., Stattin, P., Stenlund, H., Riklund, K., Grobner, G., & Bergh, A. (2011). H HRMAS NMR derived bio-markers related to tumor grade, tumor cell fraction, and cell proliferation in prostate tissue samples. Biomark Insights, 6, 39–47. https ://doi. org/10.4137/BMI.S6794.

Swanson, M. G., Keshari, K. R., Tabatabai, Z. L., Simko, J. P., Shinohara, K., Carroll, P. R., et al. (2008). Quantification of choline- and ethanolamine-containing metabolites in human prostate tissues using 1H HR-MAS total correlation spectroscopy. Magnetic Resonance in Medicine, 60(1), 33–40. https ://doi.org/10.1002/ mrm.21647.

Tessem, M. B., Swanson, M. G., Keshari, K. R., Albers, M. J., Joun, D., Tabatabai, Z. L., et al. (2008). Evaluation of lactate and alanine as metabolic biomarkers of prostate cancer using 1H HR-MAS spectroscopy of biopsy tissues. Magnetic Resonance in Medicine, 60(3), 510–516. https ://doi.org/10.1002/mrm.21694.

Trock, B. J. (2011). Application of metabolomics to prostate cancer. Urologic Oncology, 29(5), 572–581. https ://doi.org/10.1016/j. urolo nc.2011.08.002.

van Asten, J. J., Cuijpers, V., Hulsbergen-van de Kaa, C., SoedeHuijbregts, C., Witjes, J. A., Verhofstad, A., et al. (2008). High resolution magic angle spinning NMR spectroscopy for metabolic assessment of cancer presence and Gleason score in human prostate needle biopsies. MAGMA, 21(6), 435–442. https ://doi. org/10.1007/s1033 4-008-0156-9.

Vandergrift, L. A., Decelle, E. A., Kurth, J., Wu, S., Fuss, T. L., DeFeo, E. M., et al. (2018). Metabolomic prediction of human prostate cancer aggressiveness: Magnetic resonance spectroscopy of histologically benign tissue. Scientific Reports, 8(1), 4997. https :// doi.org/10.1038/s4159 8-018-23177-w.

Welch, H. G., & Black, W. C. (2010). Overdiagnosis in cancer. Journal of the National Cancer Institute, 102(9), 605–613. https: //doi. org/10.1093/jnci/djq09 9.

Yang, S. Y., Adelstein, J., & Kassis, A. I. (2010). Putative molecular signatures for the imaging of prostate cancer. Expert Review of Molecular Diagnostics, 10(1), 65–74. https ://doi.org/10.1586/ erm.09.73.

Zhang, A., Yan, G., Han, Y., & Wang, X. (2014). Metabolomics approaches and applications in prostate cancer research. Applied Biochemistry and Biotechnology, 174(1), 6–12. https ://doi. org/10.1007/s1201 0-014-0955-6.

Chapter 2 – Aims and scope

Currently, there is a clear limitation in the PCa screening options, regardless of the common use of PSA for PCa screening. In fact, PSA biomarker shows important limitations which compromises the effectiveness of PCa screening and consequently PCa diagnosis. Furthermore, despite the great efforts performed to date, PCa metabolic phenotype is not completely characterized. Considering this, the major goals of this work were to uncover new potential biomarkers for non-invasive PCa screening and to perform a comprehensive metabolic characterization of PCa dysregulations.

To achieve these goals, the following specific objectives have been established:

- To evaluate the performance of volatile compounds, present in urine as candidate markers for PCa detection, by headspace-solid-phase microextraction (HS-SPME)/GC-MS, aiming to disclose a biomarker panel with potential to be used as a non-invasive diagnostic tool for PCa.

- To validate the previously proposed PCa biomarker panel and evaluate its site specificity in a completely independent set of urine samples collected from PCa patients, cancer-free controls and patients diagnosed with other urological cancers, namely bladder cancer (BC) and renal cancer (RC).

- To understand the metabolic alterations associated with PCa development, studying matched pairs of tumor and adjacent non-malignant tissue by a multi-platform untargeted metabolomics approach (GC-MS, ^{1}H NMR spectroscopy and HILIC-MS/MS), aiming to get a more holistic fingerprint of the PCa metabolic dysregulations.

- To deepen the PCa metabolic dysregulations detected in urine by a dual-platform untargeted metabolomics approach (GC-MS and ^{1}H NMR spectroscopy), aiming to obtain a more complete overview of the excreted metabolites related to PCa disease.

Chapter 3 – PCa biomarker discovery

Section 3.1 - Identification of a biomarker panel for improvement of prostate cancer diagnosis by volatile metabolic profiling of urine

Ana Rita Lima, Joana Pinto, Ana Isabel Azevedo, Daniela Barros-Silva, Carmen Jerónimo, Rui Henrique, Maria de Lourdes Bastos, Paula Guedes de Pinho and Márcia Carvalho

The article (DOI: 10.1038/s41416-019-0585-4) presented in this chapter was published by Springer Nature, in *British Journal of Cancer*, in 2019, and is here presented in the form of “Accepted Manuscript”. It is available online on:

https://www.nature.com/articles/s41416-019-0585-4

3.1.1 Abstract

Background: The lack of sensitive and specific biomarkers for the early detection of prostate cancer (PCa) is a major hurdle to improve patient management.

Methods: A metabolomics approach based on GC-MS was used to investigate the performance of volatile organic compounds (VOCs) in general and, more specifically, volatile carbonyl compounds (VCCs) present in urine as potential markers for PCa detection.

Results: Results showed that PCa patients (*n* = 40) can be differentiated from cancer-free subjects (*n* = 42) based on their urinary volatile profile in both VOCs and VCCs models, unveiling significant differences in the levels of several metabolites. The models constructed were further validated using an external validation set (*n* = 18 PCa and *n* = 18 controls) to evaluate sensitivity, specificity and accuracy of the urinary volatile profile to discriminate PCa from controls. The VOCs model disclosed 78% sensitivity, 94% specificity and 86% accuracy, whereas the VCCs model achieved the same sensitivity, a specificity of 100% and an accuracy of 89%. Our findings unveil a panel of 6 volatile compounds significantly altered in PCa patients' urine samples that was able to identify PCa, with a sensitivity of 89%, specificity of 83%, and accuracy of 86%.

Conclusions: It is disclosed a biomarker panel with potential to be used as a non-invasive diagnostic tool for PCa.

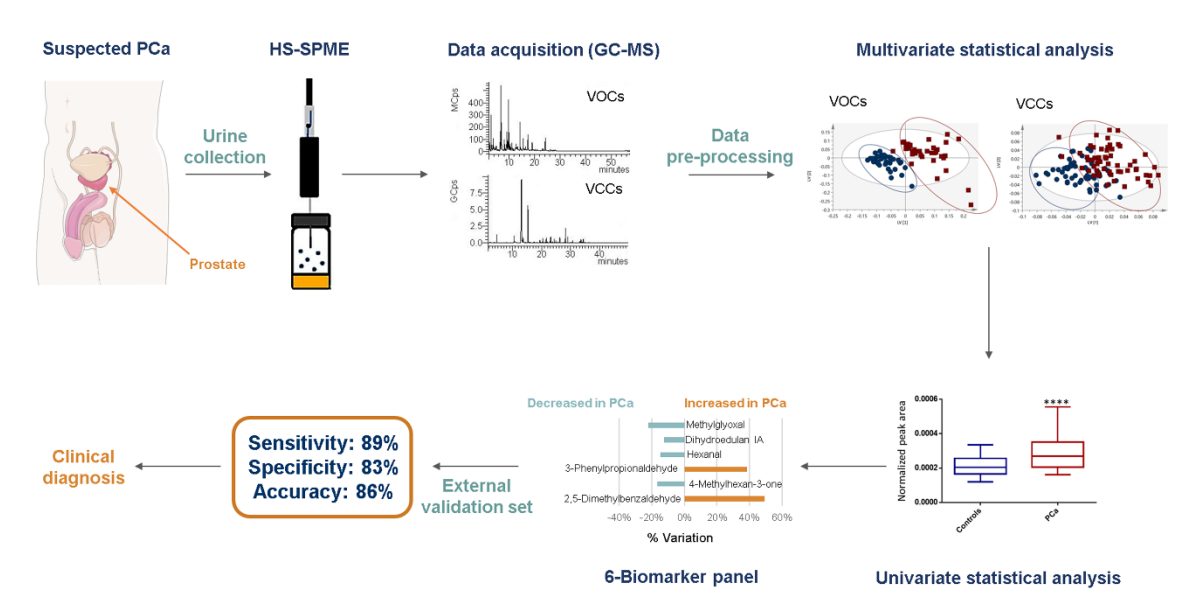

3.1.2 Background

Prostate cancer (PCa) ranks second in cancer incidence and fifth in mortality among men worldwide.[1] Diagnostic strategies currently available for patients with PCa rely on prostate biopsy (PB), which is an invasive, unpleasant and potentially harmful procedure, potentially missing clinically significant cancers due to tumor heterogeneity.[2] Prostate cancer detection based on serum PSA with a cut-off of 4.0 ng/ml has limited sensitivity (of 20.5%) and specificity (ranging from 51 to 91%),[3,4] and inability to differentiate aggressive from indolent PCa,[4] leading to false negatives, to overdiagnosis and consequent overtreatment.[5] The free/total serum PSA ratio (fPSA/tPSA) has been proposed as an alternative. However, it displays the opposite performance, with high sensitivity but low specificity.[3] Globally, this entails the performance of a large number of prostate biopsies, a significant proportion of which is deemed unnecessary. Thus, the free/total PSA ratio is not usually employed for risk-stratification of prostate cancer, but only in selected cases. The reported values for the sensitivity and specificity of this biomarker are very inconsistent among different studies, nevertheless a recent meta-analysis concluded that this biomarker shows a sensitivity of 70% and a specificity of 58%.[6] Thus, intense efforts have been devoted for development of PCa molecular biomarkers, some of which have already obtained FDA approval, like prostate cancer antigen 3 (PCA3)[7] or circulating tumor cells (CTs).[7] Notwithstanding, these biomarkers also have important limitations, such as the definition of a cut-off value (e.g., PCA3)[7] and low abundance at early stages (e.g., CTs).[7] Thus, discovery and validation of novel PCa biomarkers with improved sensitivity, non-invasive and able to detect early stage disease (when PCa is potentially curable) remains an important research aim.

Metabolomics emerged as one of the most promising approaches for discovery of new disease biomarkers as pathological conditions cause disruption of metabolic processes and consequently change the production, use and levels of many metabolites, resulting in a characteristic “metabolic signature” that can be captured through metabolic profiling. Analysis of the volatile part of the metabolome, i.e., the low molecular weight volatile organic compounds (VOCs) present in the headspace (gas phase) of clinical samples (e.g., biofluids as urine), is a promising new screening tool for several cancers, including PCa.[8–10] VOCs are end products of cellular activities and alterations in VOCs profile may reflect modifications in gene activation, gene expression, proteins and activity of enzymes involved in metabolic pathways. These volatile molecules endow biological samples with distinct odours which may even be detected by animals with highly sensitive olfactory capabilities, such as dogs,[11,12] or sophisticated analytical instrumental techniques, such as gas

chromatography-mass spectrometry (GC-MS) combined with multivariate statistical analysis (MVA).[8–10] In this regard, Smith et al.[8] studied the urine metabolomics of 13 PCa patients and 24 controls using GC-MS, disclosing 91 VOCs and unveiling significant differences between PCa and controls in 21 VOCs. However, this study has important limitations namely a small sample size and lack of external validation.[8] Khalid et al. performed the GC-MS volatile profiling of urine from PCa patients using a larger number of samples (*n* = 59 PCa and *n* = 43 controls). Overall, 196 VOCs were identified from which four (2,6-dimethy-7-octen-2-ol, pentanal, 3-octanone, and 2-octanone) were found to be statistically different between PCa and control samples.[9] More recently, Jimenez-Pacheco et al. performed a similar study using 29 PCa urine samples that were compared with 21 samples from patients with benign prostatic hyperplasia (BPH). In this study, 57 VOCs were identified, but only nine significantly differed between the two groups, highlighting furan and p-xylene as potential PCa biomarkers.[10] Interestingly, 2-octanone[8,9] and 2,6-dimethy-7octen-2-ol[9,10] were pointed as urinary PCa biomarkers in more than one study. Taken together, these studies provide convincing evidence that volatiles emanating from urine are potential biomarkers for PCa detection. Recently, the feasibility and potential of volatile signature for diagnosing PCa led to the development of chemical system sensors (so-called "electronic nose" or "e-nose").[13,14] "E-noses" are designed to mimic the mammalian olfactory system and provide a global characterization of the odorous mixtures.[15] Remarkably, the application of the "e-nose" technology to discriminate the odour of urine from patients with PCa from controls provided better diagnostic performance than serum PSA.[13,14]

Herein, we aimed to obtain a more comprehensive metabolomic profiling of volatile metabolites in urine from PCa patients, using a metabolomics approach based on headspace solid-phase microextraction coupled with GC-MS (HS-SPME/GC-MS). Two different sample preparation strategies were considered: (i) direct analysis for VOCs detection and (ii) derivatization with O-(2,3,4,5,6-pentafluorobenzyl)hydroxylamine (PFBHA), prior to HS-SPME/GC-MS analysis, to enhance the sensitive detection of volatile carbonyl compounds (VCCs). An external validation set was then used to validate a panel of discriminant volatile compounds with clinical potential for PCa diagnosis. To the best of our knowledge, this is the first time that VCCs are investigated as urinary PCa biomarkers and that a volatile biomarker panel for PCa is validated using an external set of samples.

3.1.3 Methods

3.1.3.1 Chemicals

All chemicals used were of analytical grade. Benzaldehyde (≥99.5%), 2-butanone (≥99%), (E)-2-butenal (≥99%), cyclohexanone (≥99%), 2-decanone (≥98%), (E)-2-decenal (≥92%), 2,5-dimethylbenzaldhyde (≥99%), 3,4-dimethylcyclohex-3-ene-1-carbaldehyde (≥97%), 2,6-dimethyl-6-hepten-2-ol (≥96%), 3,7-dimethylocta-1,6dien-3-ol (≥95%), 4-fluorobenzaldehyde (≥98%), 2-furfural (≥99%), heptanal (≥92%), 4-heptanone (≥97%), hexadecane (≥99%), (E,E)2,4-hexadienal (≥95%), hexanal (≥98%), 2-hexanone (≥98%), 2hydroxy-2-methyl-1-phenylpropan-1-one (≥97%), 2-methylbutanal (≥90%), 3-methylbutanal (≥97%), 2-methylcyclopentan-1-one (≥97%), 5-methyl-2-furfural (≥99%), methylglyoxal (40% aqueous solution), 5-methylheptan-2-one (≥95%), 2-methylpropanal (≥98%), 5-methyl-2-(propan-2-yl) cyclohexyl acetate (≥98%), nonanal (≥95%), 2-nonanone (≥97%), (E) -2-nonenal (≥93%), octanal (≥98%), 2-octanone (≥98%), pentanal (≥97%), (E)-2-pentenal (≥95%), 3-penten-2-one (≥70%), 3-phenylpropionaldehyde (≥95%), PFBHA (≥98%), phenylacetaldehyde (≥90%), propanal (≥97%), terpinen-4-ol (≥95%), 2,6,6,10-tetramethyl-1-oxaspiro[4.5] dec-9-ene (≥90%), and 3,7,7-trimethylbicyclo[4.1.0] hept-3-ene (≥97%) were purchased from Sigma–Aldrich (Madrid, Spain). Butanal (≥99%) and glyoxal (≥95%) were purchased from Fluka (Madrid, Spain) and 4-hydroxy-2-nonenal (≥98%) was purchased from Cayman Chemical (USA). Sodium chloride was obtained from VWR (Leuven, Belgium).

3.1.3.2 Subjects

Early morning urine samples without fasting were collected from PCa patients and controls at the Portuguese Oncology Institute of Porto (IPO Porto) and frozen at −80 °C until analysis. The study protocol was approved by the local Ethics Committee and all subjects provided their signed informed consent prior to enrolment.

A cohort of 118 men were included in this study: 58 PCa patients (age 52–77 years, mean 63) and 60 cancer-free control subjects (age 56–66 years, mean 59). Both PCa and control groups were randomly divided into two sets: (1) training (n = 40 PCa and n = 42 controls for VOCs; n = 40 PCa and n = 40 controls for VCCs) and (2) external validation (n = 18 PCa and n = 18 controls for VOCs and VCCs). Control group consisted of subjects with age related comorbidities such as hypertension, diabetes, lipid disorders and BPH, but without cancer. Detailed information on Gleason score and some important biochemical and clinical parameters of PCa patients and control subjects is provided in Table 3.1.

Table 3.1: Demographic and clinical data of the PCa patients and cancer-free controls included in the training and validation sets.

Characteristics	Prostate cancer				Control			
	Training set VOCs	*External set VOCs*	*Training set VCCs*	*External set VCCs*	*Training set VOCs*	*External set VOCs*	*Training set VCCs*	*External set VCCs*
Number of subjects	40	18	40	18	42	18	40	18
Mean Age ± SD (years)	64.4 ± 6.4	61.8 ± 5.2	63.7 ± 6.5	63.4 ± 5.3	59.3 ± 3.0	59.6 ± 2.62	59.3 ± 2.8	59.8 ± 2.7
PSA (ng/mL), *n* (%)								
<4	3 (7.5%)	1 (5.6%)	-	4 (22.2%)	-	-	-	-
4-10	24 (60%)	13 (72.2%)	28(70%)	9 (50%)	-	-	-	-
>10	13 (32.5%)	4 (22.2%)	12 (30%)	5 (27.8%)	-	-	-	-
Gleason score, *n* (%)								
≤6	6 (15%)	3 (16.7%)	8 (20%)	1 (5.6%)	-	-	-	-
=7	25 (62.5%)	12 (66.7%)	24 (60%)	13 (72.2%)	-	-	-	-
≥8	9 (22.5%)	3 (16.7%)	8 (20%)	4 (22.2%)	-	-	-	-
Clinical stage, *n* (%)								
I	3 (7.5%)	3 (16.7%)	4(10%)	2 (11.1%)	-	-	-	-
II	-	2 (11.1%)	2(4%)	-	-	-	-	-
IIA	7 /17.5%)	4 (22.2%)	9(22.5%)	2 (11.1%)	-	-	-	-
IIB	15 (37.5%)	2 (11.1%)	11 (27.5%)	6 (33.3%)	-	-	-	-
III	13 (32.5%)	5 (27.8%)	10 (25%)	8 (44.4%)	-	-	-	-
IV	2 (5%)	2 (11.1%)	4 (10%)	-	-	-	-	-
Alcoholism, *n* (%)	7 (17.5%)	4 (22.2%)	9 (22.5%)	2 (11.1%)	3 (7.1%)	-	2 (5%)	1 (5.6%)
Smoking, *n* (%)	2 (5%)	-	2 (5%)	-	5 (11.9%)	2 (11.1%)	6 (15%)	1 (5.6%)
Obesity, *n* (%)	6 (15%)	4 (22.2%)	7 (17.5%)	3 (16.7%)	7 (16.7%)	3 (16.7%)	7 (17.5%)	2 (11.1%)
Cardiac condition, *n* (%)	5 (12.5%)	6 (33.3%)	7 (17.5%)	4 (22.2%)	-	1 (5.6%)	-	1 (5.6%)
AH, *n* (%)	21 (52.5%)	8 (44.4%)	19 (47.5%)	10 (55.6%)	14 (33.3%)	9 (50%)	20 (50%)	3 (16.7%)
Dyslipidemia, *n* (%)	16 (40%)	8 (44.4%)	14 (35%)	10 (55.6%)	16 (38.1%)	9 (50%)	16 (40%)	8 (44.4%)
Diabetes, *n* (%)	9 (22.5%)	3 (16.7%)	8 (20%)	4 (22.2%)	6 (14.3%)	1 (5.6%)	5 (12.5%)	1(5.6%)
HTG, *n* (%)	2 (5%)	-	1 (2.5%)	1 (5.6%)	1 (2.4%)	-	-	1 (5.6%)
HC, *n* (%)	3 (7.5%)	-	1 (2.5%)	2 (11.1%)	4 (9.5%)	1 (5.6%)	3 (7.5%)	2 (11.1%)
BPH, n (%)	-	-	-	-	13 (31%)	4 (22.2%)	11 (27.5%)	4 (22.2%)
Prostatitis, *n* (%)	-	-	-	-	1 (2.4%)	1 (5.6%)	2 (5%)	-

AH: Arterial Hypertension; BPH: Benign prostatic hyperplasia; HC: Hypercholesteremia; HTG: Hypertriglyceridemia.

3.1.3.3 Sample preparation and metabolites extraction

Urine samples were thawed at 4 °C. For VOCs analysis, 1 mL of sample was placed in a 10 mL glass vial with 20 µL of internal standard (IS) (10 µg/mL 4-fluorobenzaldehyde in ultrapure water) and NaCl (0.27 g). To optimise the extraction conditions, a central composite design (CCD) was performed (data not shown). The optimal extraction conditions, using divinylbenzene/carboxen/ polydimethylsiloxane (DVB/CAR/PDMS) fiber coating, were 11 min of incubation and 30 min of extraction at 44 °C under continuous stirring (250 rpm).

For VCCs analysis, 250 µL of urine were placed in a 10 mL glass vial with 5 µL of IS (10 µg/mL 4-fluorobenzaldehyde in ultrapure water) and 7.5 µL of the derivatizing agent PFBHA (40 g/L in ultrapure water). Extraction was performed according to the conditions previously optimised in our lab[16] using a CombiPAL automatic autosampler (Varian, Palo Alto, CA) and a polydimethylsiloxane/divinylbenzene (PDMS/DVB) fiber coating. Briefly, urine samples were incubated at 62 °C during 6 min, followed by extraction of volatiles at the same temperature during 51 min, under continuous stirring (250 rpm). After extraction, the fiber was inserted into the GC system for thermal desorption of the analytes at 250 °C during 5 min.

In both approaches, all samples were randomly injected, with the quality control (QCs) samples being injected at the same conditions on every eight samples. QCs were prepared as aliquots of a pool of all urine samples (PCa and controls) considered in this study.

3.1.3.4 GC-MS analysis

A Scion 436-gas chromatograph coupled to a Bruker single quadrupole (SQ) equipped with a Scion SQ ion trap mass detector and a Bruker Daltonics MS workstation software version 6.8, with a Rxi-5Sil MS (30 m × 0.25 mm × 0.25 µm) column from RESTEK were used. Briefly, the carrier gas was helium C-60 (Gasin, Portugal) (flow rate 1 mL/min) and the injector port was heated at 230 °C. The oven temperature was fixed at 40 °C for 1 min, increasing to 250 °C (rate 5 °C/min), held for 5 min, followed by increasing to 300 °C (rate 5 °C/min) and held for 1 min. The temperatures of transfer line, manifold and trap were 280 °C, 50 °C and 180 °C, respectively. The emission current was 50 µA and the electron multiplier was set in relative mode to an auto tune procedure. All mass spectra were acquired in the electron impact mode (270 °C). The analysis was performed in full scan mode and the mass range used was 40–350 m/z, with a scan rate of 6 scan/s.[17]

To analyse VCCs, a 436-GC model (Bruker Daltonics) coupled to an EVOQ triple quadrupole mass spectrometer (Bruker Daltonics) and a Bruker MS workstation software

version 8.2 were used. The chromatographic separation was accomplished using a fused silica capillary column (Rxi-5Sil MS; 30 m × 0.25 mm × 0.25 µm; Restek Corporation, U.S., Bellefonte, Pennsylvania) and high purity helium C-60 (Gasin, Portugal) as carrier gas (flow rate 1 mL/min). The oven temperature was held at 40 °C for 1 min, increasing to 250 °C (rate 5 °C/min), held for 5 min, finally increasing to 300 °C (rate 20 °C/ min). The temperature of transfer line and manifold were 260 °C and 40 °C, respectively. The emission current was 50 µA and the electron multiplier was set in relative mode to an auto tune procedure. All mass spectra were acquired in the electron impact mode (270 °C). Data acquisition was performed in full scan mode and a 50–600 m/z mass range was used.[16]

The metabolite identification was accomplished by comparison of the MS spectra with standards (whenever available), the National Institute of Standards and Technology (NIST 14) database spectral library, and comparison of the experimental and theory (literature) Kovats index.

3.1.3.5 Data pre-processing

Before statistical analysis, the data was pre-processed using MZmine 2,[18] including baseline correction, peak detection, chromatogram deconvolution and alignment. The parameters used for pre-processing of VOCs data were: RT range 2.0–29.0 min, m/z range 50–400, MS data noise level 1.0×10^5, m/z tolerance 0.2, chromatogram baseline level 1.0×10^2 and peak duration range 0.06–0.70 min; whereas for VCCs were: RT range 6.5–38.0 min, m/z range 50–600, MS data noise level 5.0×10^5, m/z tolerance 0.2, chromatogram baseline level 1.0×10^4 and peak duration range 0.06–0.70 min. In both approaches, all RT-m/z pairs with a relative standard deviation greater than 30% in QCs, as well as RT-m/z pairs identified as contaminants (from column, fiber, among others), were manually removed from the matrix. The obtained data were normalised by the total area of the chromatograms and the final matrix was scaled to pareto. Furthermore, to reduce the variation from uncontrolled confounding factors and simplify the data, a variable selection method based in a univariate test,[19] namely t-test, was performed using MetaboAnalyst.[20] Consequently, all variables with p-value > 0.05 were removed from the matrix.

3.1.3.6 Statistical analysis

The statistical analysis strategy used for VOCs and VCCs data was similar and included multivariate and univariate statistical tests. From all available samples, 70% were used for the training set and 30% were randomly selected for the external set. MVA was performed

using the training set and included principal component analysis (PCA) and partial least squares discriminant analysis (PLS-DA) in SIMCA-P 15 (Umetrics, Sweden). The robustness of the PLS-DA models was confirmed through 7-fold cross validation and permutation test (200 random permutations of Y-observations, 2 components) (SIMCA-P 15, Umetrics, Sweden). To test the validity of the created models, an internal (training set) and external (external set) validation was performed. For internal and external validations, receiver operating characteristic curves (ROC), area under the curve (AUC), sensitivity, and specificity were computed (MetaboAnalyst)[20] for both PLS-DA models (VOCs and VCCs). The samples of the external set were classified as cancer or controls, taking into consideration the PLS-DA models obtained using the training sets and the sensitivity, specificity and accuracy of both PLS-DA models (VOCs and VCCs) were computed.[21]

After MVA, all metabolites with VIP (Variable Importance to the Projection) greater than one were subjected to univariate analysis (GraphPad Prism 6, USA), including a normality test (Shapiro-Wilk test) followed by unpaired Student's t-test with Welch correction test, for normal distribution, or unpaired Mann–Whitney U-test, for non-normal distribution. Percentage of variation, uncertainty of the percentage of variation, and effect size and the standard error were also determined.[22] For all significantly altered metabolites (p value < 0.05 and effect size higher than the standard error), receiver operating characteristic curves (ROC), area under the curve (AUC), sensitivity, and specificity were also computed (MetaboAnalyst).[20] Bonferroni correction was used to adjust p values in multiple comparisons.[23] Multivariate ROC exploratory analysis (Metaboanalyst)[20] was used to define a small panel of discriminant metabolites with high accuracy for prostate cancer detection, envisaging a possible translation into clinics using an "e-nose". The PLS-DA algorithm was used to evaluate the importance of each discriminant metabolite based on VIP scores through repeated random sub-sampling cross validation. The top important metabolites were used to build a PLS-DA model which was validated through ROC analysis using the training and external sets.

To better understand the biological relevance of the significantly altered VOCs and VCCs, a metabolic pathway analysis using the MetPa tool was performed in Metaboanalyst.[20] Finally, to search for possible correlations between the metabolites significantly altered in PCa, Spearman's rank correlation coefficient was computed for the set of identified and putatively annotated statistically significant compounds and represented in a heatmap, using R software (version 3.5.1).[24] Spearman's rank correlation coefficient was also computed between age and the set of metabolites found altered in PCa compared to controls.

3.1.4 Results

3.1.4.1 Urinary volatile profile of PCa patients vs. controls

In this study, a HS-SPME/GC-MS method was employed to evaluate differences in the urinary volatile profile of PCa patients compared with controls. To accomplish a more comprehensive evaluation of the urinary volatilome, we used two different sample preparation techniques which enabled the identification of 122 VOCs and 148 VCCs (seven common compounds were found).

MVA was used to evaluate the reproducibility of both analytical strategies and the discriminant capability of the PLS-DA models created using the training set. The QC samples were closely clustered in the PCA scores scatter plot (Fig. S1), which confirmed the analytical reproducibility of both methods. For construction of the PLS-DA models, a variable selection method was performed (VOCs: 3232 variables x 82 samples; VCCs: 246 variables x 80 samples) to improve the prediction power. In Fig. 3.1, the discriminant capability of the PLS-DA models, after variable selection, is clearly observed (VOCs model: LV = 2; R^2X = 0.172; R^2Y = 0.776; Q^2 = 0.599; VCCs model: LV = 2; R^2X = 0.354; R^2Y = 0.534; Q^2 = 0.443). Model robustness was also confirmed through permutation testing (Fig. S2). In the internal validation, VOCs PLS-DA model showed an AUC of 0.975, a sensitivity of 92% and specificity of 100% and the VCCs model unveiled an AUC of 0.878, a sensitivity of 71% and specificity of 91% (Fig. 3.1).

Furthermore, an external validation set was used to confirm the validity of the training models. For VOCs and VCCs, among 18 PCa samples, 14 were accurately classified and four were poorly classified. On the other hand, 17 control samples were accurately classified and only one was poorly classified for VOCs, whereas all 18 control samples were correctly classified for VCCs (Table S3). Thus, taking into consideration these results, a sensitivity of 78%, a specificity of 94% and an accuracy of 86% was obtained for VOCs, whereas VCCs disclosed equal sensitivity, a specificity of 100% and an accuracy of 89%. For VOCs, from a total of 64 metabolites with VIP > 1,31 were found significantly different between the two groups (PCa *vs*. control). The discriminant VOCs included three aldehydes, six ketones, two alcohols, two monoterpene alcohols, one alkene, one cycloalkane, two terpenes, among others, and 11 unidentified compounds (Table 3.2). Regarding VCCs analysis, 21 metabolites showed VIP > 1 and 12 significantly differed between PCa and control groups. The discriminant VCCs included two alpha-ketoaldehydes, one alkanal, one alkenal, two aromatic aldehydes, three ketones, one alkane and two unidentified compounds (Table 3.3). The chromatographic characteristics considered for identification of VOCs and VCCs are displayed in Tables S1 and S2, respectively. AUC values were superior to 0.6 for all

statistically significantly altered metabolites (Tables 3.2 and 3.3). The sensitivity and specificity of the individual metabolites was also determined and, despite the lower individual sensitivity and specificity found for the majority of the metabolites when compared to the one obtained for the models (Fig. 3.1 and Table S3), all metabolites disclosed sensitivity and specificity greater than 50 and 70%, respectively (Tables 3.2 and 3.3).

Age significantly differed between PCa and controls in VOCs (Mann–Whitney test *p*-value = 0.0002) and VCCs (Mann–Whitney test *p*-value = 0.0022) training sets (Table 3.1). Hence, a possible influence of age in the set of metabolites found altered in PCa compared to controls (Tables 3.2 and 3.3) was investigated through Spearman correlation, unveiling no statistically relevant correlations ($|r| \leq 0.36$) (Table S4). In addition, the number of individuals with arterial hypertension (AH) was higher in PCa group compared to controls in the VOCs training set (Table 3.1). The impact of AH on urine volatile profile was evaluated in the control group (AH $n = 14$ *vs*. non-HA $n = 28$), revealing no predictive power ($Q^2 = -0.145$) in the PLS-DA model (Fig. S3). Taking into consideration these results, no age- and AH-related changes were found in the urinary volatile signature of PCa patients.

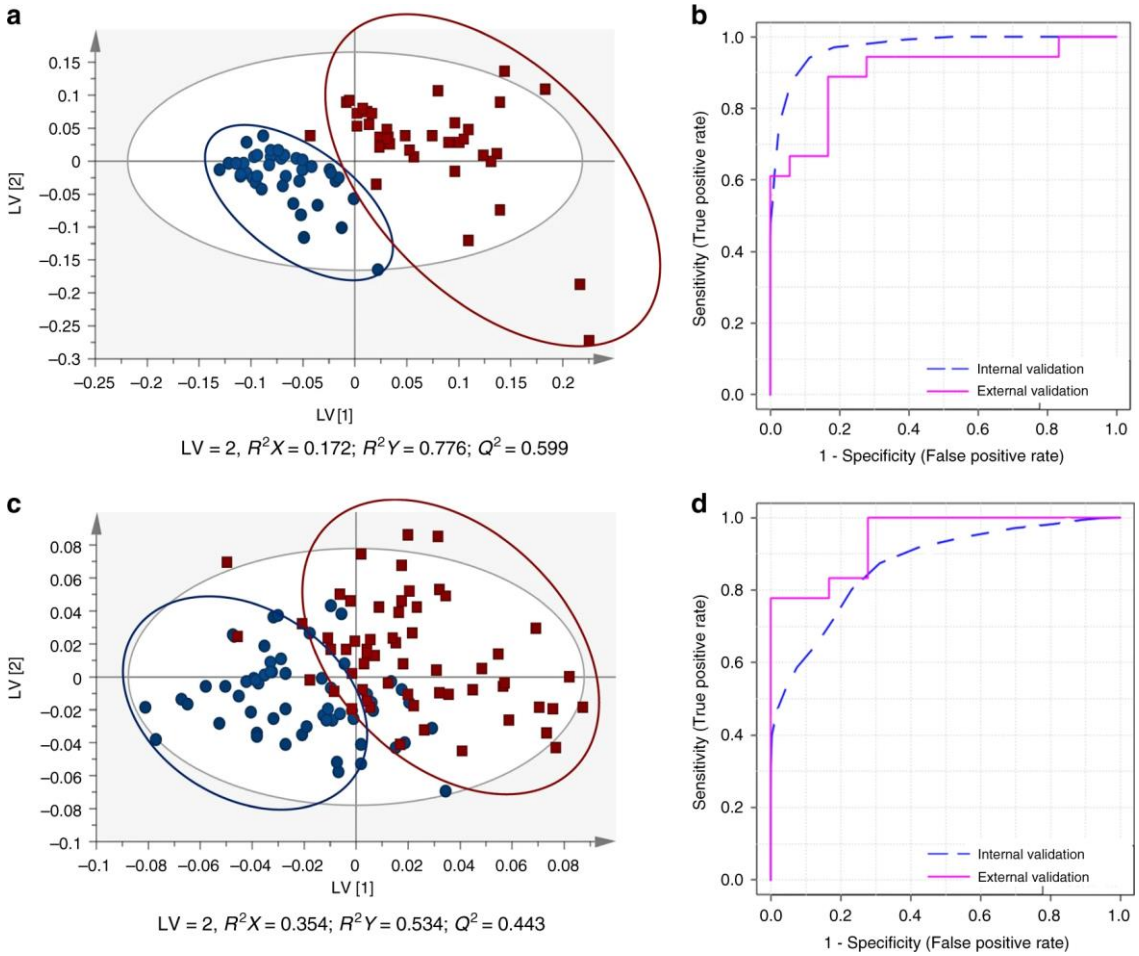

Figure 3.1: a PLS-DA scores scatter plot (Pareto scaling; 2 components) obtained for VOCs training model of PCa patients (*n* = 40, squares) *vs*. cancer-free controls (*n* = 42, circles), after variable selection; **b** Assessment of the diagnostic performance of the PLS-DA model obtained for VOCs using the training set (AUC = 0.975; sensitivity = 92%; specificity = 100%) and the external set (AUC = 0.898; sensitivity = 78%; specificity = 94%) through ROC analysis; **c** PLS-DA scores scatter plot (Pareto scaling; 2 components) obtained for VCCs training model of PCa patients (*n* = 40, squares) *vs*. cancer-free controls (*n* = 40, circles), after variable selection; **d** Assessment of the diagnostic performance of the PLS-DA model obtained for VCCs using the training set (AUC = 0.878; sensitivity = 71%; specificity = 97%) and the external set (AUC = 0.944; sensitivity = 78%; specificity = 100%) through ROC analysis.

Table 3.2: List of VOCs significantly altered in PCa group compared to controls.

Chemical name (IUPAC) or common name	*p*-value	Variation ± uncertainty (%)	Effect size ± ES_{SE}	AUC	Spec	Sens	HMDB[29]	Matrices	Potential biochemical pathway
Aldehydes									
Hexanal [L1]	0.0313	↓ 14.62 ± 6.77	↓ 0.53 ± 0.45	0.641	0.76	0.51	HMDB0005994	Blood; Cerebrospinal fluid; Feces; Saliva; Urine[29]	Steroid hormone biosynthesis[20]
3,4-Dimethylcyclohex-3-ene-1-carbaldehyde [L1]	0.0004[B]	↓ 24.09 ± 8.68	↓ 0.71 ± 0.46	0.730	0.84	0.61	NA	-	-
2,5-Dimethyl-benzaldehyde [L1]	<0.0001[B]	↑ 49.36 ± 9.90	↑ 0.91 ± 0.47	0.786	0.87	0.64	HMDB0032014	-	Alcohols and fatty acids metabolism[40,48]
Ketones									
Hexan-2-one [L1] (2-Hexanone)	0.0194	↓ 23.42 ± 10.77	↓ 0.56 ± 0.45	0.656	0.77	0.53	HMDB0005842	Urine; Feces[29]	Fatty acid metabolism[41]
2-Methylcyclopentan-1-one [L1]	0.0129	↓ 31.26 ± 12.85	↓ 0.65 ± 0.46	0.662	0.78	0.55	NA	-	Fatty acid metabolism[41]
4-Methylhexan-3-one [L2]	0.0022	↓ 16.49 ± 6.17	↓ 0.66 ± 0.46	0.701	0.82	0.59	NA	-	Fatty acid metabolism[41]
5-Methylheptan-2-one [L1]	0.0073	↓ 21.40 ± 11.34	↓ 0.48 ± 0.45	0.677	0.80	0.51	NA	Cell lines[40]	Fatty acid metabolism[41]

Chemical name (IUPAC) or common name	*p*-value	Variation ± uncertainty (%)	Effect size ± ES_{SE}	AUC	Spec	Sens	HMDB[29]	Matrices	Potential biochemical pathway
4,6-Dimethylheptan-2-one [L2]	0.0174	↓ 17.04 ± 6.67	↓ 0.63 ± 0.46	0.658	0.76	0.55	NA	-	Fatty acid metabolism[41]
2-Hydroxy-2-methyl-1-phenylpropan-1-one [L1]	0.0123	↓ 11.90 ± 4.03	↓ 0.71 ± 0.46	0.662	0.78	0.55	NA	-	-
Alcohols									
2,6-Dimethyl-6-hepten-2-ol [L1]	0.0002[B]	↓ 36.42 ± 12.89	↓ 0.78 ± 0.46	0.748	0.84	0.63	NA	-	Lipid metabolism[40]
1-Methyl-4-propan-2-ylcyclohex-2-en-1-ol [L2]	0.0026	↓ 13.49 ± 5.75	↓ 0.57 ± 0.45	0.698	0.81	0.57	NA	-	Lipid metabolism[40]
Monoterpene alcohols									
3,7-Dimethylocta-1,6-dien-3-ol (Linalool)[L1]	0.0355	↓ 28.00 ± 13.53	↓ 0.55 ± 0.45	0.635	0.75	0.51	HMDB0036100	Feces[29]	Lipid metabolism[29]
4-Methyl-1-propan-2-ylcyclohex-3-en-1-ol [L1] (Terpinen-4-ol)	<0.0001[B]	↓ 28.84 ± 8.35	↓ 0.91 ± 0.47	0.766	0.87	0.65	HMDB0035833	Feces; Cell lines[29, 40]	Lipid metabolism[29]
Alkenes									
4-Methyldec-1-ene [L2]	0.0321	↓ 18.31 ± 9.75	↓ 0.47 ± 0.45	0.635	0.75	0.52	NA	-	-

Chemical name (IUPAC) or common name	*p*-value	Variation ± uncertainty (%)	Effect size ± ES_{SE}	AUC	Spec	Sens	HMDB[29]	Matrices	Potential biochemical pathway
Cycloalkenes									
2,2,7,7-Tetramethyl-tricyclo[6.2.1.0¹,⁶]-undeca-3,5,9-triene (4,5,9,10-dehydro-isolongifolene) [L2]	0.0379	↓ 15.98 ± 8.18	↓ 0.48 ± .045	0.634	0.76	0.50	HMDB0059829	Saliva[29]	Steroid Metabolism[49]
Terpenes									
3,7,7-Trimethylbicyclo [4.1.0] hept-3-ene (3-Carene) [L1]	0.0108	↓ 16.72 ± 6.46	↓ 0.64 ± 0.46	0.672	0.78	0.54	HMDB0035619	Feces[29]	Lipid metabolism[29]
3-Methyl-6-(propan-2-ylidene)cyclohex-1-ene (Isoterpinolene) [L2]	0.0062	↓ 18.79 ± 8.17	↓ 0.58 ± 0.45	0.676	0.79	0.56	HMDB0061938	Saliva[29]	Lipid metabolism[29]
Others									
2,2,2,8a-Tetramethyl-3,4,4a,5,6,8a-hexahydro-2H-chromene (Dihydroedulan IA) [L2]	0.0251	↓ 12.58 ± 5.46	↓ 0.56 ± 0.45	0.629	0.77	0.52	NA	-	-
5-Methyl-2-(propan-2-yl)cyclohexyl acetate [L1] (Menthyl acetate)	0.0139	↓ 12.89 ± 5.09	↓ 0.61 ± 0.45	0.662	0.77	0.54	HMDB0041264	-	Lipid metabolism[29]

Chemical name (IUPAC) or common name	*p*-value	Variation ± uncertainty (%)	Effect size ± ES_{SE}	AUC	Spec	Sens	HMDB[29]	Matrices	Potential biochemical pathway
2,6,6,10-Tetramethyl-1-oxaspiro[4.5]dec-9-ene (Theaspirane) [L1]	0.0096	↓ 13.36 ± 5.23	↓ 0.62 ± 0.45	0.668	0.78	0.55	HMDB0036823	Urine[29]	Energetic metabolism; cell signaling; membrane stabilization[29]
Unidentified VOCs									
Unknown 1 [L4]	0.0137	↓ 12.70 ± 6.38	↓ 0.48 ± 0.45	0.661	0.77	0.53	NA	-	-
Unknown 2 [L4]	<0.0001[B]	↓ 49.99 ± 17.13	↓ 0.88 ± 0.47	0.822	0.92	0.73	NA	-	-
Unknown 3 [L4]	0.0006[B]	↓ 23.54 ± 8.13	↓ 0.74 ± 0.46	0.727	0.84	0.62	NA	-	-
Unknown 4 [L4]	<0.0001[B]	↓ 55.31 ± 13.34	↓ 1.30 ± 0.49	0.883	0.95	0.80	NA	-	-
Unknown 5 [L4]	0.0031	↓ 14.50 ± 6.14	↓ 0.58 ± 0.45	0.695	0.81	0.58	NA	-	-
Unknown 6 [L4]	<0.0001[B]	↓ 71.24 ± 10.61	↓ 1.12 ± 0.48	0.768	0.86	0.66	NA	-	-
Unknown 7 [L4]	0.0093	↓ 15.01 ± 6.08	↓ 0.61 ± 0.45	0.665	0.77	0.54	NA	-	-
Unknown 8 [L4]	0.0056	↓ 16.23 ± 7.55	↓ 0.53 ± 0.45	0.684	0.81	0.60	NA	-	-
Unknown 9 [L4]	<0.0001[B]	↓ 16.12 ± 6.57	↓ 0.60 ± 0.45	0.808	0.90	0.70	NA	-	-
Unknown 10 [L4]	0.0205	↓ 16.39 ± 7.42	↓ 0.55 ± 0.45	0.659	0.76	0.54	NA	-	-
Unknown 11 [L4]	0.0043	↓ 21.05 ± 7.98	↓ 0.69 ± 0.46	0.677	0.78	0.55	NA	-	-

The statistical significance (*p*-values), percentage of variation, effect size (ES), standard error (ES_{SE}), AUC, specificity (spec.) and sensitivity (sens.) are represented for each VOC, as well as the HMDB (human metabolome database) code (when available), the matrices where the compound was previously found and the potential biochemical pathways where the compound participates. NA not available. [L1]Identified metabolites (GC-MS analysis of the metabolite of interest and a chemical reference standard of suspected structural equivalence, with all analyses performed under identical analytical conditions within the same laboratory).[54] [L2] Putatively annotated compounds (spectral (MS) similarity with NIST database), when standards were not commercially available.[54]; [L4] Unidentified[54]; [B]Alterations remaining significant after Bonferroni correction, with cut-off *p*-value of 7.69 × 10−4 (0.05 divided by 65 analysed VOCs).

Table 3.3: List of VCCs significantly altered in PCa group compared to controls.

Chemical name (IUPAC) or common name	*p*-value	Variation ± uncertainty (%)	Effect size ± ES_{SE}	AUC	Spec.	Sens	HMDB[29]	Matrices	Potential biochemical pathway
Alpha-ketoaldehydes									
Oxaldehyde [L1] (Glyoxal)	0.0342	↓ 8.67 ± 4.23	↓ 0.48 ± 0.44	0.612	0.73	0.48	NA	-	Peroxidation of polyunsaturated fatty acids[50]
2-Oxopropanal [L1] (Methylglyoxal/ Pyruvaldehyde)	0.0101	↓ 22.35 ± 9.58	↓ 0.59 ± 0.45	0.638	0.76	0.53	HMDB01167	Urine; Blood[29]	Pyruvate metabolism; Glycine, serine and threonine metabolism[50]
Alkanals									
Decanal [L1]	0.0210	↓ 18.28 ± 7.52	↓ 0.60 ± 0.45	0.649	0.76	0.55	HMDB0011623	Saliva; Feces; Urine; Blood[29]	Alcohols and fatty acids metabolism; amino acids and carbohydrate catabolism[40, 48]
Alkenals									
But-2-enal [L1] (2-Butenal)	0.0040	↓ 22.64 ± 7.33	↓ 0.78 ± 0.46	0.686	0.78	0.56	HMDB0034233	Feces; Saliva[29]	Lipid peroxidation[51,52]

Chemical name (IUPAC) or common name	*p*-value	Variation ± uncertainty (%)	Effect size ± ES_{SE}	AUC	Spec.	Sens	HMDB[29]	Matrices	Potential biochemical pathway
Alkanes									
Hexadecane [L1]	0.0308	↑ 30.23 ± 10.86	↑ 0.54 ± 0.45	0.642	0.76	0.51	HMDB33792	Feces; Saliva[29]	NA
Ketones									
Butan-2-one [L1] (2-Butanone)	0.0003[B]	↑ 39.88 ± 8.81	↑ 0.84 ± 0.45	0.732	0.83	0.61	HMDB0000474	Saliva; Feces; Urine; Blood[10,29]	Fatty acid and carbohydrate metabolisms[53]
Pentan-2-one [L1] (2-Pentanone)	0.0356	↑ 53.36 ± 18.02	↑ 0.52 ± 0.45	0.638	0.75	0.51	HMDB34235	Saliva; Feces; Urine[29]	Fatty acid metabolism[41]
Cyclohexanone [L1]	0.0021[B]	↑ 30.89 ± 8.65	↑ 0.69 ± 0.45	0.704	0.82	0.59	HMDB0003315	Feces[29]	Fatty acid metabolism[41]
Aromatic aldehydes									
3-Phenylpropanal [L1] (3-Phenyl-propionaldehyde)	<0.0001[B]	↑ 38.35 ± 7.11	↑ 1.01 ± 0.47	0.757	0.85	0.65	HMDB33716	-	Alcohols and fatty acids metabolism; amino acids and carbohydrate catabolisms[40, 48]
2-Phenyl-acetaldehyde[L1] (Phenyl-acetaldehyde)	<0.0001[B]	↑ 50.66 ± 15.08	↑ 0.60 ± 0.45	0.765	0.85	0.65	HMDB06236	Feces[29]	Phenylalanine metabolism[20]

Chemical name (IUPAC) or common name	*p*-value	Variation ± uncertainty (%)	Effect size ± ES_{SE}	AUC	Spec.	Sens	HMDB[29]	Matrices	Potential biochemical pathway
Unidentified VCCs									
Unknown 12 [L4]	0.0026	↑ 136.48 ± 25.12	↑ 0.72 ± 0.45	0.698	0.81	0.58	NA	-	-
Unknown 13 [L4]	0.0126	↓ 21.71 ± 8.37	↓ 0.65 ± 0.45	0.669	0.78	0.54	NA	-	-

The statistical significance (*p*-values), percentage of variation, effect size (ES), standard error (ES_{SE}), AUC, specificity (spec.) and sensitivity (sens.) are represented for each VOC, as well as the HMDB (human metabolome database) code (when available), the matrices where the compound was previously found and the potential biochemical pathways where the compound participates. NA not available. [L1]Identified metabolites (GC-MS analysis of the metabolite of interest and a chemical reference standard of suspected structural equivalence, with all analyses performed under identical analytical conditions within the same laboratory).[54] [L2] Putatively annotated compounds (spectral (MS) similarity with NIST database), when standards were not commercially available.[54]; [L4] Unidentified[54]; [B]Alterations remaining significant after Bonferroni correction, with cut-off *p*-value of 0.0025 (0.05 divided by 20 analysed VCCs).

3.1.4.2 Definition of a multi-biomarker panel for PCa diagnosis

The smallest panel of metabolites that best predict PCa comprised 6 metabolites, namely hexanal, 2,5-dimethylbenzaldehyde, 4-methylhexan-3-one, dihydroedulan IA, methylglyoxal and 3-phenylpropionaldehyde. This panel showed an AUC of 0.856, a sensitivity of 72%, a specificity of 96% and an accuracy of 79% taking into consideration the internal validation (Fig. 3.2). Regarding the external validation set, the 6-biomarker panel showed an AUC of 0.904, a sensitivity of 89%, a specificity of 83% and an accuracy of 86% (Fig. 3.2 and Table S5).

Although integration of volatile compounds in specific biochemical pathways is still difficult to accomplish, MetPA tool[20] was used for identification of the most relevant metabolic pathways where the discriminant compounds are involved. The results revealed that methylglyoxal is involved in pyruvate metabolism and glycine, serine and threonine metabolism, phenylacetaldehyde in phenylalanine metabolism and hexanal in steroid hormone biosynthesis (Fig. S4).

To overcome the lack of knowledge about the role of volatile compounds in the metabolic pathways, Spearman's correlation indexes were computed using all identified metabolites (L1 and L2 in Tables 3.2, 3.3, S1 and S2) significantly altered in urine of PCa patients (Fig. 3.3). The magnitude and the sign of correlations can provide identification of metabolites in the same metabolic pathway or under some common regulatory mechanisms. Stronger positive correlations ($r > 0.7$ and $p < 0.0001$) were observed for 2,6,6,10-tetramethyl-1-oxaspiro[4.5]dec-9-ene with 5-methyl-2-(propan-2-yl)cyclohexyl acetate (r = 0.75), hexadecane with cyclohexanone (r = 0.72), 3-phenylpropionaldehyde with cyclohexanone (r = 0.77), 3-phenylpropionaldehyde with hexadecane (r = 0.71) and 3-phenylpropionaldehyde with phenylacetaldehyde (r = 0.76).

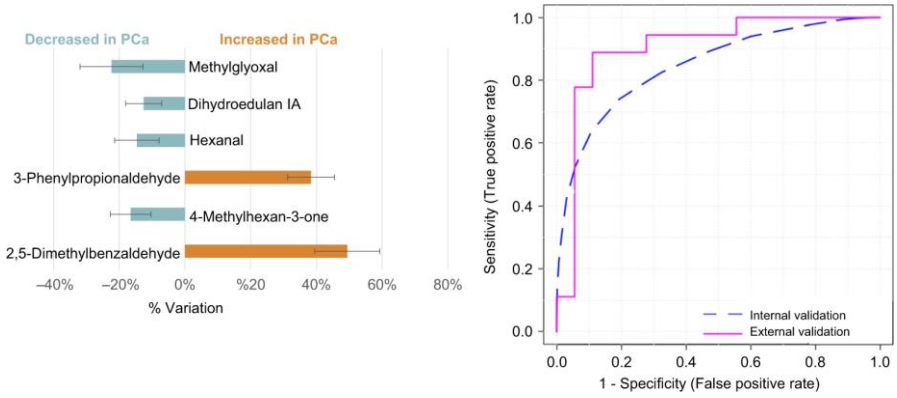

Figure 3.2: Description, % of variation and assessment of the diagnostic performance of the 6-biomarker panel using the training (AUC = 0.856; sensitivity = 72%; specificity = 96%) and the external (AUC = 0.904; sensitivity = 89%; specificity = 83%) sets through ROC analysis.

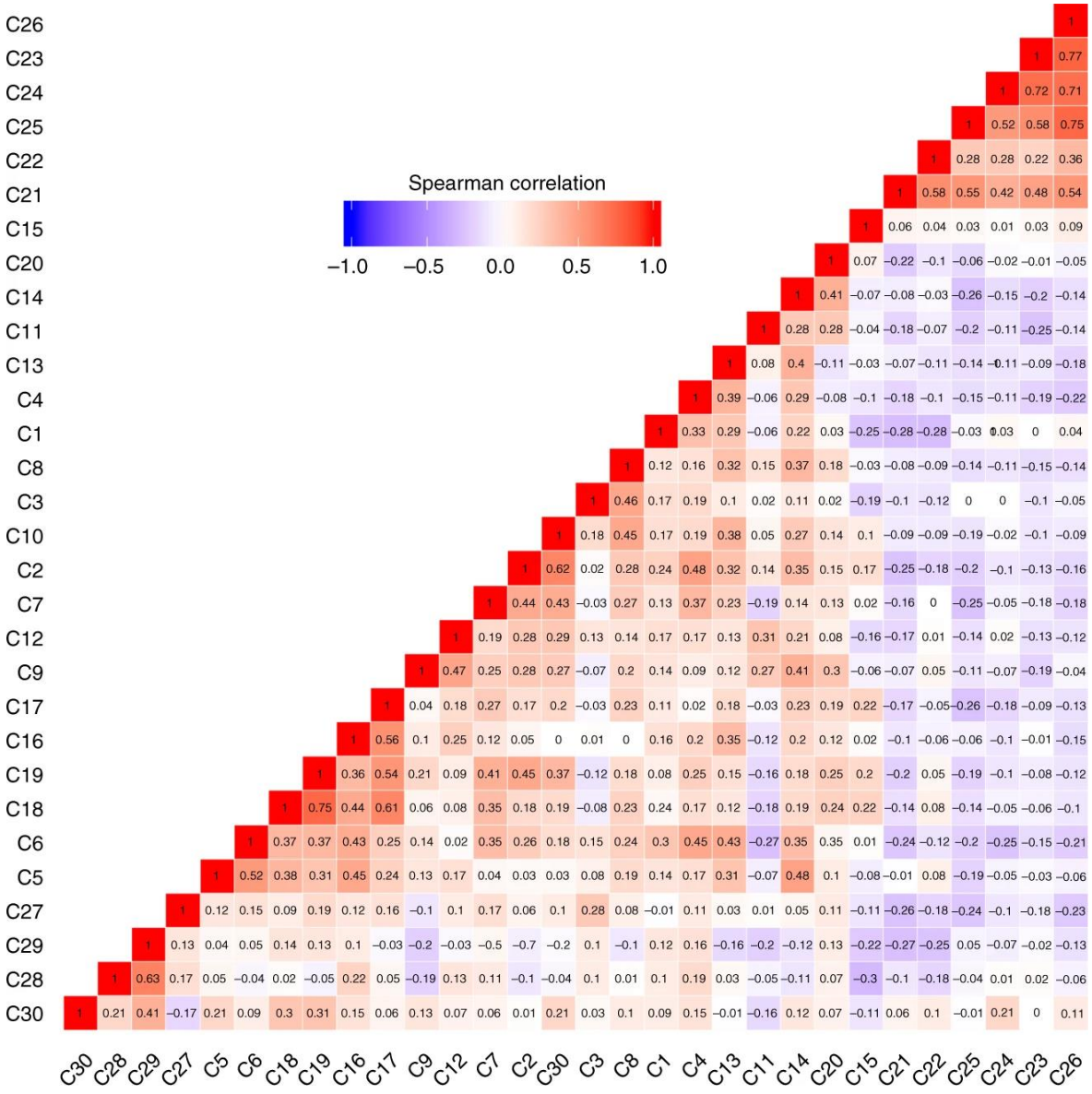

Figure 3.3: Heatmap with the Spearman's correlations among the 30 identified and putatively identified metabolites significantly altered. C1: 2-hexanone; C2: hexanal; C3: 2-methylcyclopentan-1-one; C4: 4-methylhexan-3-one; C5: 5-methylheptan-2-one; C6: 4-methyldec-1-ene; C7: 3,7,7-trimethylbicyclo[4.1.0] hept-3-ene; C8: 2,6-dimethyl-6-hepten-2-ol; C9: 3-methyl-6-(propan-2-ylidene)cyclohex-1-ene; C10: 4,6-dimethylheptan-2-one; C11: 3,7-dimethylocta-1,6-dien-3-ol; C12: 3,4-dimethylcyclohex-3-ene-1-carbaldehyde; C13: 1-methyl-4-propan-2-ylcyclohex-2-en-1-ol; C14: terpinen-4-ol; C15: 2,5-dimethylbenzaldehyde; C16: 2-hydroxy-2-methyl-1-phenylpropan-1-one; C17: dihydroedulan IA; C18: 5-methyl-2-(propan-2-yl)cyclohexyl acetate; C19: 2,6,6,10-tetramethyl-1-oxaspiro[4.5]dec-9-ene; C20: 4,5,910-dehydroisolongifolene; C21: 2-butanone; C22: 2-pentanone; C23: cyclohexanone; C24: hexadecane; C25: phenylacetaldehyde; C26: 3-phenylpropionaldehyde; C27: 2-butenal; C28: decanal; C29: glyoxal; C30: methylglyoxal

3.1.5 Discussion

In this study, two HS-SPME/GC-MS approaches were used to more comprehensively uncover the volatile profile of urine from PCa patients compared with previous reports,[8–10] unveiling a total of 263 different volatile compounds. Multivariate analysis showed that both VOCs and VCCs urinary signature allowed for accurate discrimination between PCa and control groups. A major strength of this study lies in its design, with the inclusion of an external validation set to validate the models obtained through MVA of the training sets, after variable selection. These external validation sets disclosed satisfactory sensitivity (78% for VOCs and VCCs), high specificity (94% for VOCs and 100% for VCCs) and high accuracy (86% for VOCs and 89% for VCCs). Interestingly, all false negatives observed in VOCs model were from obese and/or alcoholic subjects, whereas the false positive was a control with prostatitis (Table 3.1). Among the four false negatives observed in VCCs model, three were also obese subjects and one with ischemic heart disease, which may compromise renal function (Table 3.1). These confounding factors might justify the misclassifications. Notwithstanding, specificity and accuracy were superior to previously published in similar studies.[8,9] Furthermore, individually, all discriminant metabolites disclosed sensitivity (ranging from 48 to 80%; Tables 3.2 and 3.3) higher than the one reported for serum PSA (20.5%).[4]

The idea of using multiple biomarkers rather than a single biomarker has gained strength as a means to improved performance,[25] since the metabolomic signature of a disease is comprised of groups of connected metabolites that change in concert.[26] Furthermore, this approach ensures that an arbitrary change in a single metabolite will not lead to a false diagnosis.[26] In line with this, a biomarker panel was herein defined consisting in the combination of 6 discriminatory metabolites. A small panel of biomarkers was selected in this work envisaging the development of a sensing material[27] tuned in specificity and selectivity for these compounds to be applied in an “e-nose” in near future. This 6-biomarker panel unveiled good prediction of PCa from non-cancer patients, providing accuracies of 79% and 86% in the internal and external sets, respectively. The small sample size in external set can be considered a limiting factor in this study, though this is the first study, to our knowledge, to use an external set for validation of a volatile biomarker panel of PCa in urine. Importantly, the four patients with BPH and one patient with prostatitis included in the external set as controls were correctly classified by the panel. These prostate non-malignant conditions are well-recognized confounders in the context of serum PSA screening, as elevated levels of this biomarker are detected in BPH and prostatitis.[25] So, taking into consideration the results of the internal and external validations, the diagnostic

performance of the 6-biomarker panel outperforms not only PSA sensitivity but also fPSA / tPSA sensitivity and specificity.

In our study, three classes of compounds stood out as discriminant of PCa from controls, namely alcohols, aldehydes and ketones. A significant decrease was found in the levels of four alcohols, specifically terpinen-4-ol, 2,6-dimethyl-6-hepten-2-ol, 1-methyl-4-propan-2-ylcyclohex-2-en-1-ol, and 3,7-dimethylocta-1,6-dien-3-ol (Table 3.2). This may be related with changes in several metabolic pathways, namely hydrocarbon metabolism,[28] fatty acid β-oxidation,[29] intensification of cellular membrane synthesis[30] and alterations in the activity of some important enzymes, namely CYP 450[31] and alcohol dehydrogenases.[28] Several studies have demonstrated the intracellularly increased concentrations of reactive oxygen species (ROS) in cancer cells,[32,33] which are capable of causing the oxidation of biologically crucial molecules such as DNA, RNA, proteins and lipids. ROS-mediated oxidation of polyunsaturated fatty acids (also termed lipid peroxidation) increases alkanes formation, which after hydroxylation through CYP 450 leads to the production of alcohols.[31] Additionally, it has been proposed that terpinen-4-ol and α-terpineol (an isomer of terpinen-4-ol) can interfere with immune response, as they were able to inhibit the production of inflammatory mediators.[34] Furthermore, α-terpineol was shown to have cytotoxic and apoptotic effects in PCa cell lines, which may be correlated with down-regulation of various proteins that mediate cell proliferation, cell survival, metastasis, and angiogenesis.[35] 3,7-Dimethylocta-1,6-dien-3-ol may have an exogenous source, since it is present in several food products like cinnamon or citrus fruits.[29] However, an endogenous origin cannot be ruled out since this compound is involved in lipid metabolism.[29] In addition, the supplementation with 3,7-dimethylocta-1,6-dien-3-ol in PCa immortalised cell lines and in tumour xenografts showed an induction of apoptosis and inhibition of cell proliferation.[36]

Referring to aldehydes, urinary levels of hexanal, 3,4-dimethylcyclohex-3-ene-1-carbaldehyde, glyoxal, methylglyoxal, decanal, and 2-butenal were found significantly decreased in PCa patients, whereas 2,5-dimethylbenzaldehyde, 3-phenylpropionaldehyde and phenylacetaldehyde were significantly increased in PCa compared to controls (Tables 3.2 and 3.3). Aldehydes are involved in the metabolism of alcohols and fatty acids,[37,38] and can also be produced during amino acid and carbohydrate catabolism.[37,38] The presence of aldehydes may also be related with the excessive production of ROS,[9] known to induce lipid peroxidation, which originates the formation of over 200 types of highly reactive and extremely toxic aldehydes.[39] This may explain the higher levels of 2,5-dimethylbenzaldehyde, 3-phenylpropionaldehyde and phenylacetaldehyde detected in urine of PCa patients. In agreement with our findings, other metabolomic studies have also

observed a trend for increased production of certain aldehydes in PCa compared to control groups.[8–10]

The levels of nine ketones were also found significantly altered in urine from PCa patients, including 2-hexanone, 2-methylcyclopentan-1-one, 4-methylhexan-3-one, 5-methylheptan-2-one, 4,6-dimethylheptan-2-one, 2-hydroxy-2-methyl-1-phenyl-propan-1-one, 2-butanone, 2-pentanone and cyclohexanone (Tables 3.2 and 3.3). Of note, increased levels of 2-butanone[10] and decreased 5-methylheptan-2-one levels[40] were previously associated with PCa in urine samples and cell lines, respectively. Alterations in the levels of ketones might be related with carcinogenic processes, such as protein metabolism and ketogenic pathway dysregulations.[28] Some important ketones present in the human body are products of fatty acid metabolism, having acetyl-CoA as a precursor.[41] The increase in ketone levels can also be associated with high oxidation rate of fatty acids and glycation.[42] During glycation, ROS are formed and contribute to the glycation-induced protein modifications, normally designated glycoxidation.[43]

The exact metabolic pathways which constitute the biological origin of VOCs and VCCs is not completely elucidated yet. Thus far, only one study reported on the cancer-specific biochemical origin of VOCs.[44] This goal is very difficult to accomplish as VOCs are produced during metabolic cascades as degradation products of the metabolites directly involved in metabolic pathways, and, consequently, conservative methods are unable to determine the VOCs real metabolic origin.[44] Notwithstanding, some metabolites altered in the PCa group were associated with known biochemical pathways, namely pyruvate metabolism, glycine, serine and threonine metabolism, phenylalanine metabolism and steroid hormone biosynthesis (Fig. S4). However, it is important to take into account that some of the significantly altered metabolites may not be directly cancer-derived but reflect other local or systemic body responses (e.g., inflammation and/or necrosis).

Considering the correlation coefficient (Fig. 3.3) observed among all identified metabolites (L1 and L2 in Tables 3.2 and 3.3 and Tables S1 and S2) found significantly different between cancer and control, the significant decrease in the levels of 2,6,6,10 - tetramethyl-1-oxaspiro[4.5]dec-9-ene correlated with the significant decrease in the levels of 5-methyl-2-(propan-2-yl)cyclohexyl acetate, suggesting a possible relationship in PCa disturbed biochemical pathways. Furthermore, we also observed several strong correlations between alterations found in the levels of ketones, aldehydes and alkanes, suggesting a probable association of these compounds with PCa altered metabolism.

Despite the small sample size that may lead to bias in statistical power and precision, our results disclose a volatile biomarker panel that has the potential to be used as a non-

invasive diagnostic tool for PCa with good performance. Notwithstanding, the use of a GC-MS approach in routine clinical practice has important limitations, including high cost, non-portability, time consuming process, and the need for considerable operator expertise.[45] To overcome these limitations, the use of portable gas-sensing devices such as ‘’e-noses” is a more suitable approach for routine clinical use.[45] Some research groups have already demonstrated that “e-nose” technology is able to detect the “odour fingerprint” emanated from urine of PCa patients in a simple and fast way.[13,14]

The knowledge on the urinary volatile signature of PCa acquired with this study has the potential to allow for the development of a sensor optimized for the recognition of volatiles with chemical groups herein elucidated and consequently with greater capabilities of chemical discriminations and diagnostic accuracy. However, e-nose devices are incapable to determine the identity and concentration of individual compounds responsible for discrimination between urine samples and, therefore, do not provide information about the metabolic pathways affected by the disease.[46] Furthermore, the reproducibility of “e-nose” results can be affected by sensor drift over time, affecting instrument reproducibility.[47] In the future, a best diagnostic approach may rely in the use of low-cost “e-nose” device for assessing the presence of PCa in a rapid, non-invasive way, followed by targeted assessment of known volatile biomarkers by GC-MS technology for diagnostic confirmation. The combination of e-nose and GC-MS technologies may provide a powerful tandem diagnostic tool potentially allowing for early non-invasive diagnosis of PCa with high accuracy.

3.1.6 Conclusions

In the present study, a comprehensive volatile metabolomic signature of urine from PCa patients was obtained that covered the profile of a large number of volatile carbonyl compounds reported for the first time. A panel of 6 volatile biomarkers was established for PCa diagnosis, disclosing a good prediction of new PCa and control samples in an external validation cohort. Indeed, the 6-biomarker panel unveiled higher sensitivity and accuracy compared to serum PSA, as well as higher sensitivity and specificity than fPSA/tPSA. The knowledge gained from the definition of PCa volatile signature in urine samples has the potential to be used in the development of an electronic nose device containing sensing materials tuned for specificity and selectivity, thus improving accuracy. Furthermore, the alterations found in the levels of some metabolites (methylglyoxal, phenylacetaldehyde and hexanal) suggest dysregulations in pyruvate metabolism, glycine, serine and threonine

metabolism, phenylalanine metabolism and steroid hormone biosynthesis in prostate carcinogenesis. Nonetheless, the biochemical origin of volatile metabolites remains mostly unknown and further studies focused on the understanding of regulatory mechanisms regarding their release at cellular level are required. In conclusion, our findings strengthen the value of urinary volatilome for PCa diagnosis and disclose a biomarker panel that has potential to be used as an accurate diagnostic tool for this malignancy. Further studies will be performed in order to validate these results in an independent larger cohort.

3.1.7 References

1. Bray, F., Ferlay, J., Soerjomataram, I., Siegel, R. L., Torre, L. A. & Jemal, A. Global cancer statistics 2018: GLOBOCAN estimates of incidence and mortality worldwide for 36 cancers in 185 countries. CA Cancer J. Clin. 68, 394–424 (2018).
2. Spur, E. M., Decelle, E. A. & Cheng, L. L. Metabolomic imaging of prostate cancer with magnetic resonance spectroscopy and mass spectrometry. Eur. J Nucl. Med. Mol Imaging. 40(Suppl 1), S60–S71 (2013).
3. Kearns, J. T. & Lin, D. W. Improving the specificity of PSA screening with serum and urine markers. Curr. Urol. Rep. 19, 80 (2018).
4. Wolf, A. M., Wender, R. C., Etzioni, R. B., Thompson, I. M., D'Amico, A. V., Volk, R. J. et al. American Cancer Society guideline for the early detection of prostate cancer: update 2010. CA Cancer J. Clin. 60, 70–98 (2010).
5. Kelly, R. S., Vander Heiden, M. G., Giovannucci, E. & Mucci, L. A. Metabolomic biomarkers of prostate cancer: prediction, diagnosis, progression, prognosis, and Recurrence. Cancer Epidemiol Biomarkers Prev. 25, 887–906 (2016).
6. Huang, Y., Li, Z. Z., Huang, Y. L., Song, H. J. & Wang, Y. J. Value of free/total prostate-specific antigen (f/t PSA) ratios for prostate cancer detection in patients with total serum prostate-specific antigen between 4 and 10 ng/mL: A meta-analysis. Medicine (Baltimore) 97, e0249 (2018).
7. Filella, X., Fernandez-Galan, E., Fernandez Bonifacio, R. & Foj, L. Emerging biomarkers in the diagnosis of prostate cancer. Pharmgenomics Pers Med. 11, 83–94 (2018).
8. Smith, S., White, P., Redding, J., Ratcliffe, N. M. & Probert, C. S. J. Application of similarity coefficients to predict disease using volatile organic compounds. IEEE Sens. J. 10, 92–96 (2010).

9. Khalid, T., Aggio, R., White, P., De Lacy Costello, B., Persad, R., Al-Kateb, H. et al.Urinary volatile organic compounds for the detection of prostate cancer. PLoS ONE. 10, e0143283 (2015).

10. Jimenez-Pacheco, A., Salinero-Bachiller, M., Iribar, M. C., Lopez-Luque, A., MijanOrtiz, J. L. & Peinado, J. M. Furan and p-xylene as candidate biomarkers for prostate cancer. Urol. Oncol. 36, 243e21–e27 (2018).

11. Taverna, G., Tidu, L., Grizzi, F., Torri, V., Mandressi, A., Sardella, P. et al. Olfactory system of highly trained dogs detects prostate cancer in urine samples. J Urol. 193, 1382–1387 (2015).

12. Elliker, K. R., Sommerville, B. A., Broom, D. M., Neal, D. E., Armstrong, S. & Williams,H. C. Key considerations for the experimental training and evaluation of cancer odour detection dogs: lessons learnt from a double-blind, controlled trial of prostate cancer detection. BMC Urol. 14, 22 (2014).

13. Roine, A., Veskimäe, E., Tuokko, A., Kumpulainen, P., Koskimäki, J., Keinänen Tuomo, A. et al. Detection of prostate cancer by an electronic nose: a proof of principle study. J. Urol. 192, 230–235 (2014).

14. Asimakopoulos, A. D., Del Fabbro, D., Miano, R., Santonico, M., Capuano, R., Pennazza, G. et al. Prostate cancer diagnosis through electronic nose in the urine headspace setting: a pilot study. Prostate Cancer Prostatic Dis. 17, 206 (2014).

15. Bax, C., Taverna, G., Eusebio, L., Sironi, S., Grizzi, F., Guazzoni, G. et al. Innovative diagnostic methods for early prostate cancer detection through urine analysis: a review. Cancers. 10, 123 (2018).

16. Calejo, I., Moreira, N., Araujo, A. M., Carvalho, M., Bastos Mde, L. & de Pinho, P. G. Optimisation and validation of a HS-SPME-GC-IT/MS method for analysis of carbonyl volatile compounds as biomarkers in human urine: application in a pilot study to discriminate individuals with smoking habits. Talanta. 148, 486–493 (2016).

17. Monteiro, M., Carvalho, M., Henrique, R., Jeronimo, C., Moreira, N., de Lourdes Bastos, M. et al. Analysis of volatile human urinary metabolome by solid-phase microextraction in combination with gas chromatography-mass spectrometry for biomarker discovery: application in a pilot study to discriminate patients with renal cell carcinoma. Eur. J. Cancer 50, 1993–2002 (2014).

18. Pluskal, T., Castillo, S., Villar-Briones, A. & Oresic, M. MZmine 2: modular framework for processing, visualizing, and analyzing mass spectrometry-based molecular profile data. BMC Bioinformatics 11, 395 (2010).

19. Xi, B., Gu, H., Baniasadi, H. & Raftery, D. Statistical analysis and modeling of mass spectrometry-based metabolomics data. Methods Mol. Biol. 1198, 333–353 (2014).

20. Chong, J., Soufan, O., Li, C., Caraus, I., Li, S., Bourque, G. et al. MetaboAnalyst 4.0: towards more transparent and integrative metabolomics analysis. Nucleic Acids Res. 46(W1), W486–W494 (2018).

21. Fawcett, T. An introduction to ROC analysis. Pattern Recogn. Lett. 27, 861–874 (2006).

22. Berben, L., Sereika, S. M. & Engberg, S. Effect size estimation: methods and examples. Int. J. Nurs Stud. 49, 1039–1047 (2012).

23. Aickin, M. & Gensler, H. Adjusting for multiple testing when reporting research results: the Bonferroni vs Holm methods. American journal of public health. 86, 726–728 (1996).

24. R Core Team. R: A Language and Environment for Statistical Computing. (RFoundation for Statistical Computing, Vienna, Austria, 2014).

25. Dimakakos, A., Armakolas, A. & Koutsilieris, M. Novel tools for prostate cancer prognosis, diagnosis, and follow-up. Biomed Res Int. 2014, 890697 (2014).

26. Marchand C.R., Farshidfar F., Rattner J. & Bathe O.F. A framework for development of useful metabolomic biomarkers and their effective knowledge translation. Metabolites 8, 59 (2018).

27. Hussain A., Semeano A. T. S., Palma S., Pina A. S., Almeida J., Medrado B. F. et al. TunaBle Gas Sensing Gels By Cooperative Assembly. Adv. Funct. Mater. 27, 1700803 (2017).

28. Haick, H., Broza, Y. Y., Mochalski, P. & Ruzsanyi, V. Amann A. Assessment, origin, and implementation of breath volatile cancer markers. Chem. Soc. Rev. 43, 1423–1449 (2014).

29. Wishart, D. S., Feunang, Y. D., Marcu, A., Guo, A. C., Liang, K., Vázquez-Fresno, R.et al. HMDB 4.0: the human metabolome database for 2018. Nucleic Acids Res. 46 (D1), D608–D617 (2018).

30. Zhang, Y., Gao, G., Liu, H., Fu, H., Fan, J., Wang, K. et al. Identification of volatile biomarkers of gastric cancer cells and ultrasensitive electrochemical detection based on sensing interface of Au-Ag alloy coated MWCNTs. Theranostics. 4, 154–162 (2014).

31. Taware, R., Taunk, K., Pereira, J. A. M., Dhakne, R., Kannan, N., Soneji, D. et al. Investigation of urinary volatomic alterations in head and neck cancer: a noninvasive approach towards diagnosis and prognosis. Metabolomics. 13, 111 (2017).

32. Khandrika, L., Kumar, B., Koul, S., Maroni, P. & Koul, H. K. Oxidative stress in prostate cancer. Cancer Lett. 282, 125–136 (2009).

33. Oh, B., Figtree, G., Costa, D., Eade, T., Hruby, G., Lim, S. et al. Oxidative stress in prostate cancer patients: a systematic review of case control studies. Prostate int. 4, 71–87 (2016).

34. Nogueira, M. N., Aquino, S. G., Rossa Junior, C. & Spolidorio, D. M. Terpinen-4-oland alpha-terpineol (tea tree oil components) inhibit the production of IL-1beta, IL-6 and IL-10 on human macrophages. Inflamm Res. 63, 769–778 (2014).

35. Ryu, N. H., Park, K. R., Kim, S. M., Yun, H. M., Nam, D., Lee, S. G. et al. A hexane fraction of guava Leaves (Psidium guajava L.) induces anticancer activity by suppressing AKT/mammalian target of rapamycin/ribosomal p70 S6 kinase in human prostate cancer cells. J. Med. Food 15, 231–241 (2012).

36. Zhao, Y., Chen, R., Wang, Y., Qing, C., Wang, W. & Yang, Y. In vitro and in vivo efficacy studies of lavender angustifolia essential oil and its active constituents on the proliferation of human prostate cancer. Integr. Cancer Ther. 16, 215–226 (2017).

37. Muzio, G., Maggiora, M., Paiuzzi, E., Oraldi, M. & Canuto, R. A. Aldehyde dehydrogenases and cell proliferation. Free Radic. Biol. Med. 52, 735–746 (2012).

38. Yan, J., De Melo, J., Cutz, J. C., Aziz, T. & Tang, D. Aldehyde dehydrogenase 3A1 associates with prostate tumorigenesis. Br. J. Cancer 110, 2593–2603 (2014).

39. Li, D. & Ellis, E. M. Aldo-keto reductase 7A5 (AKR7A5) attenuates oxidative stress and reactive aldehyde toxicity in V79-4 cells. Toxicol. In Vitro. 28, 707–714 (2014).

40. Lima A. R., Araujo A. M., Pinto J., Jeronimo C., Henrique R., Bastos M. L. et al. GCMS-based endometabolome analysis differentiates prostate cancer from normal prostate cells. Metabolites. 19, pii: E23 (2018).

41. White, H. & Venkatesh, B. Clinical review: ketones and brain injury. Crit. Care. 15, 219 (2011).

42. Serrano, M., Gallego, M. & Silva, M. Analysis of endogenous aldehydes in human urine by static headspace gas chromatography-mass spectrometry. J. Chromatogr. A. 1437, 241–246 (2016).

43. Sadowska-Bartosz, I. & Bartosz, G. Effect of glycation inhibitors on aging and age-related diseases. Mech. Ageing Dev. 160, 1–18 (2016).

44. Lee, D. K., Na, E., Park, S., Park, J. H., Lim, J. & Kwon, S. W. In vitro tracking of intracellular metabolism-derived cancer volatiles via isotope labeling. ACS Cent. Sci. 4, 1037–1044 (2018).

45. Wilson, A. D. & Baietto, M. Advances in electronic-nose technologies developed for biomedical applications. Sensors (Basel). 11,1105–1176 (2011).

46. Wilson, A. D. Advances in electronic-nose technologies for the detection of volatile biomarker metabolites in the human breath. Metabolites. 5, 140–163 (2015).

47. Capelli L., Taverna G., Bellini A., Eusebio L., Buffi N., Lazzeri M. et al. Application and uses of electronic noses for clinical diagnosis on urine samples: a review. Sensors (Basel). 16, pii: E1708 (2016).

48. Bianchi, F., Riboni, N., Carbognani, P., Gnetti, L., Dalcanale, E., Ampollini, L. et al. Solid-phase microextraction coupled to gas chromatography-mass spectrometry followed by multivariate data analysis for the identification of volatile organic compounds as possible biomarkers in lung cancer tissues. J. Pharm. Biomed. Anal. 146, 329–333 (2017).

49. Taunk, K., Taware, R., More, T. H., Porto-Figueira, P., Pereira, J. A. M., Mohapatra, R.et al. A non-invasive approach to explore the discriminatory potential of the urinary volatilome of invasive ductal carcinoma of the breast. RSC Advances 8, 25040–25050 (2018).

50. Miyata, T., Inagi, R., Asahi, K., Yamada, Y., Horie, K., Sakai, H. et al. Generation of protein carbonyls by glycoxidation and lipoxidation reactions with autoxidation products of ascorbic acid and polyunsaturated fatty acids. FEBS Lett. 437, 24–28 (1998).

51. Liu, X. Y., Yang, Z. H., Pan, X. J., Zhu, M. X. & Xie, J. P. Crotonaldehyde induces oxidative stress and caspase-dependent apoptosis in human bronchial epithelial cells. Toxicol Lett. 195, 90–98 (2010).

52. Voulgaridou, G. P., Anestopoulos, I., Franco, R., Panayiotidis, M. I. & Pappa, A. DNA damage induced by endogenous aldehydes: current state of knowledge. Mutat Res. 711, 13–27 (2011).

53. Garner, C. E., Smith, S., de Lacy Costello, B., White, P., Spencer, R., Probert, C. S.et al. Volatile organic compounds from feces and their potential for diagnosis of gastrointestinal disease. FASEB J. 21, 1675–1688 (2007).

54. Viant, M. R., Kurland, I. J., Jones, M. R. & Dunn, W. B. How close are we to complete annotation of metabolomes? Curr. Opin. Chem. Biol. 36, 64–69 (2017).

3.1.8 Supporting information

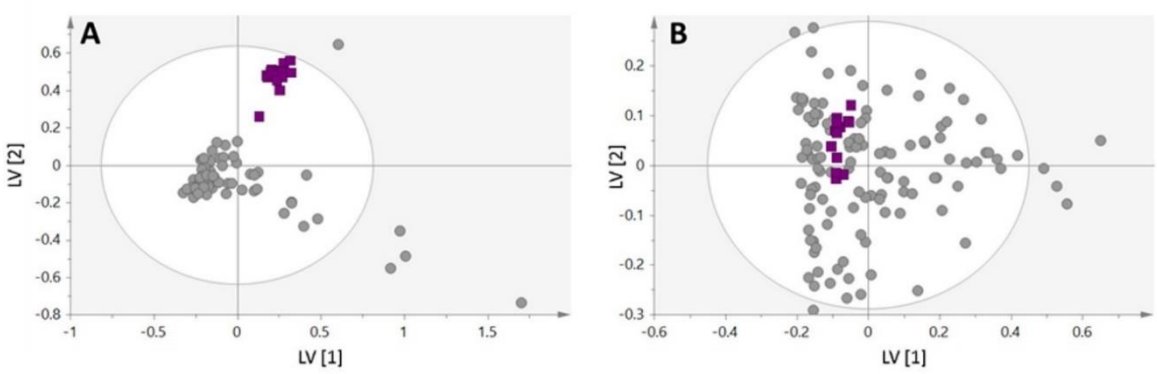

Figure S1. PCA scores scatter plot (Pareto scaling; 2 components) obtained for the HS-SPME/GC-MS chromatograms of all samples (control and PCa) (gray circles) and QCs samples (purple squares). (A) VOCs (R^2X=0.345); (B) VCCs (R^2X=0.423). QCs samples are grouped together, which prove the reproducibility of the analytical techniques.

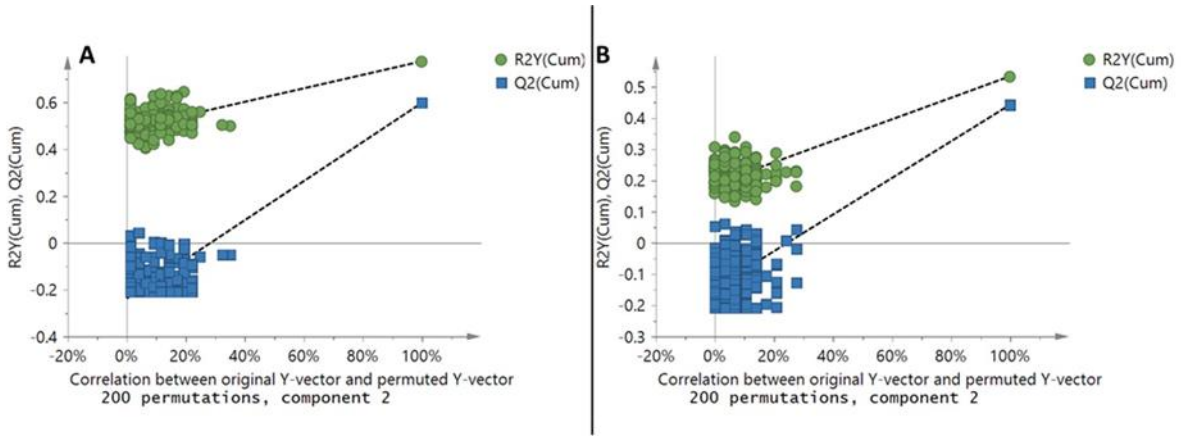

Figure S2. Statistical validation of the PLS-DA models by permutation testing (200 permutations; 2 components). (A) VOCs model (Intercepts: R^2 = (0.0, 0.487), Q^2 = (0.0, -0.237)). (B) VCCs model (Intercepts: R^2 = (0.0, 0.189), Q^2 = (0.0, -0.144)).

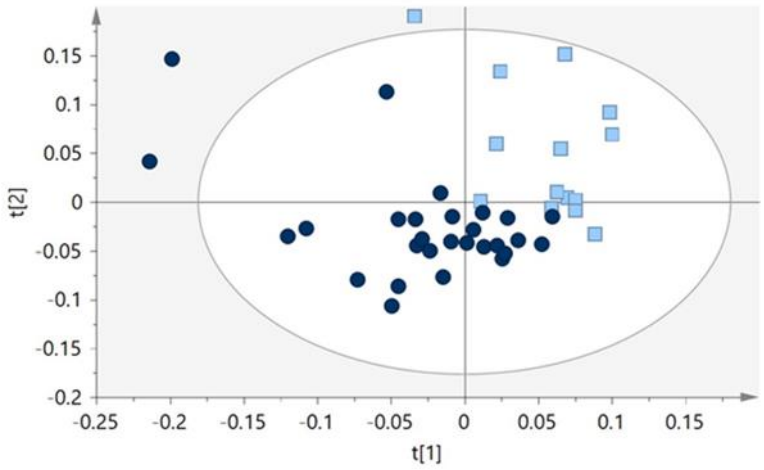

Figure S3. PLS-DA scores scatter plots (Pareto scaling; 2 components) obtained for control without hypertension (dark blue circles) *vs*. control with hypertension (light blue squares) (LV= 2, R^2X= 0.193; R^2Y = 0.617; Q^2= -0.145) (*n*= 28 controls without hypertension *vs. n* = 14 controls with hypertension).

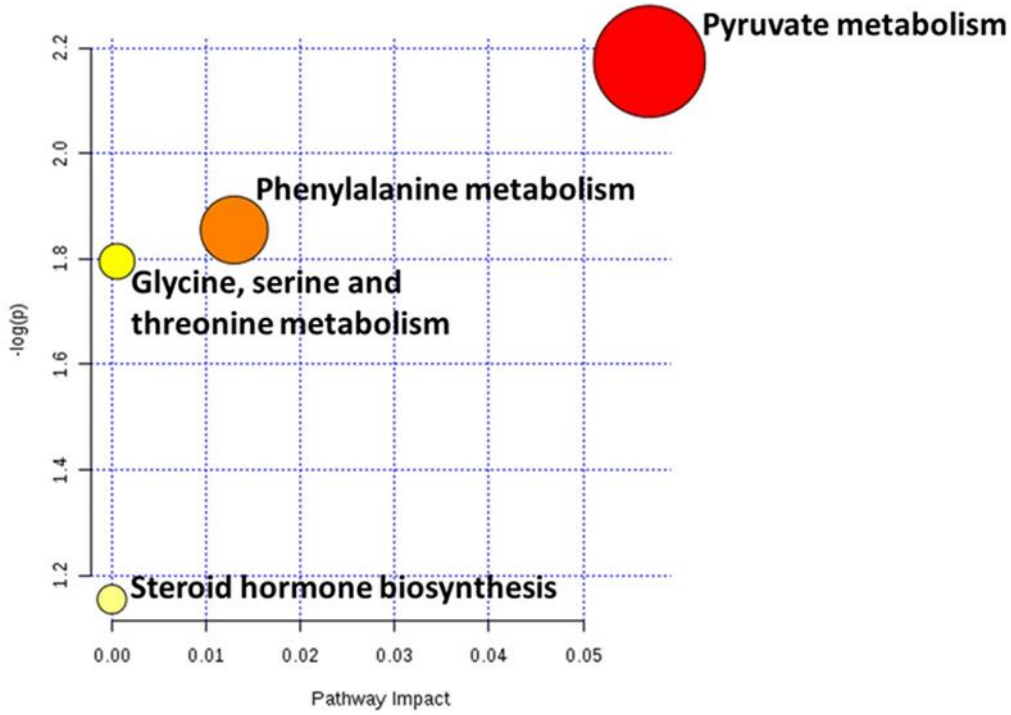

Figure S4. Metabolic pathway analysis performed by the MetPA tool in Metaboanalyst 3.0. Pathway topology analysis depicting dysregulated metabolic pathways in PCa patients. The X-axis represents the pathway impact values, and the Y-axis indicates the -log of *p*-values from the pathway enrichment analysis. The color of the nodes links to the p-values and the node radius is linked to the pathway impact values.

Table S1. List of VOCs significantly altered in PCa group compared to controls. They are characterized by their IUPAC name, retention time, characteristic ions (m/z), Kovat indices (KI) from literature, experimental Kovat indices, NIST R-match and CAS registry number.

Name	Retention time	m/z	KI from literature	Experimental KI or standards	R-match	CAS number	Identification Level[1]
Hexan-2-one (2-Hexanone)	4.61	58;57;100;85;71	790	794	785	591-78-6	L1
Hexanal	4.80	56; 57; 72; 55;99	800	802	823	66-25-1	L1
2-Methylcyclopentan-1-one	5.91	98; 55; 69;80	847	846	735	1120-72-5	L1
4-Methylhexan-3-one	6.86	57; 85; 72; 58; 114;55	853	884	920	17042-16-9	L2
Unknown 1	7.92	59; 56; 55; 76; 84; 65; 57	-	921	-	-	L4
5-Methylheptan-2-one	9.22	58; 71; 70; 55;57;56;59;87;74	971	966	659	18217-12-4	L1
4-Methyldec-1-ene	10.00	57; 56; 41;71;112;55	1041	992	685	13151-29-6	L2
3,7,7-Trimethylbicyclo[4.1.0] hept-3-ene (3-Carene)	10.40	93;79;77;92;121;80; 94;105; 136; 53	1011	1006	907	13466-78-9	L1
2,6-Dimethyl-6-hepten-2-ol	10.47	59;69;56;109;68;124	996	1008	650	32779-58-1	L1
3-Methyl-6-(propan-2-ylidene)cyclohex-1-ene (Isoterpinolene)	10.68	121; 93;136; 79; 91; 77;105;107;67; 53	1023	1015	842	586-63-0	L2
4,6-Dimethylheptan-2-one	11.82	58;85;69;84;59;57;53	1045	1052	802	19549-80-5	L2
3,7-Dimethylocta-1,6-dien-3-ol (Linalool)	13.19	71; 93; 69; 55; 80; 121; 67	1082	1098	708	78-70-6	L1
Unknown 2	13.73	119; 108; 99; 107; 70; 120; 111; 139	-	1116	-	-	L4
Unknown 3	13.84	79; 91; 94; 109;119;77;121;81	-	1120	-	-	L4
3,4-Dimethylcyclohex-3-ene-1-carbaldehyde	14.11	67;138;95;91;79;93; 105	1130	1129	805	18022-66-7	L1

Name	Retention time	m/z	KI from literature	Experimental KI or standards	R-match	CAS number	Identification Level[1]
1-Methyl-4-propan-2-ylcyclohex-2-en-1-ol	15.09	93;139;69;121;111;55;71; 81	1122	1162	675	29803-81-4	L2
Unknown 4	15.74	100; 55; 81; 70; 69; 128; 56; 67	-	1184	-	-	L4
4-Methyl-1-propan-2-ylcyclohex-3-en-1-ol (Terpinen-4-ol)	16.00	59; 93; 121; 136; 67;81;68;79;91	1189	1193	904	98-55-5	L1
Unknown 5	16.26	135; 55; 91; 164; 136; 79; 53; 65; 77; 105	-	1202	-	-	L4
Unknown 6	16.35	61;89;143;81;75;137; 135;115;55;67	-	1205	-	-	L4
2,5-Dimethylbenzaldehyde	16.50	133; 134; 105; 91; 77	1208	1176	841	5779-94-2	L1
2-Hydroxy-2-methyl-1-phenylpropan-1-one	18.45	59;77;105;50;106;51; 78	1278	1277	808	7473-98-5	L1
2,5,5,8-Tetramethyl-3,4,4,6-tetrahydro-2-H-chromene	18.60	179;107;84;55;95;91; 77;69	1293	1287	600	41678-32-4	L2
5-Methyl-2-(propan-2-yl) cyclohexyl acetate (Menthyl acetate)	18.80	95; 138; 81; 123; 96; 82; 94; 67	1304	1296	709	89-48-5	L1
2,6,6,10-Tetramethyl-1-oxaspiro[4.5]dec-9-ene (Theaspirane)	19.40	138; 82; 96; 83; 139; 109; 55; 123	1302	1312	837	36431-72-8	L1
Unknown 7	20.53	56; 67; 79; 83;147; 53;114; 89; 98; 52	-	1358	-	-	L4
Unknown 8	21.43	135; 73; 79; 70; 91; 77; 133; 55; 123; 67	-	1392	-	-	L4
Unknown 9	21.83	91; 67; 53; 79;77	-	1408	-	-	L4
Unknown 10	24.68	69; 105; 129; 59; 93; 68; 67; 77	-	1522	-	-	L4

Name	Retention time	m/z	KI from literature	Experimental KI or standards	R-match	CAS number	Identification Level[1]
Unknown 11	24.74	57; 55; 191; 113; 70; 56; 117; 69	-	1525	-	-	L4
2,2,7,7-Tetramethyltricyclo[6.2.1.0[1],[6]]undeca-3,5,9-triene (4,5,9,10-dehydroisolongifolene)	25.22	107;159;205;131;91;117;220;163;105;187	1544	1546	678	NA	L2

[1]: Viant MR, Kurland IJ, Jones MR and Dunn WB (2017) How close are we to complete annotation of metabolomes? Curr Opin Chem Biol 36:64-69. L1: Identified metabolites (GC-MS analysis of the metabolite of interest and a chemical reference standard of suspected structural equivalence, with all analyses performed under identical analytical conditions within the same laboratory); L2: Putatively annotated compounds (spectral (MS) similarity with NIST database), when standards were not commercially available; L4: Unidentified.

Table S2. List of VCCs significantly altered in PCa group compared to controls. They are characterized by their IUPAC name, retention time, characteristic ions, Kovat indices (KI) from literature, experimental Kovat indices, NIST R-match and CAS registry number.

Name	Retention time	m/z	KI from literature	Experimental KI or standards	R-match	CAS number	Identification Level
Unknown 12	16.19	163;207;164;143;113	-	1194	-	-	L4
Butan-2-one (2-Butanone)	17.35;17.43	56;250;86;195;267	1335	1235/1238	838;844	78-93-3	L1
Pentan-2-one (2-Pentanone)	19.31	253;42;41;56;72;100;182	1434	1305	868	107-87-9	L1
Buten-2-al (2-Butenal)	20.09	250;182;161;195;117 265	1339	1335	721	123-73-9	L1
Cyclohexanone	24.91	82;67;293;81;112;276; 54;55	1635	1549	759	108-94-1	L1
Hexadecane	25.69	72;57;71;85;55;56	1600	1613	836	544-76-3	L1

Name	Retention time	m/z	KI from literature	Experimental KI or standards	R-match	CAS number	Identification Level
Unknown 13	28.20	95;107;75;83;108;319; 161;182;289	-	1765	-	-	L4
Phenylacetaldehyde	29.44	91,117, 65; 182, 315, 297, 77, 161, 134	1832	1919	755	122-78-1	L1
3-Phenylpropanal (3-Phenylpropionaldehyde)	30.67	91;104;105;117;77;103; 65;271;130	1931	1980	703	104-53-0	L1
Decanal	31.80	239;170;182;55;57;69; 240	1954	2130	825	112-31-2	L1
Oxaldehyde (Glyoxal)	33.54	182;161;195;167;117;99;4 48;93;119	1935	2221	933	107-22-2	L1
2-Oxopropanal (Methylglyoxal/ Pyruvaldehyde)	34.30	182;265;161;195;167; 117;99;119;168	2174	2260	935	78-98-8	L1

[1]: Viant MR, Kurland IJ, Jones MR and Dunn WB (2017) How close are we to complete annotation of metabolomes? Curr Opin Chem Biol 36:64-69. L1: Identified metabolites (GC-MS analysis of the metabolite of interest and a chemical reference standard of suspected structural equivalence, with all analyses performed under identical analytical conditions within the same laboratory); L2: Putatively annotated compounds (spectral (MS) similarity with NIST database); L4: Unidentified.

Table S3. Confusion matrix obtained for VOCs and VCCs considering the external validation sets (*n*=18 PCa patients plus *n*=18 cancer-free controls).

		Predicted Classes			
		VOCs		VCCs	
		Case	*Control*	*Case*	*Control*
True Classes	*Case*	14	4	14	4
	Control	1	17	0	18

Table S4. Spearman's correlation indexes and corresponding *p*-values obtained for age with the set of metabolites found altered in PCa compared to controls.

Metabolites	***r***	***p***
VOCs		
2-Hexanone	-0.08	0.4578
Hexanal	0.00	0.9670
2-Methylcyclopentan-1-one	-0.10	0.3915
4-Methylhexan-3-one	-0.01	0.9114
Unknown 1	-0.15	0.1860
5-Methylheptan-2-one	-0.22	0.0514
4-Methyldec-1-ene	-0.15	0.1674
3,7,7-Trimethylbicyclo[4.1.0] hept-3-ene (3-Carene)	0.00	0.9764
2,6-Dimethyl-6-hepten-2-ol	-0.29	0.0082
3-Methyl-6-(propan-2-ylidene)cyclohex-1-ene (Isoterpinolene)	-0.22	0.0483
4,6-Dimethylheptan-2-one	-0.25	0.0249
3,7-Dimethyl-1,6-octadien-3-ol (Linalool)	-0.23	0.0358
Unknown 2	-0.28	0.0115
Unknown 3	-0.32	0.0038
3,4-Dimethylcyclohex-3-ene-1-carbaldehyde	-0.31	0.0041
1-Methyl-4-propan-2-ylcyclohex-2-en-1-ol	-0.30	0.0071
Unknown 4	-0.39	0.0004
4-Methyl-1-propan-2-ylcyclohex-3-en-1-ol (Terpinen-4-ol)	-0.36	0.0010
Unknown 5	-0.19	0.0814
Unknown 6	0.20	0.0742
2,5-Dimethylbenzaldehyde	0.19	0.0929
2-Hydroxy-2-methyl-1-phenylpropan-1-one	-0.23	0.0368
2,5,5,8-Tetramethyl-3,4,4,6-tetrahydro-2-H-chromene	-0.14	0.2157
5-Methyl-2-(propan-2-yl) cyclohexyl acetate (Menthyl acetate)	-0.16	0.1505
2,6,6,10-Tetramethyl-1-oxaspiro[4.5]dec-9-ene (Theaspirane)	-0.13	0.2397
Unknown 7	-0.09	0.4011
Unknown 8	-0.20	0.0692
Unknown 9	-0.16	0.1543
Unknown 10	-0.24	0.0333
Unknown 11	-0.05	0.6494
2,2,7,7-Tetramethyltricyclo[6.2.1.0^{1,6}]undeca-3,5,9-triene (4,5,9,10-dehydroisolongifolene)	-0.19	0.0889

Metabolites	*r*	*p*
VCCs		
Unknown 12	0.12	0.2991
2-Butanone	0.04	0.7035
2-Pentanone	0.02	0.8925
2-Butenal	-0.02	0.8418
Cyclohexanone	0.03	0.7650
Hexadecane	0.04	0.7433
Unknown 13	-0.01	0.9429
Phenylacetaldehyde	0.20	0.0705
3-Phenylpropionaldehyde	0.09	0.4186
Decanal	-0.17	0.1341
Oxaldehyde (Glyoxal)	-0.08	0.5009
2-Oxopropanal (Methylglyoxal/Pyruvaldehyde)	-0.07	0.5409

Table S5. Confusion matrix obtained for the panel of 6 metabolites considering the external validation set (*n*=18 PCa plus *n*=18 controls) (sensitivity: 88%, specificity: 83% and accuracy: 86%).

		Predicted classes	
		Case	*Control*
True Classes	*Case*	16	2
	Control	3	15

Section 3.2 - A Panel of Urinary Volatile Biomarkers for Differential Diagnosis of Prostate Cancer from Other Urological Cancers

Ana Rita Lima, Joana Pinto, Carina Carvalho-Maia, Carmen Jerónimo, Rui Henrique, Maria de Lourdes Bastos, Márcia Carvalho, Paula Guedes de Pinho

The article (DOI: 10.3390/cancers12082017.10.3390) presented in this chapter was published by MDPI, in *Cancers*, in 2020, and is here presented in the form of “Accepted Manuscript” It is available online on:

https://www.mdpi.com/2072-6694/12/8/2017

3.2.1 Abstract

Our group recently developed a urinary 6-biomarker panel for the diagnosis of prostate cancer (PCa) which has a higher level of accuracy compared to the serum prostate specific antigen (PSA) test. Herein, urine from an independent cohort of PCa patients and cancer-free controls was analyzed to further validate the discriminative power of that panel. Additionally, urine from patients diagnosed with bladder cancer (BC) and renal cancer (RC) were included to evaluate the site-specificity of the panel. Results confirmed the ability of the 6-biomarker panel to discriminate PCa patients from controls, but not from other urological cancers. To overcome this limitation, an untargeted approach was performed to unveil discriminant metabolites among the three cancer types. A 10-biomarker panel comprising the original panel plus four new metabolites was established to discriminate PCa from controls, BC, and RC, with 76% sensitivity, 90% specificity, and 92% accuracy. This improved panel also disclosed better accuracy than serum PSA test and provides the basis for a new non-invasive early detection tool for PCa.

Keywords:
Prostate cancer; Renal cancer; Bladder cancer; Volatile organic compounds; Urinary biomarkers; Detection

3.2.2 Introduction

Globally, prostate cancer (PCa) ranks first amongst all male urological cancers and second in incidence of all cancers in men [1]. Due to its asymptomatic nature at early stages, long latency period, and potential for cure [2], PCa is a perfect candidate for screening programs. Currently, early PCa detection is mostly based on digital rectal examination (DRE) and serum prostate specific antigen (PSA) assessment, which stratify patients for subsequent prostate biopsy [2,3]. However, these procedures have serious limitations and have led to overdiagnosis and consequent overtreatment of low-risk patients, unnecessary biopsies, and unwarranted radical prostatectomies [4]. Indeed, the standard serum PSA cut-off of 4 ng/mL has failed to meet the criteria required for an effective biomarker due to its limited sensitivity (20.5%), specificity (51–91%) [5,6], area under the curve (AUC) (0.53–0.83), and accuracy (62–75%) [7]. Based on these limitations, several research groups have proposed new candidate biomarkers for PCa detection (e.g., prostate cancer antigen 3 (PCA3) and prostate health index (PHI)) [8–10]. PCA3 score has 63% sensitivity, 88% specificity, and an AUC of 0.82, considering a cut-off of 35 [9]. However, the definition of the ideal cut-off for this biomarker remains controversial [8]. PHI combines total serum PSA, free PSA (fPSA), and [-2]proPSA (p2PSA) and outperforms serum PSA with an AUC ranging from 0.70 to 0.77 [10].

Metabolic rewiring has recently been recognized as a hallmark of cancer cells [11], boosting the search for innovative PCa detection strategies based on the study of tumor-associated metabolic alterations [12–15]. Volatile organic compounds (VOCs) are end products of cellular metabolism, especially promising as potential non-invasive biomarkers for translation into the clinic due to the recent advancements in the development of electronic-nose (e-nose) sensors [16]. In this vein, we have recently reported a urinary biomarker panel for PCa diagnosis comprising six volatile compounds, that outperformed PSA sensitivity and accuracy [17]. Here, we extend our previous work to further validate the biomarker panel in an independent cohort of PCa patients and also to assess the performance of the panel for discriminating PCa from other common urological cancers, namely bladder cancer (BC) and renal cancer (RC).

3.2.3 Material and Methods

3.2.3.1 Study Population

Urine samples were collected at the Portuguese Oncology Institute of Porto from a total of 80 men, comprising 20 PCa patients, 20 BC patients, 20 RC patients, and 20 cancer-free individuals (controls) (Table S1). This study was performed in accordance with the Declaration of Helsinki and approved by the Portuguese Oncology Institute of Porto (IPO Porto) Ethics Committee (Reference 282R/2017). All subjects included in the study provided signed informed consent. Early morning voided urine samples (without fasting) were centrifuged and the supernatants were immediately frozen at -80 ºC until analysis.

3.2.3.2 Sample Preparation for GC-MS Based Metabolomic Analysis

Preparation of urine samples and analytical conditions followed the protocol described by Lima et al. [17]. To detect a large number of volatile compounds, two different analysis procedures based on headspace solid-phase microextraction (HS-SPME) coupled to GC-MS were performed. VOCs were analyzed directly in the headspace of the urine, while VCCs (mostly aldehydes and ketones) were analyzed after a derivatization step of urine with O-(2,3,4,5,6-pentafluorobenzyl) hydroxylamine hydrochloride (PFBHA). Quality control (QC) samples (a pool of all urine samples) were analyzed at the same conditions on every eight samples, to ensure the reproducibility of the method. All samples were extracted and injected randomly.

3.2.3.3 GC-MS Analysis

VOCs and VCCs analyses were performed in a 436-GC (Bruker Daltonics, Billerica, MA, USA) coupled to a Bruker Scion SQ MS detector (Bruker Daltonics) and a 436-GC (Bruker Daltonics) coupled to an EVOQ TQ-MS (Bruker Daltonics), respectively. Details on software, GC and MS acquisition parameters, and metabolite identification are described in Lima et al. [17].

3.3.3.4 Data Pre-Processing and Statistical Analysis

Data pre-processing was performed in MZmine 2.18 [18] using the parameters previously described in Lima et al. [17]. In the untargeted models, a variable selection approach was applied to reduce the data and eliminate the variation from uncontrolled confounding factors [19]. This variable selection was based on the t-test (MetaboAnalyst 4.0 software) [20] and all variables with *p*-value > 0.05 were removed from the matrix.

Finally, the untargeted models were scaled to pareto and the models based in the biomarker panel were scaled to unit variance (UV).

Multivariate statistical analysis (MVA) included principal component analysis (PCA) to detect trends and possible outliers, followed by partial least squares discriminant analysis (PLS-DA). In addition, the robustness of all PLS-DA models was confirmed through 7-fold cross validation and permutation test in SIMCA-P 15 (Umetrics, Umeå, Sweden).

Unpaired Student's t-test with Welch correction test (normal distribution) or unpaired Mann–Whitney U-test (non-normal distribution) were applied to all metabolites with VIP higher than 1 in the untargeted models (VOCs and VCCs) (GraphPad Prism 6, San Diego, CA, USA). In addition, percentage of variation and effect size were computed for all statistically significant metabolites. The metabolites significantly altered in all comparisons (PCa *vs*. BC, PCa *vs*. RC, and PCa *vs*. controls) were considered specific for PCa.

To select the most important metabolites among these, a PLS-DA algorithm was applied. The selected biomarker panel was used to construct a classification model and the corresponding receiver operating characteristic (ROC) curve using the MetaboAnalyst 4.0 software [20].

3.2.4 Results

3.2.4.1 Evaluation of the Diagnostic Performance of 6-Volatile Biomarker Panel

A targeted metabolomics approach (Figure 3.4a) was first performed to build a partial least squares discriminant analysis (PLS-DA) model comprising only the six volatile metabolites included in the previously defined PCa biomarker panel, specifically 2,5-dimethylbenzaldehyde, 3-phenylpropionaldehyde, 4-methylhexan-3-one, dihydroedulan IA, hexanal, and methylglyoxal (MG). The classification model confirmed that this 6-biomarker panel was able to discriminate PCa from controls (Figure S1A), as validated by permutation tests (Figure S2A), with 84% sensitivity, 80% specificity, 82% accuracy, and an AUC of 0.83 (Figure S2B). However, the panel was unable to discriminate PCa from either BC (Figure S1B) or RC (Figure S1C). To overcome this limitation, an untargeted approach was conducted, seeking to identify new biomarkers able to discriminate PCa from the other urological cancers.

3.2.4.2 Untargeted Volatile Profiling Unveils Discriminant Metabolites among Urological Cancers

The untargeted approach consisted on the comparison of the urinary volatile profiles (VOCs and volatile carbonyl compounds (VCCs)) of PCa patients with that of BC and RC patients. Results disclosed a good separation of PCa from BC and RC in the PLS-DA models (Table S2). Overall, 50 metabolites showed a variable importance to the projection (VIP) higher than 1 comparing PCa *vs*. BC, from which 35 were found significantly different. Comparison of PCa *vs*. RC unveiled a total of 62 metabolites with VIP > 1, from which 47 were significantly different. Subsequently, only the metabolites that met the criteria of statistical significance in the three comparisons (PCa *vs*. BC, PCa *vs*. RC, and PCa *vs*. controls) were considered for further analysis, namely ethylbenzene, heptan-3-one, heptan-2-one, 4-(2-methylpropoxy)butan-2-one, methyl benzoate, 3-methyl-benzaldehyde, and an unknown metabolite (Figure S3; Tables S3 and S4).

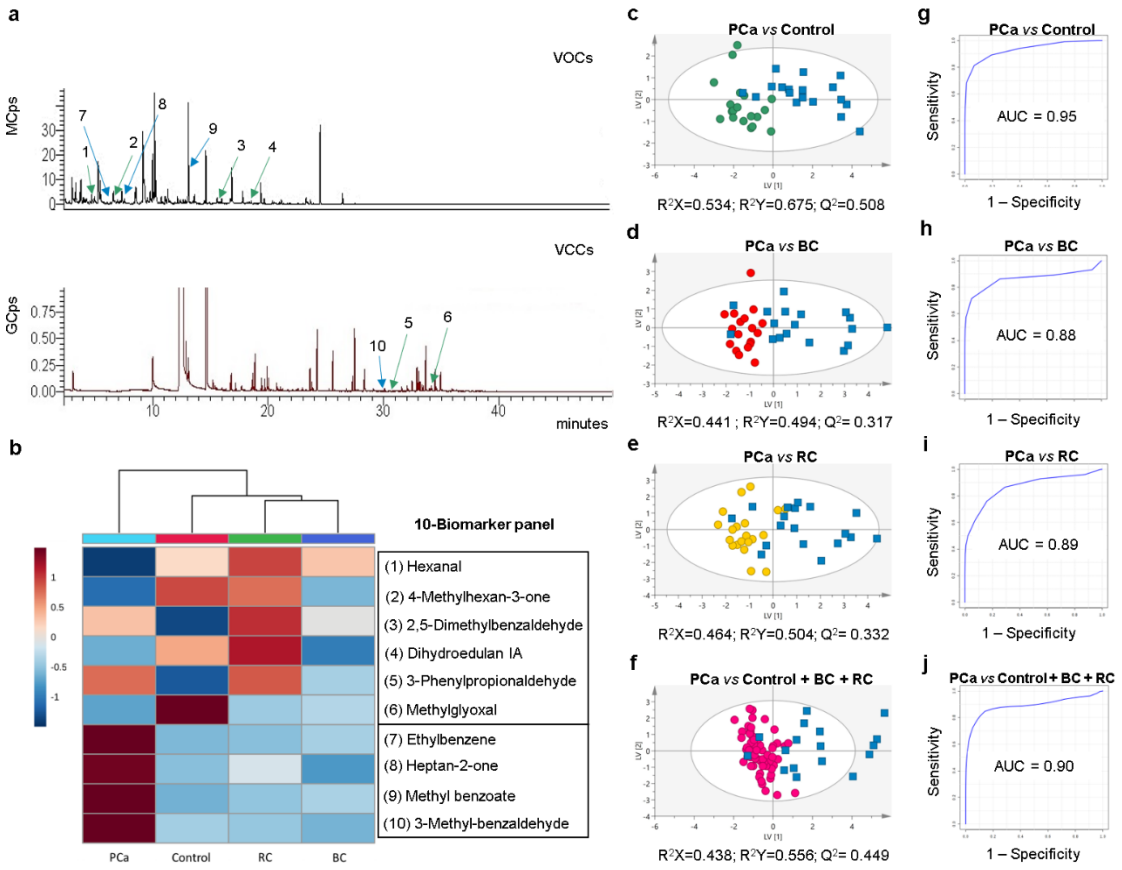

Figure 3.4: (a) Representative GC-MS chromatograms of VOCs and VCCs present in urine of PCa patients (green arrows indicate the 6 volatiles (numbers 1-6) in former biomarker panel and blue arrows the surplus 4 volatiles (numbers 7-10), with the correspondence of numbers to metabolite identities present in b). **(b)** Heatmap illustrating the mean levels (normalized peak areas) of metabolites included in the 10-biomarker panel. Rows correspond to the mean normalized peak area of each metabolite with the sample groups in the columns. **(c- f)** PLS-DA scores scatter plots (UV scaling; 2 components) obtained for the 10-biomarker panel of **(c)** PCa (*n* = 18, blue squares) *vs.* cancer-free controls (*n* = 19, green circles), **(d)** PCa (n = 18, blue squares) *vs*. BC (*n* = 18, red circles), **(e)** PCa (*n* = 18, blue squares) *vs.* RC (*n* = 20, yellow circles), **(f)** PCa (*n* = 17, blue squares) *vs.* cancer-free controls plus BC and RC (*n* = 58, pink circles). **(g, h, i, j)** Assessment of the diagnostic performance of the PLS-DA models obtained for the 10-biomarker panel of **(g)** PCa *vs*. cancer-free controls (AUC = 0.95; sensitivity = 78%; specificity = 100%; accuracy = 89%), **(h)** PCa *vs.* BC (AUC = 0.88; sensitivity = 72%; specificity = 100%; accuracy = 86%), **(i)** PCa *vs.* RC (AUC = 0.89; sensitivity = 72%; specificity = 90%; accuracy = 82%), **(j)** PCa *vs.* cancer-free controls plus BC and RC (AUC = 0.90; sensitivity = 76%; specificity = 97%; accuracy = 92%).

3.2.4.3 Definition of an Improved Biomarker Panel for PCa Diagnosis

The seven candidate biomarkers disclosed by untargeted analysis were assessed for their ability to perfect an extended biomarker panel providing the best combination of sensitivity, specificity, and accuracy for PCa detection. Considering a PLS-DA based algorithm, four metabolites were selected, namely ethylbenzene, heptan-2-one, methyl benzoate, and 3-methylbenzaldehyde (Figure S4). Therefore, a final 10-biomarker panel was defined for PCa diagnosis (Figure 3.4b), composed by hexanal, 4-methylhexan-3-one, dihydroedulan IA and MG (significantly decreased), and 3-phenylpropionaldehyde, 2,5-dimethylbenzaldehyde, ethylbenzene, heptan-2-one, methyl benzoate, and 3-methylbenzaldehyde (significantly increased). Finally, PLS-DA models obtained with this improved biomarker panel revealed a clear separation between PCa *vs*. controls (Figure 3.4c), PCa *vs*. BC (Figure 3.4d), and PCa *vs*. RC (Figure 3.4e). Furthermore, the panel disclosed 78% sensitivity, 100% specificity, 89% accuracy, and an AUC of 0.95 for PCa *vs*. controls (Figure 3.4g); 72% sensitivity, 100% specificity, 86% accuracy, and an AUC of 0.88 for PCa *vs*. BC (Figure 3.4h); and 72% sensitivity, 90% specificity, 82% accuracy, and an AUC of 0.89 for PCa *vs*. RC (Figure 3.4i). To provide a more global perspective of the 10-biomarker panel performance, a final PLS-DA model was computed comparing PCa *vs*. controls plus BC plus RC (Figure 3.4f). This model showed a good separation between the two groups with 76% sensitivity, 97% specificity, 92% accuracy, and an AUC of 0.90 (Figure 3.4j). The robustness of all PLS-DA models was confirmed through permutation testing (Figure S5).

3.2.5 Discussion

The major novelty of this study design was the inclusion of patients with other urological cancers to evaluate the performance of the biomarker panel to discriminate not only PCa *vs.* cancer-free individuals, but also PCa *vs.* BC and RC (2nd and 3rd most common urological cancers in males, respectively) [21]. This critical point is often overlooked in traditional biomarker studies, thus disregarding the cancer site specificity of the biomarker (s). Although the performance of our 6-biomaker panel to accurately identify PCa patients *vs.* control subjects was confirmed, it failed to discriminate PCa from both BC and RC. This result was not completely surprising as tumor cells share some metabolic abnormalities to promote cancer cell survival and growth [11], which may make the discrimination among different cancer types difficult. Indeed, three out of the six biomarkers included in the panel (2,5-dimethylbenzaldehyde, 3-phenylpropionaldehyde, and MG) disclosed the same trend

in all urological cancers *vs*. controls (Figure 3.4b), explaining the lack of discriminatory power. One well-established metabolic feature of cancer cells is increased aerobic glycolysis over oxidative respiration, which unavoidably leads to MG accumulation [19]. Particularly, MG is known as a highly toxic and reactive carbonyl compound that spontaneously glycates proteins, nucleic acids, and lipids [22]. MG detoxification is accomplished mainly by glyoxalase-1, and both high expression and activity of this enzyme have been demonstrated in PCa, BC, and RC [23], explaining the decrease in MG urinary levels in all urological cancers compared to controls.

Those results demonstrated that BC or RC patients may be false positives in a PCa screening strategy based on the 6-biomarker panel, constituting a relevant limitation in clinical practice. To overcome this, we performed an untargeted metabolomic study to look for new biomarkers capable of discriminating PCa from the other urological cancers. This approach allowed the improvement of the previously established biomarker panel through the addition of four new volatile compounds, discriminative of PCa *vs*. BC and RC. Thus, the improved panel included five aldehydes (hexanal, 2,5-dimethylbenzaldehyde, 3-phenylpropionaldehyde, MG, 3-methylbenzaldehyde), two ketones (4-methylhexan-3-one, heptan-2-one), two aromatic hydrocarbons (methyl benzoate and ethylbenzene), and one polycyclic organic compound (dihydroedulan IA). From these, only hexanal [24–27], MG [28], heptan-2-one [25,29], and ethylbenzene [26,30] were previously associated with cancer. Besides MG, it is difficult to ascertain the metabolic origin of these volatile compounds since they are end products of several cellular processes, including lipid peroxidation, protein carbonylation, glycation, and amino acid and lipid metabolisms [31–33].

In the last decade, several candidate biomarkers have been proposed using metabolomic approaches, including mainly amino acids and derivatives, organic acids, and sugars [15]. Overall, the 10-biomarker panel disclosed similar or even better performance for PCa detection compared with those candidate biomarkers. Moreover, the discrimination of PCa from other urological cancers has been understudied, comprising only one study which failed to demonstrate discriminative power [34]. Hence, the accurate classification of PCa using the 10-biomarker panel in a cohort comprising other urological cancers is an important achievement. Notably, the 10-biomarker panel outperforms not only PSA [5–7], but also PCA3 [9] and PHI [10] in differentiating PCa patients from controls.

These results emphasize the potential of volatile biomarkers for development of a non-invasive screening tool for clinical diagnosis. However, the analytical techniques used in metabolomic approaches might not be feasible for real-time diagnostic applications due to

several limitations, such as low sample throughput, high costs, and the requirement for trained personnel and sophisticated software. Thus, future research may rely on the translation of the volatile signatures detected by GC-MS analysis to the application of a fast, cheap, and portable e-nose device. In this regard, our defined panel holds the potential for development of an optimized e-nose with sensor arrays targeting specific PCa-related volatile compounds for routine clinical use with high accuracy for PCa diagnosis.

3.2.5 Conclusions

In conclusion, we propose an improved volatile urinary biomarker panel to simultaneously discriminate PCa from cancer-free subjects and carriers of other common urological cancers, holding the potential for the development of a non-invasive early detection tool for PCa that outperforms serum PSA sensitivity and accuracy. In the future, we plan to extend the PCa-specificity of this novel panel, testing larger cohorts of cancer patients and controls, including common non-urological cancers in males (e.g., lung and colorectal cancers). Furthermore, taking into consideration that benign prostate hyperplasia, urinary tract infection, and prostatitis are important confounding factors in PSA test, we also plan to include urine samples from patients with these diseases.

3.2.6 References

1. Bray, F.; Ferlay, J.; Soerjomataram, I.; Siegel, R.L.; Torre, L.A.; Jemal, A. Global cancer statistics 2018: GLOBOCAN estimates of incidence and mortality worldwide for 36 cancers in 185 countries. CA Cancer J. Clin. 2018, 68, 394–424.
2. Bax, C.; Taverna, G.; Eusebio, L.; Sironi, S.; Grizzi, F.; Guazzoni, G.; Capelli, L. Innovative Diagnostic Methods for Early Prostate Cancer Detection through Urine Analysis: A Review. Cancers 2018, 10, 123.
3. Grignon, D.J. Prostate cancer reporting and staging: Needle biopsy and radical prostatectomy specimens. Mod. Pathol. 2018, 31, S96–S109.
4. Loeb, S.; Bjurlin, M.A.; Nicholson, J.; Tammela, T.L.; Penson, D.F.; Carter, H.B.; Carroll, P.; Etzioni, R. Overdiagnosis and overtreatment of prostate cancer. Eur. Urol. 2014, 65, 1046–1055.
5. Kearns, J.T.; Lin, D.W. Improving the Specificity of PSA Screening with Serum and Urine Markers. Curr. Urol. Rep. 2018, 19, 80.

6. Wolf, A.M.; Wender, R.C.; Etzioni, R.B.; Thompson, I.M.; D'Amico, A.V.; Volk, R.J.; Brooks, D.D.; Dash, C.; Guessous, I.; Andrews, K.; et al. American Cancer Society guideline for the early detection of prostate cancer: Update 2010. CA Cancer J. Clin. 2010, 60, 70–98.

7. Louie, K.S.; Seigneurin, A.; Cathcart, P.; Sasieni, P. Do prostate cancer risk models improve the predictive accuracy of PSA screening? A meta-analysis. Ann. Oncol. 2015, 26, 848–864.

8. Filella, X.; Fernandez-Galan, E.; Fernandez Bonifacio, R.; Foj, L. Emerging biomarkers in the diagnosis of prostate cancer. Pharmgenom. Personal. Med. 2018, 11, 83–94.

9. Cui, Y.; Cao, W.; Li, Q.; Shen, H.; Liu, C.; Deng, J.; Xu, J.; Shao, Q. Evaluation of prostate cancer antigen 3 for detecting prostate cancer: A systematic review and meta-analysis. Sci. Rep. 2016, 6, 25776.

10. Filella, X.; Gimenez, N. Evaluation of [-2] proPSA and Prostate Health Index (phi) for the detection of prostate cancer: A systematic review and meta-analysis. Clin. Chem. Lab. Med. 2013, 51, 729–739.

11. Pavlova, N.N.; Thompson, C.B. The Emerging Hallmarks of Cancer Metabolism. Cell Metab. 2016, 23, 27–47.

12. Sreekumar, A.; Poisson, L.M.; Rajendiran, T.M.; Khan, A.P.; Cao, Q.; Yu, J.; Laxman, B.; Mehra, R.; Lonigro, R.J.; Li, Y.; et al. Metabolomic profiles delineate potential role for sarcosine in prostate cancer progression. Nature 2009, 457, 910–914.

13. Kelly, R.S.; Vander Heiden, M.G.; Giovannucci, E.; Mucci, L.A. Metabolomic Biomarkers of Prostate Cancer:
Prediction, Diagnosis, Progression, Prognosis, and Recurrence. Cancer Epidemiol. Biomark. Prev. 2016, 25, 887–906.

14. Khalid, T.; Aggio, R.; White, P.; De Lacy Costello, B.; Persad, R.; Al-Kateb, H.; Jones, P.; Probert, C.S.; Ratcliffe, N. Urinary Volatile Organic Compounds for the Detection of Prostate Cancer. PLoS ONE 2015, 10, e0143283.

15. Kdadra, M.; Hockner, S.; Leung, H.; Kremer, W.; Schiffer, E. Metabolomics Biomarkers of Prostate Cancer: A Systematic Review. Diagnostics 2019, 9, 21.

16. Capelli, L.; Taverna, G.; Bellini, A.; Eusebio, L.; Buffi, N.; Lazzeri, M.; Guazzoni, G.; Bozzini, G.; Seveso, M.; Mandressi, A.; et al. Application and Uses of Electronic Noses for Clinical Diagnosis on Urine Samples: A Review. Sensors 2016, 16, 1708.

17. Lima, A.R.; Pinto, J.; Azevedo, A.I.; Barros-Silva, D.; Jeronimo, C.; Henrique, R.; de Lourdes Bastos, M.; Guedes de Pinho, P.; Carvalho, M. Identification of a biomarker panel

for improvement of prostate cancer diagnosis by volatile metabolic profiling of urine. Br. J. Cancer 2019, 121, 857–868.

18. Pluskal, T.; Castillo, S.; Villar-Briones, A.; Oresic, M. MZmine 2: Modular framework for processing, visualizing, and analyzing mass spectrometry-based molecular profile data. BMC Bioinform. 2010, 11, 395.

19. Xi, B.; Gu, H.; Baniasadi, H.; Raftery, D. Statistical analysis and modeling of mass spectrometry-based metabolomics data. Methods Mol. Biol. 2014, 1198, 333–353.

20. Chong, J.; Soufan, O.; Li, C.; Caraus, I.; Li, S.; Bourque, G.; Wishart, D.S.; Xia, J. MetaboAnalyst 4.0: Towards more transparent and integrative metabolomics analysis. Nucleic Acids Res. 2018, 46, W486–W494.

21. Siegel, R.L.; Miller, K.D.; Jemal, A. Cancer statistics, 2019. CA Cancer J. Clin. 2019, 69, 7–34.

22. Bellahcene, A.; Nokin, M.J.; Castronovo, V.; Schalkwijk, C. Methylglyoxal-derived stress: An emerging biological factor involved in the onset and progression of cancer. Semin. Cancer Biol. 2018, 49, 64–74.

23. Antognelli, C.; Talesa, V.N. Glyoxalases in Urological Malignancies. Int. J. Mol. Sci. 2018, 19, 415.

24. Cauchi, M.; Weber, C.M.; Bolt, B.J.; Spratt, P.B.; Bessant, C.; Turner, D.C.; Willis, C.M.; Britton, L.E.; Turner, C.; Morgan, G. Evaluation of gas chromatography mass spectrometry and pattern recognition for the identification of bladder cancer from urine headspace. Anal. Methods 2016, 8, 4037–4046.

25. Porto-Figueira, P.; Pereira, J.; Miekisch, W.; Camara, J.S. Exploring the potential of NTME/GC-MS, in the establishment of urinary volatomic profiles. Lung cancer patients as case study. Sci. Rep. 2018, 8, 13113.

26. Opitz, P.; Herbarth, O. The volatilome—Investigation of volatile organic metabolites (VOM) as potential tumor markers in patients with head and neck squamous cell carcinoma (HNSCC). J. Otolaryngol. Head Neck Surg. 2018, 47, 42.

27. Silva, C.L.; Passos, M.; Camara, J.S. Investigation of urinary volatile organic metabolites as potential cancer biomarkers by solid-phase microextraction in combination with gas chromatography-mass spectrometry. Br. J. Cancer 2011, 105, 1894–1904.

28. Monteiro, M.; Moreira, N.; Pinto, J.; Pires-Luis, A.S.; Henrique, R.; Jeronimo, C.; Bastos, M.L.; Gil, A.M.; Carvalho, M.; Guedes de Pinho, P. GC-MS metabolomics-based approach for the identification of a potential VOC-biomarker panel in the urine of renal cell carcinoma patients. J. Cell Mol. Med. 2017, 21, 2092–2105.

29. Perez Anton, A.; Ramos, A.G.; Del Nogal Sanchez, M.; Pavon, J.L.; Cordero, B.M.; Pozas, A.P. Headspace-programmed temperature vaporization-mass spectrometry for the rapid determination of possible volatile biomarkers of lung cancer in urine. Anal. Bioanal. Chem. 2016, 408, 5239–5246.
30. Jobu, K.; Sun, C.; Yoshioka, S.; Yokota, J.; Onogawa, M.; Kawada, C.; Inoue, K.; Shuin, T.; Sendo, T.; Miyamura, M. Metabolomics study on the biochemical profiles of odor elements in urine of human with bladder cancer. Biol. Pharm. Bull. 2012, 35, 639–642.
31. Haick, H.; Broza, Y.Y.; Mochalski, P.; Ruzsanyi, V.; Amann, A. Assessment, origin, and implementation of breath volatile cancer markers. Chem. Soc. Rev. 2014, 43, 1423–1449.
32. Filipiak, W.; Mochalski, P.; Filipiak, A.; Ager, C.; Cumeras, R.; Davis, C.E.; Agapiou, A.; Unterkofler, K.; Troppmair, J. A Compendium of Volatile Organic Compounds (VOCs) Released By Human Cell Lines. Curr. Med. Chem. 2016, 23, 2112–2131.
33. Hakim, M.; Broza, Y.Y.; Barash, O.; Peled, N.; Phillips, M.; Amann, A.; Haick, H. Volatile organic compounds of lung cancer and possible biochemical pathways. Chem. Rev. 2012, 112, 5949–5966.
34. Gamagedara, S.; Kaczmarek, A.T.; Jiang, Y.; Cheng, X.; Rupasinghe, M.; Ma, Y. Validation study of urinary metabolites as potential biomarkers for prostate cancer detection. Bioanalysis 2012, 4, 1175–1183.

3.2.7 Supporting information

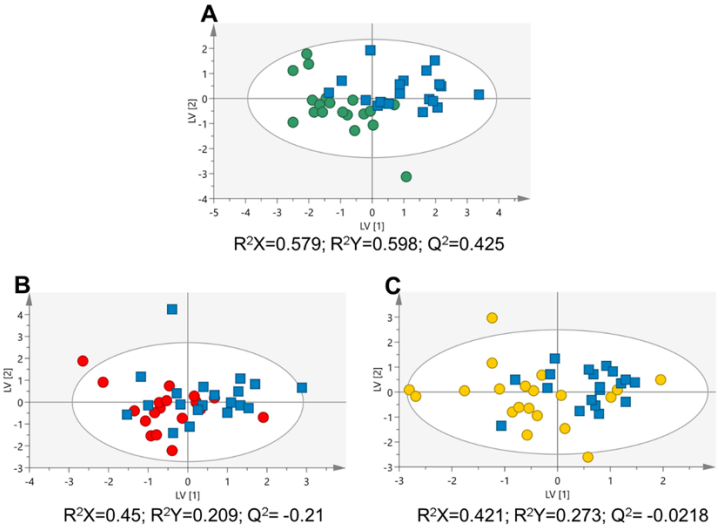

Supplementary Figure 1. PLS-DA scores scatter plots (UV scaling; 2 components) obtained for the urinary 6-biomarker panel of **(A)** PCa patients (*n* = 19, blue squares) *vs*. cancer-free controls (*n* = 20, green circles); **(B)** PCa (*n* = 20, blue squares) *vs*. BC (*n* = 19, red circles); and **(C)** PCa (*n* = 19, blue squares) *vs*. RC (*n* = 20, yellow circles).

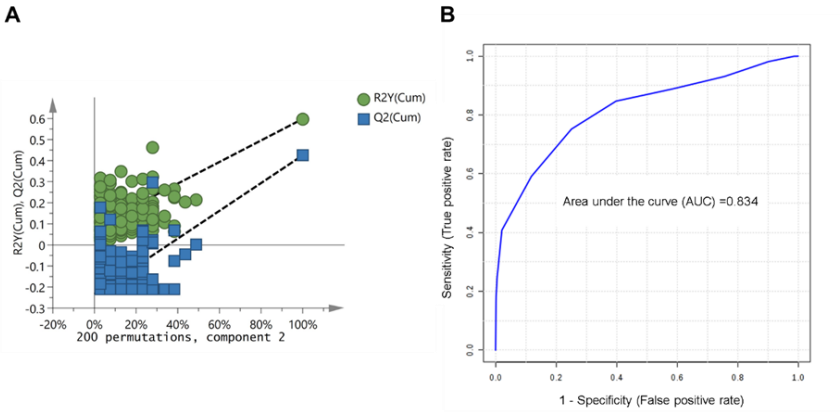

Supplementary Figure 2. (A) Statistical validation of the PLS-DA model obtained for the 6-biomarker panel, by permutation testing (200 permutations; 2 components) PCa *vs.* cancer-free controls [Intercepts: R^2 = (0.0, 0.0866), Q^2 = (0.0, -0.234)]; **(B)** Assessment of the diagnostic performance of the PLS-DA model obtained for the 6-biomarker panel through receiver operating characteristic (ROC) curve, PCa *vs*. controls (AUC = 0.834; sensitivity = 84%; specificity = 80%; accuracy = 82%).

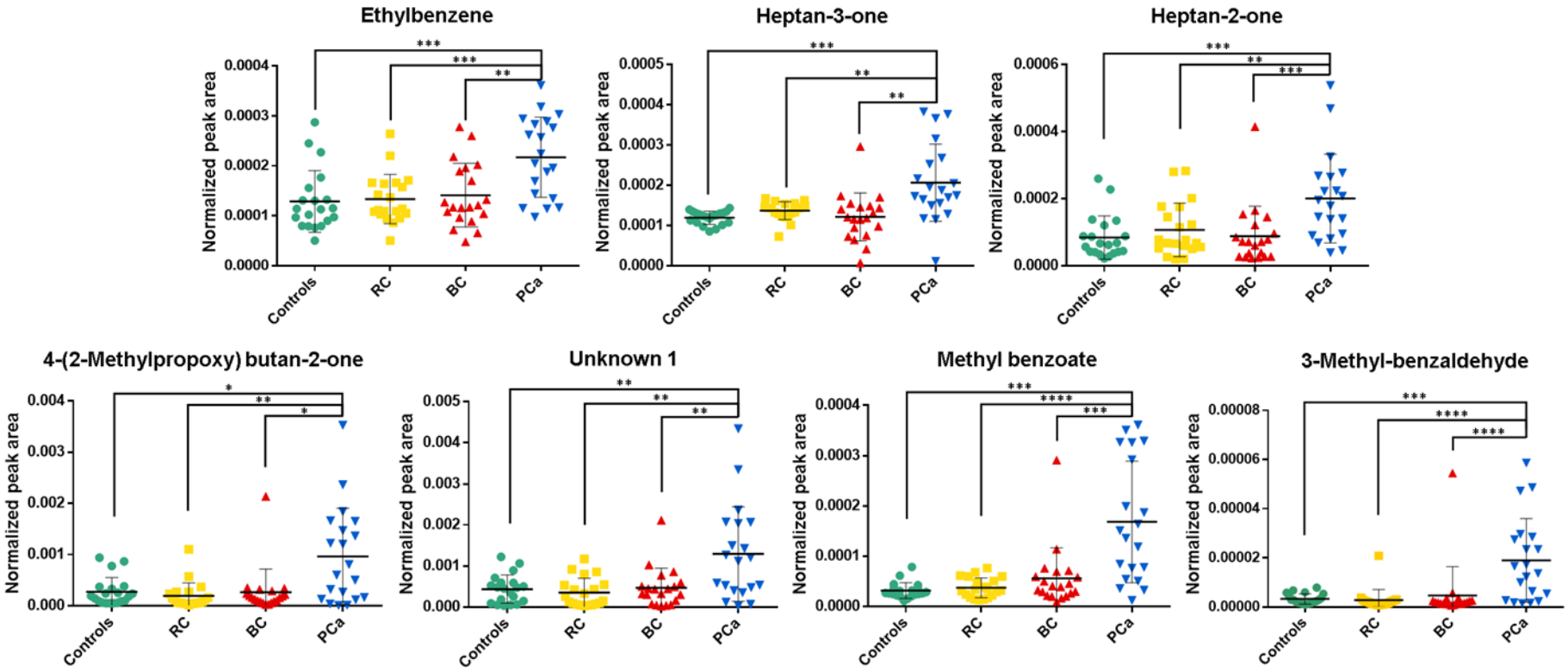

Supplementary Figure 3. Boxplots from all metabolites that were simultaneously significantly different between PCa *vs*. BC, PCa *vs.* RC and PCa *vs.* cancer free-controls (****p-value < 0.0001, ***p-value < 0.001, **p-value < 0.01, *p-value < 0.05).

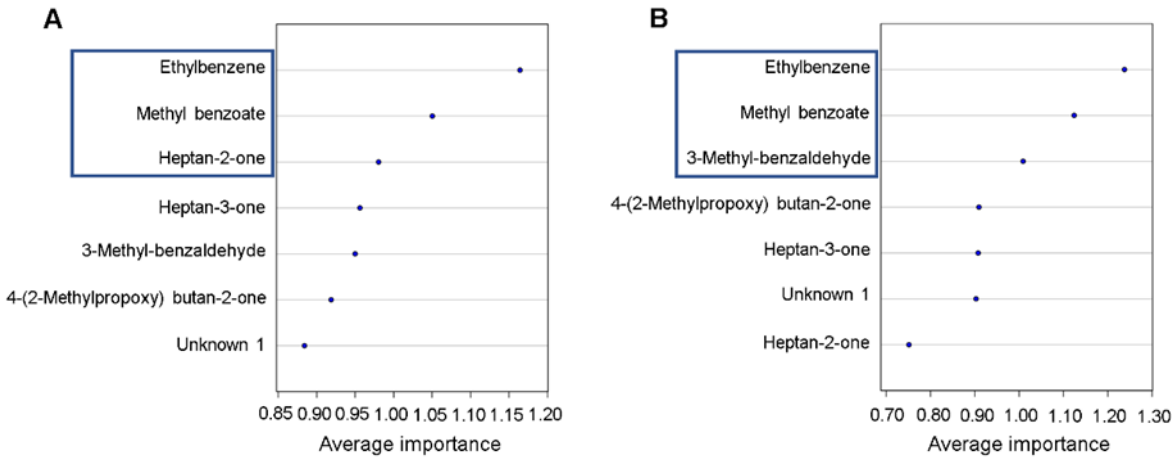

Supplementary Figure 4. VIP scores computed through a PLS-DA based algorithm to select the metabolites that best discriminate the groups: **(A)** PCa *vs*. BC; **(B)** PCa *vs*. RC.

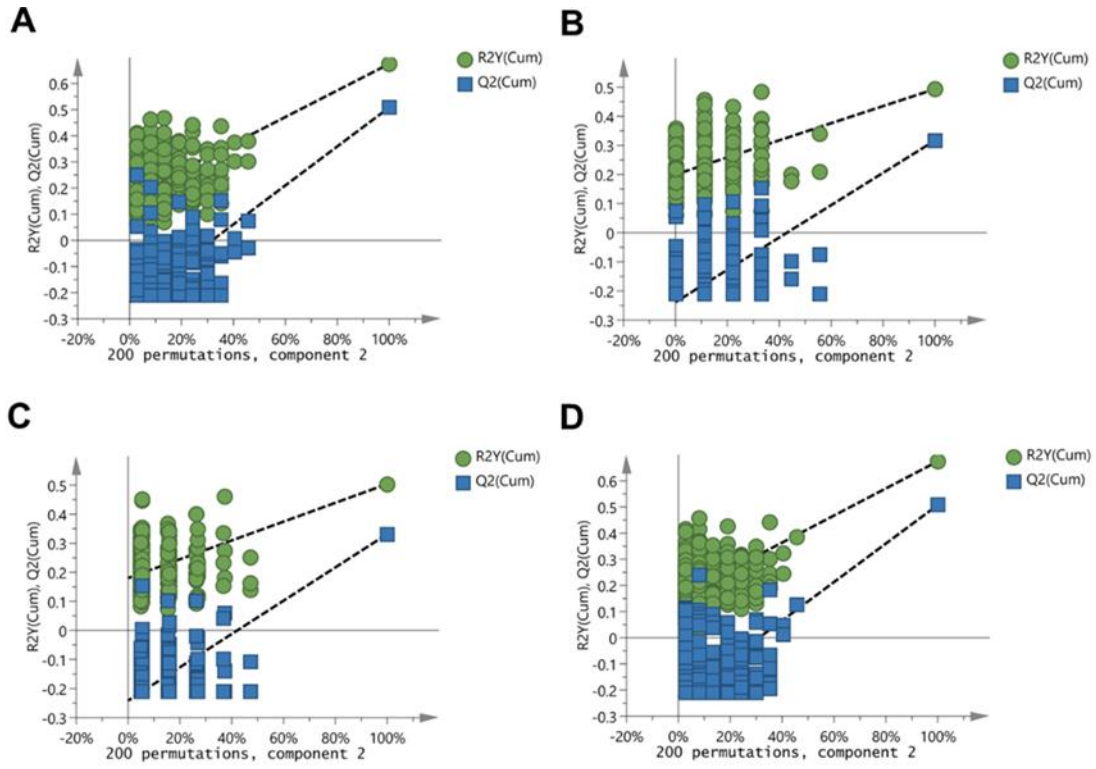

Supplementary Figure 5. Statistical validation of the PLS-DA model obtained for the 10-biomarker panel, by permutation testing (200 permutations; 2 components). **(A)** PCa *vs.* controls [Intercepts: R^2 = (0.0, 0.167), Q^2 = (0.0, -0.237)]; **(B)** PCa *vs.* BC [Intercepts: R^2 = (0.0, 0.2), Q^2 = (0.0, -0.238)]; **(C)** PCa *vs*. RC [Intercepts: R^2 = (0.0, 0.18), Q^2 = (0.0, -0.241)]; **(D)** PCa *vs.* controls plus BC and RC [Intercepts: R^2 = (0.0, 0.157), Q^2 = (0.0, -0.229)].

Supplementary Table 1. Demographic and clinical data of prostate cancer (PCa), bladder cancer (BC) and renal cancer (RC) patients and cancer-free controls included in this study.

Characteristics	PCa	BC	RC	Controls
Number of subjects	20	20	20	20
Mean Age ± SD (years)	67 ± 8.1	69 ± 8.6	71 ± 7.7	58 ± 2.8
Clinical stage, *n* (%)				
0	-	9 (47%)	2 (10%)	-
I	7 (35%)	6 (32%)	11 (55%)	-
II	3 (15%)	2 (11%)	1 (5%)	-
III	2 (10%)	-	5 (25%)	-
IV	6 (30%)	2 (11%)	1 (5%)	-
Not available	2 (10%)	-	-	-

Supplementary Table 2. 7-Fold cross validation parameters obtained for PLS-DA models of VOCs and VCCs in the untargeted approach.

	VOCs				VCCs			
Comparison	**LV**	**R^2X**	**R^2Y**	**Q^2**	**LV**	**R^2X**	**R^2Y**	**Q^2**
PCa *vs.* BC	2	0.544	0.773	0.655	2	0.414	0.742	0.554
PCa *vs.* RC	2	0.403	0.772	0.477	2	0.702	0.628	0.394

Supplementary Table 3. List of VOCs and VCCs significantly altered in PCa group compared to BC, RC and cancer-free controls.

		PCa *vs.* BC			PCa *vs.* RC			PCa *vs.* Controls		
Chemical name (IUPAC)	***Protocol***	***p-value***	***Variation ± uncertainty (%)***	***Effect size ± ES_{SE}***	***p-value***	***Variation ± uncertainty (%)***	***Effect size ± ES_{SE}***	***p-value***	***Variation ± uncertainty (%)***	***Effect size ± ES_{SE}***
Ethylbenzene	VOCs	0.0021	91.15 ± 16.80	0.83 ± 0.45	0.0004	62.77 ± 12.00	1.23 ± 0.67	0.0002	68.59 ± 13.07	1.21 ± 0.66
Heptan-3-one	VOCs	0.0021	69.75 ± 15.41	1.04 ± 0.65	0.0048	50.64 ± 12.83	0.98 ± 0.64	0.0007	72.56 ± 13.35	1.24 ±0.67
Heptan-2-one (2-Heptanone)	VOCs	0.0005	126.37 ± 24.58	0.98 ± 0.64	0.0082	87.09 ± 22.36	0.84 ± 0.63	0.0003	137.2 ± 23.00	1.10 ±0.65
Methyl benzoate	VOCs	0.0002	200.05 ± 26.93	1.15 ± 0.66	<0.0001	350.68 ± 26.59	1.48 ± 0.69	<0.0001	430.1 ± 27.21	1.56 ± 0.70
Unknown 1	VOCs	0.0061	175.99 ± 31.57	0.92 ± 0.64	0.0013	267.36 ± 32.60	1.09 ± 0.65	0.0075	195.7 ± 30.10	0.99 ± 0.65
3-Methyl-benzaldehyde	VCCs	<0.0001	305.49 ± 39.22	0.96 ± 0.64	<0.0001	572.98 ± 36.09	1.27 ± 0.67	0.0003	476.8 ± 34.50	1.27 ± 0.67

The statistical significance (*p*-values), percentage of variation, effect size (ES), standard error (ES_{SE}) are represented for each volatile compound.

Supplementary Table 4. List of VOCs and VCCs significantly altered in PCa group compared to BC, RC and cancer-free controls. They are characterized by their IUPAC name, retention time, characteristic ions (*m/z*), Kovat indices (KI) from literature, experimental KI, NIST R-match, CAS registry number and human metabolome database (HMDB) code.

Chemical name (IUPAC)	Protocol	Retention time	*m/z*	KI from literature	Experimental KI	R-match	CAS number	Identification Level [1]	HMDB [2]
Ethylbenzene	VOCs	6.44	91; 106; 51; 65; 77;78; 92; 50; 105	855	-	853	100-41-4	L1	HMDB0059905
Heptan-3-one	VOCs	7.10	57; 85; 72; 114	877	884	845	106-35-4	L2	HMDB0031482
Heptan-2-one	VOCs	7.20	58; 71; 59	891	887	835	110-43-0	L1	HMDB0003671
4-(2-Methylpropoxy) butan-2-one	VOCs	8.47	71;72; 57; 55; 101; 89	964	-	735	31576-33-7	L2	-
Methyl benzoate	VOCs	13.29	105; 77; 55; 51; 136; 57; 71; 50	1094	-	856	93-58-3	L1	HMDB0033968
Unknown 1	VOCs	10.75	57; 59; 69; 89; 56; 71; 87; 58	-	1009	-	-	L4	-
3-Methyl-benzaldehyde	VCCs	29.98	315; 77; 91; 182; 65; 79; 285; 78, 89	1845	-	788	620-23-5	L1	HMDB0029637

L1: Identified metabolites (GC-MS analysis of the metabolite of interest and a chemical reference standard of suspected structural equivalence, with all analyses performed under identical analytical conditions within the same laboratory); L2: Putatively annotated compounds (spectral (MS) similarity with NIST database); L4: Unidentified.

Supporting References

1. Viant, M.R.; Kurland, I.J.; Jones, M.R.; Dunn, W.B. How close are we to complete annotation of metabolomes? Curr Opin Chem Biol 2017, 36, 64-69, doi:10.1016/j.cbpa.2017.01.001.

2. Wishart, D.S.; Feunang, Y.D.; Marcu, A.; Guo, A.C.; Liang, K.; Vazquez-Fresno, R.; Sajed, T.; Johnson, D.; Li, C.; Karu, N., et al. HMDB 4.0: the human metabolome database for 2018. Nucleic Acids Res 2018, 46, D608-D617, doi:10.1093/nar/gkx1089.

Chapter 4 – Metabolic characterization of PCa

Section 4.1 - Comprehensive metabolomics and lipidomics profiling of prostate cancer tissue reveals metabolic dysregulations associated with disease development

Ana Rita Lima, Márcia Carvalho, Susana S. Aveiro, Tânia Melo, M. Rosário Domingues, Catarina Macedo-Silva, Nuno Coimbra, Carmen Jerónimo, Rui Henrique, Maria de Lourdes Bastos, Paula Guedes de Pinho and Joana Pinto

The article presented in this chapter was submitted to *Cancers* and is here presented in the form of “Submitted Manuscript”.

4.1.1 Abstract

Prostate cancer (PCa) is a global health problem that affects millions of men every year. In the last decade, metabolomics and related subareas, such as lipidomics, have demonstrated an enormous potential to identify novel mechanisms underlying PCa development and progression, providing a good basis for the development of new and more effective therapies and diagnostics. In this study, a multi-platform metabolomics and lipidomics approach, combining untargeted mass spectrometry (MS) and nuclear magnetic resonance (NMR)-based techniques, was applied to PCa tissues to investigate dysregulations associated with PCa development, in a cohort of 40 patients submitted to radical prostatectomy for PCa. Results revealed significant alterations in the levels of 27 metabolites and 21 phospholipid species in PCa tissue compared with adjacent non-malignant tissue, suggesting dysregulation in 13 metabolic pathways associated with PCa development. The most affected metabolic pathways were amino acid metabolism, nicotinate and nicotinamide metabolism, purine metabolism, and glycerophospholipid metabolism. A clear interconnection between metabolites and phospholipid species participating in these pathways was observed through correlation analysis. Overall, these dysregulations may reflect the reprogramming of metabolic responses to produce high levels of cellular building blocks required for rapid PCa cell proliferation.

Keywords: prostate cancer; tissue; metabolomics; lipidomics; mass spectrometry; nuclear magnetic resonance spectroscopy; metabolic pathways

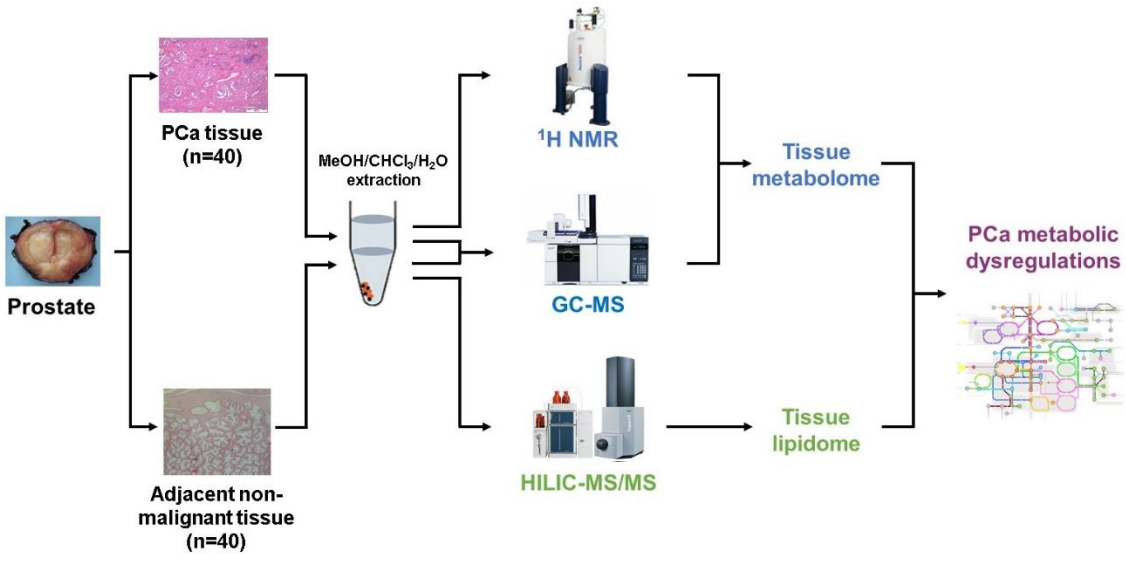

4.1.2 Introduction

In 2020, prostate cancer (PCa) was the second most diagnosed cancer and the fifth leading cause of mortality in men, worldwide (1). The majority of new cases were diagnosed in men between 65-74 years of age (median of 66 years), while the median age of death was 80 years (2). As life expectancy has increased over the past few decades, it is expected that the number of PCa cases will increase accordingly. Hence, timely detection of PCa is important to assure treatment with fewer side-effects and a better quality of life. Currently, early PCa detection mostly relies on prostate specific antigen (PSA) blood test, but PSA screening is a controversial topic since this biomarker is prostate-specific but not cancer-specific (3), entailing overdiagnosis and overtreatment (4). Imaging techniques (e.g., transrectal ultrasound, multiparametric magnetic resonance imaging) have also been used for PCa detection but concerns remain regarding their ability to detect small yet clinically significant cancers (5). Hence, prostate biopsy (PB), an invasive procedure that can result in health complications (e.g., haemoejaculate, haematuria, fever, pain) (6), is mandatory for definitive PCa diagnosis (7). After PCa's histopathological confirmation, the Gleason score (GS) (the most common PCa grading system) and clinical stage are key to determine which treatment modality [e.g., active surveillance, radical prostatectomy (RP), radiotherapy, androgen deprivation therapy (ADT)] should be applied (8). Despite the high likelihood of cure offered by RP as primary treatment for localized PCa, approximately 20-40% of patients will develop biochemical recurrence (BCR) after RP (9, 10). Thus, there is an urgent need for more effective diagnostic tools and precision therapies tackling tumor aggressiveness and risk of recurrence.

Metabolomics has been widely used, in parallel with other -omics approaches (e.g., genomics, transcriptomics, proteomics), to unravel the complexity of PCa development and progression, disclosure of new diagnostic and prognostic biomarkers and new potential therapeutic targets (11-13). These studies have been performed using urine, serum/plasma, tissue, or cell lines (14). In particular, metabolomic studies performed in PCa tissue focused on the investigation of altered metabolic pathways involved in PCa development and identification of potential therapeutic targets. The use of tissues has the advantage of matching samples collected from the same individual, thus allowing to substantially reduce confounding factors, such as age, comorbidities, or lifestyle (15). Some metabolic alterations associated with PCa development in several studies, performed in different matrixes (e.g. urine and tissue), included a significant decrease in citrate levels and an increase in the levels of lactate, alanine, succinate, malate, and fumarate (14, 16, 17), suggesting alterations in tricarboxylic acid (TCA) cycle and energetic metabolism. In

addition, decreased levels of polyamines (e.g., spermine and spermidine) were reported, indicating that PCa cells lose their capability to synthesize polyamines (14, 16, 17). Important alterations in amino acid metabolism have also been associated with PCa, due to the significant alterations in the levels of glutamate, tyrosine, arginine, proline, and sarcosine (14, 16, 17). Finally, alterations in lipid profile are also a hallmark of PCa (14, 16, 17), particularly dysregulations in the levels of several fatty acids (14, 16, 17) and metabolites involved in cellular membrane metabolism, like choline, choline-related compounds and phospholipids (PL) (16).

Herein, we report on a multi-platform metabolomics and lipidomics study, combining untargeted mass spectrometry (MS) and nuclear magnetic resonance (NMR)-based approaches, which investigated the metabolic alterations characterizing PCa tissues compared with matched adjacent non-malignant tissues. To the best of our knowledge, this is the first study that integrates the metabolome and lipidome fingerprints of PCa tissues to unravel the metabolic dysregulations associated with PCa development.

4.1.3 Material and Methods

4.1.3.1 Chemicals

All chemicals were of analytical grade. Aspartic acid (99%), benzoic acid (99.5%), chloroform (≥99.9%), desmosterol (≥84%), deuterium oxide containing 0.05 wt% 3-(trimethylsilyl) propionic- 2,2,3,3-d4 acid (TSP) sodium salt, glutamine (98%), malic acid (97%), methanol (≥ 99.9%), methoxyamine hydrochloride, *myo*-inositol (≥99%), N,O-bis(trimethylsilyl) trifluoroacetamide (BSTFA with 1% of trimethylchlorosilane), nonanoic acid (≥97%), phenylalanine (≥98%), proline (≥99%), serine (≥ 98%), tyrosine (≥ 98%), uracil (≥ 99%), urea (99%), were purchased from Sigma Aldrich (Madrid, Spain). Deuterium oxide (D2O) was provided by Eurisotop (Saint-Aubin, France). HPLC grade dichloromethane was purchased from Fisher Scientific Ltd. (Loughborough, UK). Ammonium molybdate, sodium dihydrogen phosphate dihydrate and perchloric acid were purchased from Panreac (Barcelona, Spain), Riedell-de Haen (Seelze, Germany) and Chem-Lab NV (Zedelgem, Germany), respectively. PL standards were purchased from Avanti Polar Lipids, Inc. (Alabaster, AL, USA). Mobile phase constituents namely acetonitrile and methanol were purchased from Fisher Scientific (Leicestershire, UK) with a degree of purity suitable for HPLC.

4.1.3.2 Subjects and sample collection

All tissue samples included in this study were collected after RP at the Portuguese Oncology Institute of Porto (IPO Porto) from PCa patients without previous neoadjuvant therapy. The study was approved by the Ethics Committee of the IPO-Porto (Reference 282R/2017) and informed written consent was obtained from all patients. Matched PCa and adjacent non-malignant tissues were collected from a cohort comprising 40 patients. PCa (*n* = 40) and adjacent non-malignant tissues (*n* = 40) were divided into slices, immediately frozen and stored at -80 ºC until analysis. An experienced pathologist evaluated all collected samples to distinguish between tumoral and adjacent non-malignant tissue (Figure 4.1). Detailed information of the patients is provided in Table 4.1.

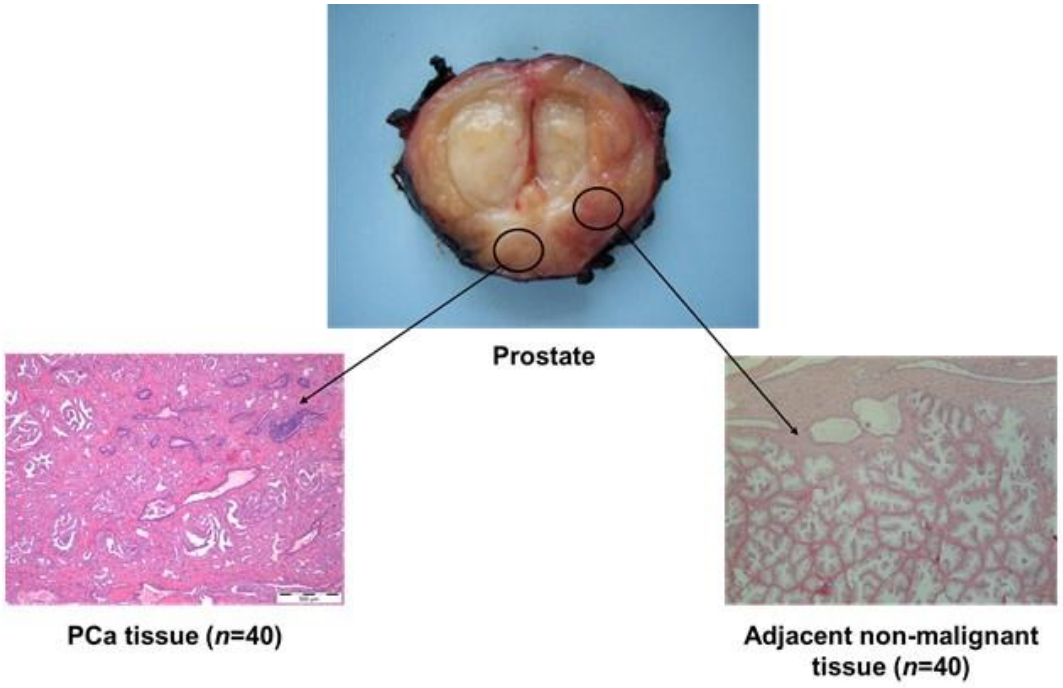

Figure 4.1: Schematic representation of PCa and adjacent non-malignant tissue collected from one patient included in the study.

Table 4.1: Clinical data of the PCa patients

PCa patients (*n*=40)	
Age	
Mean (standard deviation)	63.3 (5.5)
Serum PSA (ng/mL)	
4-10	22 (55%)
>10	16 (40%)
NA	2 (5%)
Gleason score	
5	1 (2.5%)
6	15 (37.5%)
7	23 (57.6%)
8	1 (2.5%)

NA: Not available

4.1.3.3 Sample extraction and preparation

Polar and lipophilic metabolites were extracted from tissue samples using a method previously described (18). Briefly, a combination of methanol (4 mL/g), chloroform (4 mL/g), and water (0.85 mL/g plus 2 mL/g) was added to 100 mg (± 10 mg) of each tissue sample. The solvents were added stepwise (three steps), between each stepwise addition of extraction solvents, the samples were vigorously agitated (vortex). After solvent addition, samples were centrifuged (1000 g for 15 min at 4 ºC), which allowed the separation of an upper phase containing the polar metabolites (methanol/water), a lower phase with lipophilic compounds (chloroform) and the sediment with tissue debris and other cellular components. For gas chromatography-mass spectrometry (GC-MS) analysis, 100 µL of polar phase was combined with 60 µL of the lipophilic phase. The remaining polar and lipophilic phases were used for proton (^{1}H) NMR spectroscopy and hydrophilic interaction liquid chromatography-tandem mass spectrometry (HILIC-MS/MS) analyses, respectively. For both GC-MS and HILIC-MS/MS, an aliquot of all samples was pooled to define a quality control (QC) for evaluation of analytical precision. All extracts were dried under a stream of nitrogen and stored at -80 ºC until analysis.

Sample preparation for GC-MS consisted in the treatment of the dried extracts with methoxyamine followed by derivatization with BSTFA containing 1% TCMS, accordingly to a previously described protocol (19). For NMR analyses, the dry aqueous extracts were resuspended in phosphate buffer (100 mM, pH 7.4, in D2O containing 0.05 mM TSP), centrifuged (12 000 g for 5 min at 4 ºC) and transferred to 5 mm NMR tubes, as previously

described (20). Finally, for lipidomics HILIC-MS/MS analyses, the total amount of PL present in the lipidic extracts was first quantified using the phosphorus assay previously described (21). After PL quantification, the dried lipid extracts were resuspended in dichloromethane to achieve a PL concentration of 1µg/µL. Finally, 10 µL of each sample, containing 10 µg of PL, was mixed with the internal standards [8 µL of a PL standard mixture containing 0.04 µg 1,2-dimyristoyl-sn-glycero-3-phosphocholine (dMPC), 0.04 µg 1,2-dimyristoyl-sn-glycero-3-phosphoethanolamine (dMPE), 0.04 µg N-palmitoyl-D-erythro-sphingosyl-phosphorylcholine (NPSM), 0.04 µg 1-nonadecanoyl-2-hydroxy-sn-glycero-3-phosphocholine (LPC), 0.16 µg 1,2-dipalmitoyl-sn-glycero-3-phosphatidylinositol (dPPI), 0.024 µg 1,2-dimyristoyl-sn-glycero-3-phospho-(10-rac-) glycerol (dMPG), 0.08 µg 1,2-dimyristoyl-sn-glycero-3-phospho-L-serine (dMPS), 0.16 µg 1,2-dimyristoyl-sn-glycero-3-phosphate (dMPA), 0.04 µg C17 Ceramide (d35:1)] and 82 µL of starting eluent, performing a total volume of 100 µL (22). Samples were randomly analyzed in all methodologies, and QC samples were injected on every 10 samples in GC-MS and HILIC-MS/MS analyses.

4.1.3.4 GC-MS analysis

The GC-MS conditions were the same used in previous studies (23, 24). Briefly, the analysis was performed in a 436-GC model, equipped with a column Rxi-5Sil MS (30 m × 0.25 mm × 0.25 µm) (Restek Corporation, U.S., Bellefonte, PA, USA), coupled with a EVOQ triple quadrupole (TQ) mass spectrometer (Bruker Daltonics, Bremen, Germany). A Bruker MS workstation software (version 8.2.1, Bruker Daltonics, Bremen, Germany) was used. The oven temperature was fixed at 70 ºC for 2 min, then increased to 250 ºC (rate 15 ºC/min), held for 2 min, and finally increased to 300 ºC (rate 10 ºC/min) and held for 8 min. The injection was performed in split mode (ratio 1/5) and the carrier gas was helium C-60 (Gasin, Porto, Portugal) with a flow rate of 1 mL/min. The temperatures of injector port, transfer line, and manifold were 250 ºC, 250 ºC and 40 ºC, respectively. The emission current was 50 µA and the electron multiplier was set in relative mode to an auto tune procedure. The analysis was performed in full scan mode and all mass spectra were acquired in the electron impact (EI) mode with a mass range of 50 to 1000 m/z (24).

Metabolites were identified by comparison of the mass spectra and Kovats indices (KI), determined using a commercial hydrocarbon mixture (C8-C20), obtained for tissue samples with the National Institute of Standards and Technology database (NIST 14, Gaithersburg, MD, USA). Metabolite identification was confirmed using standard compounds analyzed under the same conditions, when commercially available.

4.1.3.5 ^{1}H NMR analysis

The parameters considered in ^{1}H NMR analysis were based in a previous work (20). The 1D ^{1}H NMR analysis was performed on a Bruker Avance III HD 600 MHz spectrometer (Bruker BioSpin, Rheinstetten, Germany) equipped with a cryoprobe, at 26.85 °C (300 K). Briefly, the acquisition parameters of the standard pulse sequence (noesypr1d) were: 4 s relaxation delay, 100 ms mixing time, 256 transients, 64k complex data points, 10 080.646 Hz spectral width and 3.25 s acquisition time. Each free induction decay was multiplied by a 1.0 Hz exponential line-broadening function, manually phased and baseline corrected, and chemical shifts referenced internally to TSP at δ = 0.0 ppm.

For metabolite identification, 2D NMR experiments, namely total correlation spectroscopy (TOCSY) and heteronuclear single quantum coherence (HSQC) spectra, literature (25, 26), and the Biological Magnetic Resonance Data Bank (27) were used.

4.1.3.6 Lipidomic HILIC-MS/MS analysis

The lipid extracts were analyzed by HILIC-MS/MS on a high-performance liquid chromatography system (Ultimate 3000 Dionex, Thermo Fisher scientific, Bremen, Germany) equipped with an autosampler coupled online to the Q-Exactive hybrid quadrupole Orbitrap mass spectrometer, using a method previously described with some modifications (22). The solvent system consisted of two mobile phases: mobile phase A [acetonitrile/methanol/water, 50:25:25 (v/v/v) with 5 mM ammonium acetate] and mobile phase B [acetonitrile/methanol, 60:40 (v/v) with 5 mM ammonium acetate]. Initially, 5% of mobile phase A was held isocratically for 2 min, followed by a linear increase to 48% of A within 8 min. A new linear increase to 65% A within 5 min was followed by a maintenance period of 2 min, returning to the initial conditions in 3 min and held for more 10 min. A volume of 5 µL of each sample, was injected into the Ascentis Si column HPLC Pore column (15 cm × 2.1 mm, 2.7 µm, Sigma-Aldrich), with a flow rate of 200 µL/min, at 35 ºC.

The mass spectrometer was operated using a positive/negative switching toggles between positive (electrospray voltage 3.0 kV) and negative (electrospray voltage -2.7 kV) ion modes. The capillary temperature and the sheath gas flow were 250 °C and 15 U, respectively. Data was acquired at full scan mode with a high resolution of 70 000, automatic gain control (AGC) target of 1×106, in a m/z range of 400-1600, 2 microscans, and maximum inject time (IT) of 100 ms. The tandem mass spectra (MS/MS) were obtained with a resolution of 17 500, AGC target of 1×105, 1 microscan, maximiun IT of 50 ms. The cycles consisted of one full-scan mass spectrum and ten data-dependent MS/MS scans, which were repeated continuously throughout the experiments with a dynamic exclusion of 60 s

and intensity threshold of 2×104. Normalized collision energyTM (CE) ranged between 25, 30 and 35 eV. Data acquisition was performed using the Xcalibur data system (V3.3, Thermo Fisher Scientific, Bremen, Germany).

Putative identification of lipid species was performed through MZmine 2.53 (28) using a custom database search build using the retention time (RT) of internal standards and the exact masses from Lipid Maps database (29). The phosphatidylcholine (PC) and sphingomyelin (SM) species were identified and semi-quantified in the positive mode as $[M + H]^+$ ions, whereas the negative mode as $[M - H]^-$ ions was considered for phosphatidylethanolamine (PE) and phosphatidylinositol (PI). Class confirmation and identification of fatty acid composition was achieved through MS/MS analysis as described in reference (30). The MS/MS spectra representative of each class are shown in Figures S1-S4. Briefly, PC and SM class confirmations were accomplished through the MS/MS of $[M + H]^+$ ions by detection of the product ion of exact mass 184.0739, corresponding to the phosphocholine polar head. Confirmation of PE class was accomplished by the identification of the typical neutral loss of 141 Da, characteristic of the polar head of phosphoethanolamine, seen in the MS/MS of $[M + H]^+$ ions. Finally, PI class was confirmed by the detection of the phosphoinositol head group (m/z 241.0113) in the MS/MS spectra of the $[M - H]^-$ ions. Fatty acid composition of each PC, PE and PI species was determined in analysis of the MS/MS data in negative mode, respectively by the analysis of MS/MS spectra of the $[M + CH3COO]^-$ ions for the PC species and analysis of MS/MS spectra of the $[M - H]^-$ ions for the PE and PI species and by detecting the product ions corresponding to the fatty acyl chains ($[RCOO]^-$). For SM class, the sphingoid base and fatty acyl amide substituent were deduced in MS/MS spectra of $[M + H]^+$ ions. In addition, ions were confirmed by retention time and accuracy of the mass measurements < 5 ppm. Relative quantification of each class was achieved by summing the normalized ion areas of all PL species within each class.

4.1.3.7 Data pre-processing

MZmine 2.53 (28) was used for pre-processing of GC-MS and HILIC-MS/MS data, comprising baseline correction, peak detection, chromatogram deconvolution and alignment. The parameters used for pre-processing of GC-MS data were: RT range 4.4-26.0 min, m/z range 50-600, MS data noise level 1.5×105, m/z tolerance 0.2, chromatogram baseline level 1.5×104 and peak duration range 0.02-1.18 min. All RT-m/z pairs identified as contaminants (e.g., from column, fiber, among others) were manually removed from the matrix. Data was normalized by the total area of the chromatograms and scaled to pareto.

The parameters used for pre-processing of HILIC-MS/MS data acquired in the positive mode were: RT range 0.9-12 min, m/z range 400-1420, MS data noise level 1.0×105, m/z tolerance 0.01, chromatogram baseline level 9×104 and peak duration range 0.03-2.00 min; while for HILIC-MS/MS negative mode were: RT range 0.01-20 min, m/z range 400-1000, MS data noise level 1.0×105, m/z tolerance 0.01, chromatogram baseline level 9×104 and peak duration range 0.03-2.00 min. Data from the positive and negative modes were combined, duplicate peaks were removed and the final matrix was normalized by the total area of all identified lipid species and scaled to pareto. For ^{1}H NMR, water resonances were removed from de matrix and the spectra were aligned using the recursive segment-wise peak alignment method (31) (R 3.3.3 software). The final matrix was normalized by the total area of the spectrum and scaled to unit variance (UV). For all data, an additional step of variable selection was applied to remove uninformative variables (32), based on an univariate test (t-test) and considering a significance level of 0.05 (MetaboAnalyst) (33).

4.1.3.8 Statistical analysis

The strategy used for statistical analysis was the same for all methodologies carried out in this work and comprised both multivariate statistical analysis (MVA) and univariate statistical analysis. MVA was performed using SIMCA-P 15 (Umetrics, Sweden) and included principal component analysis (PCA) and partial least squares discriminant analysis (PLS-DA). PCA was used to visualize sample distribution including QCs clustering, while PLS-DA was applied to evaluate the discriminant capability of the data. Furthermore, sevenfold cross-validation and permutation test (200 permutations) were performed to validate the PLS-DA models. Additionally, receiver operating characteristic analysis (ROC) was performed, along with the area under the curve (AUC), sensitivity, specificity, and accuracy (MetaboAnalyst) (33). For all metabolites and lipid species with variable importance to the projection (VIP) greater than one, univariate statistical analysis was performed, including a normality test (Shapiro–Wilk test), unpaired Student's t-test with Welch correction for normal distribution, and unpaired Mann-Whitney test for non-normal distribution. Additionally, percentage of variation and uncertainty, effect size and standard error (ES_{SE}) (34), Bonferroni correction (35) and AUC were computed for each discriminant metabolite and lipid species.

Metabolic pathway analysis was performed in the MetPA tool (Metaboanalyst) (33) using all significantly altered metabolites and lipid species to disclose which metabolic pathways were dysregulated in PCa tissue. Only statistically different metabolic pathways ($p < 0.05$) involving at least two significantly altered metabolites or lipid species were

considered. Finally, the Spearman's rank correlation coefficient was computed between all the significantly altered metabolites and lipid species defining a threshold of $p \leq 0.0001$ (R version 4.0.3) (36). The correlation matrix was created using the R package Hmisc (37).

4.1.4 Results and Discussion

To increase the metabolome coverage of PCa tissue, three complementary analytical platforms were used for characterization of PCa and adjacent non-malignant tissue samples. GC-MS and ^{1}H NMR spectroscopy enabled the detection of polar and semi-polar metabolites, such as amino acids, organic acids, sugars, among others, while HILIC-MS/MS was applied to detect complex lipid species, such as PLs. Overall, 151 metabolites were detected, corresponding to 110 by GC-MS and 62 by ^{1}H NMR (21 in common with GC-MS), and 477 lipid species by HILIC-MS/MS. As recommended for MS-based untargeted metabolomic approaches (38), QCs were included in the GC-MS and HILIC-MS/MS analyses to provide a representation of the variability within the data acquired. As depicted in Figure S5, the cluster of QC samples in the PCA model was more compact than the distribution of all biological samples under study, confirming the reproducibility of the GC-MS and HILIC-MS/MS analyses.

To examine trends and possible outliers in the metabolic and lipid profiles of PCa and adjacent non-malignant tissue samples, PCA was first performed using the data obtained by GC-MS, ^{1}H NMR and HILIC-MS/MS (Figure S6). Overall, no separation was observed in PCA models and only one outlier was excluded from GC-MS data. The metabolic differences existing between PCa and adjacent non-malignant tissue were further investigated through PLS-DA (Figure 4.2A, C and E). The three models showed a satisfactory performance to discriminate both groups. The GC-MS model showed an AUC of 0.88, 82% sensitivity, 90% specificity and 86% accuracy (Figure 4.2B), while the ^{1}H NMR model unveiled an AUC of 0.84, 78% sensitivity, 70% specificity and 74% accuracy (Figure 4.2D) and, finally, the HILIC-MS/MS model showed an AUC of 0.83, 83% sensitivity, 75% specificity and 79% accuracy (Figure 4.2F). All PLS-DA models were validated through permutation tests (Figure S7).

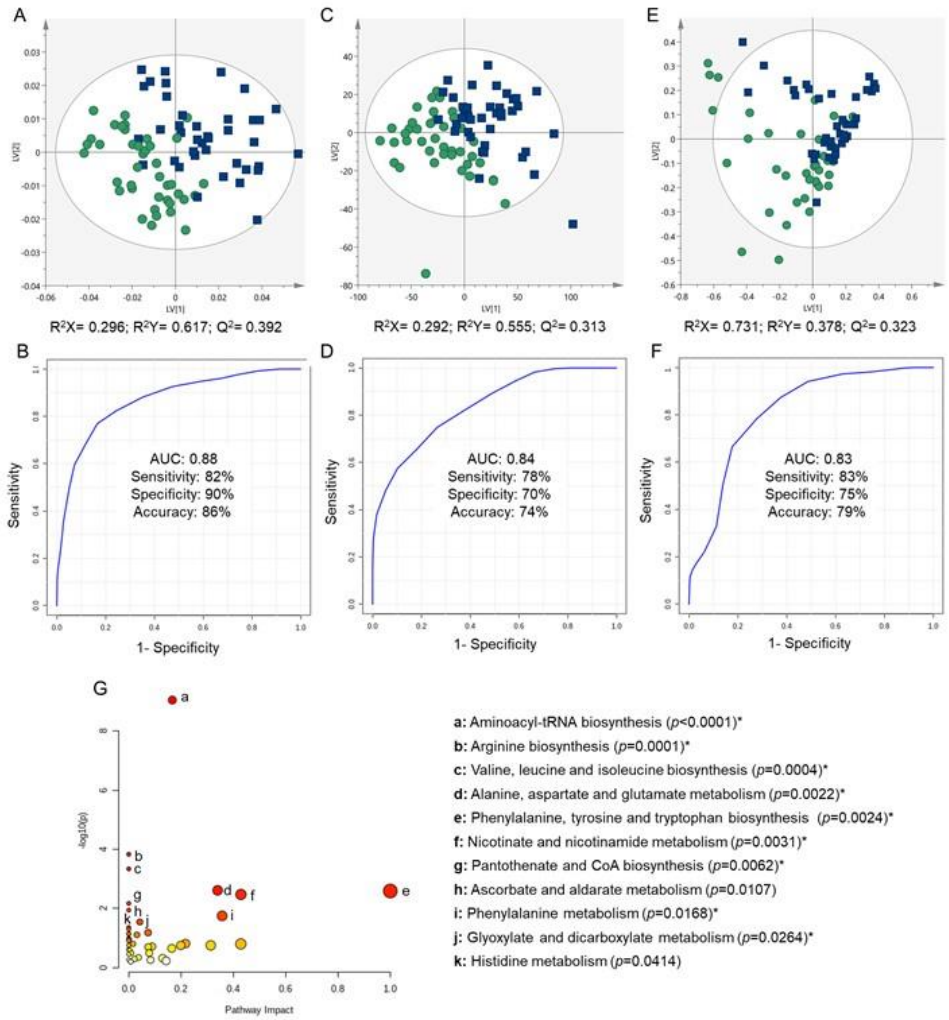

Figure 4.2: (A) PLS-DA scores scatter plot (pareto scaling; 2 latent variables) obtained for the GC–MS metabolic profile of PCa tissue (*n*=39, blue squares) vs. adjacent non-malignant tissue (*n*=40, green circles), after variable selection; **(B)** ROC curve of the PLS-DA model obtained through GC–MS; **(C)** PLS-DA scores scatter plot (UV scaling; 2 latent variables) obtained for the ^{1}H NMR metabolic profile of PCa tissue (*n*=40, blue squares) *vs*. adjacent non-malignant tissue (*n*=40, green circles), after variable selection; **(D)** ROC curve of the PLS-DA model obtained through ^{1}H NMR; **(E)** PLS-DA scores scatter plot (pareto scaling; 2 latent variables) obtained for the HILIC–MS/MS metabolic profile of PCa tissue (*n*=40, blue squares) *vs*. adjacent non-malignant tissue (*n*=40, green circles), after variable selection; **(F)** ROC curve of the PLS-DA model obtained through HILIC-MS/MS. **(G)** Pathway topology analysis depicting the dysregulated metabolic pathways associated with PCa development, performed using the set of metabolites and PL species found statistically different between PCa and adjacent non-malignant tissue.The node colors represent the *p*-values from the pathway enrichment analysis and the node radius indicate the pathway impact values. Dysregulations in metabolic pathways corroborated by correlation analysis are marked with asterisks.

Considering all analytical platforms, 48 metabolites/PL species showed VIP >1 in PLS-DA models and significantly altered levels (p-value < 0.05) between PCa and adjacent non-malignant tissue, namely 15 from GC-MS, 12 from ^{1}H NMR and 21 from HILIC-MS/MS (Table 4.2, Tables S1, S2 and S3). These metabolites included 14 amino acids and derivatives, 3 fatty acids and derivatives, 2 nucleotide derivatives, 4 organic acids and derivatives, 1 pyridine derivative,1 pyrimidine derivative, 1 purine derivative, 1 sugar alcohol and 21 PL species [6 phosphatidylcholines (PCs), 9 phosphatidylethanolamines (PEs), 4 phosphatidylinositols (PIs) and 2 sphingomyelins (SMs)]. From the 48 metabolites/PL species, 17 remained statistically significant after Bonferroni correction (Table 4.2), namely alanine, aspartic acid, proline, serine, taurine, oleamide, uracil, benzoic acid, malic acid, urea, niacinamide, *myo*-inositol, and 5 PL species [PE(34:2), PE(36:3), PI(36:1), PI (36:2) and PI (38:2)]. Regarding the relative comparison of total PL classes (Table S4), significantly altered levels were found for lysophosphatidylglycerol (LPG), phosphatidylglycerol (PG) and PI classes, which were upregulated in PCa, and diacylglycerols (DG) and SM classes, which were downregulated.

Most of the amino acids, organic acids and nucleotide derivatives were previously found altered in PCa tissue compared with adjacent non-malignant tissue (39-44). To our knowledge, 9 metabolites were, for the first time, detected as significantly altered in PCa tissue, namely 1-methylhistidine, serine, tryptophan, benzoic acid, nonanoic acid, UDP-glucose/UDP-galactose, niacinamide, oleamide, and urea. Though, 4 metabolites were previously found altered in PCa by analysis of other sample matrices (urine and serum), namely serine (45), tryptophan (46), 1-methylhistidine (46, 47), and benzoic acid (45). Furthermore, arachidonic acid was previously reported as significantly increased in PCa tissues (48), which contradicts our results as a significant decrease of the levels of this metabolite was observed in this study.

Regarding the PL species identified in the present study, PC(34:2), PC(36:3), PC(36:2), PC(36:1), PI(36:1), PI(38:2) and SM(d34:1) were previously found altered in PCa tissue and implicated in PCa development (49-51). In addition, the significant decrease of the SM class in PCa agrees with previous literature (43), while a significant increased in the levels of SM(d42:1) was previously reported (51) contradicting our results. To the best of our knowledge, the significant alterations in the levels of DG, LPG, PG and PI classes, as well as, PC(34:3), PC(38:7), PI(34:1) and PI(36:2) species, were detected in PCa tissue for the first time in this study. Moreover, the identification of specific PE molecular species (Table S3) changing in PCa tissue was seen in this work for the first time, despite alterations in the levels of PE class have been previously described (43, 52).

Table 4.2: List of metabolites and PL species found significantly altered in PCa tissue compared to adjacent non-malignant tissue by GC–MS, ^{1}H NMR spectroscopy and HILIC-MS/MS.

Name	*p*-value	Variation ± uncertainty (%)	Effect size ± ES_{SE}	AUC	Up/ down regulated	Analytical platform
Amino acids and derivatives						
1-Methyl-histidine [L2]	0.0125	13.1 ± 4.8	0.57 ± 0.45	0.66	Up	^{1}H NMR
Alanine [L2]	0.0006[B]	15.6 ± 4.0	0.80 ± 0.46	0.70	Up	^{1}H NMR
Aspartic acid [L1]	<0.0001[B]	8194 ± 26.1	1.73 ± 0.52	0.85	Up	GC-MS
Creatine [L2]	0.0037	-15.65 ± 5.37	-0.71 ± 0.45	0.69	Down	^{1}H NMR
Glutamine [L1]	0.0085	98.4 ± 23.7	0.63 ± 0.45	0.67	Up	GC-MS
Isoleucine [L2]	0.0073	9.8 ± 3.8	0.56 ± 0.45	0.67	Up	^{1}H NMR
Leucine [L2]	0.0021	12.1 ± 3.7	0.70 ± 0.45	0.70	Up	^{1}H NMR
Phenylalanine [L1]	0.0152	26.1 ± 10.2	0.57 ± 0.45	0.66	Up	GC-MS
Proline [L1]	<0.0001[B]	241 ± 16.4	1.53 ± 0.50	0.85	Up	GC-MS
Serine [L1]	0.0008[B]	105 ± 26.9	0.58 ± 0.45	0.72	Up	GC-MS
Taurine [L2]	0.0001[B]	-19.6 ± 5.0	-0.98 ± 0.46	0.74	Down	^{1}H NMR
Tryptophan [L2]	0.0086	26.3 ± 8.6	0.60 ± 0.45	0.68	Up	^{1}H NMR
Tyrosine [L1]	0.0041	53.6 ± 15.7	0.61 ± 0.45	0.69	Up	GC-MS
Valine [L2]	0.0244	8.3 ± 3.4	0.51 ± 0.45	0.66	Up	^{1}H NMR
Fatty acids and derivatives						
Arachidonic acid [L2]	0.0093	-36.3 ± 17.7	-0.56 ± 0.45	0.67	Down	GC-MS
Nonanoic acid [L1]	0.0208	-8.2 ± 3.8	-0.51 ± 0.45	0.65	Down	GC-MS
Oleamide [L2]	<0.0001[B]	-31.8 ± 8.3	-1.02 ± 0.47	0.79	Down	GC-MS
Nucleotide derivatives						
NAD^{+} [L2]	0.0021	-35.6 ± 13.7	-0.71 ± 0.45	0.70	Down	^{1}H NMR
UDP-Glucose/ UDP-Galactose[L2]	0.0023	25.7 ± 7.2	0.71 ± 0.45	0.70	Up	^{1}H NMR
Organic acids and derivatives						
Benzoic acid [L1]	<0.0001[B]	-23.3 ± 8.7	-0.68 ± 0.45	0.76	Down	GC-MS
Fumaric acid [L2]	0.0352	19.1 ± 8.1	0.48 ± 0.45	0.66	Up	^{1}H NMR
Malic acid [L1]	<0.0001[B]	153 ± 14.5	1.34 ± 0.49	0.87	Up	GC-MS
Urea [L1]	<0.0001[B]	48.9 ± 10.0	0.89 ± 0.46	0.75	Up	GC-MS
Pyridine derivative						
Niacinamide [L2]	0.0003[B]	25.8 ± 6.1	0.84 ± 0.46	0.72	Up	^{1}H NMR

Name	*p*-value	Variation ± uncertainty (%)	Effect size ± ES_{SE}	AUC	Up/ down regulated	Analytical platform
Pyrimidine derivative						
Uracil [L1]	0.0011[B]	76.2 ± 15.8	0.79 ± 0.46	0.71	Up	GC-MS
Purine derivative						
Hypoxanthine [L2]	0.0096	34.3 ± 11.0	0.61 ± 0.45	0.64	Up	GC-MS
Sugar alcohol						
Myo-inositol [L1]	0.0007[B]	-39.7 ± 11.6	-0.95 ± 0.47	0.71	Down	GC-MS
Phosphatidylcholine species						
PC(34:2) [L2]	0.0332	18.38 ± 6.12	0.62 ± 0.45	0.64	Up	HILIC-MS/MS
PC(34:3) [L2]	0.0310	-11.41 ± 5.14	-0.53 ± 0.45	0.64	Down	HILIC-MS/MS
PC(36:1) [L2]	0.0319	12.45 ± 5.36	0.49 ± 0.45	0.62	Up	HILIC-MS/MS
PC(36:2) [L2]	0.0216	15.95 ± 5.35	0.62 ± 0.45	0.65	Up	HILIC-MS/MS
PC(36:3) [L2]	0.0050	17.37 ± 5.53	0.65 ± 0.45	0.67	Up	HILIC-MS/MS
PC(38:7) [L2]	0.0028	-17.85 ± 6.19	-0.71 ± 0.45	0.69	Down	HILIC-MS/MS
Phosphatidylethanolamine species						
PE(34:1) [L2]	0.0231	22.02 ± 8.55	0.52 ± 0.45	0.65	Up	HILIC-MS/MS
PE(34:2) [L2]	<0.0001[B]	45.93 ± 8.08	1.03 ± 0.47	0.75	Up	HILIC-MS/MS
PE(36:1) [L2]	0.0370	17.06 ± 7.41	0.48 ± 044	0.62	Up	HILIC-MS/MS
PE(36:3) [L2]	<0.0001[B]	43.68 ± 7.96	1.01 ± 0.47	0.76	Up	HILIC-MS/MS
PE(38:3) [L2]	0.0155	22.56 ± 7.88	0.58 ± 0.45	0.65	Up	HILIC-MS/MS
PE(38:5) [L2]	0.0342	18.12 ± 7.71	0.48 ± 0.45	0.62	Up	HILIC-MS/MS
PE(40:6) [L2]	0.0019	30.38 ± 7.71	0.77 ± 0.45	0.70	Up	HILIC-MS/MS
PE(P-38:5) [L2]	0.0415	-10.59 ± 5.39	-0.46 ± 0.44	0.64	Down	HILIC-MS/MS
PE(P-40:7) [L2]	0.0152	-13.98 ± 6.04	-0.57 ± 0.48	0.68	Down	HILIC-MS/MS
Phosphatidylinositol species						
PI(34:1) [L2]	0.0118	24.45 ± 8.43	0.58 ± 0.45	0.66	Up	HILIC-MS/MS
PI(36:1) [L2]	<0.0001[B]	40.40 ± 7.63	0.99 ± 0.46	0.77	Up	HILIC-MS/MS
PI(36:2) [L2]	<0.0001[B]	40.58 ± 6.32	1.19 ± 0.48	0.79	Up	HILIC-MS/MS
PI(38:2) [L2]	0.0001[B]	36.48 ± 7.63	0.90 ± 0.46	0.63	Up	HILIC-MS/MS
Sphingomyelin species						
SM(d34:1) [L2]	0.0059	-11.81 ± 4.42	-0.64 ± 0.45	0.67	Down	HILIC-MS/MS
SM(d42:1) [L2]	0.0027	-14.69 ± 5.10	-0.70 ± 0.45	0.70	Down	HILIC-MS/MS

[L1]: Formally identified metabolites by comparison of a reference standard analyzed under the same conditions within the same laboratory (53); [L2]: Putatively annotated compounds according to similarity with databases (53); B: Alterations remaining significant after Bonferroni correction, with a *p*-value cut-off of 0.0015 (0.05 divided by 33 tested metabolites) for GC–MS data, *p*-value cut-off of 0.0018 (0.05 divided by 28 tested PL species) for ^{1}H NMR and p-value cut-off of 0.0016 (0.05 divided by 31 tested metabolites) for HILIC-MS/MS.

The altered metabolites suggested significant (*p*-value <0.05) dysregulations in 11 metabolic pathways associated with the development of PCa using the MetPA tool (54) (Figure 4.2G, Table S5), namely aminoacyl-tRNA biosynthesis (phenylalanine, glutamine, aspartic acid, serine, valine, alanine, isoleucine, leucine, tryptophan, tyrosine, proline), arginine biosynthesis (aspartic acid, glutamine, urea, fumaric acid), valine, leucine and isoleucine biosynthesis (isoleucine, leucine, valine), alanine, aspartate and glutamate metabolism (aspartic acid, alanine, glutamine, fumaric acid), phenylalanine, tyrosine and tryptophan biosynthesis (phenylalanine, tyrosine), nicotinate and nicotinamide metabolism (aspartic acid, NAD^+, niacinamide), pantothenate and CoA biosynthesis (valine, aspartic acid, uracil), ascorbate and aldarate metabolism (*myo*-inositol, UDP-glucose), phenylalanine metabolism (phenylalanine, tyrosine), glyoxylate and dicarboxylate metabolism (malic acid, serine, glutamine), and histidine metabolism (1-methylhistidine, aspartic acid). To evaluate a potential relationship among the metabolites participating in the same metabolic pathway, correlation analysis was performed using all metabolites/PL species found significantly different between PCa *vs*. adjacent non-malignant tissue. From these, 39 metabolites/PL species revealed relevant positive and negative correlations (*p*-value ≤ 0.0001) (Figure 4.3, Table S6), corroborating potential dysregulations in aminoacyl-tRNA biosynthesis, arginine biosynthesis, valine, leucine and isoleucine biosynthesis, alanine, aspartate and glutamate metabolism, phenylalanine, tyrosine and tryptophan biosynthesis, nicotinate and nicotinamide metabolism, pantothenate and CoA biosynthesis, phenylalanine metabolism, and glyoxylate and dicarboxylate metabolism. Moreover, dysregulations in purine metabolism (glutamine, hypoxanthine and urea) and glycerophospholipid metabolism (PCs and PEs) were supported by strong correlations among the participating metabolites/PL species, despite the lack of statistical significance in the MetPA tool (Table S5 and S6). Interestingly, strong correlations were also observed between metabolites participating in different metabolic pathways, such as uracil with several amino acids (leucine, alanine, tryptophan, phenylalanine, aspartic acid), and niacinamide and taurine with several PL species (Figure 4.3, Table S6).

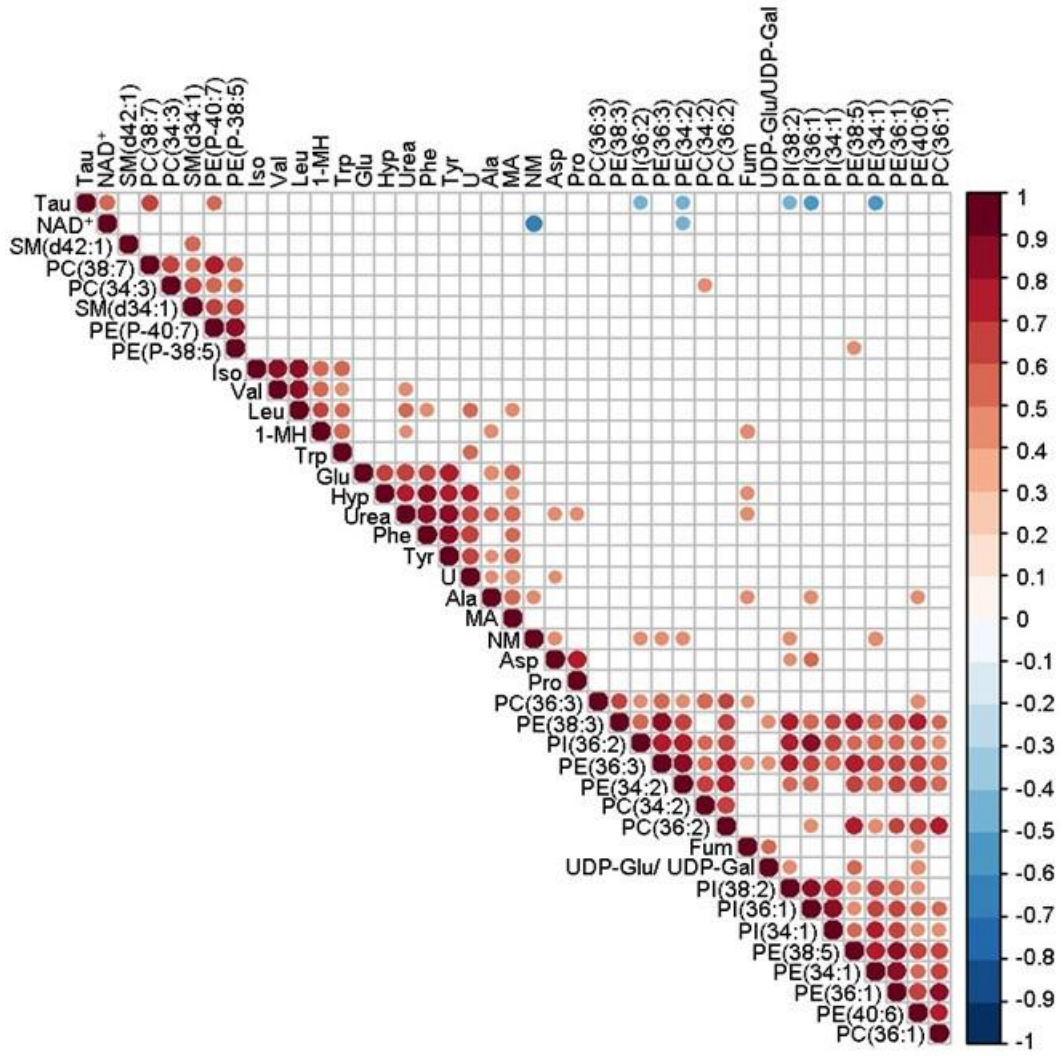

Figure 4.3: Correlation matrix obtained from the significantly altered metabolites/PL species found between PCa and adjacent non-malignant tissue. Circle size is proportional to the correlation coefficient and only correlations with *p*-value ≤ 0.0001 are represented. Metabolite abbreviations: 1-MH, 1-methylhistidine; Ala, alanine; Asp, aspartic acid; Fum, fumaric acid; Glu, glutamine; Hyp, hypoxanthine; Iso, Isoleucine; Leu, leucine; MA, malic acid; NM, niacinamide; Phe, phenylalanine; Pro, proline; Tau, taurine; Trp, tryptophan; Tyr, tyrosine; U, uracil; UDP-Glu/UDP-Gal, UDP-glucose/UDP-galactose; Val, valine.

Most of the metabolic pathways found dysregulated in PCa in this study were associated with the upregulation of several amino acids and derivatives, namely aminoacyl-tRNA biosynthesis, arginine biosynthesis, valine, leucine and isoleucine biosynthesis, alanine, aspartate and glutamate metabolism, phenylalanine, tyrosine and tryptophan biosynthesis, phenylalanine metabolism, and histidine metabolism. Importantly,

dysregulations in these pathways were corroborated by strong correlations among amino acids participating in the same pathway. Amino acids are key intermediates in several biological reactions, providing intermediates for TCA cycle (energetic metabolism), nucleotide synthesis, pyridine synthesis, purines and thymidylate production, and lipid synthesis (17, 55-59). Furthermore, amino acids have the ability to activate the mammalian target of rapamycin (mTOR), which is essential for anabolic metabolism, cell growth (60-62), tumor progression and therapy resistance (63), and, ultimately, reprogramming of metabolic responses in cancer cells. Hence, the significant alterations in amino acid levels observed in our study suggest an upregulation of amino acid metabolism to produce high levels of cellular building blocks required for rapid PCa cell proliferation. This assumption is corroborated by the observed alteration in purine metabolism, which provides essential components for DNA and RNA synthesis, as well as energy and cofactors to stimulate cell survival and proliferation (64). Purine and amino acid metabolisms are closely interconnected because several amino acids (e.g., glutamine, glycine, aspartic acid) are substrates required for purine *de novo* biosynthetic pathway, particularly in rapid proliferating cancer cells (64).

Dysregulations in nicotinate and nicotinamide metabolism were corroborated by the negative correlation (Table S6) between NAD^+ and niacinamide (also known as nicotinamide), which is expected since NAD^+ is produced *de novo* from niacinamide in a short sequence of enzyme-catalyzed reactions referred as salvage pathway (65). NAD^+ is essential for aerobic glycolysis and other energy metabolic pathways (e.g., TCA cycle, oxidative phosphorylation, fatty acid metabolism), as well as for DNA repair mechanisms and several cellular signaling regulatory pathways. The NAD^+ levels in cells can be modulated by enzymatic consumption, particularly by cyclic ADP-ribose (ADPR) synthases such as CD38, which is the primary NAD'ase in mammalian cells (66). However, a decreased expression of CD38 and consequent increase in NAD^+ levels have been reported in PCa (66), which contrasts with the downregulation of NAD^+ and upregulation of niacinamide observed in our study. Still, Dudka et al. also reported significantly lower NAD^+ levels in PCa compared with adjacent non-malignant tissue (43), in accordance with our findings. Regarding the correlations found between niacinamide and several PL species (particularly PEs) in this study, it may be explained by the essential role of nicotinamide phosphoribosyl transferase (NAMPT) for PL synthesis in PCa cells (67), which may link nicotinate and nicotinamide metabolism with glycerophospholipid metabolism.

Regarding glycerophospholipid metabolism, a significant increase in the levels of several PEs and PCs was observed in PCa tissue. PEs and PCs are the most abundant PL

species in cellular membranes, playing a major role in their structure and function (68). Considering that cancer cells disclose a highly proliferative phenotype, and consequent high demand of cellular membrane components, this increase in the levels of the major cellular membrane components might be expected (60). Interestingly, the PCs and PEs found upregulated in PCa were mainly composed by palmitic acid (16:0), stearic acid (18:0), oleic acid (18:1), and linoleic acid (18:2). In addition, two plasmalogen PEs, namely PE(P-38:5) and PE(P-40:7), stand out as they were downregulated in PCa tissue. The significant decrease in the levels of alkenyl-ether lipid species was previously associated with other cancers (e.g. pancreatic cancer (69) and esophageal cancer (70)). The role of plasmalogens in cancer metabolism is not fully understood, although several potential biological functions have been associated with these lipid species, including reduction of PL surface tension and viscosity, control of cellular membrane fusion and remodeling, regulation of membrane proteins, membrane vesicle structure, storage of cellular messengers, and cellular signaling (71, 72). Most importantly, plasmalogens act as endogenous antioxidants (71), which may justify the observed significant decrease in the levels of these PL species in PCa tissue.

Concerning PIs, we observed a significant increase in the levels of this class of lipids in PCa tissue, particularly composed by stearic (18:0) and oleic (18:1) acids, which is in accordance with a previous study (49). PIs are key regulators of membrane binding of proteins and protein activity at the cell interface (73), contributing for cell membrane fluidity (49). Furthermore, PIs are an important precursor of signaling molecules (73), including the lipid secondary messenger phosphatidylinositol (3,4,5)-trisphosphate (PIP3), a key participant in PI3-kinase pathway (63). Thus, the increase in the levels of PIs in PCa tissue might be related with the role of these molecules in intracellular signal transduction of PI3-kinase pathway. Indeed, the oncogenic activation of PI3K pathway has been associated with PCa (63).

Finally, we also observed a significant decrease in the levels of SMs. These lipid species are essential bioactive components of cell membrane (74, 75), as they can interact with proteins and cholesterol at the membrane surface (76). The decrease in the levels of SMs may be associated with the activation of sphingomyelinase since these enzymes can be activated by the metabolic products of arachidonic acid (50). Remarkably, a significant decrease in the levels of arachidonic acid was also observed in our study. Furthermore, the arachidonic acid pathway has previously been associated with PCa development and progression (50).

4.1.5 Conclusions

This work unveiled alterations in the levels of 27 metabolites and 21 PL species participating in 13 metabolic pathways, in PCa. Novel and significant alterations included the upregulation of 1-methylhistine, serine, tryptophan, UDP-glucose/UDP-galactose, niacinamide, urea, and several PC, PE and PI species, and the downregulation of nonanoic acid, benzoic acid, oleamide, two plasmalogen PEs and one SM specie. Interestingly, the dysregulated PL species included mainly palmitic (16:0), stearic (18:0), oleic (18:1) and linoleic (18:2) acids in their composition.

The metabolic pathways most affected in PCa tissue were amino acid metabolism, nicotinate and nicotinamide metabolism, purine metabolism, and glycerophospholipid metabolism. Importantly, a clear interconnection among these pathways was observed through correlation analysis. Dysregulation in these metabolic pathways may be related with activation of mTOR and PI3-kinase pathway to produce high levels of cellular building blocks required for rapid PCa cell proliferation. These results emphasize that the combination of GC-MS and NMR-based metabolomics with lipidomics provides a more comprehensive characterization of PCa tissue and a better understanding of metabolic alterations occurring in PCa development.

4.1.6 References

1. Sung H, Ferlay J, Siegel RL, Laversanne M, Soerjomataram I, Jemal A, et al. Global cancer statistics 2020: GLOBOCAN estimates of incidence and mortality worldwide for 36 cancers in 185 countries. CA Cancer J Clin. 2021.

2. Siegel RL, Miller KD, Jemal A. Cancer statistics, 2020. CA Cancer J Clin. 2020;70(1):7-30.

3. Schalken J, Dijkstra S, Baskin-Bey E, van Oort I. Potential utility of cancer-specific biomarkers for assessing response to hormonal treatments in metastatic prostate cancer. Ther Adv Urol. 2014;6(6):245-52.

4. Ziglioli F, Granelli G, Cavalieri D, Bocchialini T, Maestroni U. What chance do we have to decrease prostate cancer overdiagnosis and overtreatment? A narrative review. Acta Biomed. 2019;90(4):423-6.

5. Sarkar S, Das S. A Review of Imaging Methods for Prostate Cancer Detection. Biomed Eng Comput Biol. 2016;7(Suppl 1):1-15.

6. Das CJ, Razik A, Sharma S, Verma S. Prostate biopsy: when and how to perform. Clin Radiol. 2019;74(11):853-64.

7. Hubner N, Shariat S, Remzi M. Prostate biopsy: guidelines and evidence. Curr Opin Urol. 2018;28(4):354-9.

8. Mottet N, van den Bergh RCN, Briers E, Van den Broeck T, Cumberbatch MG, De Santis M, et al. EAU-EANM-ESTRO-ESUR-SIOG Guidelines on Prostate Cancer-2020 Update. Part 1: Screening, Diagnosis, and Local Treatment with Curative Intent. European urology. 2021;79(2):243-62.

9. Fakhrejahani F, Madan RA, Dahut WL. Management Options for Biochemically Recurrent Prostate Cancer. Curr Treat Options Oncol. 2017;18(5):26.

10. Tourinho-Barbosa R, Srougi V, Nunes-Silva I, Baghdadi M, Rembeyo G, Eiffel SS, et al. Biochemical recurrence after radical prostatectomy: what does it mean? Int Braz J Urol. 2018;44(1):14-21.

11. Armitage EG, Ciborowski M. Applications of Metabolomics in Cancer Studies. Adv Exp Med Biol. 2017;965:209-34.

12. Kumar A, Misra BB. Challenges and Opportunities in Cancer Metabolomics. Proteomics. 2019;19(21-22):e1900042.

13. Sharma U, Jagannathan NR. Metabolism of prostate cancer by magnetic resonance spectroscopy (MRS). Biophys Rev. 2020;12(5):1163-73.

14. Lima AR, Bastos Mde L, Carvalho M, Guedes de Pinho P. Biomarker Discovery in Human Prostate Cancer: an Update in Metabolomics Studies. Transl Oncol. 2016;9(4):357-70.

15. Jung K, Reszka R, Kamlage B, Bethan B, Stephan C, Lein M, et al. Tissue metabolite profiling identifies differentiating and prognostic biomarkers for prostate carcinoma. International journal of cancer. 2013;133(12):2914-24.

16. Lima AR, Pinto J, Bastos ML, Carvalho M, Guedes de Pinho P. NMR-based metabolomics studies of human prostate cancer tissue. Metabolomics. 2018;14(7):88.

17. Lima AR, Pinto J, Amaro F, Bastos MdL, Carvalho M, Guedes de Pinho P. Advances and Perspectives in Prostate Cancer Biomarker Discovery in the Last 5 Years through Tissue and Urine Metabolomics. Metabolites. 2021;11(3):181.

18. Beckonert O, Keun HC, Ebbels TM, Bundy J, Holmes E, Lindon JC, et al. Metabolic profiling, metabolomic and metabonomic procedures for NMR spectroscopy of urine, plasma, serum and tissue extracts. Nat Protoc. 2007;2(11):2692-703.

19. Chan EC, Pasikanti KK, Nicholson JK. Global urinary metabolic profiling procedures using gas chromatography-mass spectrometry. Nat Protoc. 2011;6(10):1483-99.

20. Beckonert O, Keun HC, Ebbels TMD, Bundy J, Holmes E, Lindon JC, et al. Metabolic profiling, metabolomic and metabonomic procedures for NMR spectroscopy of urine, plasma, serum and tissue extracts. Nature Protocols. 2007;2(11):2692-703.

21. Neves B, Duarte S, Domingues P, Pérez-Sala D, Oliveira MM, Domingues MDR, et al. Advancing Target Identification of Nitrated Phospholipids in Biological Systems by HCD Specific Fragmentation Fingerprinting in Orbitrap Platforms. Molecules (Basel, Switzerland). 2020;25(9).

22. Colombo S, Melo T, Martínez-López M, Carrasco MJ, Domingues MR, Pérez-Sala D, et al. Phospholipidome of endothelial cells shows a different adaptation response upon oxidative, glycative and lipoxidative stress. Scientific reports. 2018;8(1):12365.

23. Lima AR, Pinto J, Barros-Silva D, Jeronimo C, Henrique R, Bastos ML, et al. New findings on urinary prostate cancer metabolome through combined GC-MS and (1)H NMR analytical platforms. Metabolomics. 2020;16(6):70.

24. Lima AR, Araujo AM, Pinto J, Jeronimo C, Henrique R, Bastos ML, et al. GC-MS-Based Endometabolome Analysis Differentiates Prostate Cancer from Normal Prostate Cells. Metabolites. 2018;8(1).

25. Diaz SO, Barros AS, Goodfellow BJ, Duarte IF, Carreira IM, Galhano E, et al. Following healthy pregnancy by nuclear magnetic resonance (NMR) metabolic profiling of human urine. J Proteome Res. 2013;12(2):969-79.

26. Monteiro MS, Barros AS, Pinto J, Carvalho M, Pires-Luís AS, Henrique R, et al. Nuclear Magnetic Resonance metabolomics reveals an excretory metabolic signature of renal cell carcinoma. Scientific reports. 2016;6(1):37275.

27. Ulrich EL, Akutsu H, Doreleijers JF, Harano Y, Ioannidis YE, Lin J, et al. BioMagResBank. Nucleic Acids Res. 2008;36(Database issue):D402-8.

28. Pluskal T, Castillo S, Villar-Briones A, Oresic M. MZmine 2: modular framework for processing, visualizing, and analyzing mass spectrometry-based molecular profile data. BMC Bioinformatics. 2010;11:395.

29. Liebisch G, Fahy E, Aoki J, Dennis EA, Durand T, Ejsing CS, et al. Update on LIPID MAPS classification, nomenclature, and shorthand notation for MS-derived lipid structures. Journal of lipid research. 2020;61(12):1539-55.

30. Guerra IMS, Diogo L, Pinho M, Melo T, Domingues P, Domingues MR, et al. Plasma Phospholipidomic Profile Differs between Children with Phenylketonuria and Healthy Children. J Proteome Res. 2021.

31. Veselkov KA, Lindon JC, Ebbels TM, Crockford D, Volynkin VV, Holmes E, et al. Recursive segment-wise peak alignment of biological (1)h NMR spectra for improved metabolic biomarker recovery. Anal Chem. 2009;81(1):56-66.

32. Xi B, Gu H, Baniasadi H, Raftery D. Statistical analysis and modeling of mass spectrometry-based metabolomics data. Methods Mol Biol. 2014;1198:333-53.

33. Chong J, Soufan O, Li C, Caraus I, Li S, Bourque G, et al. MetaboAnalyst 4.0: towards more transparent and integrative metabolomics analysis. Nucleic Acids Res. 2018;46(W1):W486-W94.

34. Berben L, Sereika SM, Engberg S. Effect size estimation: Methods and examples. International Journal of Nursing Studies. 2012;49(8):1039-47.

35. Aickin M, Gensler H. Adjusting for multiple testing when reporting research results: the Bonferroni vs Holm methods. Am J Public Health. 1996;86(5):726-8.

36. Team RC. R: A Language and Environment for Statistical Computing. R Foundation for Statistical Computing, Vienna, Austria; 2017.

37. Harrell Jr F. Hmisc: Harrell Miscellaneous [Available from: https://cran.r-project.org/web/packages/Hmisc/]

38. Broadhurst D, Goodacre R, Reinke SN, Kuligowski J, Wilson ID, Lewis MR, et al. Guidelines and considerations for the use of system suitability and quality control samples in mass spectrometry assays applied in untargeted clinical metabolomic studies. Metabolomics. 2018;14(6):72.

39. Shao Y, Ye G, Ren S, Piao HL, Zhao X, Lu X, et al. Metabolomics and transcriptomics profiles reveal the dysregulation of the tricarboxylic acid cycle and related mechanisms in prostate cancer. International journal of cancer. 2018;143(2):396-407.

40. Vandergrift LA, Decelle EA, Kurth J, Wu S, Fuss TL, DeFeo EM, et al. Metabolomic Prediction of Human Prostate Cancer Aggressiveness: Magnetic Resonance Spectroscopy of Histologically Benign Tissue. Scientific reports. 2018;8(1):4997.

41. Franko A, Shao Y, Heni M, Hennenlotter J, Hoene M, Hu C, et al. Human Prostate Cancer is Characterized by an Increase in Urea Cycle Metabolites. Cancers (Basel). 2020;12(7).

42. Zheng H, Dong B, Ning J, Shao X, Zhao L, Jiang Q, et al. NMR-based metabolomics analysis identifies discriminatory metabolic disturbances in tissue and biofluid samples for progressive prostate cancer. Clin Chim Acta. 2020;501:241-51.

43. Dudka I, Thysell E, Lundquist K, Antti H, Iglesias-Gato D, Flores-Morales A, et al. Comprehensive metabolomics analysis of prostate cancer tissue in relation to tumor aggressiveness and TMPRSS2-ERG fusion status. BMC Cancer. 2020;20(1):437.

44. Stenman K, Stattin P, Stenlund H, Riklund K, Grobner G, Bergh A. H HRMAS NMR Derived Bio-markers Related to Tumor Grade, Tumor Cell Fraction, and Cell Proliferation in Prostate Tissue Samples. Biomark Insights. 2011;6:39-47.

45. Yumba-Mpanga A, Struck-Lewicka W, Wawrzyniak R, Markuszewski M, Roslan M, Kaliszan R, et al. Metabolomic Heterogeneity of Urogenital Tract Cancers Analyzed by Complementary Chromatographic Techniques Coupled with Mass Spectrometry. Curr Med Chem. 2019;26(1):216-31.

46. Derezinski P, Klupczynska A, Sawicki W, Palka JA, Kokot ZJ. Amino Acid Profiles of Serum and Urine in Search for Prostate Cancer Biomarkers: a Pilot Study. Int J Med Sci. 2017;14(1):1-12.

47. Fernandez-Peralbo MA, Gomez-Gomez E, Calderon-Santiago M, Carrasco-Valiente J, Ruiz-Garcia J, Requena-Tapia MJ, et al. Prostate Cancer Patients-Negative Biopsy Controls Discrimination by Untargeted Metabolomics Analysis of Urine by LC-QTOF: Upstream Information on Other Omics. Scientific reports. 2016;6:38243.

48. Zhou X, Mei H, Agee J, Brown T, Mao J. Racial differences in distribution of fatty acids in prostate cancer and benign prostatic tissues. Lipids Health Dis. 2019;18(1):189.

49. Goto T, Terada N, Inoue T, Nakayama K, Okada Y, Yoshikawa T, et al. The expression profile of phosphatidylinositol in high spatial resolution imaging mass spectrometry as a potential biomarker for prostate cancer. PLoS One. 2014;9(2):e90242.

50. Goto T, Terada N, Inoue T, Kobayashi T, Nakayama K, Okada Y, et al. Decreased expression of lysophosphatidylcholine (16:0/OH) in high resolution imaging mass spectrometry independently predicts biochemical recurrence after surgical treatment for prostate cancer. Prostate. 2015;75(16):1821-30.

51. Buszewska-Forajta M, Pomastowski P, Monedeiro F, Walczak-Skierska J, Markuszewski M, Matuszewski M, et al. Lipidomics as a Diagnostic Tool for Prostate Cancer. Cancers (Basel). 2021;13(9).

52. Li J, Ren S, Piao HL, Wang F, Yin P, Xu C, et al. Integration of lipidomics and transcriptomics unravels aberrant lipid metabolism and defines cholesteryl oleate as potential biomarker of prostate cancer. Scientific reports. 2016;6:20984.

53. Viant MR, Kurland IJ, Jones MR, Dunn WB. How close are we to complete annotation of metabolomes? Current Opinion in Chemical Biology. 2017;36:64-9.

54. Pang Z, Chong J, Li S, Xia J. MetaboAnalystR 3.0: Toward an Optimized Workflow for Global Metabolomics. Metabolites. 2020;10(5):186.

55. Eidelman E, Twum-Ampofo J, Ansari J, Siddiqui MM. The Metabolic Phenotype of Prostate Cancer. Front Oncol. 2017;7:131.

56. Kwon H, Oh S, Jin X, An YJ, Park S. Cancer metabolomics in basic science perspective. Arch Pharm Res. 2015;38(3):372-80.

57. Zadra G, Loda M. Metabolic Vulnerabilities of Prostate Cancer: Diagnostic and Therapeutic Opportunities. Cold Spring Harb Perspect Med. 2018;8(10).

58. Lloyd SM, Arnold J, Sreekumar A. Metabolomic profiling of hormone-dependent cancers: a bird's eye view. Trends Endocrinol Metab. 2015;26(9):477-85.

59. Nelson DL. Lehninger principles of biochemistry: Fourth edition. New York : W.H. Freeman, 2005.; 2005.

60. Zhang BK, Moran AM, Bailey CG, Rasko JEJ, Holst J, Wang Q. EGF-activated PI3K/Akt signalling coordinates leucine uptake by regulating LAT3 expression in prostate cancer. Cell Commun Signal. 2019;17(1):83.

61. Linares Juan F, Duran A, Reina-Campos M, Aza-Blanc P, Campos A, Moscat J, et al. Amino Acid Activation of mTORC1 by a PB1-Domain-Driven Kinase Complex Cascade. Cell Reports. 2015;12(8):1339-52.

62. Xu Y, Chen S, Balk SP. Androgen receptor signaling induces prostate cancer cell proliferation through mTOR activation and post-transcriptional increases in cyclin D proteins. Cancer Research. 2006;66(8 Supplement):688.

63. Shorning BY, Dass MS, Smalley MJ, Pearson HB. The PI3K-AKT-mTOR Pathway and Prostate Cancer: At the Crossroads of AR, MAPK, and WNT Signaling. Int J Mol Sci. 2020;21(12):4507.

64. Yin J, Ren W, Huang X, Deng J, Li T, Yin Y. Potential Mechanisms Connecting Purine Metabolism and Cancer Therapy. Front Immunol. 2018;9:1697.

65. Kennedy BE, Sharif T, Martell E, Dai C, Kim Y, Lee PW, et al. NAD(+) salvage pathway in cancer metabolism and therapy. Pharmacol Res. 2016;114:274-83.

66. Chmielewski JP, Bowlby SC, Wheeler FB, Shi L, Sui G, Davis AL, et al. CD38 Inhibits Prostate Cancer Metabolism and Proliferation by Reducing Cellular NAD(+) Pools. Mol Cancer Res. 2018;16(11):1687-700.

67. Bowlby SC, Thomas MJ, D'Agostino RB, Jr., Kridel SJ. Nicotinamide phosphoribosyl transferase (Nampt) is required for *de novo* lipogenesis in tumor cells. PLoS One. 2012;7(6):e40195.

68. Gibellini F, Smith TK. The Kennedy pathway-*De novo* synthesis of phosphatidylethanolamine and phosphatidylcholine. IUBMB Life. 2010;62(6):414-28.

69. Ritchie SA, Akita H, Takemasa I, Eguchi H, Pastural E, Nagano H, et al. Metabolic system alterations in pancreatic cancer patient serum: potential for early detection. BMC Cancer. 2013;13(1):416.

70. Merchant TE, de Graaf PW, Minsky BD, Obertop H, Glonek T. Esophageal cancer phospholipid characterization by 31P NMR. NMR in Biomedicine. 1993;6(3):187-93.

71. Messias MCF, Mecatti GC, Priolli DG, de Oliveira Carvalho P. Plasmalogen lipids: functional mechanism and their involvement in gastrointestinal cancer. Lipids in Health and Disease. 2018;17(1):41.

72. Jimenez-Rojo N, Riezman H. On the road to unraveling the molecular functions of ether lipids. FEBS Lett. 2019;593(17):2378-89.

73. Christie WW. The LIPIDWEB: Phosphatidylinositol and Related Phosphoinositides: LIPID MAPS Lipidomics Gateway; 2021 [updated 2021. Available from: https://www.lipidmaps.org/resources/lipidweb/index.php?page=lipids/complex/pi/index.htm

74. Perrotti F, Rosa C, Cicalini I, Sacchetta P, Del Boccio P, Genovesi D, et al. Advances in Lipidomics for Cancer Biomarkers Discovery. Int J Mol Sci. 2016;17(12).

75. Andersen MK, Giskeødegård GF, Tessem M-B. Metabolic alterations in tissues and biofluids of patients with prostate cancer. Current Opinion in Endocrine and Metabolic Research. 2020;10:23-8.

76. Christie WW. The LIPIDWEB: Sphingomyelin and Related Sphingophospholipids: LIPID MAPS Lipidomics Gateway; 2021 [updated 2021. Available from: https://www.lipidmaps.org/resources/lipidweb/index.php?page=lipids/sphingo/sph/index.htm.

4.1.7 Supporting information

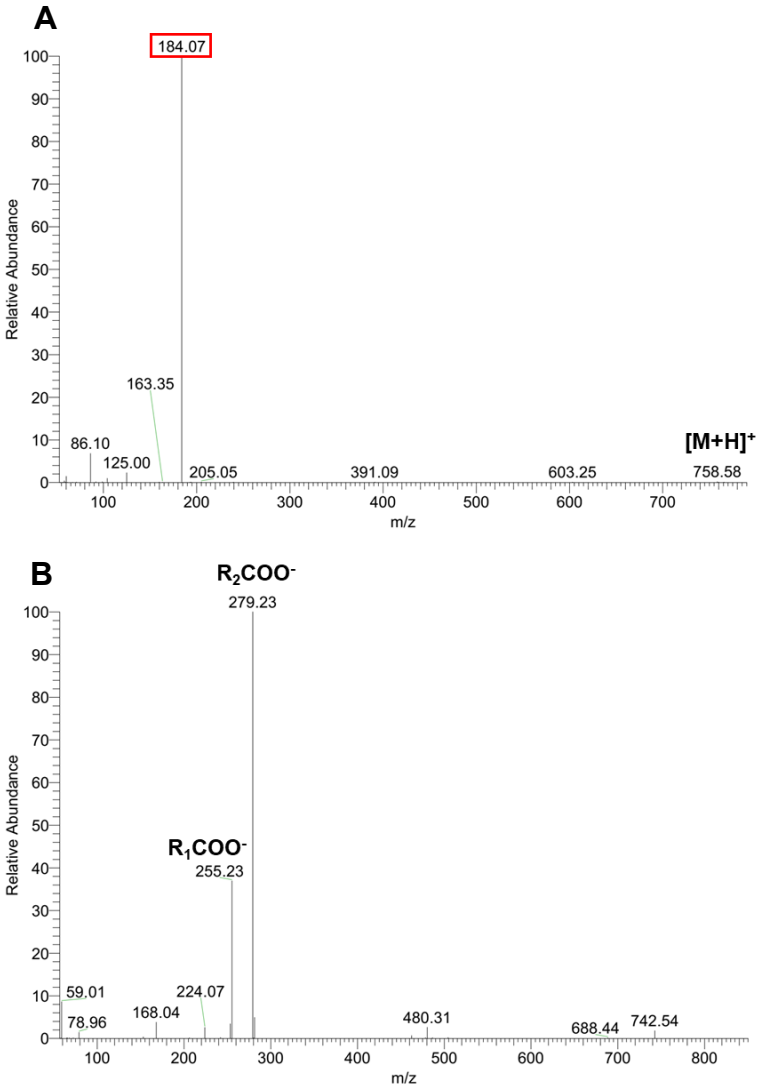

Figure S1: Representative MS/MS spectra of phosphatidylcholine (PC) lipid species. **A)** HILIC-MS/MS spectrum of the $[M + H]^+$ ion at *m/z* 758.6 of the lipid species PC (34:2). Confirmation of PL class was achieved by the identification of phosphocholine polar head, ion at *m/z* 184.1 (formula: $C_5H_{15}NO_4P$; exact mass: 184.0739); **B)** HILIC-MS/MS spectrum of the $[M + CH3COO]^-$ ion at *m/z* 816.6 of the lipid species PC (34:2). The typical neutral loss of 74 Da, corresponding to the loss of methyl acetate (i.e., $-CH_3COOCH_3$ with formation of ions at *m/z* 742.5), and the product ions at *m/z* 168.0 (formula: $C_4H_{11}NO_4P$; exact mass:168.0425), corresponding to the N-dimethylaminoethylphosphate anion (i.e., phosphocholine polar head without a methyl group), corroborate the identification of the PC class. Fatty acid composition was confirmed by the identification of product ions corresponding to the fatty acyl chains as $[RCOO]^-$. The product ions observed at *m/z* 255.2 and 279.2, corresponding to fatty acyl carboxylate anions 16:0 (R_1COO^-) and 18:2 (R_2COO^-) allowed to identify the fatty acyl composition of PC (16:0/18:2).

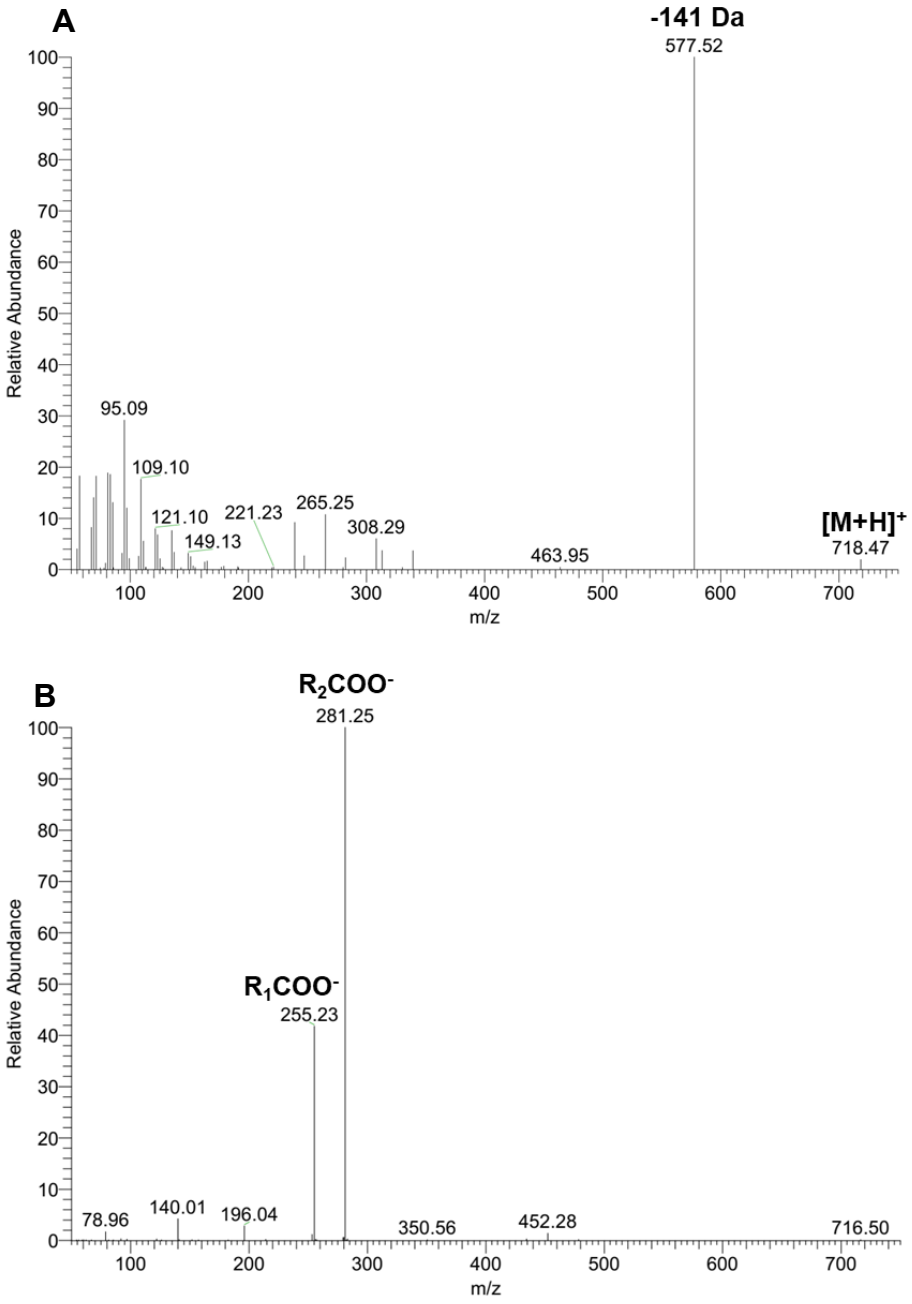

Figure S2: Representative MS/MS spectra of phosphatidylethanolamine (PE) lipid species. **A)** HILIC-MS/MS spectrum of the $[M + H]^+$ ion at *m/z* 718.5 of the lipid species PE (34:1). Confirmation of the PL class was achieved by the identification of phosphoethanolamine polar head corresponding to the neutral loss of 141 Da (formula: $C_2H_8NO_4P$; exact mass: 141.0191). **B)** HILIC-MS/MS spectrum of the $[M + H]^-$ ion at *m/z* 716.5 of the lipid species PE (34:1). The class confirmation was accomplished by the presence of the phosphoethanolamine polar head that correspond to the product ion at *m/z* 140.0 (formula: $C_2H_7NO_4P$; exact mass: 140.0113). Fatty acid composition was confirmed by the identification of product ions corresponding to the fatty acyl chains as $[RCOO]^-$. The product ions observed at *m/z* 255.2 and 281.2, corresponding to fatty acyl carboxylate anions of 16:0 (R_1COO^-) and 18:1 (R_2COO^-), allowed to identify the fatty acyl composition of PE (16:0/18:1).

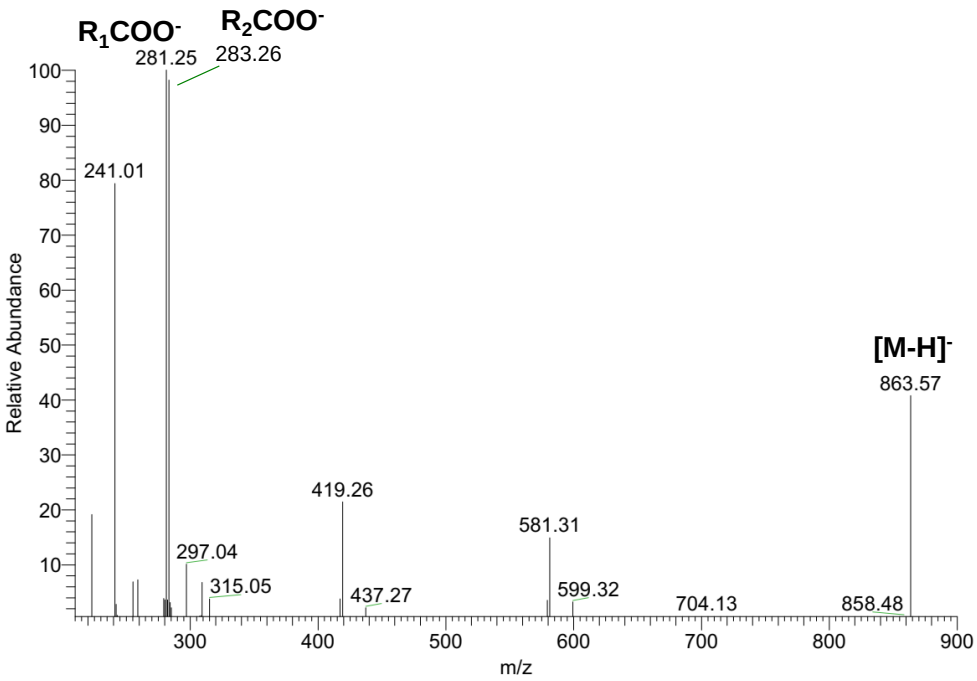

Figure S3: Representative MS/MS spectrum of phosphatidylinositol (PI) lipid species. HILIC-MS/MS spectrum of the $[M + H]^-$ ion at *m/z* 863.6 of the lipid species PI (36:1). Confirmation of PL class was achieved by the identification of the phosphoinositol head group that correspond to the product ion at *m/z* 241.0 (formula: $C_6H_{10}O_8P$; exact mass: 241.0113). Fatty acid composition was confirmed by the identification of product ions corresponding to the fatty acyl chains as $[RCOO]^-$. The product ions observed at *m/z* 281.3 and 283.3, corresponding to fatty acyl carboxylate anions of 18:1 (R_1COO^-) and 18:0 (R_2COO^-) allowed to identify the fatty acyl composition of PI (18:0/18:1).

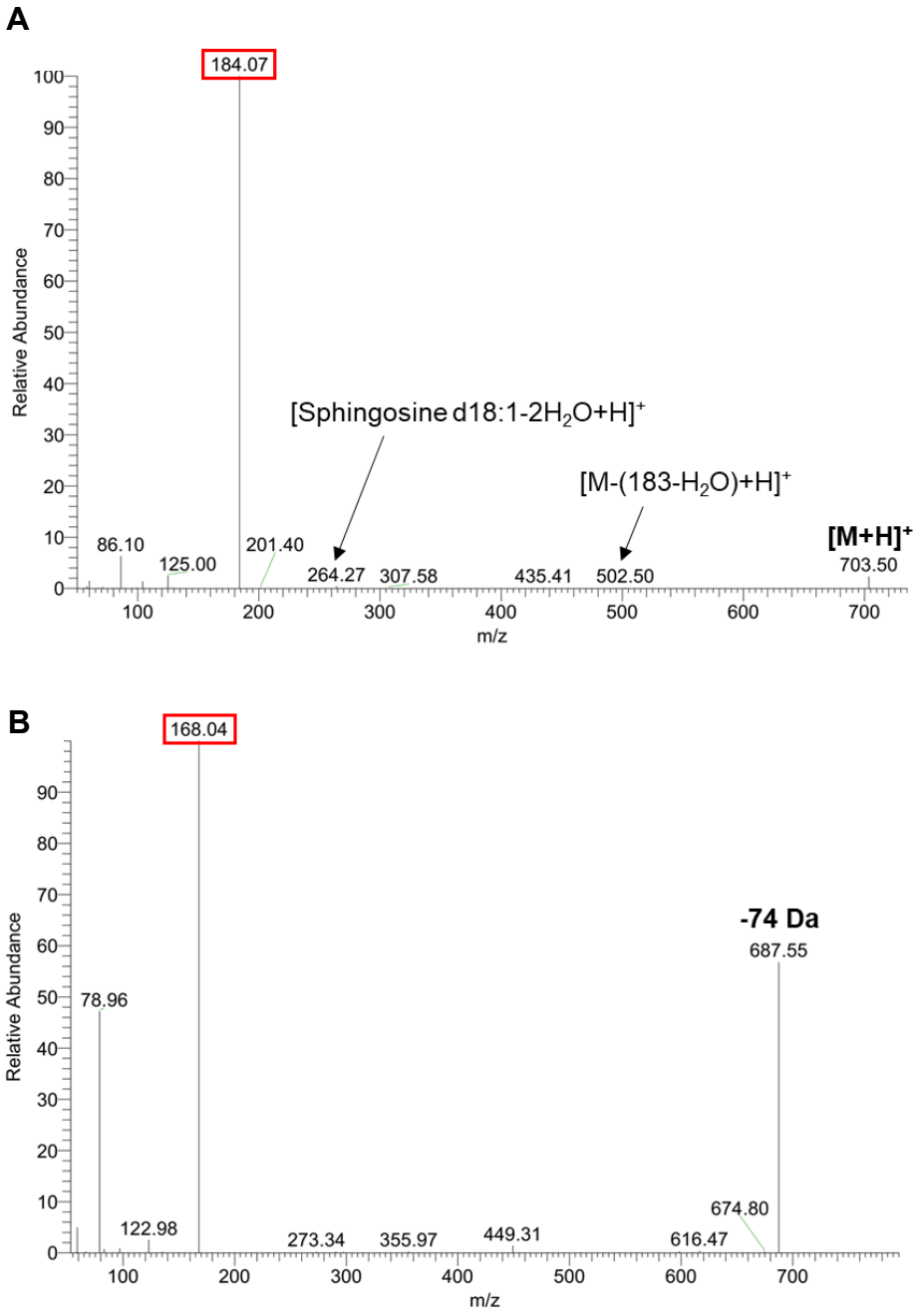

Figure S4: Representative MS/MS spectra of sphingomyelin (SM) lipid species. **A)** HILIC-MS/MS spectrum of the $[M + H]^+$ ion at *m/z* 703.5 of the lipid species SM (d34:1). Confirmation of PL class was achieved by the identification of the phosphocholine polar head corresponding to the product ion at *m/z* 184.1 (formula: $C_5H_{15}NO_4P$; exact mass: 184.0739), and the product ion of sphingoid base at *m/z* 264.3, corresponding to $[Sphingosine\ d18:1\text{-}2H_2O+H]^+$. The mass difference of 238 Da between the product ions at *m/z* 502.5 ($[M\text{-}(183\text{-}H_2O)+H]^+$) and 264.3, plus 18 Da, allowed to infer the presence of 16:0 as fatty acyl amide substituent. **B)** HILIC-MS/MS spectrum of the $[M + CH_3COO]^-$ ion at *m/z* 761.5 of the lipid species SM (d34:1). The typical loss of 74 Da corresponding to the loss of methyl acetate (formula: C3H6O2; exact mass: 74.0368) and the product ion at m/z 168.0 (formula: C4H11NO4P; exact mass:168.0425), corresponding to the phosphocholine polar head without a methyl group, corroborate the identification of the SM class.

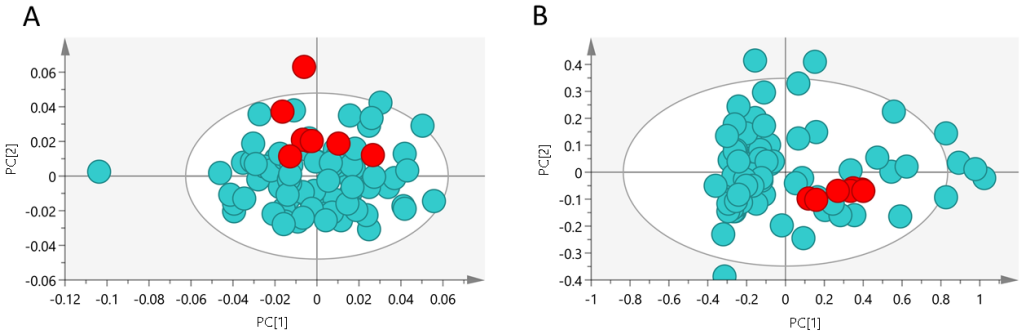

Figure S5: PCA scores scatter plots (Pareto scaling; 2 components) obtained for (A) GC-MS (R^2X=0.346) and (B) HILIC-MS/MS (R^2X=0.749) data of all samples under study (*n* = 80, blue circles) and QCs (*n* = 8, red circles).

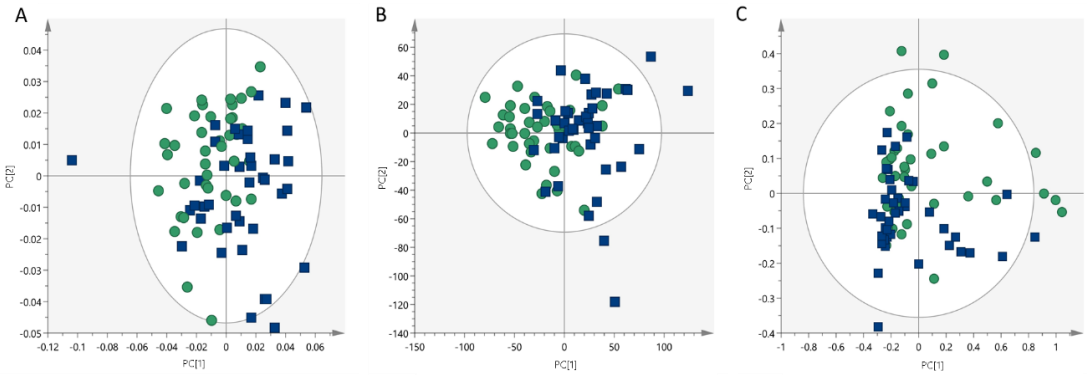

Figure S6: PCA scores scatter plots obtained for (A) GC-MS data (Pareto scaling; 2 components, R^2X=0.354), (B) ^{1}H NMR data (UV scaling; 2 components, R^2X=0.233) and HILIC-MS/MS data (Pareto scaling; 2 components, R^2X=0.741) of PCa (*n* = 40, blue squares) compared with adjacent non-malignant tissue (*n* = 40, green circles).

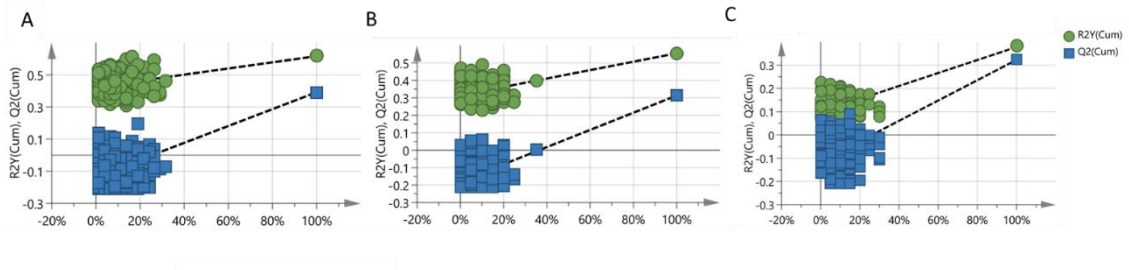

Figure S7: Statistical validation of the PLS-DA models obtained for (A) GC-MS [Intercepts: R^2 = (0.0, 0.425); Q^2 = (0.0, -0.133)], (B) ^{1}H NMR [Intercepts: R^2 = (0.0, 0.315); Q^2 = (0.0, -0.179)], and (C) HILIC-MS/MS [Intercepts: R^2 = (0.0, 0.0989); Q^2 = (0.0, -0.114)] data of PCa vs. adjacent non-malignant tissue by permutation testing (200 permutations; 2 components).

Table S1: List of metabolites significantly altered in PCa *vs*. adjacent non-malignant tissue detected through GC-MS. Metabolites are characterized by their retention time (RT), most characteristic ions (*m/z*), Kovats indices (KI) from literature, experimental KI, R match (NIST), identification level, as well as the HMDB (Human Metabolome Database) code.

Name	RT	*m/z*	KI from literature	Experimental KI [a]	R match	Identification level [b]	HMDB [c]
Urea	7.13	147/189/73	-	-	910	L1	HMDB0000294
Benzoic acid	7.25	105/179/77	-	-	906	L1	HMDB0001870
Serine	7.32	116/132/73	-	-	751	L1	HMDB0000187
Proline	7.71	142/73/143	-	-	912	L1	HMDB0000162
Uracil	8.07	241/99/255	-	-	867	L1	HMDB0000300
Nonanoic acid	8.31	73/75/215	-	-	781	L1	HMDB0000847
Aspartic acid	8.87	73/160/130	-	-	823	L1	HMDB0000191
Malic acid	9.38	73/147/233	-	-	928	L1	HMDB0000156
Phenyl-alanine	10.55	73/218/192	-	-	886	L1	HMDB0000159
Glutamine	11.61	73/156/155	-	-	896	L1	HMDB0000641

Name	RT	*m/z*	KI from literature	Experimental KI [a]	R match	Identification level [b]	HMDB [c]
Hypoxanthine	11.88	265/73/280	1811	1809	920	L2	HMDB0000157
Tyrosine	12.76	218/73/219	-	-	959	L1	HMDB0000158
Myo-inositol	13.73	73/147/217	-	-	937	L1	HMDB0000211
Arachidonic acid	15.79	73/75/79	2417	2463	860	L2	HMDB0001043
Oleamide	16.23	75/131/73	2427	2512	912	L2	HMDB0002117

[a]: Experimental Kovats RI determined using a commercial hydrocarbon mixture (C8–C20); [b]: Viant MR, Kurland IJ, Jones MR, Dunn WB. How close are we to complete annotation of metabolomes? Curr Opin Chem Biol. 2017;36:64-9. [c]: Wishart DS, Tzur D, Knox C, Eisner R, Guo AC, Young N, et al. HMDB: the Human Metabolome Database. Nucleic Acids Res. 2007;35(Database issue):D521-6; L1: Identified metabolites (GC-MS analysis of the metabolite of interest and a chemical reference standard of suspected structural equivalence, with all analyses performed under identical analytical conditions within the same laboratory); L2: Putatively annotated compounds (MS spectral similarity with NIST database).

Table S2: List of metabolites significantly altered in PCa *vs.* adjacent non-malignant tissue detected through ^{1}H NMR spectroscopy. Metabolites are characterized by their ^{1}H chemical shift (multiplicity), the identification level, as well as the HMDB (Human Metabolome Database) code.

Name	δH ppm (multiplicity)	Identification level [a]	HMDB [b]
1-Methylhistidine	7.12 (s), 8.12 (s)	L2	HMDB0000001
Alanine	1.47 (d), 3.78 (q)	L2	HMDB0000161
Creatine	3.04(s), 3.93 (s)	L2	HMDB0000064
Fumaric acid	6.51 (s)	L2	HMDB0000134
Isoleucine	0.94 (t), 1.02 (d), 1.25 (m), 1.46(m), 1.96 (m), 3.64 (d)	L2	HMDB0000172
Leucine	0.96 (d), 0.97 (d), 1.67 (m), 1.70 (m), 3.73 (m)	L2	HMDB0000687
NAD^{+}	4.23 (m), 4.37 (m), 4.42 (dd), 4.49 (m), 4.54 (m), 4.76 (t), 6.04 (d), 6.08 (d), 8.18 (s), 8.20 (m), 8.43 (s), 8.84 (d), 9.15 (d), 9.34 (s)	L2	HMDB0000902

Name	δH ppm (multiplicity)	Identification level [a]	HMDB [b]
Niacinamide	7.58 (dd), 8.24 (dd), 8.70(dd), 8.94 (s)	L2	HMDB0001406
Taurine	3.28 (t), 3.41 (t)	L2	HMDB0000251
Tryptophan	3.30 (dd), 3.47 (dd), 4.05 (dd), 7.19 (m), 7.27 (m), 7.31 (s), 7.54 (d), 7.72 (d)	L2	HMDB0000929
UDP-Galactose	5.62 (dd), 5.99 (d), 6.00 (d), 7.96 (d)	L2	HMDB0012305
UDP-Glucose	5.55 (dd), 5.9 (d), 5.99 (d), 7.96 (d)	L2	HMDB0000286
Valine	1.00 (d), 1.05 (d), 2.26 (m), 3.60 (d)	L2	HMDB0000883

[a]: Levels of confidence in metabolite identification defined as described in Viant MR, Kurland IJ, Jones MR, Dunn WB. How close are we to complete annotation of metabolomes? Curr Opin Chem Biol. 2017;36:64-9. L2: Putatively annotated compounds (spectral similarity with database). [b]: Metabolite ID as described in Wishart DS, Tzur D, Knox C, Eisner R, Guo AC, Young N, et al. HMDB: the Human Metabolome Database. Nucleic Acids Res. 2007;35 (Database issue):D521-6; s: singlet, d: doublet, t: triplet, dd: doublet of doublets, m: multiplet

Table S3: List of metabolites significantly altered in PCa *vs.* adjacent non-malignant tissue, detected through HILIC-MS/MS. Lipid species are characterized by their retention time (RT), molecular ions (*m/z*) in positive and negative modes, fatty acid chains identified by MS/MS, formula, and identification level. Lipid species are labelled as X(C:N), where X is the lipid class abbreviation, C is the number of carbon atoms in fatty acids and N is the number of double bonds. The 'P-' prefix is used for plasmenyl species to indicate the alk-1-enyl ether substituent. All lipid species were identified by retention time, mass accuracy and confirmation of polar head group by MS/MS, whenever possible the fatty acid chains were also identified by MS/MS. Molecular species with known fatty acyl constituents are labelled using (sn-1/sn-2) nomenclature, considering that smaller and saturated fatty acids are commonly present at the sn-1 position in animals, while unsaturation fatty acids are located at sn-2. Lipid class abbreviations: PC, phosphatidylcholine; SM, sphingomyelin; PE, phosphatidylethanolamine; PI, phosphatidylinositol.

Lipid species (C:N)	RT	Calculated *m/z*	Observed *m/z*	Error (ppm)	Fatty acyl chains (C:N)	Formula	Identification level [a]
PC identified as $[M + H]^+$							
PC(34:2)	6.60	758.5700	758.5701	0.1556	(16:0/18:2)	$C_{42}H_{80}NO_8P$	L2
PC(34:3)	6.78	756.5543	756.5541	-0.3053	(16:1/18:2)	$C_{42}H_{78}NO_8P$	L2
PC(36:1)	6.45	788.6169	788.6160	-1.2059	(18:0/18:1)	$C_{44}H_{86}NO_8P$	L2

Lipid species (C:N)	RT	Calculated *m/z*	Observed *m/z*	Error (ppm)	Fatty acyl chains (C:N)	Formula	Identification level [a]
PC(36:2)	6.46	786.6013	786.6006	-0.8670	(18:1/18:1) and (18:0/18:2)	$C_{44}H_{84}NO_8P$	L2
PC(36:3)	6.47	784.5856	784.5842	-1.8338	-	$C_{44}H_{82}NO_8P$	L2
PC(38:7)	6.30	804.5543	804.5543	-2.8973	-	$C_{46}H_{78}NO_8P$	L2
PE identified as $[M-H]^-$							
PE(34:1)	2.73	716.5230	716.5234	0.5583	(16:0/18:1)	$C_{39}H_{76}NO_8P$	L2
PE(34:2)	2.74	714.5070	714.5082	1.6795	(16:0/18:2) and (16:1/18:1)	$C_{39}H_{74}NO_8P$	L2
PE(36:1)	2.68	744.5543	744.5546	0.4029	(18:0/18:1) and (16:0/20:1)	$C_{41}H_{80}NO_8P$	L2
PE(36:3)	2.68	740.5230	740.5251	2.8358	(18:1/18:2) and (16:0/20:3)	$C_{41}H_{76}NO_8P$	L2
PE(38:3)	2.63	768.5540	768.5545	0.7055	(18:1/20:2)	$C_{43}H_{80}NO_8P$	L2
PE(38:5)	2.61	764.5230	764.5243	1.7004	(18:1/20:4) and (16:0/22:5)	$C_{43}H_{76}NO_8P$	L2
PE(40:6)	2.53	790.5300	790.5385	-0.2530	(18:0/22:6)	$C_{45}H_{78}NO_8P$	L2
PE(P-38:5)	2.57	748.5280	748.5295	2.0040	(P-18:1/20:4) and (P-16:0/22:5)	$C_{43}H_{76}NO_7P$	L2
PE(P-40:7)	2.53	772.5280	772.5278	-0.2589	(P-18:1/22:6)	$C_{45}H_{76}NO_7P$	L2
PI identified as $[M-H]^-$							
PI(34:1)	1.30	835.5340	835.5340	<0.0001	(16:0/18:1)	$C_{43}H_{81}O_{13}P$	L2
PI(36:1)	1.30	863.5650	863.5643	-0.8106	(18:0/18:1)	$C_{45}H_{85}O_{13}P$	L2
PI(36:2)	1.30	861.5490	861.5494	0.4643	(18:1/18:1) and (18:0/18:2)	$C_{45}H_{83}O_{13}P$	L2
PI(38:2)	1.30	889.5810	889.5789	-2.3607	(18:0/20:2) and (18:1/20:1)	$C_{475}H_{87}O_{13}P$	L2
SM identified as $[M+H]^+$							
SM(d34:1)	7.79	703.5754	703.5748	-0.8542	(d18:1/16:0)	$C_{39}H_{79}N_2O_6P$	L2

Lipid species (C:N)	RT	Calculated *m/z*	Observed *m/z*	Error (ppm)	Fatty acyl chains (C:N)	Formula	Identification level [a]
SM(d42:1)	7.20	815.7006	815.7003	-0.3690	-	$C_{47}H_{95}N_2O_6P$	L2

[a]: Levels of confidence in metabolite identification defined as described in Viant MR, Kurland IJ, Jones MR, Dunn WB. How close are we to complete annotation of metabolomes? Curr Opin Chem Biol. 2017;36:64-9; L2: Putatively annotated compounds according to similarity with databases and MS/MS spectra.

Table S4: List of lipid classes significantly altered in PCa tissue compared to adjacent non-malignant tissue by HILIC-MS/MS. Relative comparison of each lipid class was performed by sum of normalized ion areas of all lipid species (identified only by RT and mass accuracy) within each class.

Class	*p*-value	Variation ± uncertainty (%)	Effect size ± ES_{SE}	AUC	Up/ down regulated
DGs	0.0102	-29.7 ± 13.2	-0.59 ± 0.45	0.65	Down
LPGs	0.0141	43.3 ± 15.0	0.53 ± 0.45	0.76	Up
PGs	0.0195	27.5 ± 9.6	0.56 ± 0.45	0.65	Up
PIs	0.0082	17.4 ± 5.2	0.70 ± 0.45	0.67	Up
SMs	0.0244	-9.5 ± 4.4	-0.51 ± 0.45	0.65	Down

DGs: diacylglycerols; LPGs: lysophosphatidylglycerol; PGs: Phosphatidylglycerols; PIs: phosphatidylinositols; SMs: sphingomyelins.

Table S5: Dysregulated metabolic pathways associated with PCa obtained from the metabolic pathway analysis performed in the MetPA tool (Metaboanalyst) considering all metabolites/PL species found statistically different between PCa and adjacent non-malignant tissue.

Metabolic pathway	Metabolites	*p*-value	Source
Aminoacyl-tRNA biosynthesis	Phenylalanine; Glutamine; Aspartic acid; Serine; Valine; Alanine; Isoleucine; Leucine; Tryptophan; Tyrosine; Proline	<0.0001	KEGG
Arginine biosynthesis	Aspartic acid; Glutamine; Urea; Fumaric acid	0.0001	KEGG
Valine, leucine and isoleucine biosynthesis	Leucine; Isoleucine; Valine	0.0004	KEGG, SMP
Alanine, aspartate and glutamate metabolism	Aspartic acid; Alanine; Glutamine; Fumaric acid	0.0022	KEGG, SMP
Phenylalanine, tyrosine and tryptophan biosynthesis	Phenylalanine; Tyrosine	0.0024	KEGG, SMP
Nicotinate and nicotinamide metabolism	Aspartic acid; NAD^+; Niacinamide	0.0031	KEGG, SMP
Pantothenate and CoA biosynthesis	Valine; Aspartic acid; Uracil	0.0062	KEGG, SMP

Metabolic pathway	Metabolites	*p*-value	Source
Ascorbate and aldarate metabolism	*Myo*-inositol; UDP-Glucose	0.0107	KEGG
Phenylalanine metabolism	Phenylalanine; Tyrosine	0.0168	KEGG, SMP
Glyoxylate and dicarboxylate metabolism	Malic acid; Serine; Glutamine	0.0264	KEGG
Histidine metabolism	1-Methylhistidine; Aspartic acid	0.0414	KEGG, SMP
Valine, leucine and isoleucine degradation	Valine; Isoleucine; Leucine	0.0471	KEGG, SMP
Citrate cycle (TCA cycle)	Malic acid; Fumaric acid	0.0623	KEGG, SMP
beta-Alanine metabolism	Aspartic acid; Uracil	0.0680	KEGG, SMP
Galactose metabolism	UDP-Glucose; *Myo*-inositol	0.1053	KEGG, SMP
Glycine, serine and threonine metabolism	Serine; Creatine	0.1469	KEGG, SMP
Purine metabolism	Glutamine; Hypoxanthine; Urea	0.1475	KEGG, SMP
Glycerophospholipid metabolism	PC; PE	0.1688	KEGG
Arginine and proline metabolism	Creatine; Proline	0.1837	KEGG, SMP
Pyrimidine metabolism	Glutamine; Uracil	0.1913	KEGG, SMP
Tyrosine metabolism	Tyrosine; Fumaric acid	0.2142	KEGG, SMP

PC, phosphatidylcholine; PE, phosphatidylethanolamine

Table S6: Spearman's rank correlation coefficient obtained between all significantly altered metabolites/PL species in PCa *vs.* adjacent non-malignant tissue, with a threshold of $p \leq 0.0001$.

Metabolite pair		*r*	*p*-value	Metabolic pathways
Val	Iso	0.87	<0.0001	Aminoacyl-tRNA biosynthesis; Valine, leucine and isoleucine biosynthesis; Valine, leucine and isoleucine degradation
Val	Leu	0.90	<0.0001	Aminoacyl-tRNA biosynthesis; Valine, leucine and isoleucine biosynthesis; Valine, leucine and isoleucine degradation
Iso	Leu	0.87	<0.0001	Aminoacyl-tRNA biosynthesis, Valine, leucine and isoleucine biosynthesis; Valine, leucine and isoleucine degradation
Tau	NAD	0.57	<0.0001	-
Ala	Fum	0.48	<0.0001	Alanine, aspartate and glutamate metabolism
Val	1-MH	0.57	<0.0001	-
Iso	1-MH	0.58	<0.0001	-

Metabolite pair		*r*	*p*-value	Metabolic pathways
Leu	1-MH	0.60	<0.0001	-
Ala	1-MH	0.44	0.0001	-
Fum	1-MH	0.50	<0.0001	-
Val	Trp	0.45	<0.0001	Aminoacyl-tRNA biosynthesis
Iso	Trp	0.57	<0.0001	Aminoacyl-tRNA biosynthesis
Leu	Trp	0.53	<0.0001	Aminoacyl-tRNA biosynthesis
1MH	Trp	0.59	<0.0001	-
Ala	NM	0.44	0.0001	-
NAD	NM	-0.65	<0.0001	Nicotinate and nicotinamide metabolism
Fum	UDP-Glu/ UDP-Gal	0.55	<0.0001	-
PC(34:2)	PC(36:2)	0.69	<0.0001	Glycerophospholipid metabolism
Fum	PC(36:3)	0.43	0.0001	-
PC(34:2)	PC(36:3)	0.56	<0.0001	Glycerophospholipid metabolism
PC(36:2)	PC(36:3)	0.60	<0.0001	Glycerophospholipid metabolism
Tau	PC(38:7)	0.66	<0.0001	-
SM(d34:1)	PC(38:7)	0.53	<0.0001	-
Tau	PE(34:1)	-0.50	<0.0001	-
NM	PE(34:1)	0.50	<0.0001	-
PC(36:2)	PE(34:1)	0.50	<0.0001	Glycerophospholipid metabolism
Tau	PI(36:2)	-0.43	0.0001	-
NM	PI(36:2)	0.45	<0.0001	-
PC(34:2)	PI(36:2)	0.50	<0.0001	Glycerophospholipid metabolism
PC(36:2)	PI(36:2)	0.67	<0.0001	Glycerophospholipid metabolism
PC(36:3)	PI(36:2)	0.46	<0.0001	Glycerophospholipid metabolism
PE(34:1)	PI(36:2)	0.57	<0.0001	Glycerophospholipid metabolism
Fum	PE(36:3)	0.46	<0.0001	-
NM	PE(36:3)	0.44	<0.0001	-
UDP-Glu/ UDP-Gal	PE(36:3)	0.47	<0.0001	-
PC(34:2)	PE(36:3)	0.52	<0.0001	Glycerophospholipid metabolism
PC(36:2)	PE(36:3)	0.77	<0.0001	Glycerophospholipid metabolism
PC(36:3)	PE(36:3)	0.58	<0.0001	Glycerophospholipid metabolism
PE(34:1)	PE(36:3)	0.68	<0.0001	Glycerophospholipid metabolism
PI(36:2)	PE(36:3)	0.79	<0.0001	Glycerophospholipid metabolism
Ala	PI(36:1)	0.45	<0.0001	-
Tau	PI(36:1)	-0.50	<0.0001	-
PC(36:2)	PI(36:1)	0.45	<0.0001	Glycerophospholipid metabolism
PE(34:1)	PI(36:1)	0.68	<0.0001	Glycerophospholipid metabolism
PI(36:2)	PI(36:1)	0.82	<0.0001	Glycerophospholipid metabolism
PE(36:3)	PI(36:1)	0.66	<0.0001	Glycerophospholipid metabolism
Tau	PE(34:2)	-0.45	<0.0001	-
NAD	PE(34:2)	-0.45	<0.0001	-
NM	PE(34:2)	0.45	<0.0001	-
PC(34:2)	PE(34:2)	0.66	<0.0001	Glycerophospholipid metabolism

Metabolite pair		*r*	*p*-value	Metabolic pathways
PC(36:2)	PE(34:2)	0.75	<0.0001	Glycerophospholipid metabolism
PC(36:3)	PE(34:2)	0.44	0.0001	Glycerophospholipid metabolism
PE(34:1)	PE(34:2)	0.60	<0.0001	Glycerophospholipid metabolism
PI(36:2)	PE(34:2)	0.76	<0.0001	Glycerophospholipid metabolism
PE(36:3)	PE(34:2)	0.84	<0.0001	Glycerophospholipid metabolism
PI(36:1)	PE(34:2)	0.56	<0.0001	Glycerophospholipid metabolism
PC(36:2)	PE(36:1)	0.61	<0.0001	Glycerophospholipid metabolism
PE(34:1)	PE(36:1)	0.89	<0.0001	Glycerophospholipid metabolism
PI(36:2)	PE(36:1)	0.58	<0.0001	Glycerophospholipid metabolism
PE(36:3)	PE(36:1)	0.68	<0.0001	Glycerophospholipid metabolism
PI(36:1)	PE(36:1)	0.65	<0.0001	Glycerophospholipid metabolism
PE(34:2)	PE(36:1)	0.64	<0.0001	Glycerophospholipid metabolism
Tau	PE(P-40:7)	0.52	<0.0001	-
SM(d34:1)	PE(P-40:7)	0.65	<0.0001	Glycerophospholipid metabolism
PC(38:7)	PE(P-40:7)	0.78	<0.0001	Glycerophospholipid metabolism
Ala	PE(40:6)	0.46	<0.0001	-
Fum	PE(40:6)	0.45	<0.0001	-
UDP-Glu/UDP-Gal	PE(40:6)	0.49	<0.0001	-
PC(36:2)	PE(40:6)	0.66	<0.0001	Glycerophospholipid metabolism
PC(36:3)	PE(40:6)	0.50	<0.0001	Glycerophospholipid metabolism
PE(34:1)	PE(40:6)	0.55	<0.0001	Glycerophospholipid metabolism
PI(36:2)	PE(40:6)	0.54	<0.0001	Glycerophospholipid metabolism
PE(36:3)	PE(40:6)	0.68	<0.0001	Glycerophospholipid metabolism
PI(36:1)	PE(40:6)	0.54	<0.0001	Glycerophospholipid metabolism
PE(34:2)	PE(40:6)	0.69	<0.0001	Glycerophospholipid metabolism
PE(36:1)	PE(40:6)	0.69	<0.0001	Glycerophospholipid metabolism
SM(d34:1)	PE(P-38:5)	0.64	<0.0001	Glycerophospholipid metabolism
PC(38:7)	PE(P-38:5)	0.58	<0.0001	Glycerophospholipid metabolism
PE(P-40:7)	PE(P-38:5)	0.86	<0.0001	Glycerophospholipid metabolism
PE(34:1)	PI(34:1)	0.75	<0.0001	Glycerophospholipid metabolism
PI(36:2)	PI(34:1)	0.66	<0.0001	Glycerophospholipid metabolism
PE(36:3)	PI(34:1)	0.59	<0.0001	Glycerophospholipid metabolism
PI(36:1)	PI(34:1)	0.85	<0.0001	Glycerophospholipid metabolism
PE(36:1)	PI(34:1)	0.63	<0.0001	Glycerophospholipid metabolism
PE(40:6)	PI(34:1)	0.49	<0.0001	Glycerophospholipid metabolism
SM(d34:1)	SM(d42:1)	0.58	<0.0001	Glycerophospholipid metabolism
UDP-Glu/ UDP-Gal	PE(38:3)	0.46	<0.0001	-
PC(36:2)	PE(38:3)	0.66	<0.0001	Glycerophospholipid metabolism
PC(36:3)	PE(38:3)	0.60	<0.0001	Glycerophospholipid metabolism
PE(34:1)	PE(38:3)	0.60	<0.0001	Glycerophospholipid metabolism
PI(36:2)	PE(38:3)	0.60	<0.0001	Glycerophospholipid metabolism
PE(36:3)	PE(38:3)	0.84	<0.0001	Glycerophospholipid metabolism
PI(36:1)	PE(38:3)	0.56	<0.0001	Glycerophospholipid metabolism

Metabolite pair		*r*	*p*-value	Metabolic pathways
PE(34:2)	PE(38:3)	0.62	<0.0001	Glycerophospholipid metabolism
PE(36:1)	PE(38:3)	0.63	<0.0001	Glycerophospholipid metabolism
PE(40:6)	PE(38:3)	0.71	<0.0001	Glycerophospholipid metabolism
PI(34:1)	PE(38:3)	0.61	<0.0001	Glycerophospholipid metabolism
UDP-Glu/ UDP-Gal	PE(38:5)	0.50	<0.0001	-
PC(36:2)	PE(38:5)	0.71	<0.0001	Glycerophospholipid metabolism
PE(34:1)	PE(38:5)	0.77	<0.0001	Glycerophospholipid metabolism
PI(36:2)	PE(38:5)	0.52	<0.0001	Glycerophospholipid metabolism
PE(36:3)	PE(38:5)	0.79	<0.0001	Glycerophospholipid metabolism
PI(36:1)	PE(38:5)	0.48	<0.0001	Glycerophospholipid metabolism
PE(34:2)	PE(38:5)	0.66	<0.0001	Glycerophospholipid metabolism
PE(36:1)	PE(38:5)	0.82	<0.0001	Glycerophospholipid metabolism
PE(40:6)	PE(38:5)	0.67	<0.0001	Glycerophospholipid metabolism
PE(P-38:5)	PE(38:5)	0.44	0.0001	Glycerophospholipid metabolism
PI(34:1)	PE(38:5)	0.52	<0.0001	Glycerophospholipid metabolism
PE(38:3)	PE(38:5)	0.72	<0.0001	Glycerophospholipid metabolism
PC(34:2)	PC(34:3)	0.47	<0.0001	Glycerophospholipid metabolism
SM(d34:1)	PC(34:3)	0.66	<0.0001	Glycerophospholipid metabolism
PC(38:7)	PC(34:3)	0.70	<0.0001	Glycerophospholipid metabolism
PE(P-40:7)	PC(34:3)	0.59	<0.0001	Glycerophospholipid metabolism
PE(P-38:5)	PC(34:3)	0.52	<0.0001	Glycerophospholipid metabolism
PC(36:2)	PC(36:1)	0.71	<0.0001	Glycerophospholipid metabolism
PE(34:1)	PC(36:1)	0.62	<0.0001	Glycerophospholipid metabolism
PI(36:2)	PC(36:1)	0.48	<0.0001	Glycerophospholipid metabolism
PE(36:3)	PC(36:1)	0.58	<0.0001	Glycerophospholipid metabolism
PI(36:1)	PC(36:1)	0.52	<0.0001	Glycerophospholipid metabolism
PE(34:2)	PC(36:1)	0.56	<0.0001	Glycerophospholipid metabolism
PE(36:1)	PC(36:1)	0.80	<0.0001	Glycerophospholipid metabolism
PE(40:6)	PC(36:1)	0.75	<0.0001	Glycerophospholipid metabolism
PI(34:1)	PC(36:1)	0.47	<0.0001	Glycerophospholipid metabolism
PE(38:3)	PC(36:1)	0.54	<0.0001	Glycerophospholipid metabolism
PE(38:5)	PC(36:1)	0.67	<0.0001	Glycerophospholipid metabolism
Tau	PI(38:2)	-0.47	<0.0001	-
NM	PI(38:2)	0.46	<0.0001	-
UDP-Glu/ UDP-Gal	PI(38:2)	0.44	0.0001	-
PE(34:1)	PI(38:2)	0.68	<0.0001	Glycerophospholipid metabolism
PI(36:2)	PI(38:2)	0.74	<0.0001	Glycerophospholipid metabolism
PE(36:3)	PI(38:2)	0.72	<0.0001	Glycerophospholipid metabolism
PI(36:1)	PI(38:2)	0.81	<0.0001	Glycerophospholipid metabolism
PE(34:2)	PI(38:2)	0.54	<0.0001	Glycerophospholipid metabolism
PE(36:1)	PI(38:2)	0.56	<0.0001	Glycerophospholipid metabolism
PE(40:6)	PI(38:2)	0.46	<0.0001	Glycerophospholipid metabolism
PI(34:1)	PI(38:2)	0.77	<0.0001	Glycerophospholipid metabolism

Metabolite pair		*r*	*p*-value	Metabolic pathways
PE(38:3)	PI(38:2)	0.70	<0.0001	Glycerophospholipid metabolism
PE(38:5)	PI(38:2)	0.49	<0.0001	Glycerophospholipid metabolism
Leu	U	0.51	<0.0001	-
Ala	U	0.43	0.0001	-
Trp	U	0.53	<0.0001	-
Leu	Phe	0.45	<0.0001	Aminoacyl-tRNA biosynthesis
U	Phe	0.70	<0.0001	-
Fum	Hyp	0.43	0.0001	-
U	Hyp	0.72	<0.0001	-
Phe	Hyp	0.83	<0.0001	-
NM	Asp	0.46	<0.0001	Nicotinate and nicotinamide metabolism
PI(36:1)	Asp	0.54	<0.0001	-
PI(38:2)	Asp	0.42	0.0001	-
U	Asp	0.43	0.0001	Pantothenate and CoA biosynthesis; beta-Alanine metabolism
Asp	Pro	0.79	<0.0001	Aminoacyl-tRNA biosynthesis
Leu	MA	0.44	<0.0001	-
Ala	MA	0.56	<0.0001	-
U	MA	0.49	<0.0001	-
Phe	MA	0.51	<0.0001	-
Hyp	MA	0.45	<0.0001	-
Val	Urea	0.45	<0.0001	-
Leu	Urea	0.52	<0.0001	-
Ala	Urea	0.51	<0.0001	-
Fum	Urea	0.44	0.0001	Arginine biosynthesis
1-MH	Urea	0.43	0.0001	-
U	Urea	0.66	<0.0001	-
Phe	Urea	0.87	<0.0001	-
Hyp	Urea	0.74	<0.0001	Purine metabolism
Asp	Urea	0.46	<0.0001	Arginine biosynthesis
Pro	Urea	0.46	<0.0001	-
MA	Urea	0.59	<0.0001	-
Ala	Glu	0.49	<0.0001	Aminoacyl-tRNA biosynthesis; Alanine, aspartate and glutamate metabolism
Phe	Glu	0.63	<0.0001	Aminoacyl-tRNA biosynthesis
Hyp	Glu	0.63	<0.0001	Purine metabolism
MA	Glu	0.56	<0.0001	Glyoxylate and dicarboxylate metabolism
Urea	Glu	0.69	<0.0001	Arginine biosynthesis; Purine metabolism
Ala	Tyr	0.42	0.0001	Aminoacyl-tRNA biosynthesis
U	Tyr	0.62	<0.0001	-
Phe	Tyr	0.87	<0.0001	Aminoacyl-tRNA biosynthesis; Phenylalanine, tyrosine and tryptophan biosynthesis; Phenylalanine metabolism
Hyp	Tyr	0.74	<0.0001	-
MA	Tyr	0.57	<0.0001	-
Urea	Tyr	0.84	<0.0001	-

Metabolite pair		*r*	*p*-value	Metabolic pathways
Glu	Tyr	0.78	<0.0001	Aminoacyl-tRNA biosynthesis

Metabolite abbreviations: 1-MH, 1-methylhistidine; Ala, alanine; Asp, aspartic acid; Fum, fumaric acid; Glu, glutamine; Hyp, hypoxanthine; Iso, isoleucine; Leu, leucine; MA, malic acid; NM, niacinamide; PC, phosphatidylcholine; PE, phosphatidylethanolamine; PI, phosphatidylinositol. Phe, phenylalanine; Pro, proline; SM, sphingomyelin; Tau, taurine; Trp, tryptophan; Tyr, tyrosine; U, uracil; UDP-Glu/UDP-Gal, UDP-glucose/UDP-galactose; Val, valine.

Section 4.2 - New findings on urinary prostate cancer metabolome through combined GC–MS and ^{1}H NMR analytical platforms

---

Ana Rita Lima, Joana Pinto, Daniela Barros-Silva, Carmen Jerónimo, Rui Henrique, Maria de Lourdes Bastos, Márcia Carvalho, Paula Guedes de Pinho

The article (DOI: 10.1007/s11306-020-01691-1) presented in this chapter was published by Springer Nature, in *Metabolomics*, in 2020, and is here presented in the form of “Accepted Manuscript”. It is available online on:

https://link.springer.com/article/10.1007/s11306-020-01691-1

4.2.1 Abstract

Introduction: The inherent sensitivity of metabolomics allows the detection of subtle alterations in biological pathways, making it a powerful tool to study biomarkers and the mechanisms that underlie cancer.

Objectives: The purpose of this work was to characterize the urinary metabolic profile of prostate cancer (PCa) patients and cancer-free controls to obtain a holistic coverage of PCa metabolome.

Methods: Two groups of samples, a training set (*n* = 41 PCa and *n* = 42 controls) and an external validation set (*n* = 18 PCa and *n* = 18 controls) were analyzed using a dual analytical platform, namely gas chromatography-mass spectrometry (GC– MS) and proton nuclear magnetic resonance spectroscopy (^{1}H NMR).

Results: The multivariate analysis models revealed a good discrimination between cases and controls with an AUC higher than 0.8, a sensitivity ranging from 67 to 89%, a specificity ranging from 74 to 89% and an accuracy from 73 to 86%, considering the training and external validation sets. A total of 28 metabolites (15 from GC–MS and 13 from ^{1}H NMR) accounted for the separation. These discriminant metabolites are involved in 14 biochemical pathways, indicating that PCa is highly linked to dysregulation of metabolic pathways associated with amino acids and energetic metabolism.

Conclusion: These findings confirmed the complementary information provided by GC–MS and ^{1}H NMR, enabling a more comprehensive picture of the altered metabolites, underlying pathways and deepening the understanding of PCa development and progression.

Keywords:

Prostate cancer; Metabolome; Gas chromatography–mass spectrometry; Proton nuclear magnetic resonance spectroscopy; Urine; Biomarkers

4.2.2 Introduction

Metabolomics is a powerful technology which allows to define a metabolic snapshot that can be used for identifying novel biomarkers of numerous diseases (Lucarelli et al. 2015). Prostate cancer (PCa), represents an attractive model for metabolite profiling owing to the fact that, in addition to the metabolic features associated with cancer development and progression common to all malignancies (e.g., high glycolytic metabolism) (Warburg 1956), PCa cells lose their capacity to accumulate zinc, which in turn is assumed to inhibit the ability to accumulate citrate (Pértega-Gomes and Baltazar 2014). Since this feature is unique to neoplastic prostate cells, it may be hypothesized that metabolomic alterations result in a distinctive and specific metabolic signature of these cells.

Several metabolomic studies have been conducted to study the metabolome of urine from PCa patients, mainly through GC–MS (Bianchi et al. 2011; Jentzmik et al. 2010; Khan et al. 2013; Lima et al. 2019; Stabler et al. 2011; Struck-Lewicka et al. 2015; Wu et al. 2011), while studies performed through ^{1}H NMR are more scarce (MacKinnon et al. 2019; Pérez-Rambla et al. 2017; Zaragoza et al. 2014; Zheng et al. 2017), and none has combined these two analytical approaches for a more comprehensive analysis of the PCa metabolome. MS and ^{1}H NMR provide complementary information about different metabolites, so the integration of both techniques can be a major advantage to obtain a more holistic coverage of the metabolome (Aboud and Weiss 2013; Lindon et al. 2004). Previous metabolomic studies performed in urine from PCa patients have associated PCa with alterations in amino acids metabolism (Bianchi et al. 2011; Khan et al. 2013; Pérez-Rambla et al. 2017; Sreekumar et al., 2009; Stabler et al. 2011; Struck-Lewicka et al. 2015), mainly in glycine, serine and threonine metabolism (Bianchi et al. 2011; Khan et al. 2013; Sreekumar et al. 2009; Stabler et al. 2011). Beyond alteration in amino acid metabolism, PCa has been also associated with alterations in lipid (Struck-Lewicka et al. 2015; Zheng et al. 2017) and energetic (Struck-Lewicka et al. 2015; Wu et al. 2011) metabolisms.

In this study we sought to further explore the metabolic fingerprint of urine from PCa patients by applying a combination of GC–MS and ^{1}H NMR analytical platforms. In addition, biological interpretation of the observed metabolic changes was undertaken to better understand the metabolic reprogramming associated with PCa development.

4.2.3 Materials and methods

4.2.3.1 Chemicals

All chemicals were of analytical grade. l-(-)-arabitol (≥ 98%), gluconic acid (≥ 99%), d-glucose (≥ 99.5%), d-mannitol (≥ 98%), methanol (≥ 99.9%), methoxamine hydrochloride, *myo*-inositol (≥ 99%), *N,O*-bis(trimethylsilyl) trifluoroacetamide (BSTFA with 1% of trimethylchlorosilane), oxalic acid (≥ 99%), propylene glycol (≥ 98%), sarcosine (≥ 97%), sodium hydroxide (≥ 97%), l-(+)-threose (≥ 60%) and d-threitol (≥ 99%) were purchased from SigmaAldrich (Madrid, Spain). Deuterium oxide and deuterium oxide containing 0.05 wt% 3-(trimethylsilyl) propionic-2,2,3,3-d4 acid (TSP) sodium salt were supplied by Eurisotop (Saint-Aubin, France) and Sigma-Aldrich (Madrid, Spain), respectively.

4.2.3.2 Subjects

All urine samples were collected at the Portuguese Oncology Institute of Porto, centrifuged (3076×g, 20 min at 4 °C) and the supernatants were immediately frozen at − 80 °C until analysis. All 119 individuals (59 PCa patients and 60 cancer-free control subjects) enrolled in this study signed an informed consent. Detailed information on Gleason score and some important biochemical and clinical parameters of PCa patients and control subjects is provided in Supplementary Table 1. Both PCa and control samples were randomly divided into two groups, a training set, comprising 70% of all samples (41 PCa and 42 cancer-free controls), and an external set, corresponding to 30% of all samples (18 PCa and 18 cancer-free controls). This study was approved by the Ethics Committee of the Portuguese Oncology Institute of Porto (Reference 282R/2017).

4.2.3.3 Sample preparation

For GC–MS analysis, urine samples (200 µL) were prepared according to the protocol described by Chan et al. (2011). Quality controls (QCs) samples, consisting of a pool of all urine samples, were also analyzed by GC–MS on every eight samples under the same experimental conditions. For ^{1}H NMR analysis, 800 µL of urine from each sample were prepared according to the protocol described by Pinto et al. (2016). All samples were randomly prepared and analyzed.

4.2.3.4 GC–MS analysis

The GC–MS analysis was performed in an EVOQ-436 gas chromatograph, equipped with a CombiPAL automatic autosampler (Varian, Palo Alto, CA) and a Bruker Triple

Quadrupole mass detector. The injections were performed in split mode (ratio 1/5) and the acquisition conditions were previously described (Lima et al. 2018).

For metabolite identification, reference standards were used, whenever available. Alternatively, a putative identification was performed using the National Institute of Standards and Technology (NIST 14) database spectral library, and a comparison of the experimental and theoretical Kovats index.

4.2.3.5 ^{1}H NMR analysis

The ^{1}H NMR spectra were recorded on a Bruker Avance III HD 600 MHz spectrometer equipped with a cryoprobe, at 26.85 °C (300 K). An 1D ^{1}H NMR spectrum was acquired using a standard pulse sequence (noesypr1d) with 4 s relaxation delay, 100 ms mixing time, 128 transients, 64k complex data points, 10,080.646 Hz spectral width and 1.82 s acquisition time. Each free induction decay was multiplied by a 1.0 Hz exponential line-broadening function, manually phased and baseline corrected, and chemical shifts referenced internally to TSP at δ = 0.0 ppm. Peak assignments were carried out with basis on 2D NMR experiments (total correlation spectroscopy, TOCSY; and heteronuclear single quantum coherence, HSQC), literature (Diaz et al. 2013; Monteiro et al. 2016) and the Biological Magnetic Resonance Bank (Ulrich et al. 2008).

4.2.3.6 Data pre-processing

MZmine 2 (Pluskal et al. 2010) was used for pre-processing of GC–MS data. The parameters used were: RT range 4.4–26.0 min, m/z range 50–600, MS data noise level 1.0 × 105, m/z tolerance 0.2, chromatogram baseline level 1.0 × 104 and peak duration range 0.02–1.2 min. To refine the data, all RT-m/z pairs identified as contaminants and with a relative standard deviation higher than 30% in QCs samples, were removed from the matrix; ^{1}H NMR data preprocessing included the exclusion of water (δ 4.71–4.89) and urea (δ 5.66–5.99) signals, followed by alignment using the recursive segment-wise peak alignment method (Veselkov et al. 2009) (R 3.3.3 software).

In both approaches, the data were normalized by the total area of the chromatograms and, to remove uninformative variables and simplify the data, a variable selection method was applied (Xi et al. 2014). This variable selection was based in a univariate test (t test), and was performed using MetaboAnalyst (Chong et al. 2018). Consequently, all variables disclosing $p \geq 0.05$ were removed from the matrix. Finally, GC–MS and ^{1}H NMR data were scaled to pareto and unit variance (UV), respectively.

4.2.3.7 Statistical analysis

GC–MS and ^{1}H NMR data were used to perform multivariate (MVA) and univariate statistical treatments. MVA included unsupervised analysis (Principal Component Analysis [PCA]) and supervised analysis (Partial Least Squares Discriminant Analysis [PLS-DA]). To confirm that no overfitting was observed in PLS-DA models, a sevenfold cross validation and permutation test were performed (SIMCA-P 15, Umetrics, Sweden). For GC–MS and ^{1}H NMR data, receiver operating characteristic curves (ROC), area under the curve (AUC), sensitivity, specificity and accuracy were computed (MetaboAnalyst) (Chong et al. 2018) using both internal and external sets.

The univariate statistical analysis (GraphPad Prism 6, USA) was performed for all metabolites with Variable Importance to the Projection (VIP) greater than one. This analysis included: normality test (Shapiro–Wilk test); unpaired Student's t test with Welch correction test (normal distribution), or unpaired Mann–Whitney test (non-normal distribution); percentage of variation; effect size (Berben et al. 2012); and Bonferroni correction (Aickin and Gensler 1996). For all metabolites significantly altered, AUC, sensitivity, and specificity were calculated (Chong et al. 2018).

To better understand the biological relevance of the significantly altered metabolites, a metabolic enrichment analysis using the MetPa tool of Metaboanalyst was performed (Chong et al. 2018). Moreover, a correlation network analysis (Gephi 0.9.2, Bastian et al. 2009) of all significantly altered metabolites was carried out to search for possible correlations between metabolites.

Finally, the Spearman's rank correlation coefficient was computed between age and the set of metabolites found altered in PCa in order to discard age as a potential confounding factor. In addition, the possible influence of arterial hypertension (AH) and dyslipidemia in the urinary metabolic profile was also studied through PLS-DA using the control group (Supplementary Table 1).

4.2.4 Results and discussion

4.2.4.1 Urinary metabolic profile of PCa vs. control

In this study, a total of 193 metabolites were detected in urine of PCa patients and controls through the combination of GC–MS (yield: 151 metabolites) and ^{1}H NMR spectroscopy (yield: 52 metabolites, of which 10 were common to both analytical techniques) (Supplementary Fig. 1).

The projection of all samples (PCa, controls and QCs) in a PCA model revealed a good reproducibility of the GC–MS acquisition since a QCs clustering was observed in the scores scatter plot (Supplementary Fig. 2). Furthermore, PCA was also performed for both GC–MS and ^{1}H NMR data to detect trends and possible outliers among the samples. In GC–MS data, two outlier PCa urine samples were excluded from the model, whereas in ^{1}H NMR data, four PCa and one control urine samples were excluded (Supplementary Fig. 1). The PLS-DA models obtained for the training sets after variable selection (Fig. 4.4) showed a clear separation between PCa and control groups for both analytical strategies. In addition, permutation testing unveiled no overfitting of the GC–MS and ^{1}H NMR data (Supplementary Fig. 4). For GC–MS model, an AUC of 0.840, a sensitivity of 73%, a specificity of 74% and an accuracy of 73% (Fig. 4.4) was obtained, whereas the ^{1}H NMR model showed an AUC of 0.874, a sensitivity of 78%, a specificity of 83% and an accuracy of 81% (Fig. 4.4) (internal validation). Furthermore, considering the external validation set, 16 PCa and 15 control urine samples (from a total of 18 samples per group) were correctly classified by the GC–MS approach, while 12 PCa and 16 controls were correctly classified by the ^{1}H NMR model. Therefore, taking into consideration the external sets, the GC–MS model showed an AUC of 0.960, a sensitivity of 89%, a specificity of 83% and an accuracy of 86%, and the ^{1}H NMR model unveiled an AUC of 0.824, a sensitivity of 67%, a specificity of 89% and an accuracy of 78% (Fig. 4.4 and Supplementary Table 2). However, the small sample size, in the validation set, may lead to bias in statistical power and precision.

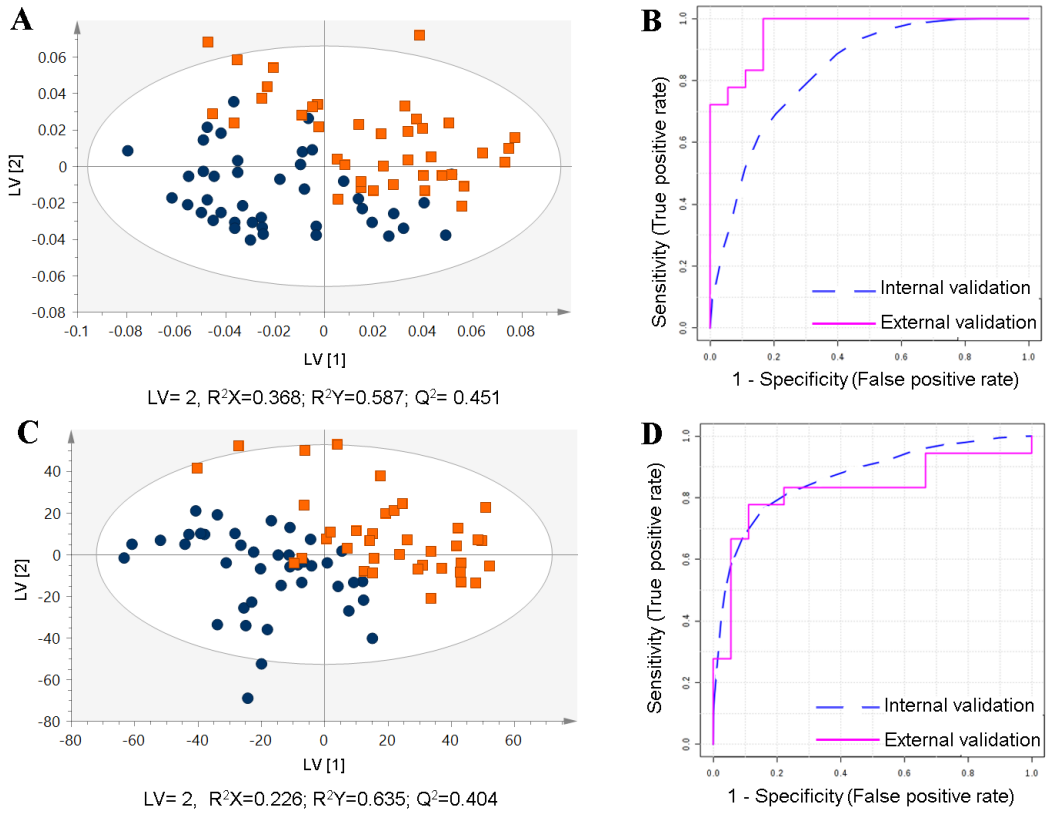

Figure 4.4: A: PLS-DA scores scatter plot (Pareto scaling; two components) obtained for the GC–MS metabolic profle of urine of PCa patients (orange squares) *vs.* cancer-free controls (blue circles) (training model), after variable selection; **B:** Assessment of the diagnostic performance of the PLS-DA model obtained for GC–MS using the training set (AUC = 0.840, sensitivity = 73%, specifcity = 74%, accuracy = 73%) and the external set (AUC = 0.960, sensitivity = 89%, specifcity = 83%, accuracy = 86%) through ROC analysis; **C:** PLS-DA scores scatter plot (UV scaling; 2 components) obtained for the ^{1}H NMR metabolic profle of urine of PCa patients (orange squares) *vs*. cancer-free controls (blue circles) (training model), after variable selection; **D:** Assessment of the diagnostic performance of the PLS-DA model obtained for ^{1}H NMR using the training set (AUC = 0.874, sensitivity = 78%, specifcity = 83%, accuracy = 81%) and the external set (AUC = 0.824, sensitivity = 67%, specificity = 89%, accuracy = 78%) through ROC analysis.

Since a statistically significant difference (*p*-value ≤ 0.001) in age was observed between PCa (64.3 ± 6.1 years for GC–MS and 63.1 ± 5.3 years for ^{1}H NMR) and controls (59.2 ± 2.6 years for GC–MS and 58.81 ± 2.7 years for ^{1}H NMR), its potential contribution as a confounding factor in the set of metabolites found altered between PCa and controls was evaluated, but no statistically relevant correlations were found (|r|≤ 0.38, p > 0.001) (Supplementary Table 3). The impact of AH and dyslipidemia on urine metabolic profile was also evaluated in the control group, revealing no predictive power (Q^2 = 0.137 and Q^2 =

0.011 for GC–MS and ^{1}H NMR, respectively) in the PLS-DA models (Supplementary Fig. 5), so AH and dyslipidemia were not confounding factors.

For the GC–MS approach, 34 metabolites showed a VIP > 1; among them, 15 were found significantly different between the two groups under study (PCa *vs*. control) (Table 4.3, Supplementary Table 4). For the ^{1}H NMR approach, 19 metabolites disclosed a VIP > 1, from which 13 were significantly different between PCa and control groups (Table 4.3, Supplementary Table 5). These discriminant metabolites included four amino acids, six organic acids, eight sugars, two ketones, one alkaloid and seven unidentified compounds (Table 4.3, Supplementary Tables 4 and 5).

Among the metabolites significantly altered in PCa, we highlight sarcosine, which was previously reported as a non-invasive biomarker for PCa diagnosis and progression (Sreekumar et al. 2009). As matter of fact, our results confirmed the results of Sreekumar et al. (2009), since in that study sarcosine showed an AUC of 0.67 in urine supernatants and a similar AUC value (0.65) was found in our study (Table 4.3) (Sreekumar et al. 2009).

Table 4.3: List of metabolites significantly altered in urine from PCa patients compared to controls by GC-MS and ^{1}H NMR spectroscopy.

Name	*p*-value	Variation ± uncertainty (%)	Effect size ± ES_{SE}	AUC	Sens	Spec	Analytical platform
Amino acids-derivatives							
2-Furoyl-glycine [L2]	0.0009	↓ 44.02 ± 16.00	↓ 0.78 ± 0.46	0.74	0.85	0.62	^{1}H NMR
Leucine [L2]	0.0048	↑ 9.73 ± 3.80	↑ 0.57 ± 0.45	0.68	0.80	0.55	^{1}H NMR
Sarcosine [L1]	0.0167	↑ 48.18 ± 14.46	↑ 0.60 ± 0.44	0.65	0.68	0.60	GC-MS
Valine [L2]	0.0336	↑ 11.47 ± 5.07	↑ 0.51 ± 0.45	0.67	0.80	0.54	^{1}H NMR
Organic acids/alcohol							
2-Hydroxy-isobutyrate [L2]	0.0034	↑ 12.66 ± 3.94	↑ 0.69 ± 0.46	0.67	0.80	0.55	^{1}H NMR
2-Hydroxy-valerate [L2]	<0.0001[B]	↑ 15.64 ± 3.62	↑ 0.93 ± 0.47	0.76	0.86	0.61	^{1}H NMR
Gluconate [L1]	0.0103	↓ 18.33 ± 8.20	↓ 0.55 ± 0.44	0.66	0.50	0.79	GC-MS
Oxalate [L1]	0.0137	↑ 50.02 ± 14.45	↑ 0.62 ± 0.44	0.65	0.73	0.55	GC-MS

Name	*p*-value	Variation ± uncertainty (%)	Effect size ± ES_{SE}	AUC	Sens	Spec	Analytical platform
Pyruvate [L2]	0.0233	↑ 30.71 ± 10.64	↑ 0.58 ± 0.45	0.65	0.77	0.51	^{1}H NMR
Propylene glycol [L1]	0.0218	↑ 299.2 ± 57.35	↑ 0.48 ± 0.44	0.65	0.50	0.79	GC-MS
Sugars							
D-Glucose [L1]	0.0023	↓ 28.97 ± 10.39	↓ 0.72 ± 0.45	0.69	0.70	0.69	GC-MS
D-Mannitol [L1]	0.0027	↓ 33.81 ± 14.29	↓ 0.62 ± 0.44	0.69	0.78	0.60	GC-MS
D-Threitol [L1]	0.0120	↑ 40.25 ± 16.85	↑ 0.48 ± 0.44	0.66	0.70	0.62	GC-MS
L-Arabitol [L1]	0.0173	↓ 27.59 ± 11.59	↓ 0.61 ± 0.44	0.65	0.68	0.57	GC-MS
L-Fucitol [L2]	0.0037	↓ 15.56 ± 12.19	↓ 0.65 ± 0.44	0.69	0.63	0.67	GC-MS
L-Threose [L1]	0.0169	↑ 17.10 ± 6.86	↑ 0.51 ± 0.44	0.65	0.70	0.67	GC-MS
Myo-inositol [L1]	0.0091	↓ 15.44 ± 10.51	↓ 0.55 ± 0.44	0.67	0.63	0.76	GC-MS
Ribitol [L2]	0.0202	↓ 27.30 ± 13.44	↓ 0.51 ± 0.44	0.65	0.65	0.64	GC-MS
Ketones							
Acetone [L2]	0.0066	↑ 11.38 ± 3.87	↑ 0.63 ± 0.46	0.68	0.79	0.55	^{1}H NMR
Hydroxy-acetone [L2]	0.0420	↑ 17.52 ± 8.07	↑ 0.53 ± 0.45	0.64	0.76	0.51	^{1}H NMR
Alkaloid							
Trigonelline [L2]	0.0344	↓ 23.75 ± 12.42	↓ 0.49 ± 0.45	0.63	0.76	0.50	^{1}H NMR
Unknowns							
Unknown 1 [L4]	0.0370	↓ 23.11 ± 12.37	↓ 0.47 ± 0.44	0.63	0.63	0.60	GC-MS
Unknown 2 [L4]	0.0392	↑ 22.98 ± 9.10	↑ 0.50 ± 0.44	0.64	0.60	0.60	GC-MS
Unknown 3 [L4]	0.0004[B]	↓ 34.25 ± 13.71	↓ 0.69 ± 0.45	0.73	0.74	0.80	GC-MS
Unknown 4 [L4]	0.0006[B]	↑ 16.36 ± 4.46	↑ 0.78 ± 0.46	0.73	0.83	0.61	^{1}H NMR
Unknown 5 [L4]	0.0094	↑ 14.175 ± 5.26	↑ 0.58 ± 0.45	0.67	0.79	0.56	^{1}H NMR
Unknown 6 [L4]	0.0011	↓ 49.49 ± 19.05	↓ 0.75 ± 0.46	0.72	0.83	0.60	^{1}H NMR

Name	*p*-value	Variation ± uncertainty (%)	Effect size ± ES_{SE}	AUC	Sens	Spec	Analytical platform
Unknown 7 [L4]	0.0392	↓ 45.40 ± 17.75	↓ 0.72 ± 0.46	0.73	0.83	0.62	^{1}H NMR

[L1]: Identified metabolites (GC-MS applied to the analysis of both the metabolite of interest and a chemical reference standard of suspected structural equivalence, with all analyses performed under identical analytical conditions within the same laboratory) (Viant et al., 2017); [L2]: Putatively annotated compounds (similarity with databases) (Viant et al., 2017); [L4]: Unidentified (Viant et al., 2017); B: Alterations remaining significant after Bonferroni correction, with cut-off *p*-value of 0.0015 (0.05 divided by 34 tested metabolites) for GC-MS data, and cut-off *p*-value of 0.0003 (0.05 divided by 19 analyzed metabolites) for ^{1}H NMR; NA: Not available

Besides sarcosine, seven other compounds found altered in PCa urines in this study were also previously associated with PCa in other metabolomic studies, namely the significant increases in valine (Pérez-Rambla et al. 2017), leucine (Pérez-Rambla et al. 2017) and pyruvate (Kumar et al. 2015) levels and the significant decreases in arabitol (Struck-Lewicka et al. 2015), *myo*-inositol (Stenman et al. 2011), gluconate (Jung et al. 2013) and glucose (Vaz et al. 2012) levels. Importantly, to the best of our knowledge, this study is the first to report significant increased levels of 2-hydroxyisobutyrate, 2-hydroxyvalerate, oxalate, propylene glycol, d-threitol, l-threose, acetone and hydroxyacetone, as well as significant decreased levels of 2-furoylglycine, mannitol, l-fucitol, ribitol and trigonelline in urine of PCa patients.

4.2.4.2 Biological interpretation

Using the MetPA tool (Chong et al. 2018), 14 metabolic pathways were found significantly altered ($p < 0.05$) in PCa (Fig. 4.5), namely valine, leucine and isoleucine synthesis and degradation; pentose phosphate pathway; glycine, serine and threonine metabolism; pentose and glucuronate interconversions; pantothenate and CoA biosynthesis; glycolysis or gluconeogenesis; pyruvate metabolism; propanoate metabolism; galactose metabolism; nicotinate and nicotinamide metabolism; ascorbate and aldarate metabolism; synthesis and degradation of ketone bodies; and glyoxylate and dicarboxylate metabolism. The most significantly altered metabolic pathways were those associated with amino acids metabolism, although most of the dysregulated pathways were involved in energy metabolism. Dysregulations of energetic metabolism are expected since cancer cells have a greater need for energy to sustain high cell proliferation levels (Pértega-Gomes and Baltazar 2014). It is now recognized that cancer cells upregulate the glycolytic pathway, even in the presence of oxygen, to produce energy (the so called “Warburg effect”) (Warburg 1956). Moreover, it has been demonstrated that glucose-6-phosphate dehydrogenase (G6PD), a key enzyme in energetic metabolism (pentose phosphate

pathway), is upregulated in PCa cells (Tsouko et al. 2014), promoted by androgen receptor (AR) signaling. AR signaling also upregulates glycolysis and glucose transporters (GLUT), subsequently increasing glucose uptake (Fraga et al. 2015; Gonzalez-Menendez et al. 2018). GLUT also has an important role in tumor progression and regulation of cell death (Fraga et al. 2015; Gonzalez-Menendez et al. 2018), highlighting the close relationship alteration in energetic metabolism and PCa development and progression (Tsouko et al. 2014).

On the other hand, amino acids also play an important role in metabolism of glucose, lipids, and protein synthesis, which are essential for cell division and, consequently, cancer progression (Pérez-Rambla et al. 2017). In addition, branched-chain amino acids (leucine, valine and isoleucine) can activate mammalian target of rapamycin (mTOR), which is an important regulator of cell growth, proliferation and migration (Pópulo et al. 2012).

To better understand the metabolic alterations associated with PCa, a correlation network was computed using the set of significantly altered metabolites (Fig. 4.6). Three main clusters were identified, namely: Cluster A, linking most of the metabolites found significantly decreased in PCa and reflecting mainly alterations in sugar metabolism; Cluster B, connecting pyruvate, oxalate, sarcosine and two unidentified compounds, which may be attributed to the alterations in glycine, serine and threonine metabolism, and glyoxylate and dicarboxylate metabolism; and Cluster C, linking valine, leucine, acetone, 2-hydroxyvalerate and 2-hydroxyisobutyrate, which may reflect the alteration in the biosynthesis and degradation of valine, leucine and isoleucine and in propanoate metabolism.

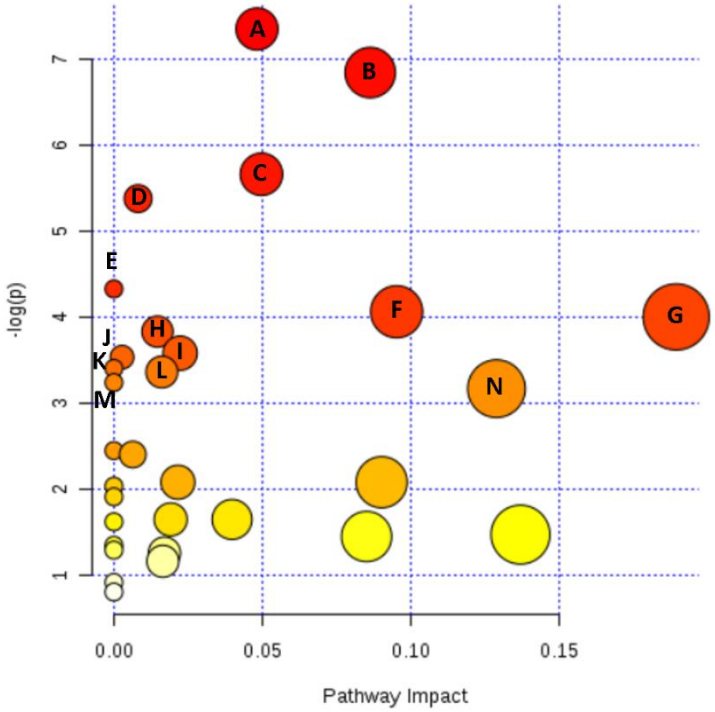

Figure 4.5: Metabolic pathway analysis of the set of metabolites found statistically different between PCa and controls. Pathway topology analysis depicting dysregulated metabolic pathways in PCa patients. The X-axis represents the pathway impact values, and the Y-axis indicates the -log of *p*-values from the pathway enrichment analysis. The node colors represent the *p*-values and the node radius indicate the pathway impact values. *(***A:** Valine, leucine and isoleucine biosynthesis (pyruvate, leucine and valine) *(p* = 0.0006*);* **B***:* Pentose phosphate pathway (gluconic acid, d-glucose and pyruvate) (*p* = 0.0011); **C:** Glycine, serine and threonine metabolism (sarcosine, pyruvate and hydroxyacetone) (*p* = *0.0035*); **D:** Pentose and glucuronate interconversions (l-arabitol, ribitol and pyruvate) (*p* = 0.0046); **E:** Pantothenate and CoA biosynthesis (pyruvate and valine) (*p* = 0.0132); **F:** Glycolysis or gluconeogenesis (pyruvate and glucose) (*p* = 0.0172); **G:** Pyruvate metabolism (pyruvate and propylene glycol) (*p* = 0.0183); **H:** Propanoate metabolism (valine and acetone) (*p* = 0.0217); **I:** Valine, leucine and isoleucine degradation (leucine and valine) (*p* = 0.0279); **J:** Galactose metabolism (d-glucose and *myo*-inositol) (*p* = 0.0292); **K:** Nicotinate and nicotinamide metabolism (pyruvate and trigonelline) (*p* = 0.0333); **L:** Ascorbate and aldarate metabolism (pyruvate and *myo*-inositol) (*p* = 0.0347); **M:** Synthesis and degradation of ketone bodies (acetone) (*p* = 0.0393); **N:** Glyoxylate and dicarboxylate metabolism (oxalate and pyruvate) (*p* = 0.0422)).

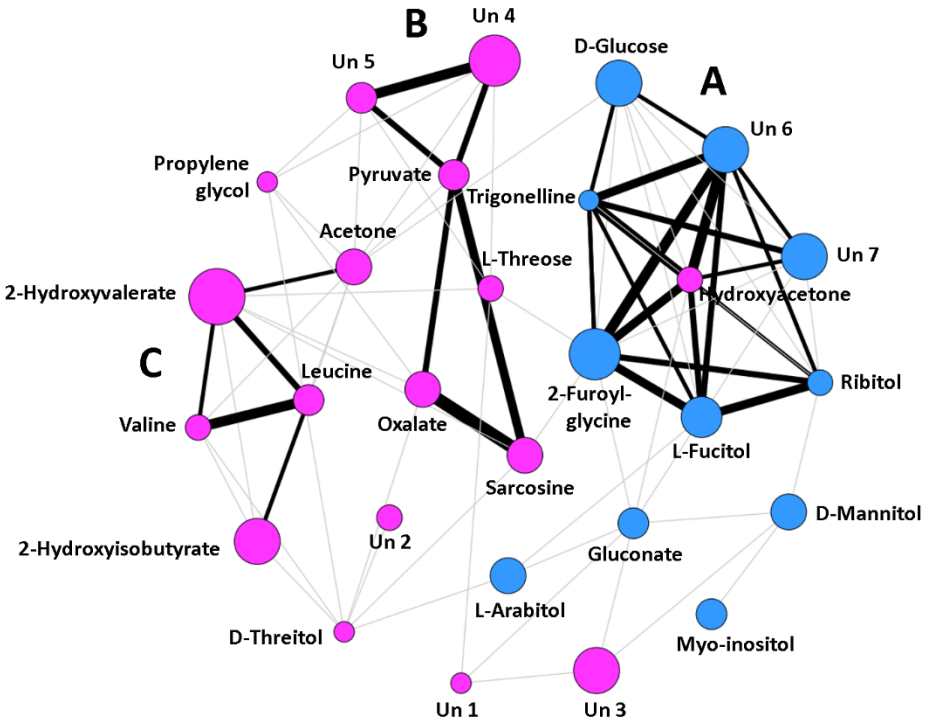

Figure 4.6: Correlation network of all significantly altered metabolites found in urine from PCa patients compared with controls, unveiling three main clusters **(A-C)** of metabolite correlations. Node colors indicate variation direction (pink for metabolites significantly increased and blue for metabolites significantly decreased in PCa) and node size reflects the effect size of variation in PCa compared with controls. Only relevant ($p < 0.01$) positive correlations were found, and grey and black lines correspond to $r < 0.5$ and $r \geq 0.5$, respectively. Line thickness represents correlation coefficient magnitude with thicker lines reflecting stronger correlations.

4.2.5 Conclusions

Metabolic reprogramming of cancer cells is essential to support tumor survival and progression. As a consequence, metabolic pathways altered in cancer have attracted increasing attention as potential targets for therapeutic exploitation. The combined GC–MS and ^{1}H NMR metabolomics approach used in the present study provided a more holistic understanding of the metabolic pathways associated with PCa development and progression. Significant alterations in the levels of 21 metabolites were found in urine of PCa patients, of which 13 were reported for the first time as associated with PCa disease (namely, 2-hydroxyisobutyrate, 2-hydroxyvalerate, oxalate, propylene glycol, d-threitol, l-threose, acetone, hydroxyacetone, 2-furoylglycine, mannitol, l-fucitol, ribitol and trigonelline) and 8 corroborated previously reported studies (sarcosine, valine, leucine, pyruvate,

arabitol, *myo*-inositol, gluconate and glucose). The majority of the significantly altered metabolites was associated with dysregulations in 14 metabolic pathways mainly related to valine, leucine and isoleucine biosynthesis; pentose phosphate pathway; and glycine, serine and threonine metabolism, which denotes that PCa development and progression is deeply connected to alterations in amino acids and energetic metabolism of cancer cells. This work highlights the complementarity between GC–MS and ^{1}H NMR analytical techniques, thus allowing the definition of a more comprehensive picture of the dysregulated metabolic pathways associated with PCa and deepening the understanding of PCa development and progression. Further studies based on a larger cohort of patients are needed to validate these promising results.

4.2.6 References

Aboud, O. A., & Weiss, R. H. (2013). New opportunities from the cancer metabolome. Clinical Chemistry, 59, 138–146.

Aickin, M., & Gensler, H. (1996). Adjusting for multiple testing when reporting research results: The Bonferroni vs Holm methods. American Journal of Public Health, 86, 726–728.

Bastian, M., Heymann, S., & Jacomy, M. (2009). Gephi: An open source software for exploring and manipulating networks. ICWSM, 8, 361–362.

Berben, L., Sereika, S. M., & Engberg, S. (2012). Effect size estimation: Methods and examples. International Journal of Nursing Studies, 49, 1039–1047.

Bianchi, F., Dugheri, S., Musci, M., Bonacchi, A., Salvadori, E., Arcangeli, G., et al. (2011). Fully automated solid-phase microextraction–fast gas chromatography–mass spectrometry method using a new ionic liquid column for high-throughput analysis of sarcosine and N-ethylglycine in human urine and urinary sediments. Analytica Chimica Acta, 707, 197–203.

Chan, E. C. Y., Pasikanti, K. K., & Nicholson, J. K. (2011). Global urinary metabolic profiling procedures using gas chromatography–mass spectrometry. Nature Protocols, 6, 1483.

Chong, J., Soufan, O., Li, C., Caraus, I., Li, S., Bourque, G., et al. (2018). MetaboAnalyst 4.0: Towards more transparent and integrative metabolomics analysis. Nucleic Acids Research, 46, W486–W494.

Diaz, S. O., Barros, A. S., Goodfellow, B. J., Duarte, I. F., Carreira, I. M., Galhano, E., et al. (2013). Following healthy pregnancy by nuclear magnetic resonance (NMR) metabolic profiling of human urine. Journal of Proteome Research, 12, 969–979.

Fraga, A., Ribeiro, R., Principe, P., Lopes, C., & Medeiros, R. (2015). Hypoxia and prostate cancer aggressiveness: A tale with many endings. Clinical Genitourinary Cancer, 13, 295–301.

Gonzalez-Menendez, P., Hevia, D., Mayo, J. C., & Sainz, R. M. (2018). The dark side of glucose transporters in prostate cancer: Are they a new feature to characterize carcinomas? International Journal of Cancer, 142, 2414–2424.

Jentzmik, F., Stephan, C., Miller, K., Schrader, M., Erbersdobler, A., Kristiansen, G., et al. (2010). Sarcosine in urine after digital rectal examination fails as a marker in prostate cancer detection and identification of aggressive tumours. European Urology, 58, 12–18.

Jung, K., Reszka, R., Kamlage, B., Bethan, B., Stephan, C., Lein, M., et al. (2013). Tissue metabolite profiling identifies differentiating and prognostic biomarkers for prostate carcinoma. International Journal of Cancer, 133, 2914–2924.

Khan, A. P., Rajendiran, T. M., Ateeq, B., Asangani, I. A., Athanikar, J. N., Yocum, A. K., et al. (2013). The role of sarcosine metabolism in prostate cancer progression. Neoplasia (New York, NY), 15, 491–501.

Kumar, D., Gupta, A., Mandhani, A., & Sankhwar, S. N. (2015). Metabolomics-derived prostate cancer biomarkers: Fact or fiction? Journal of Proteome Research, 14, 1455–1464.

Lima, A. R., Araujo, A. M., Pinto, J., Jeronimo, C., Henrique, R., Bastos, M. L., et al. (2018). GC-MS-based endometabolome analysis differentiates prostate cancer from normal prostate cells. Metabolites, 8, 23.

Lima, A. R., Pinto, J., Azevedo, A. I., Barros-Silva, D., Jeronimo, C., Henrique, R., et al. (2019). Identification of a biomarker panel for improvement of prostate cancer diagnosis by volatile metabolic profiling of urine. British Journal of Cancer, 121(10), 857–868.

Lindon, J. C., Holmes, E., Bollard, M. E., Stanley, E. G., & Nicholson, J. K. (2004). Metabonomics technologies and their applications in physiological monitoring, drug safety assessment and disease diagnosis. Biomarkers, 9, 1–31.

Lucarelli, G., Rutigliano, M., Galleggiante, V., Giglio, A., Palazzo, S., Ferro, M., et al. (2015). Metabolomic profiling for the identification of novel diagnostic markers in prostate cancer. Expert Review of Molecular Diagnostics, 15, 1211–1224.

MacKinnon, N., Ge, W., Han, P., Siddiqui, J., Wei, J. T., Raghunathan, T., et al. (2019). NMR-based metabolomic profiling of urine: Evaluation for application in prostate cancer detection. Natural Product Communications. https ://doi.org/10.1177/19345 78X19 84997 8.

Monteiro, M. S., Barros, A. S., Pinto, J., Carvalho, M., Pires-Luís, A. S., Henrique, R., et al. (2016). Nuclear magnetic resonance metabolomics reveals an excretory metabolic signature of renal cell carcinoma. Scientific Reports, 6, 37275–37275.

Pérez-Rambla, C., Puchades-Carrasco, L., García-Flores, M., RubioBriones, J., López-Guerrero, J. A., & Pineda-Lucena, A. (2017). Non-invasive urinary metabolomic profiling discriminates prostate cancer from benign prostatic hyperplasia. Metabolomics, 13, 52.

Pértega-Gomes, N., & Baltazar, F. (2014). lactate transporters in the context of prostate cancer metabolism: What do we know? International Journal of Molecular Sciences, 15, 18333–18348.

Pinto, J., Diaz, S. O., Aguiar, E., Duarte, D., Barros, A. S., Galhano, E., et al. (2016). Metabolic profiling of maternal urine can aid clinical management of gestational diabetes mellitus. Metabolomics, 12, 105.

Pluskal, T., Castillo, S., Villar-Briones, A., & Oresic, M. (2010). MZmine 2: Modular framework for processing, visualizing, and analyzing mass spectrometry-based molecular profile data. BMC Bioinformatics, 11, 395.

Pópulo, H., Lopes, J. M., & Soares, P. (2012). The mTOR signalling pathway in human cancer. International Journal of Molecular Sciences, 13, 1886–1918.

Sreekumar, A., Poisson, L. M., Rajendiran, T. M., Khan, A. P., Cao, Q., Yu, J., et al. (2009). Metabolomic profiles delineate potential role for sarcosine in prostate cancer progression. Nature, 457, 910–914.

Stabler, S., Koyama, T., Zhao, Z., Martinez-Ferrer, M., Allen, R. H., Luka, Z., et al. (2011). Serum methionine metabolites are risk factors for metastatic prostate cancer progression. PLoS ONE, 6, e22486.

Stenman, K., Stattin, P., Stenlund, H., Riklund, K., Gröbner, G., & Bergh, A. (2011). H HRMAS NMR derived bio-markers related to tumor grade, tumor cell fraction, and cell proliferation in prostate tissue samples. Biomarker Insights, 6, 39–47.

Struck-Lewicka, W., Kordalewska, M., Bujak, R., Yumba Mpanga, A., Markuszewski, M., Jacyna, J., et al. (2015). Urine metabolic fingerprinting using LC–MS and GC–MS reveals metabolite changes in prostate cancer: A pilot study. Journal of Pharmaceutical and Biomedical Analysis, 111, 351–361.

Tsouko, E., Khan, A. S., White, M. A., Han, J. J., Shi, Y., Merchant, F. A., et al. (2014). Regulation of the pentose phosphate pathway by an androgen receptor-mTOR-mediated mechanism and its role in prostate cancer cell growth. Oncogenesis, 3, e103.

Ulrich, E. L., Akutsu, H., Doreleijers, J. F., Harano, Y., Ioannidis, Y. E., Lin, J., et al. (2008). BioMagResBank. Nucleic Acids Research, 36, D402–D408.

Vaz, C. V., Alves, M. G., Marques, R., Moreira, P. I., Oliveira, P. F., Maia, C. J., et al. (2012). Androgen-responsive and nonresponsive prostate cancer cells present a distinct glycolytic metabolism profile. International Journal of Biochemistry & Cell Biology, 44, 2077–2084.

Veselkov, K. A., Lindon, J. C., Ebbels, T. M. D., Crockford, D., Volynkin, V. V., Holmes, E., et al. (2009). Recursive segmentwise peak alignment of biological 1H NMR spectra for improved metabolic biomarker recovery. Analytical Chemistry, 81, 56–66.

Viant, M. R., Kurland, I. J., Jones, M. R., & Dunn, W. B. (2017). How close are we to complete annotation of metabolomes? Current Opinion in Chemical Biology, 36, 64–69.

Warburg, O. (1956). On the origin of cancer cells. Science, 123, 309–314.

Wu, H., Liu, T., Ma, C., Xue, R., Deng, C., Zeng, H., et al. (2011). GC/ MS-based metabolomic approach to validate the role of urinary sarcosine and target biomarkers for human prostate cancer by microwave-assisted derivatization. Analytical and Bioanalytical Chemistry, 401, 635–646.

Xi, B., Gu, H., Baniasadi, H., & Raftery, D. (2014). Statistical analysis and modeling of mass spectrometry-based metabolomics data. Methods in Molecular Biology, 1198, 333–353.

Zaragoza, P., Ruiz-Cerda, J. L., Quintas, G., Gil, S., Costero, A. M., Leon, Z., et al. (2014). Towards the potential use of (1)H NMR spectroscopy in urine samples for prostate cancer detection. Analyst, 139, 3875–3878.

Zheng, H., Cai, A., Zhou, Q., Xu, P., Zhao, L., Li, C., et al. (2017). Optimal preprocessing of serum and urine metabolomic data fusion for staging prostate cancer through design of experiment. Analytica Chimica Acta, 991, 68–75.

4.2.7 Supporting information

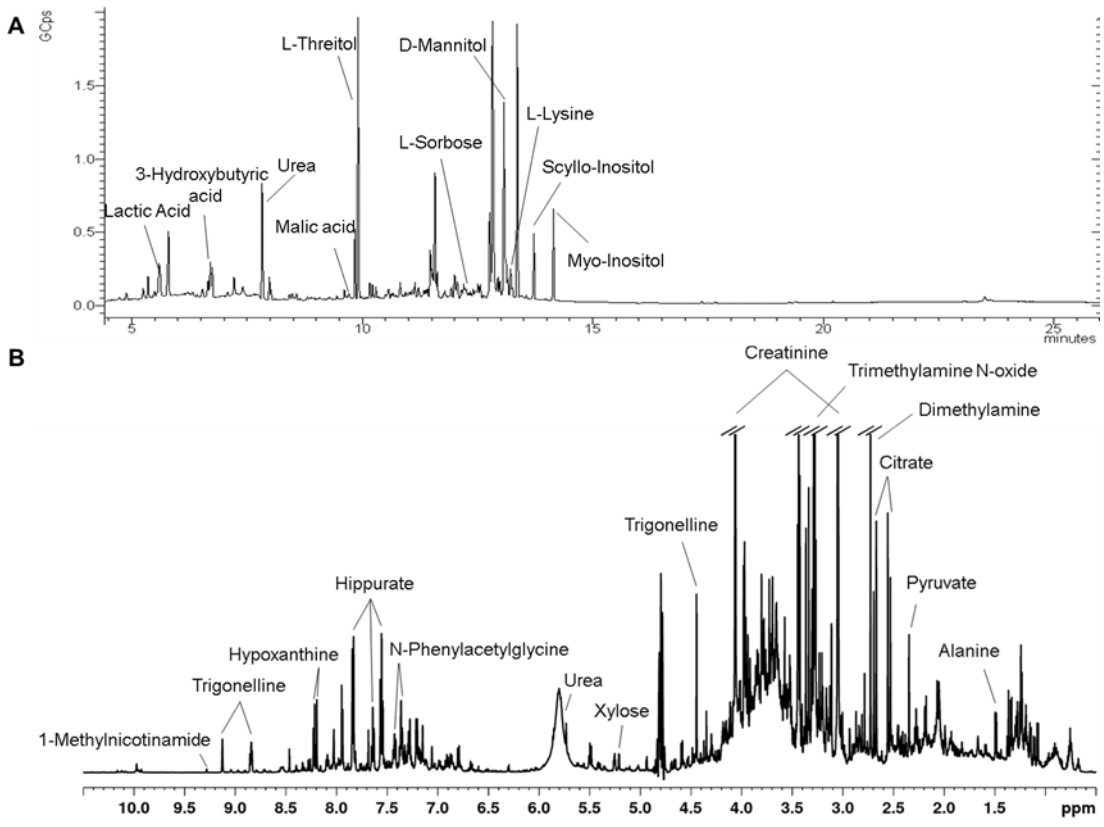

Supplementary Figure 1: Representative (A) GC-MS chromatogram and (B) ^{1}H NMR spectrum of a urine sample from a control individual.

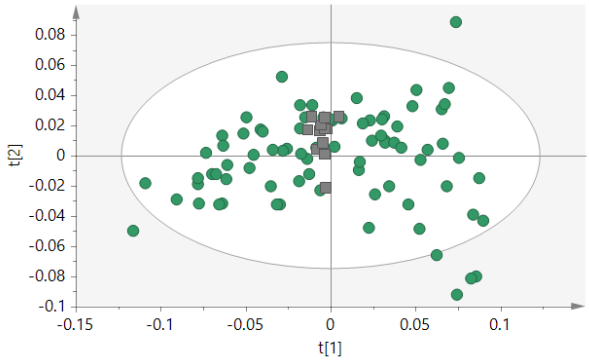

Supplementary Figure 2: PCA scores scatter plot (Pareto scaling; 2 components) obtained for the GC-MS chromatograms of all samples (control and PCa) (green circles) and QCs (grey squares) (R^2X=0.415). QCs are grouped together, thus proving the reproducibility of the analytical technique.

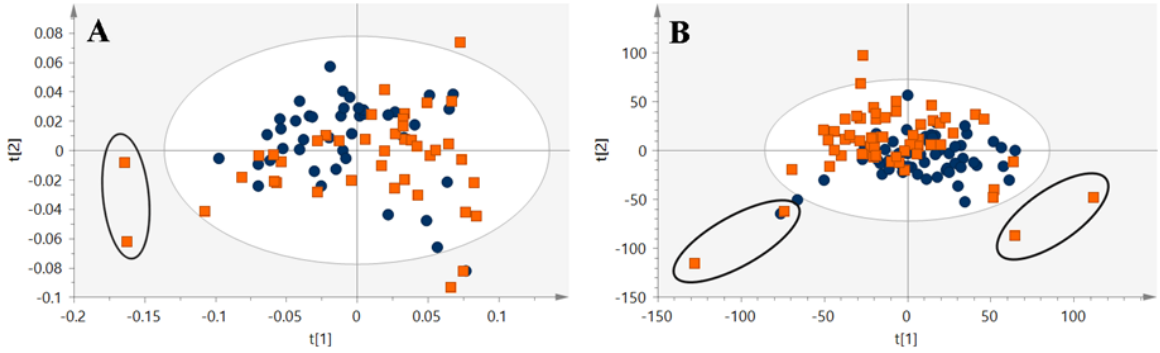

Supplementary Figure 3: PCA scores scatter plot obtained for (A) the GC-MS data (Pareto scaling; 2 components) (R^2X=0.444), and (B) ^{1}H NMR data (UV scaling; 2 components) (R^2X=0.293) of PCa samples (orange squares) and controls (blue circles). The circumvent samples were considered outliers.

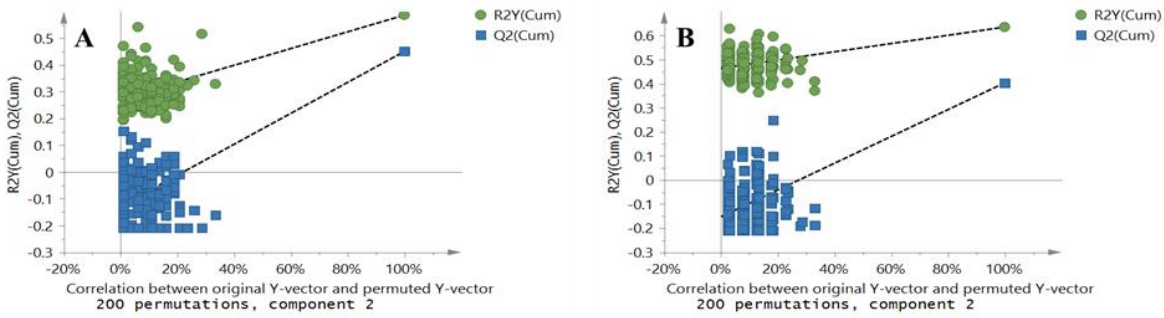

Supplementary Figure 4: Statistical validation of the PLS-DA models by permutation testing (200 permutations; 2 components). (A) GC-MS model (Intercepts: R^2= (0.0, 0.269), Q^2= (0.0, -0.132). (B) ^{1}H NMR model (Intercepts: R^2= (0.0, 0.469), Q^2= (0.0, -0.144)).

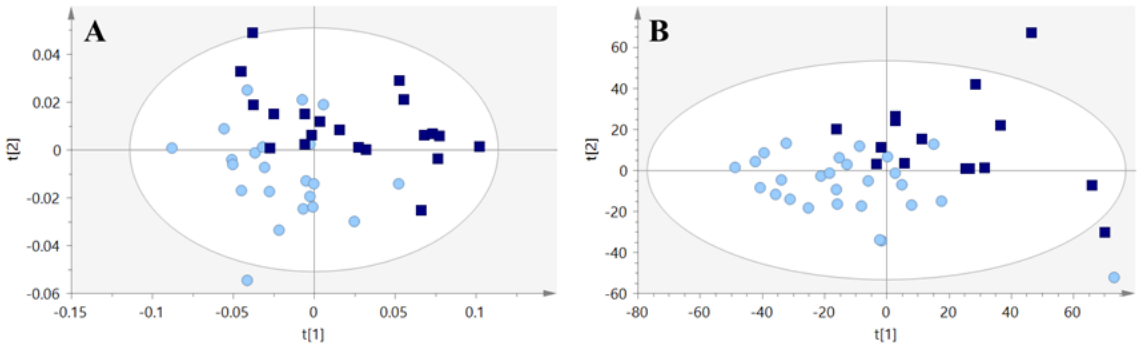

Supplementary Figure 5: PLS-DA scores scatter plots: (A) obtained for control individuals without dyslipidemia (dark blue circles) *vs.* with dyslipidemia (light blue squares) (GC-MS data) (Pareto scaling; 2 components) (LV= 2, R^2X=0.404; R^2Y=0.501; Q^2= 0.137) (Dyslipidemia *n*=20 *vs.* non-dyslipidemia *n*=22); (B) obtained for control individuals without hypertension (dark blue circles) vs. with hypertension (light blue squares) (^{1}H NMR data) (UV scaling; 2 components) (LV= 2, R^2X=0.285; R^2Y=0.557; Q^2= 0.011) (Hypertension *n*=15 *vs*. non-hypertension *n*=27).

Supplementary Table 1: Demographic and clinical data of the PCa patients and cancer-free controls included in the training and external validation sets.

Characteristics	PCa patients				Controls			
	Training set GC-MS	*External set GC-MS*	*Training set ^{1}H NMR*	*External set ^{1}H NMR*	*Training set GC-MS*	*External set GC-MS*	*Training set ^{1}H NMR*	*External set ^{1}H NMR*
Number of subjects	41	18	41	18	42	18	42	18
Age (years)								
Mean (standard deviation)	64.3 (6.12)	61.8 (5.90)	63.1 (5.25)	64.8 (7.80)	59.2 (2.60)	60.2 (3.35)	59.8 (2.73)	58.7 (3.03)
Serum PSA (ng/mL)								
<4	3 (7.3%)	1 (5.6%)	2 (4.9%)	2 (11.1%)	-	-	-	-
4-10	23 (56.2%)	14 (77.8%)	26 (63.4%)	11 (61.1%)	-	-	-	-
>10	15 (36.6%)	3 (16.7%)	13 (31.7%)	5 (27.8%)	-	-	-	-
Gleason score (GS)								
3+3	7 (17.1%)	2 (11.1%)	7 (17.1%)	2 (11.1%)	-	-	-	-
3+4	14 (34.2%)	12 (66.7%)	18 (43.9%)	8 (44.4%)	-	-	-	-
4+3	9 (22%)	2 (11.1%)	9 (22%)	2 (11.1%)	-	-	-	-
4+4	6 (14.6%)	1 (5.6%)	4 (9.8%)	3 (16.7%)	-	-	-	-
4+5	5 (12.2%)	-	3 (7.3%)	2 (11.1%)	-	-	-	-
5+4	-	1 (5.6%)	-	1 (5.6%)	-	-	-	-
Clinical stage								
I	4 (9.8%)	2 (11.1%)	3 (7.3%)	3 (16.5%)	-	-	-	-
II	19 (46.4%)	11 (61.1%)	20 (48.8%)	10 (55.6%)				
III	15 (36.6%)	4 (22.2%)	15 (36.6%)	4 (22.2%)	-	-	-	-
IV	3 (7.3%)	1 (5.6%)	3 (7.3%)	1 (5.6%)	-	-	-	-
Alcoholism	5 (12.2%)	6 (33.3%)	8 (19.5%)	3 (16.7%)	3 (7.1%)	-	3 (7.1%)	-
Smoking	-	2 (11.1%)	1 (2.4%)	1(5.6%)	6 (14.3%)	1 (5.6%)	4 (9.5%)	3 (16.7%)
Obesity	7 (17.1%)	3 (16.7%)	7 (17.1%)	3 (16.7%)	8 (19%)	2 (11.1%)	7 (16.7%)	3 (16.7%)
Cardiac condition	9 (22%)	2 (11.1%)	6 (14.6%)	5 (27.8%)	1 (2.4%)	-	1 (2.4%)	-
Arterial hypertension	18 (43.9%)	11 (61.1%)	22 (53.7%)	7 (38.9%)	14 (33.3%)	9 (50%)	15 (35.7%)	8 (44.4%)
Dyslipidemia	14 (34.1%)	11 (61.1%)	18 (43.9%)	7 (38.9%)	20 (47.6%)	5 (25.8%)	18 (42.9%)	7 (38.9%)
Diabetes mellitus	7 (17.1%)	5 (27.8%)	9 (22%)	3 (16.7%)	5 (11.9%)	2 (11.1%)	6 (14.3%)	1 (5.6%)
Hypertriglyceridemia	1 (2.4%)	-	1 (2.4%)	-	-	-	-	-
Hypercholesterolemia	2 (4.9%)	1 (5.6%)	2 (4.9%)	1 (5.6%)	4 (9.5%)	1 (5.6%)	3 (7.1%)	2 (11.1%)

Characteristics	PCa patients				Controls			
	Training set GC-MS	*External set GC-MS*	*Training set ^{1}H NMR*	*External set ^{1}H NMR*	*Training set GC-MS*	*External set GC-MS*	*Training set ^{1}H NMR*	*External set ^{1}H NMR*
Benign prostatic hyperplasia	-	-	-	-	12 (28.6%)	5 (25.8%)	15 (35.7%)	2 (11.1%)
Prostatitis	-	-	-	-	2 (4.8%)	-	1 (2.4%)	1 (5.6%)

Supplementary Table 2: Confusion matrix obtained for GC-MS and ^{1}H NMR data considering the external validation sets (*n*=18 PCa samples plus *n*=18 control samples) (sensitivity: 89%, specificity: 83% and accuracy: 86% for GC-MS and sensitivity: 67%, specificity: 89% and accuracy: 86% for ^{1}H NMR).

		Predicted classes			
		GC-MS		**^{1}H NMR**	
True Classes		***Case***	***Control***	***Case***	***Control***
	Case	16	2	12	6
	Control	3	15	2	16

Supplementary Table 3: Spearman's correlation indexes and corresponding *p*-values obtained for age with the set of metabolites found altered in PCa compared to controls.

Metabolites	**r**	***p***
GC-MS		
Propylene glycol	-0.05	0.661
Unknown 1	0.01	0.894
Sarcosine	0.30	0.006
Oxalate	0.24	0.027
L-Threose	0.09	0.408
L-Threitol	-0.03	0.785
L-Fucitol	-0.20	0.066
Ribitol	-0.15	0.186
L-Arabitol	-0.25	0.022
D-Glucose	-0.27	0.014
Gluconate	-0.19	0.094
D-Mannitol	-0.27	0.013
Unknown 2	0.20	0.065
Myo-inositol	-0.08	0.457
Unknown 3	-0.21	0.054
^{1}H NMR		
2-Hydroxyvalerate	0.12	0.308
Leucine	0.14	0.236
Valine	0.11	0.345
2-Hydroxyisobutyrate	0.10	0.374
Acetone	0.25	0.028
Pyruvate	0.38	0.001
Unknown 4	0.33	0.004
Unknown 5	0.27	0.016
Hydroxyacetone	-0.21	0.064
Trigonelline	-0.22	0.055
2-Furoylglycine	-0.30	0.008
Unknwon 6	-0.25	0.025
Unknown 7	-0.25	0.026

Supplementary Table 4: List of metabolites significantly altered in PCa group compared to controls detected through GC-MS. Metabolites are characterized by their name, retention time, most characteristic ions (m/z), Kovat indices (KI) from literature, experimental KI, R match (NIST), identification level, as well as the HMDB (human metabolome database) code, the matrices where the compound was previously found and the potential biochemical pathways in which the compound participates.

Name	Retention time	m/z	KI from literature	Experimental KI	R match	Identification Level (Viant et al., 2017)	HMDB (Wishart et al., 2018)	Matrices	Potential biochemical pathway
Propylene glycol	4.88	117; 73; 147; 118; 148; 66; 75; 133; 59	-	-	717	L1	HMDB0001881	Blood; Cerebrospinal Fluid; Feces; Saliva; Urine; Sweat (Wishart et al., 2018)	Pyruvate metabolism (Chong et al., 2018)
Unknown 1	5.93	93; 151; 121; 95; 73; 50; 91; 77; 59; 63	-	1086	-	L4	-	-	-
Sarcosine	6.31	116; 73; 147; 117; 59; 190; 74; 233; 75	-	-	784	L1	HMDB0000271	Blood; Cerebrospinal Fluid; Feces; Saliva; Urine; Tissue (Kumar et al., 2015; Putluri et al., 2011; Sreekumar et al., 2009; Wishart et al., 2018)	Glycine, serine and threonine metabolism (Chong et al., 2018)

Name	Retention time	m/z	KI from literature	Experimental KI	R match	Identification Level (Viant et al., 2017)	HMDB (Wishart et al., 2018)	Matrices	Potential biochemical pathway
Oxalate	6.41	73; 147; 148; 74; 149; 66; 72; 59; 219; 190; 113	-	-	650	L1	HMDB0002329	Blood; Feces; Saliva; Urine; Sweat (Wishart et al., 2018)	Glyoxylate and dicarboxylate metabolism (Chong et al., 2018)
L-Threose	9.61	73;147; 205; 117; 103; 161; 89; 133; 74	-	-	711	L1	NA	-	Non-enzymatic glycation by ascorbate (Nagaraj and Monnier, 1995)
L-Threitol	9.91	73; 147; 217; 103; 205; 117; 204; 189; 133; 191	-	-	927	L1	HMDB0004136	Blood; Cerebrospinal Fluid; Feces; Urine (Wishart et al., 2018)	Carbohydrate metabolism (Wishart et al., 2018)
L-Fucitol	11.93	73; 117; 147; 217; 103; 205; 219; 319; 231; 129	1770	1751	864	L2	HMDB0041500	-	Carbohydrate metabolism (Wishart et al., 2018)
Ribitol	12.01	73; 103; 147; 217; 74; 205; 129; 117; 75	1747	1761	787	L2	HMDB0000508	Blood; Cerebrospinal Fluid; Feces; Urine (Wishart et al., 2018)	Pentose and glucuronate intercom-versions (Chong et al., 2018)

Name	Retention time	m/z	KI from literature	Experimental KI	R match	Identification Level (Viant et al., 2017)	HMDB (Wishart et al., 2018)	Matrices	Potential biochemical pathway
L-Arabitol	12.43	73; 147; 103; 217; 205; 129; 307; 117; 319; 218	-	-	812	L1	HMDB0001851	Blood; Cerebrospinal Fluid; Feces; Urine (Struck-Lewicka et al., 2015; Wishart et al., 2018)	Pentose and glucuronate inter-conversions (Chong et al., 2018)
D-Glucose	12.66	73; 105; 77; 51; 206; 147; 75; 134; 135; 217	-	-	625	L1	HMDB0000122	Blood; Breast Milk; Cerebrospinal Fluid; Feces; Saliva; Sweat; Urine; Cell lines (Vaz et al., 2012) (Wishart et al., 2018)	Pentose phosphate pathway; Glycolysis or Gluconeo-genesis Galactose metabolism (Chong et al., 2018)
Gluconate	12.73	73; 147; 205; 319; 160; 217; 74; 117; 103	-	-	636	L1	HMDB0000625	Blood; Feces; Urine; Tissue (Jung et al., 2013; Wishart et al., 2018)	Pentose phosphate pathway (Chong et al., 2018)
D-Mannitol	13.04	73; 147; 217; 103; 204; 189; 219; 205; 75; 74; 451		-	662	L1	HMDB0000765	Cerebrospinal Fluid; Feces; Saliva; Urine (Wishart et al., 2018)	Fructose and mannose metabolism (Wishart et al., 2018)

Name	Retention time	m/z	KI from literature	Experimental KI	R match	Identification Level (Viant et al., 2017)	HMDB (Wishart et al., 2018)	Matrices	Potential biochemical pathway
Unknown 2	13.81	73; 75; 119; 217; 57; 103; 71; 193; 204; 117	-	2128	-	L4	-	-	-
Myo-inositol	14.14	71; 115; 84; 95; 149; 120; 89; 97; 90; 101	-	-	902	L1	HMDB0000211	Blood; Breast Milk; Cerebrospinal Fluid; Feces; Saliva; Sweat; Urine; Prostatic fluid; Tissue (Serkova et al., 2008; Stenman et al., 2011; Wishart et al., 2018)	Galactose metabolism; Ascorbate and aldarate metabolism (Chong et al., 2018)
Unknown 3	17.47	130; 117; 131; 57; 101; 55; 129; 71; 75;	-	2636	-	L4	-	-	-

L1: Identified metabolites (GC-MS analysis of the metabolite of interest and a chemical reference standard of suspected structural equivalence, with all analyses performed under identical analytical conditions within the same laboratory); L2: Putatively annotated compounds (MS spectral similarity with NIST database); L4: Unidentified.

Supplementary Table 5: List of metabolites significantly altered in urine from PCa compared to controls, detected through ^{1}H NMR spectroscopy. Metabolites are characterized by their ^{1}H chemical shift (multiplicity), the identification level, as well as the HMDB (human metabolome database) code, the matrices where the compound was previously found and the potential biochemical pathways in which the compound participates.

Name	δH ppm (multiplicity)	Identification level (Viant et al., 2017)	HMDB (Wishart et al., 2018)	Matrices	Potential biochemical pathway
2-Furoylglycine	3.93 (s); 6.65 (dd); 7.19 (d); 7.70 (d)	L2	HMDB0000439	Blood; Feces; Urine (Wishart et al., 2018)	Fatty acids metabolism (Wishart et al., 2018)
2-Hydroxy-isobutyrate	1.36 (s)	L2	HMDB0000729	Blood; Feces; Saliva; Urine (Wishart et al., 2018)	-
2-Hydroxyvalerate	0.85 (t); 1.35 (m); 1.60 (m); 1.70 (m); 4.00 (dd)	L2	HMDB0001863	Blood; Feces; Urine (Wishart et al., 2018)	Lipid metabolism (Wishart et al., 2018)
Acetone	2.22 (s)	L2	HMDB0001659	Blood; Breast Milk; Cerebro-spinal Fluid; Feces; Saliva; Urine (Wishart et al., 2018)	Propanoate metabolism; Synthesis and degradation of ketone bodies (Chong et al., 2018)
Hydroxyacetone	2.14 (s); 4.39 (s)	L2	HMDB0006961	Feces; Urine (Wishart et al., 2018)	Glycine, serine and threonine metabolism (Chong et al., 2018)
Leucine	0.96 (t); 1.70 (m); 3.73 (m)	L2	HMDB0000687	Blood; Breast Milk; Cerebro-spinal Fluid; Feces; Saliva; Sweat; Urine; Cell lines; Tissue (Lodi and Ronen, 2011; Sreekumar et al., 2009; Wishart et al., 2018)	Valine, leucine and isoleucine biosynthesis; Valine, leucine and isoleucine degradation (Chong et al., 2018)

Name	δH ppm (multiplicity)	Identification level (Viant et al., 2017)	HMDB (Wishart et al., 2018)	Matrices	Potential biochemical pathway
Pyruvate	2.35 (s)	L2	HMDB0000243	Blood; Breast Milk; Cellular Cytoplasm; Cerebro-spinal Fluid; Feces; Saliva; Sweat; Urine (Kumar et al., 2015; Wishart et al., 2018)	Valine, leucine and isoleucine biosynthesis; Pentose phosphate pathway; Glycine, serine and threonine metabolism; Pantothenate and CoA biosynthesis; Glycolysis or Gluconeogenesis; Pyruvate metabolism; Nicotinate and nicotinamide metabolism; Ascorbate and aldarate metabolism; Glyoxylate and dicarboxylate metabolism; Pentose and glucuronate interconversions (Chong et al., 2018)
Trigonelline	4.44 (s); 8.09 (t); 8.84 (d); 8.85 (d); 9.13 (s)	L2	HMDB0000875	Blood; Feces; Urine (Wishart et al., 2018)	Nicotinate and nicotinamide metabolism (Chong et al., 2018)
Valine	0.99 (d); 1.05 (d); 2.28 (m); 3.61 (d)	L2	HMDB0000883	Blood; Breast Milk; Cerebro-spinal Fluid; Feces; Saliva; Sweat; Urine; Cell line (Lodi and Ronen, 2011; Wishart et al., 2018)	Valine, leucine and isoleucine biosynthesis; Pantothenate and CoA biosynthesis; Propanoate metabolism; Valine, leucine and isoleucine degradation (Chong et al., 2018)
Unknown 4	3.66-3.65 (s)	L4	-	-	-
Unknown 5	3.68-3.67 (s)	L4	-	-	-
Unknown 6	8.81-8.77 (d)	L4	-	-	-
Unknown 7	9.078-9.006 (s)	L4	-	-	-

L2: Putatively annotated compounds (spectral similarity with database); s: singlet, d: doublet, t: triplet, dd: doublet of doublets, m: multiplet; L4: Unidentified.

Supporting references

Chong, J., Soufan, O., Li, C., Caraus, I., Li, S., Bourque, G., Wishart, D.S. and Xia, J. (2018) MetaboAnalyst 4.0: towards more transparent and integrative metabolomics analysis. Nucleic Acids Res 46, W486-W494.

Jung, K., Reszka, R., Kamlage, B., Bethan, B., Stephan, C., Lein, M. and Kristiansen, G. (2013) Tissue metabolite profiling identifies differentiating and prognostic biomarkers for prostate carcinoma. Int J Cancer 133, 2914-24.

Kumar, D., Gupta, A., Mandhani, A. and Sankhwar, S.N. (2015) Metabolomics-derived prostate cancer biomarkers: fact or fiction? J Proteome Res 14, 1455-64.

Lodi, A. and Ronen, S.M. (2011) Magnetic resonance spectroscopy detectable metabolomic fingerprint of response to antineoplastic treatment. PLoS One 6, e26155.

Nagaraj, R.H. and Monnier, V.M. (1995) Protein modification by the degradation products of ascorbate: formation of a novel pyrrole from the Maillard reaction of l-threose with proteins. Biochimica et Biophysica Acta (BBA) - Protein Structure and Molecular Enzymology 1253, 75-84.

Putluri, N., Shojaie, A., Vasu, V.T., Nalluri, S., Vareed, S.K., Putluri, V., Vivekanandan-Giri, A., Byun, J., Pennathur, S., Sana, T.R., Fischer, S.M., Palapattu, G.S., Creighton, C.J., Michailidis, G. and Sreekumar, A. (2011) Metabolomic profiling reveals a role for androgen in activating amino acid metabolism and methylation in prostate cancer cells. PLoS One 6, e21417.

Serkova, N.J., Gamito, E.J., Jones, R.H., O'Donnell, C., Brown, J.L., Green, S., Sullivan, H., Hedlund, T. and Crawford, E.D. (2008) The metabolites citrate, myo-inositol, and spermine are potential age-independent markers of prostate cancer in human expressed prostatic secretions. The Prostate 68, 620-628.

Sreekumar, A., Poisson, L.M., Rajendiran, T.M., Khan, A.P., Cao, Q., Yu, J., Laxman, B., Mehra, R., Lonigro, R.J., Li, Y., Nyati, M.K., Ahsan, A., Kalyana-Sundaram, S., Han, B., Cao, X., Byun, J., Omenn, G.S., Ghosh, D., Pennathur, S., Alexander, D.C., Berger, A., Shuster, J.R., Wei, J.T., Varambally, S., Beecher, C. and Chinnaiyan, A.M. (2009) Metabolomic profiles delineate potential role for sarcosine in prostate cancer progression. Nature 457, 910-4.

Stenman, K., Stattin, P., Stenlund, H., Riklund, K., Gröbner, G. and Bergh, A. (2011) H HRMAS NMR Derived Bio-markers Related to Tumor Grade, Tumor Cell Fraction, and Cell Proliferation in Prostate Tissue Samples. Biomarker insights 6, 39-47.

Struck-Lewicka, W., Kordalewska, M., Bujak, R., Yumba Mpanga, A., Markuszewski, M., Jacyna, J., Matuszewski, M., Kaliszan, R. and Markuszewski, M.J. (2015) Urine metabolic fingerprinting using LC–MS and GC–MS reveals metabolite changes in prostate cancer: A pilot study. Journal of Pharmaceutical and Biomedical Analysis 111, 351-361.

Vaz, C.V., Alves, M.G., Marques, R., Moreira, P.I., Oliveira, P.F., Maia, C.J. and Socorro, S. (2012) Androgen-responsive and nonresponsive prostate cancer cells present a distinct glycolytic metabolism profile. Int J Biochem Cell Biol 44, 2077-84.

Viant, M.R., Kurland, I.J., Jones, M.R. and Dunn, W.B. (2017) How close are we to complete annotation of metabolomes? Current opinion in chemical biology 36, 64-69.

Wishart, D.S., Feunang, Y.D., Marcu, A., Guo, A.C., Liang, K., Vázquez-Fresno, R., Sajed, T., Johnson, D., Li, C., Karu, N., Sayeeda, Z., Lo, E., Assempour, N., Berjanskii, M., Singhal, S., Arndt, D., Liang, Y., Badran, H., Grant, J., Serra-Cayuela, A., Liu, Y., Mandal, R., Neveu, V., Pon, A., Knox, C., Wilson, M., Manach, C. and Scalbert, A. (2018) HMDB 4.0: the human metabolome database for 2018. Nucleic acids research 46, D608-D617

.

Chapter 5 – Integrated discussion

It is well established that reprogramming of cellular metabolism is one of the defining features of cancers, including PCa (Eidelman et al. 2017; Zadra et al. 2018). Considering that metabolomics is defined as the characterization of all metabolites in a biological sample (Bujak et al. 2015), it is easy to understand why this approach is ideal to uncover the metabolic phenotype associated with PCa development and progression. As a matter of fact, several previous studies successfully applied metabolomics to accomplish this goal (reviewed in Lima et al. 2016; Lima et al. 2021; Lima et al. 2018). Considering the success of these studies, the two main goals of this thesis were to uncover new potential biomarkers for the non-invasive PCa screening and to perform a comprehensive characterization of the metabolic alterations associated with PCa development and progression.

In **Chapter 3**, the urinary volatile signature of PCa patients was characterized through HS-SPME-GC-MS in order to provide new potential biomarkers for the non-invasive screening of PCa. Results showed that the urinary volatile profile was able to clearly discriminate between PCa and cancer-free controls (**Section 3.1**). PCa presence was associated with dysregulation in the levels of 43 volatile compounds. Despite the difficulty to associate volatile compounds with known biochemical pathways (Lee et al. 2018), some metabolites altered in the PCa group were link to dysregulation in 4 metabolic pathways, namely pyruvate metabolism, glycine, serine and threonine metabolism, phenylalanine metabolism and steroid hormone biosynthesis. However, the most relevant result was the disclosure of a 6-biomarker panel, comprising hexanal, 2,5-dimethylbenzaldehyde, 4-methylhexan-3-one, dihydroedulan IA, methylglyoxal and 3-phenylpropionaldehyde, able to differentiate between PCa and control urine samples. Considering the internal set, this 6-biomarker panel showed an area under the curve (AUC) of 0.856, 72% sensitivity, 96% specificity and 79% accuracy. Considering the external set, this 6-biomarker panel showed an area under the curve (AUC) of 0.904, 89% sensitivity, 83% specificity and 86% accuracy. Thus, this biomarker panel outperforms PSA accuracy (62–75%) (Louie et al. 2015), sensitivity (20.5%) (Kearns et al. 2018; Wolf et al. 2010) and AUC (varying from 0.53 to 0.83) (Louie et al. 2015), and showed a similar specificity (ranging from 51 to 91%) (Kearns et al. 2018; Wolf et al. 2010). One of the most important confounding factors for PSA test is the presence of other prostate diseases like benign prostate hyperplasia (BPH) and prostatitis (Dimakakos et al. 2014). Importantly, in our study (**Section 3.1**), the cancer-free control group of the external set included patients with both pathologies that were correctly classified by the defined panel. The application of external validation set is extremely important since it allows to independently confirm the predictive accuracy of the model,

proving that no overfitting occurs and consequently providing statistical strength to the obtained results (Gholamy 2018; Liu et al. 2017). Furthermore, the inclusion of an external validation set, in our study, is a step forward compared to previous volatilomic works performed in PCa urine (Jiménez-Pacheco et al. 2018; Khalid et al. 2015; Smith et al. 2010).

We next sought to validate the urinary 6-biomarker panel in an independent set of samples collected from PCa patients and cancer-free controls (**Section 3.2**). Importantly, in this second study, the site specificity of this 6-biomarker panel was also explored, with the inclusion of urine samples from patients with other urological cancers, namely bladder cancer (BC) and renal cancer (RC). BC and RC are anatomically close to the prostate, and both are also highly prevalent cancers in men (Bray et al. 2018). A target approach was initially employed to confirm the discriminant capability of the 6-biomarker panel defined in **Section 3.1**. When considering only PCa and cancer-free control samples, the results attested the discriminant capability of the 6-biomarker panel, with a performance similar to the one obtained in the first study (**Section 3.1**), namely an AUC of 0.83, 84% sensitivity, 80% specificity and 82% accuracy. However, the 6-biomarker panel failed to discriminate PCa from BC and RC (**Section 3.2**). The site-specificity of a biomarker panel is frequently disregarded in metabolomic studies. To the best of our knowledge, only two previous studies tried to discriminate PCa from other cancers, but also without success (Gamagedara et al. 2012; Peng et al. 2010). This lack of discrimination between different cancers was expected since it is well established that tumor cells share some metabolic abnormalities to promote cancer cell survival and proliferation. These studies strengthen the idea that discrimination between different cancers should be more studied to obtain a specific biomarker panel of each tumor. Remarkably, the study presented in **Section 3.2** proved that the addition of 4 biomarkers, namely ethylbenzene, heptan-2-one, methyl benzoate, and 3-methylbenzaldehyde, to the former 6-biomarker panel, solved the problem of site specificity. Indeed, this improved 10-biomarker panel shows an excellent discriminant capability between PCa samples and all other samples included in the study (cancer-free controls, BC and RC) with an AUC of 0.90, 76% sensitivity, 97% specificity and 92% accuracy, proving the huge potential of urinary volatolome as a source for PCa screening biomarkers.

Unfortunately, the GC-MS applicability in clinical practice is limited due to high-cost, non-portability, laborious process, and the need of a highly qualify operator (Wilson et al. 2011). Contrastingly, chemical system sensors, like “electronic nose” (“e-nose”), are inexpensive, portable and allow a quick analysis of volatile signature of urine samples, but they are unable to identify the volatile compounds (Capelli et al. 2016; Wilson et al. 2011).

Thus, the combination of GC-MS and e-nose technologies may be an ideal approach to achieve a non-invasive test for PCa screening. Therefore, the proposed 10-biomarker panel could be applied for the development of an optimized e-nose in the future, to detect specifically this PCa volatile signature and be used in clinical practice for inexpensive, non-invasive and high throughput PCa screening.

In **Chapter 4**, tissue (**Section 4.1**) and urine (**Section 4.2**) samples from PCa patients were analyzed through different analytical platforms to provide an in-depth understanding of the metabolic alterations associated with PCa development and progression.

Tissue is the ideal matrix to disclose metabolic alterations specific of cancer cells and allow to greatly reduce confounding factors, through the use of matched samples (samples from the same patient) but tissue collection is extremely invasive. In contrast, urine is a non-invasive matrix, with high availability, and low complexity when compared with other biofluids (e.g., serum or plasma) (Bujak et al. 2015; Gomez-Cebrian et al. 2019). However, it is important to take into consideration that urine composition can be affected by several external factors, such as genetic factors and/ or presence of other comorbidities (Nagrath et al. 2011; Walsh et al. 2006). Therefore, the study of both matrices is complementary.

A multi-platform metabolomics strategy, combining GC-MS, ^{1}H NMR, and HILIC-MS/MS, was employed to allow a more holistic study of the PCa tissue metabolome (**Section 4.1**). All analytical platforms were able to provide a good discrimination between PCa and adjacent non-malignant tissue (from the same patient after prostatectomy), and the combination of all methodologies allows to associate PCa with alterations in the levels of 27 metabolites and 21 phospholipid species and suggesting dysregulations in 14 metabolic pathways, predominantly in amino acid and glycerophospholipid metabolisms.

To obtain a more holistic characterization of urine metabolome, the non-volatile compounds present in the same urine samples used in **Section 3.1** were analyzed through GC-MS and ^{1}H NMR (**Section 4.2**). Interestingly, when comparing the diagnostic performance of the volatile metabolome (**Section 3.1**), with the discriminatory performance obtained for the non-volatile urinary metabolome, using the external set, it is possible to infer that the volatilomic approach allows a better separation between PCa and cancer-free controls, once almost all the evaluated parameters have better performances in volatilomics models. These results reinforce the idea that volatilomic studies are the ideal approach to uncover new biomarkers for PCa screening.

Importantly in **Sections 4.1 and 4.2**, MS-based techniques and NMR showed high complementarity and the combination of these analytical platforms allowed a more

comprehensive coverage of the metabolome. However, it is also possible to infer that GC-MS data allowed a better discrimination between samples than NMR data. The lower performance of NMR may be related with a lower sensitivity (from micromolar to millimolar) (Crook et al. 2020), the absence of separation step and most importantly with the physiochemical characteristic of the metabolites (Lima et al. 2018; Turi et al. 2018).

When comparing the metabolic alterations associated with PCa presence in tissue (**Section 4.1**) and urine **(Section 4.2**) samples, only three metabolites were reported concordantly altered in both studies, namely leucine, valine, *myo*-inositol. This apparent low translatability between urine and tissue samples could have several explanations. Firstly, urinary metabolome contains information of cancer-derived metabolites, but also of metabolites related with other local or systemic body responses to PCa development and progression, while tissue metabolome is more specific of PCa cell. Secondly, tissue studies evaluate the metabolic alterations directly in their origin, whereas metabolites present in urine samples undergo to an excretion process that include several steps, like renal concentration (Wishart 2019). Finally, it is important to consider that non-malignant adjacent tissue was considered as control in the tissue metabolomic study (**Section 4.1**). The tissue collection was performed by an experienced pathologist, but metabolic alterations could precede histological alterations, so adjacent non-malignant tissue may not be metabolically similar to healthy/ normal prostate tissue (Boudonck et al. 2009; Sun et al. 2018). Considering that the urinary study (**Section 4.2**) was performed using cancer-free controls, this difference in the health state of the control group may limit the potential translatability of the results between tissue and urine.

Notably, it must be stressed that concordant results were found between tissue (**Section 4.1**) and urine (**Section 4.2**) when considering the dysregulated metabolic pathways in PCa. Indeed, 5 metabolic pathways were associated with PCa presence in both studies (**Sections 4.1 and 4.2**), namely ascorbate and aldarate metabolism, glyoxylate and dicarboxylate metabolism, nicotinate and nicotinamide metabolism, pantothenate and CoA biosynthesis and valine, leucine and isoleucine synthesis (Figure 5.1). Furthermore, one metabolic pathway reported in the volatilomics profile of PCa urine samples was also associated with PCa in the tissue metabolome study (**Sections 3.1 and 4.1**), namely the phenylalanine metabolism. Interestingly, one metabolic pathway was associated with PCa development and progression in all three studies (glycine, serine and threonine metabolism) (**Sections 3.1, 4.1 and 4.2**). A summary of these metabolic pathways and their potential role in PCa development and progression will be given hereafter (Figure 5.2).

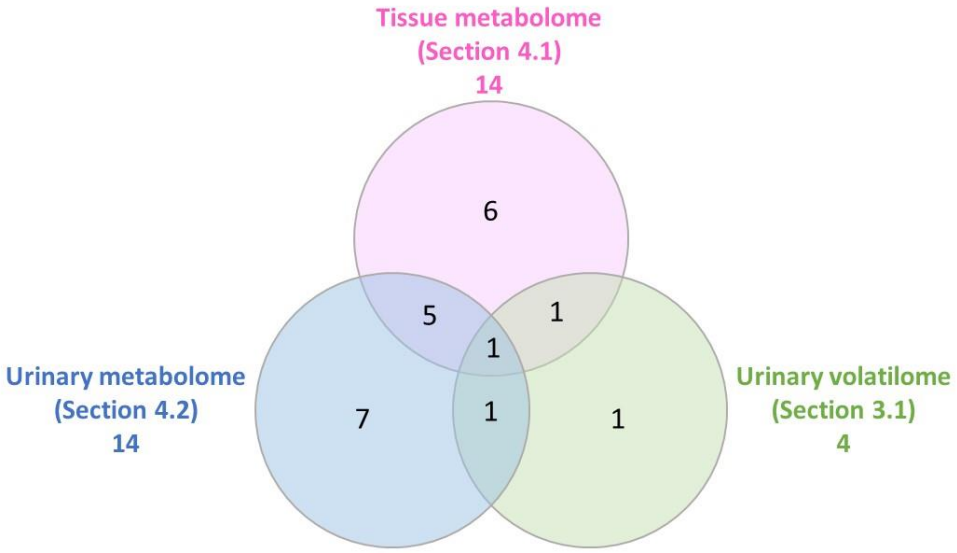

Figure 5.1: Venn diagram of all potentially metabolic pathways dysregulated in PCa, described in **Sections 3.1, 4.1** and **4.2.**

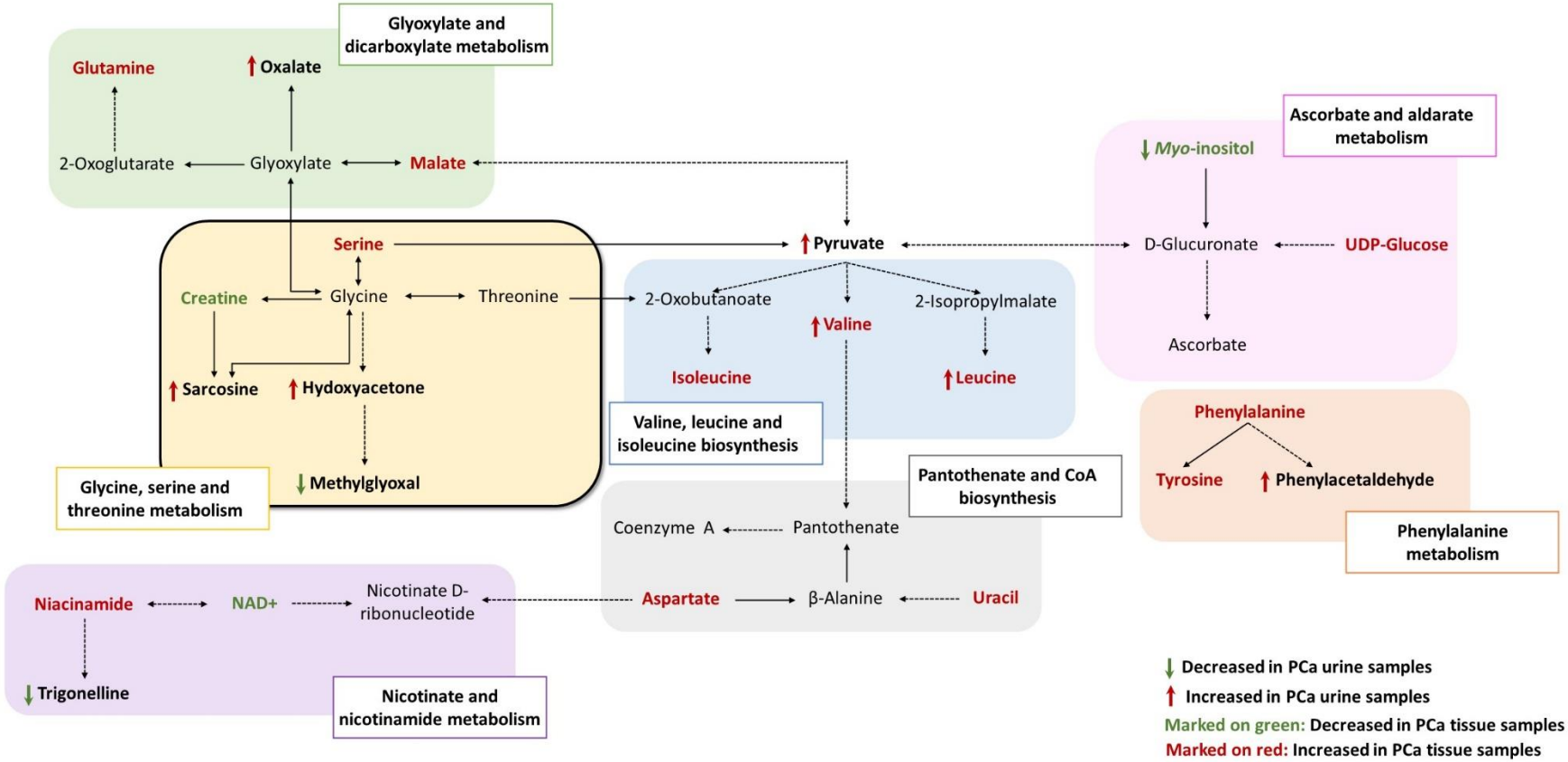

Figure 5.2: Simplified schematic representation of the seven metabolic pathways associated with PCa development and progression in both urine and tissue samples (**Sections 3.1, 4.1 and 4.2**). The dashed lines represent multiple step reactions.

.

Glycine, serine and threonine metabolism was the only metabolic pathway that was associated with PCa in all three studies (**Sections 3.1, 4.1 and 4.2**) highlighting its importance in PCa metabolism. Overall, it is well established that alteration in the enzymes involved in this metabolic pathway play an important role in proliferation, invasion and cell death (Khan et al. 2013; Lima et al. 2016; Sreekumar et al. 2009). Furthermore, upregulation of this pathway was associated with oncogenesis and tumor maintenance (Pérez-Rambla et al. 2017). Additionally, serine and glycine metabolism provide essential precursors for proteins, nucleic acids and lipids synthesis, which are crucial building-blocks for cancer cell progression (di Salvo et al. 2013) and sarcosine is an intermediate compound in choline metabolism, which is crucial for cellular membrane components synthesis (Smith-Palmer 2019).

Other two metabolic pathways directly related with amino acid metabolism were also associated with PCa, namely valine, leucine and isoleucine synthesis (**Section 4.1 and 4.2**) and phenylalanine metabolism (**Section 3.1 and 4.1**). Branched-chain amino acids (BCAAs) (valine, leucine, and isoleucine) are involved in the metabolism of glucose, lipid, and protein synthesis (Wishart et al. 2018). Furthermore, BCAAs can also be used by the cells to produce energy (Pérez-Rambla et al. 2017). Additionally, BCAAs can activate mTOR, an important regulator of cell growth, proliferation and migration (Holecek 2018; Wishart et al. 2018), being well established that mTOR activation plays a central role in cancer development and progression (Populo et al. 2012). On the other hand, restriction in levels of tyrosine and phenylalanine have several consequences in PCa cell lines, including alterations in glucose metabolism, induction of cell death (Fu et al. 2010) and inhibition of invasion and metastasis (Fu et al. 2003). These results highlighted the close relationship between PCa development and amino acid metabolism.

The significant alteration in the levels of pyruvate (**Section 4.2**), *myo*-inositol (**Sections 4.1 and 4.2**) and UDP-glucose (**Section 4.1**) indicates that PCa development and progression are associated with an alteration in ascorbate and aldarate metabolism. This metabolic pathway is related with both carbohydrate (Tao et al. 2015) and glutathione metabolisms, so the alteration in ascorbate and aldarate metabolism could be correlated with both energetic metabolism and redox homeostasis, which are known to play an important role in cancer development and progression (Park et al. 2018).

The other metabolic pathways associated with PCa are involved mainly in energetic metabolism, namely nicotinate and nicotinamide metabolism, pantothenate and CoA biosynthesis, and glyoxylate and dicarboxylate metabolism. Importantly, glyoxylate and dicarboxylate metabolism is directly correlated with glycine, serine, and threonine

metabolism, once this last pathway provides essential metabolites (hydroxypyruvate and glyoxylate) for glyoxylate and dicarboxylate metabolism (Kanehisa et al. 2000), highlighting the interconnection between the different metabolic pathways that were involved in PCa development and progression. Nicotinate and nicotinamide metabolism leads to the production of the coenzymes nicotinamide-adenine dinucleotide (NAD) and nicotinamide-adenine dinucleotide phosphate (NADP) (Frolkis et al. 2010; Jewison et al. 2014). NAD is important in several cellular processes including redox homeostasis, mitochondrial function, and cell death (Sampath et al. 2015). Furthermore, nicotinamide phosphoribosyltransferase (NAMPT), a key enzyme in this pathway, is overexpressed in PCa. The inhibition of NAMPT shows anti-tumor activity leading to ATP depletion and consequently cell death (Sampath et al. 2015). Finally, pantothenate and CoA biosynthesis was other metabolic pathway associated with PCa development. Pantothenate, is a precursor of coenzyme A (CoA) (Leonardi et al. 2007) and CoA is a key compound in several cellular mechanisms, including cell growth, synthesis of phospholipids, synthesis and degradation of fatty acids, and tricarboxylic acid (TCA) cycle (Leonardi et al. 2007).

Chapter 6 – Conclusions and future perspectives

The recognition that “omic” technologies, in particular metabolomics and its subareas volatilomics and lipidomics, are crucial tools to detect early metabolic alterations that occur in cancer development and progression opens the window to the study of potential applications of these alterations in clinical practice. Metabolomics has the potential to provide biomarkers for cancer diagnosis, for the development of new therapeutic targets and to disclose the molecular mechanisms involved in cancer development and progression. The experimental work performed under the scope of this thesis highlights the importance of metabolomic studies in PCa research area.

Regarding to PCa screening, the urinary volatilomics analysis was suitable to define a 10-biomarker panel for PCa screening (accuracy of 92%) that outperforms PSA accuracy (62-75%). Importantly, this biomarker panel was able to discriminate not only PCa from cancer-free controls but also from other urological cancers (renal and bladder cancers). So, these results revealed that the urinary volatile profiling encompasses a huge potential for non-invasive PCa screening.

The metabolic characterization of PCa samples performed in this thesis allowed to extend the knowledge about PCa metabolic phenotype and to corroborate some previous findings, e.g., the association of PCa development and progression with dysregulation in amino acid metabolism, highlighting the complementarity among different analytical platforms (GC-MS, ^{1}H NMR and HILIC-MS/MS), as well as the complementarity between urinary and tissue metabolomic studies. Notably, the dysregulation in ascorbate and aldarate metabolism, glycine, serine and threonine metabolism, glyoxylate and dicarboxylate metabolism, nicotinate and nicotinamide metabolism, pantothenate and CoA biosynthesis, valine, leucine and isoleucine synthesis and phenylalanine metabolism were reported in urine and tissue metabolomic studies. Furthermore, the detailed characterization of PCa tissue lipidome was one of the most important achievements of the present work, especially considering that this is an understudied subarea of metabolomics in PCa research.

Despite the promising results obtained, more studies are needed to fully understand the PCa metabolome and take advantages of these findings in clinical practice. For future research directions, we highlight the importance to validate the proposed 10-biomarker panel in a larger cohort including indolent and aggressive PCa and other prostate pathologies (e.g., BPH or prostatitis), and include patients with other high prevalent cancers (e.g., lung and colon cancer). The development of an “e-nose” apparatus with specificity for the detection of this panel may provide a new accurate, non-invasive, rapid and low-cost tool for PCa screening. Moreover, it will be crucial to clearly understand the biological origin

of the volatile biomarkers, which may be performed by fluxomic studies using isotopically labeled compounds. Finally, target studies to evaluate the enzymatic activity of the enzymes involved in the metabolic pathways proposed as important for PCa development and progression are also needed.

References

Boudonck KJ, Mitchell MW, Nemet L, Keresztes L, Nyska A, Shinar D, et al. Discovery of metabolomics biomarkers for early detection of nephrotoxicity. Toxicol Pathol. 2009;37(3):280-92.

Bray F, Ferlay J, Soerjomataram I, Siegel RL, Torre LA, Jemal A. Global cancer statistics 2018: GLOBOCAN estimates of incidence and mortality worldwide for 36 cancers in 185 countries. CA Cancer J. Clin. 2018;68(6):394-424.

Bujak R, Struck-Lewicka W, Markuszewski MJ, Kaliszan R. Metabolomics for laboratory diagnostics. J Pharm Biomed Anal. 2015;113:108-20.

Capelli L, Taverna G, Bellini A, Eusebio L, Buffi N, Lazzeri M, et al. Application and Uses of Electronic Noses for Clinical Diagnosis on Urine Samples: A Review. Sensors. 2016;16(10).

Crook AA, Powers R. Quantitative NMR-Based Biomedical Metabolomics: Current Status and Applications. Molecules. 2020;25(21).

di Salvo ML, Contestabile R, Paiardini A, Maras B. Glycine consumption and mitochondrial serine hydroxymethyltransferase in cancer cells: the heme connection. Med Hypotheses. 2013;80(5):633-6.

Dimakakos A, Armakolas A, Koutsilieris M. Novel tools for prostate cancer prognosis, diagnosis, and follow-up. BioMed Res Int. 2014;2014:890697.

Eidelman E, Twum-Ampofo J, Ansari J, Siddiqui MM. The Metabolic Phenotype of Prostate Cancer. Front Oncol. 2017;7:131.

Frolkis A, Knox C, Lim E, Jewison T, Law V, Hau DD, et al. SMPDB: The Small Molecule Pathway Database. Nucleic Acids Res. 2010;38(Database issue):D480-7.

Fu YM, Lin H, Liu X, Fang W, Meadows GG. Cell death of prostate cancer cells by specific amino acid restriction depends on alterations of glucose metabolism. J Cell Physiol. 2010;224(2):491-500.

Fu YM, Yu ZX, Li YQ, Ge X, Sanchez PJ, Fu X, et al. Specific amino acid dependency regulates invasiveness and viability of androgen-independent prostate cancer cells. Nutr Cancer. 2003;45(1):60-73.

Gamagedara S, Kaczmarek AT, Jiang Y, Cheng X, Rupasinghe M, Ma Y. Validation study of urinary metabolites as potential biomarkers for prostate cancer detection. Bioanalysis. 2012;4(10):1175-83.

Gholamy A, Kreinovich, V., and Kosheleva, O. Why 70/30 or 80/20 Relation Between Training and Testing Sets: A Pedagogical Explanation. IJITAS. 2018;11(2):105-11.

Gomez-Cebrian N, Rojas-Benedicto A, Albors-Vaquer A, Lopez-Guerrero JA, Pineda-Lucena A, Puchades-Carrasco L. Metabolomics Contributions to the Discovery of Prostate Cancer Biomarkers. Metabolites. 2019;9(3).

Holecek M. Branched-chain amino acids in health and disease: metabolism, alterations in blood plasma, and as supplements. Nutr Metab. 2018;15:33.

Jewison T, Su Y, Disfany FM, Liang Y, Knox C, Maciejewski A, et al. SMPDB 2.0: big improvements to the Small Molecule Pathway Database. Nucleic Acids Res. 2014;42(Database issue):D478-84.

Jiménez-Pacheco A, Salinero-Bachiller M, Iribar MC, López-Luque A, Miján-Ortiz JL, Peinado JM. Furan and p-xylene as candidate biomarkers for prostate cancer. Urol Oncol. 2018;36(5):243.e21-.e27.

Kanehisa M, Goto S. KEGG: Kyoto Encyclopedia of Genes and Genomes. Nucleic Acids Res. 2000;28(1):27-30.

Kearns JT, Lin DW. Improving the Specificity of PSA Screening with Serum and Urine Markers. Curr Urol Rep. 2018;19(10):80.

Khalid T, Aggio R, White P, De Lacy Costello B, Persad R, Al-Kateb H, et al. Urinary Volatile Organic Compounds for the Detection of Prostate Cancer. PLoS One. 2015;10(11):e0143283.

Khan AP, Rajendiran TM, Ateeq B, Asangani IA, Athanikar JN, Yocum AK, et al. The role of sarcosine metabolism in prostate cancer progression. Neoplasia. 2013;15(5):491-501.

Lee DK, Na E, Park S, Park JH, Lim J, Kwon SW. In Vitro Tracking of Intracellular Metabolism-Derived Cancer Volatiles via Isotope Labeling. ACS Cent Sci. 2018;4(8):1037-44.

Leonardi R, Jackowski S. Biosynthesis of Pantothenic Acid and Coenzyme A. EcoSal Plus. 2007;2(2).

Lima AR, Bastos Mde L, Carvalho M, Guedes de Pinho P. Biomarker Discovery in Human Prostate Cancer: an Update in Metabolomics Studies. Transl Oncol. 2016;9(4):357-70.

Lima AR, Pinto J, Amaro F, Bastos ML, Carvalho M, Guedes de Pinho P. Advances and Perspectives in Prostate Cancer Biomarker Discovery in the Last 5 Years through Tissue and Urine Metabolomics. Metabolites. 2021;11(3).

Lima AR, Pinto J, Bastos ML, Carvalho M, Guedes de Pinho P. NMR-based metabolomics studies of human prostate cancer tissue. Metabolomics. 2018;14(7):88.

Liu H, Cocea M. Semi-random partitioning of data into training and test sets in granular computing context. Granul Comput. 2017;2(4):357-86.

Louie KS, Seigneurin A, Cathcart P, Sasieni P. Do prostate cancer risk models improve the predictive accuracy of PSA screening? A meta-analysis. Ann Oncol. 2015;26(5):848-64.

Nagrath D, Caneba C, Karedath T, Bellance N. Metabolomics for mitochondrial and cancer studies. Biochim Biophys Acta. 2011;1807(6):650-63.

Park S, Ahn S, Shin Y, Yang Y, Yeom CH. Vitamin C in Cancer: A Metabolomics Perspective. Front Physiol. 2018;9(762).

Peng G, Hakim M, Broza YY, Billan S, Abdah-Bortnyak R, Kuten A, et al. Detection of lung, breast, colorectal, and prostate cancers from exhaled breath using a single array of nanosensors. Br J Cancer. 2010;103(4):542-51.

Pérez-Rambla C, Puchades-Carrasco L, García-Flores M, Rubio-Briones J, López-Guerrero JA, Pineda-Lucena A. Non-invasive urinary metabolomic profiling discriminates prostate cancer from benign prostatic hyperplasia. Metabolomics. 2017;13(5):52-.

Populo H, Lopes JM, Soares P. The mTOR signalling pathway in human cancer. Int J Mol Sci. 2012;13(2):1886-918.

Sampath D, Zabka TS, Misner DL, O'Brien T, Dragovich PS. Inhibition of nicotinamide phosphoribosyltransferase (NAMPT) as a therapeutic strategy in cancer. Pharmacol Ther. 2015;151:16-31.

Smith-Palmer T. Clinical Analysis | Sarcosine, Creatine, and Creatinine☆. In: Worsfold P, Poole C, Townshend A, Miró M, editors. Encyclopedia of Analytical Science (Third Edition). Oxford: Academic Press; 2019. p. 163-72.

Smith S, White P, Redding J, Ratcliffe NM, Probert CSJ. Application of Similarity Coefficients to Predict Disease Using Volatile Organic Compounds. IEEE Sensors Journal. 2010;10(1):92-6.

Sreekumar A, Poisson LM, Rajendiran TM, Khan AP, Cao Q, Yu J, et al. Metabolomic profiles delineate potential role for sarcosine in prostate cancer progression. Nature. 2009;457(7231):910-4.

Sun X, Stewart DA, Sandhu R, Kirk EL, Pathmasiri WW, McRitchie SL, et al. Correlated metabolomic, genomic, and histologic phenotypes in histologically normal breast tissue. PLoS One. 2018;13(4):e0193792.

Tao C, Sun J, Zheng WJ, Chen J, Xu H. Colorectal cancer drug target prediction using ontology-based inference and network analysis. Database. 2015;2015.

Turi KN, Romick-Rosendale L, Ryckman KK, Hartert TV. A review of metabolomics approaches and their application in identifying causal pathways of childhood asthma. J Allergy Clin Immunol. 2018;141(4):1191-201.

Walsh MC, Brennan L, Malthouse JP, Roche HM, Gibney MJ. Effect of acute dietary standardization on the urinary, plasma, and salivary metabolomic profiles of healthy humans. Am J Clin Nutr. 2006;84(3):531-9.

Wilson AD, Baietto M. Advances in electronic-nose technologies developed for biomedical applications. Sensors. 2011;11(1):1105-76.

Wishart DS. Metabolomics for Investigating Physiological and Pathophysiological Processes. Physiol Rev. 2019;99(4):1819-75.

Wishart DS, Feunang YD, Marcu A, Guo AC, Liang K, Vázquez-Fresno R, et al. HMDB 4.0: the human metabolome database for 2018. Nucleic Acids Res. 2018;46(D1):D608-D17.

Wolf AM, Wender RC, Etzioni RB, Thompson IM, D'Amico AV, Volk RJ, et al. American Cancer Society guideline for the early detection of prostate cancer: update 2010. CA Cancer J. Clin. 2010;60(2):70-98.

Zadra G, Loda M. Metabolic Vulnerabilities of Prostate Cancer: Diagnostic and Therapeutic Opportunities. Cold Spring Harb Perspect Med. 2018;8(10).